Performance and Reliability Evaluation for DSRC Vehicular Safety Communication

by

Xiaoyan Yin

Department of Electrical and Computer Engineering
Duke University

Date:_____

Approved:

_____
Kishor S. Trivedi, Supervisor

_____
Benjamin C. Lee

_____
Jeffrey H. Derby

_____
Loren W. Nolte

_____
Xiaomin Ma

Dissertation submitted in partial fulfillment of the requirements for the degree of Doctor of Philosophy in the Department of Electrical and Computer Engineering in the Graduate School of Duke University

2013

ABSTRACT

Performance and Reliability Evaluation for DSRC Vehicular Safety Communication

by

Xiaoyan Yin

Department of Electrical and Computer Engineering
Duke University

Date:_____

Approved:

_____
Kishor S. Trivedi, Supervisor

_____
Benjamin C. Lee

_____
Jeffrey H. Derby

_____
Loren W. Nolte

_____
Xiaomin Ma

An abstract of a dissertation submitted in partial fulfillment of the requirements for the degree of Doctor of Philosophy in the Department of Electrical and Computer Engineering in the Graduate School of Duke University

2013

Abstract

Inter-Vehicle Communication (IVC) is a vital part of Intelligent Transportation System (ITS), which has been extensively researched in recent years. Dedicated Short Range Communication (DSRC) is being seriously considered by automotive industry and government agencies as a promising wireless technology for enhancing transportation safety and efficiency of road utilization. In the DSRC based vehicular ad hoc networks (VANETs), the transportation safety is one of the most crucial features that needs to be addressed. Safety applications usually demand direct vehicle-to-vehicle ad hoc communication due to a highly dynamic network topology and strict delay requirements. Such direct safety communication will involve a broadcast service because safety information can be beneficial to all vehicles around a sender. Broadcasting safety messages is one of the fundamental services in DSRC. In order to provide satisfactory quality of services (QoS) for various safety applications, safety messages need to be delivered both timely and reliably. To support the stringent delay and reliability requirements of broadcasting safety messages, researchers have been seeking to test proposed DSRC protocols and suggesting improvements. A major hurdle in the development of VANET for safety-critical services is the lack of methods that enable one to determine the effectiveness of VANET design mechanism for predictable QoS and allow one to evaluate the tradeoff between network parameters. Computer simulations

are extensively used for this purpose. A few analytic models and experiments have been developed to study the performance and reliability of IEEE 802.11p for safety-related applications. In this thesis, we propose to develop detailed analytic models to capture various safety message dissemination features such as channel contention, backoff behavior, concurrent transmissions, hidden terminal problems, channel fading with path loss, multi-channel operations, multi-hop dissemination in 1-Dimentional or 2-Dimentional traffic scenarios. MAC-level and application-level performance metrics are derived to evaluate the performance and reliability of message broadcasting, which provide insights on network parameter settings. Extensive simulations in either Matlab or NS2 are conducted to validate the accuracy of our proposed models.

Contents

List of Tables

List of Figures

Acknowledgements

I would like to express my deepest gratitude to my advisor, Dr. Kishor S. Trivedi, for his guidance, patience, and encouragement during my research at Duke University. Dr. Kishor S. Trivedi is a brilliant, extraordinary, and inspiring professor, who taught me invaluable research skills, and helped me overcome many difficulties. He is always there for me whenever I needed advice. The completion of this dissertation would be impractical without his continuous academic and passionate support.

I will also forever be thankful to Prof. Xiaomin Ma, who gave me insightful suggestions and invaluable comments on my work. During our research cooperation, he has been extremely helpful in providing his scientific advice and knowledge through many fruitful meetings and discussions. I sincerely treasure the collaboration experiences with Prof. Ma.

I would like to thank my committee members during my research work, Dr. John A. Board, Dr. Krishnendu Chakrabarty, Dr. Loren W. Nolte, and Dr. Matt Reynolds for their kindness to serve on my committee and provide constructive suggestions to my research.

I would like to thank the generous financial support for my research work from National Science Foundation, Duke University Graduate School and Electrical and Computer Engineering Department, General Motors and NEC Corporation.

I thank my colleagues at Duke University, Javier Alonso, Ermeson Andrade, Rahul Ghosh, DongSeong Kim, Jae Shik Lim, Amita Devaraj, Fumio Machida, Arpan Roy, Ruofan Xia, and Yang Zhao for their generous help and the wonderful working environment that they created.

I would like to thank my farther Huasheng Yin, mother Zhiying Liu, elder sister Dayan Yin and younger brother Jinzhong Yin for their unconditional love and encouragement during the pursuit of my PhD degree. I am deeply grateful to my husband Lei Zhang, who has been a true and great supporter during my good and bad times. It is also a great pleasure and a wonderful life experience to have my beloved daughter Jen Zhang born during this unique period of time.

1. Introduction

1.1 Overview of DSRC Safety Communication

Vehicle safety is an important issue for our society. Although severity amelioration technologies such as air bags, seat belts, and automatic braking system (ABS) have been applied for years to provide passive protection to vehicle occupants, nearly 6.2 million police-reported motor vehicle crashes occur annually in the United States (*i.e.*, one every 5 seconds). On the average, a person is injured in a police-reported motor vehicle crash every 12 seconds, and someone is killed every 12 minutes. The related economic loss due to crashes is $230.6 billion annually. The development of Intelligent Transportation System (ITS) [113] is to progress towards safe and smooth driving without excessive delay. Vehicular ad hoc network (VANET) is one of the key enabling technologies in ITS. Dedicated Short Range Communication (DSRC) radio technology being standardized as IEEE 802.11p [1][112] is projected to support low-latency wireless data communications between vehicles and from vehicles to roadside units. Such a communication technology is being seriously considered by automotive industry and government agencies, and the radio devices are expected to be installed in future vehicles and work with sensors for enhancing transportation safety and efficiency of road utilization.

Currently, DSRC is under active development in the United States, Europe, Japan and other countries. Various safety and non-safety applications will be enabled

through information exchange using Vehicle-to-Vehicle (V2V) communication, and Vehicle-to-Infrastructure (V2I) communication. Compared to non-safety applications (*e.g.*, toll collection, traffic indication, commercial services), safety applications (*e.g.*, collision avoidance, emergency vehicle warning, slow vehicle indication) are more critical to prevent collisions on the road and hence save thousands of lives. U.S. Department of Transportation (DOT) has estimated that V2V safety communication based on DSRC can assist drivers in preventing 76 percent of the crashes on the roadway, thereby reducing fatalities and injuries that occur each year.

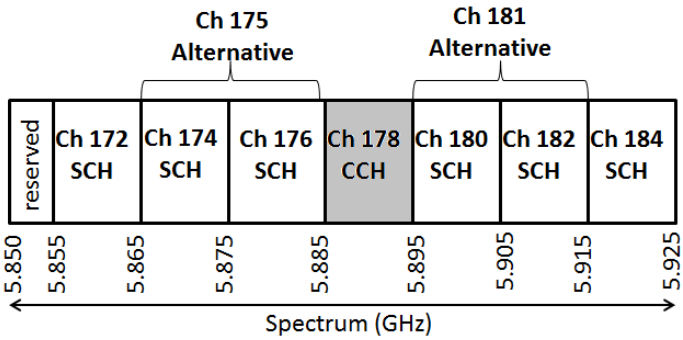

Figure 1.1: U.S. DSRC channel allocation

In U.S., Federal Communications Commission (FCC) has allocated 75 MHz of spectrum in the 5.9 GHz band, which consists of one control channel (CCH) and six service channels (SCHs), for DSRC to be used by ITS as shown in Fig. 1.1 [45]. DSRC is a secure, high speed (3 *Mbps*~27 *Mbps*), short range (100 *m*~1000 *m*) wireless interface between vehicles and surface transportation infrastructure that enables rapid communication of vehicle data and other content between On Board Equipment (OBE) and OBE, and between OBE and Road Side Equipment (RSE).

DSRC standards for various layers are under development in U.S. to support DSRC communications. Fig. 1.2 shows the protocol stack [45] for DSRC communication. According to the updated version of the DSRC standard IEEE 802.11p [44], the DSRC physical layer follows the same frame structure, modulation scheme and training sequences specified by IEEE 802.11a physical layer standard with minor changes; MAC layer of the DSRC is equivalent to the Enhanced Distribution Coordination Access (EDCA) 802.11e that has four different access classes (ACs). IEEE 1609.4 [69] as an extension for MAC layer provides channel switching for multi-channel operations, whereas 1609.3 [70] and 1609.2 [71] deal with network services and security services respectively. Internet protocols for Network and Transport layer are also supported in DSRC communication, which are mainly used for non-safety applications.

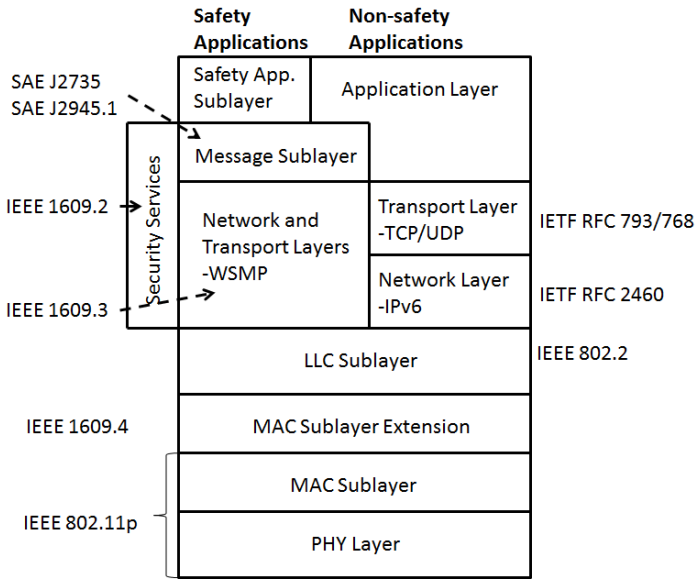

Figure 1.2: Protocol stack for DSRC communication

In the DSRC based vehicular ad hoc networks (VANETs), the transportation safety is one of the most crucial features that need to be addressed. Safety applications usually demand direct V2V ad hoc communication due to a highly dynamic network topology and strict delay requirements. Such direct safety communication will involve a broadcast service because safety information can be beneficial to all vehicles around a sender. Broadcasting safety messages is one of the fundamental services in DSRC. The safety messages can be categorized into two: basic safety message (BSM) and event-driven safety message (ESM). The BSMs are periodically sent and also referred as periodic beacon messages. The BSM contains information related to the status of vehicle (*e.g.*, position, velocity and direction) and is periodically broadcast by each vehicle to announce other vehicles about their existence. Neighboring vehicles utilize such messages to become aware of their surroundings out of sight and avoid potential dangers (*e.g.*, rear-end collision warning, slow vehicle indication, emergency vehicle warning *etc.*) [58]. The ESMs are generated and broadcast by a vehicle to warn neighbors around when an abnormal condition or an imminent danger is detected (*e.g.*, road hazard warning, traffic condition warning, signal violation warning *etc.*) [58]. In order to provide satisfactory quality of services (QoS) for various safety applications, safety messages need to be delivered in both reliably and timely manner.

1.2 Research Problems Addressed

To support the stringent delay and reliability requirements of broadcasting safety messages, researchers have been seeking to test proposed DSRC protocols and suggesting improvements. A major hurdle in the development of VANET for safety-critical services is the lack of methods that enable one to determine the effectiveness of VANET design mechanism for predictable QoS and allow one to evaluate the tradeoff between network parameters. Hence, we aim to evaluate important performance and reliability metrics under various traffic scenarios to assess the effectiveness of message dissemination schemes for safety applications.

Several types of methods have been utilized in the literature to analyze the performance and reliability for safety communication. Computer simulations are extensively used, which usually take long time to collect sufficient data for accurate performance analysis. Several real world experiments are also conducted to capture more practical network dynamics. However, due to the high equipment cost, the experimental testbed usually only consists of a very few vehicles. Even though some techniques are used to create a large scale virtual communication network using a small number of vehicles, the resulting virtual network is still only capable of capturing sparse network scenarios. Analytic modeling is a more attractive alternative due to lower cost of solving the model while covering a large network parameter space. However, there are very few accurate analytic models developed for safety applications evaluation. Our

main goal for this dissertation is to propose comprehensive and high fidelity analytic models for the performance and reliability analysis under various safety communication scenarios. The accuracy and efficiency of the analytic models are validated through extensive simulations.

1.3 Contributions of the Dissertation

In this dissertation, the following contributions are made:

(1) **Developed comprehensive and high fidelity analytic models.** In V2V safety communications, vehicles on the road compete for the channel resource to transmit their own safety messages. To reduce the complexity for developing and solving monolithic models, we utilize the model decomposition technique and propose interacting stochastic models based on the semi-Markov process (SMP) to capture vehicles' channel contention and backoff behavior. Due to the interactions between vehicles, fixed-point iteration is used to obtain converged solutions, based on which important performance and reliability metrics are further derived.

(2) **Evaluated different types of safety messages.** As mentioned earlier, the safety messages can be categorized into two: basic safety message (BSM) and event-driven safety message (ESM). A simplified SMP model is first developed for the ESM evaluation, and a more precise SMP model is developed for the BSM evaluation. The analytic-numerical results for these two approaches are also compared in Chapter 5. The obtained results show that the performance and reliability metrics for BSM and

ESM are similar when their average message generation intervals are the same. In addition, we conclude that the simplified SMP model for ESM evaluation with Poisson message arrivals can be used to approximate the BSM evaluation with periodic message arrivals. Many papers [6][8][41][52][62][117] have used Poisson arrival process to approximate BSM arrival process without any proof.

(3) **Evaluated multiple services over a single channel.** The control channel (CCH) is the default channel for V2V safety communication. If different types of safety messages need to be transmitted to support multiple safety services, it is possible that the control channel will be shared. Enhance distributed channel access (EDCA) is the access mechanism specified in IEEE 802.11p protocol to support multiple types of services with priorities. Therefore, analytic models are proposed for the performance and reliability analysis of three types of vehicular safety-related services using EDCA mechanism in the DSRC system on highways. Several important observations are drawn. The results show that EDCA mechanism, which utilizes different channel sensing time and backoff counters for different services, can only provide service differentiation in terms of transmission delay, but cannot help improve the reliability for higher priority services. Another important conclusion is that higher priority service should choose shorter packet length, higher date rate and larger carrier sensing range to ensure high packet transmission reliability.

(4) **Evaluated multi-channel operations for the BSM.** The control channel (CCH) is dedicated to support safety communications, and BSM is most likely to be transmitted via CCH. The SCH channel 172 in Fig. 1.1 is reserved probably for critical V2V safety communications, and hence the ESM (which is sent in presence of an emergency event and hence is more critical than BSM) can be transmitted on this channel to avoid the channel contention with the more frequently generated BSMs. In addition, other SCHs in Fig. 1.1 are most likely to be used for non-safety applications. At the early stage of the DSRC deployment, a vehicle may only have a single-radio device installed due to the cost constraints. To support both safety and non-safety applications, this single-radio device can switch between different channels, one channel at a time. IEEE 1609.4 [69] is an extension for MAC layer to provide channel switching mechanism for multi-channel operations. Analytic models are developed to evaluate the impact of such multi-channel operations on the performance and reliability of BSMs transmitted via the CCH. The results show that channel switching mechanism can greatly degrade the performance and reliability of the BSM transmission.

(5) **Evaluated multi-hop transmissions for the ESM.** To ensure high reliability for ESMs, which are more critical than BSMs, a channel (probably channel 172) may be reserved specifically for ESM broadcasting. In addition, some event-driven safety applications (*e.g.*, post-crash notification, road hazard warning) may be required to

cover longer distances than the one-hop communication range. Therefore, multi-hop ESM dissemination is necessary in such scenarios. A robust relay selection strategy utilizing distance-based timers is proposed in this dissertation and an accurate analytic model is proposed to evaluate multi-hop propagation of ESMs. Important conclusions are drawn to provide deeper insight into the ESM transmission behavior from different angles.

(6) **Evaluated 2-Dimensional traffic scenarios.** Most analytic models proposed in the literature concentrate on 1-Dimensional (1-D) highway traffic to simplify the model. Unfortunately, very few of network scenarios in real applications can be abstracted as 1-D models. Therefore, in this dissertation, we first developed an analytic model on the performance and reliability evaluation of 2-Dimensional (2-D) traffic at open field to capture more realistic message transmission behaviors.

(7) **Incorporated various factors for the performance and reliability metrics derivation.** In this dissertation, we considered various important factors that can influence the message transmission including channel contention, backoff behavior, concurrent transmissions, hidden terminals problems and channel fading with path loss. The degree of impact of concurrent transmission, hidden terminals problem and channel fading with path loss is also assessed. The results presented in Section 3.5.3, Section 5.5.6 and Section 6.5.3 show that concurrent transmission has very

minor impact, whereas hidden terminals problem and channel fading with path loss have significant impact on the performance and reliability.

(8) **Conducted simulations for cross validation purposes.** We conducted extensive simulations in either Matlab or NS2 for comparison purposes in each Chapter. The good match between analytic-numerical results and simulation results under a large range of network parameters validate the accuracy of our proposed models. In addition, the time consumed to solve analytic models and for simulations is compared, which shows that the analytic models are much more efficient than simulations.

Our contribution can also be summarized from different aspects according to the interest of people from various areas:

(1) **Provide valuable insights for protocol development.** First, we proposed an efficient and accurate approach to easily evaluate whether the given network parameter can satisfy the QoS and highlight how to tune the parameters in order to meet the QoS. In addition, EDCA protocol is proven in this dissertation that it does not support service differentiation regarding to broadcast reliability. Such observation may form the background to support other effective protocols development for service prioritization. Moreover, even though IEEE 802.11p is the standardized protocol analyzed in this dissertation, our proposed models are based on characterizing the operation flow for the DCF function, which forms the basic medium access

mechanism in many other protocols. Therefore, our models can be easily extended to analyze other protocols.

(2) **Provide more effective approach than simulation and experiment based methods.** To evaluate the effectiveness of our proposed analytical models, we conducted simulations in every chapter for comparison purposes. Our models can be easily solved within a few seconds or minutes, while simulations usually take up to several hours. Hence, our models are much more efficient than simulation methods and can deliver valuable results much faster for the development of DSRC safety communication. Furthermore, most experiments are limited to a few vehicles due to extremely high cost of purchasing vehicles, which results in the insufficiency for capturing realistic and important factors that influence the safety communication, such as hidden terminal problem. Therefore, the advantage of our model is that it effectively considers various factors and can be easily extended to incorporate more factors of interest without any resource limit.

(3) **Provide more accurate approach than other analytic models.** Even though there are many analytic models proposed in the literature to analyze the performance and reliability of safety communication, most of them are based on Bianchi's discrete-time Markov chain (DTMC) model [27]. The system's continuous time behavior for channel sensing and deferring in message transmission are completely ignored, which results in inaccuracy. Our model considers more accurate message

transmission behavior in MAC layer by using semi-Markov Process (SMP) model without discretizing the time. The comparison of our model with several DTMC based analytic models presented in many chapters verifies that our model is more accurate than prevalent DTMC models. In addition, most analytic models only consider MAC-level performance metrics, whereas our model also considers application-level metrics to better fulfill the safety application's QoS requirement. Moreover, several important factors such as distance-based channel fading, hidden terminal problem and channel switching mechanism are not evaluated in vast analytic approaches, while we constructed much more accurate and practical model by taking into account of those essential factors.

1.4 Outline of the Dissertation

This dissertation is organized as follows:

Chapter 2 describes the background on DSRC-related topics and stochastic modeling. Since the MAC layer channel access for safety communication follows distributed coordination function (DCF) for one type of safety message according to IEEE 802.11 protocol, the detailed DCF access control technique is first described. We also introduce the related analytic modeling methods used throughout this dissertation.

Chapter 3 presents a general analytic model to evaluate the performance of safety message broadcasting, which is suitable for ESMs. Poisson message arrival is assumed for event-driven message generation. Infinite MAC-layer queue for each

vehicle is assumed since the ESMs are too critical to be dropped. Hence, the generation and service of ESMs in each vehicle is modeled by a generalized M/G/1 queue. The overall model is a set of interacting M/G/1 queues, one queue for each vehicle. To produce a simplified yet high fidelity analytic model, we decompose the overall model and use semi-Markov process (SMP) model to capture shared channel medium's behavior from a single vehicle's perspective. Due to the interactions between vehicles, fixed-point iteration is utilized to obtain converged solutions. Important MAC-level performance and reliability metrics are subsequently derived. Simulations in Matlab are developed to validate the accuracy and efficiency of the proposed analytic model.

Chapter 4 describes a more accurate analytic model to capture the BSM broadcasting in a channel (probably the control channel), where associated features such as periodic message generation, out-dated message replacement and no queuing in MAC-layer are incorporated. Such a model for BSMs is compared with the model presented in Chapter 3 for ESMs. The results prove that the simplified analytic model for ESMs can be used to approximately evaluate the BSMs transmission. Besides MAC-level performance and reliability metrics, application-level metrics are also evaluated. Simulations in Matlab are conducted for the comparison purpose.

Since the control channel is the default channel for V2V safety communication, multiple types of safety messages (including the ESM and BSM) can be transmitted together in the control channel (CCH). Therefore, in Chapter 5, multiple types of services

transmissions over a single channel (*e.g.*, control channel) are evaluated based on the extension of the analytic model developed in Chapter 3. The EDCA mechanism specified in the IEEE 802.11p protocol is shown to be ineffective to guarantee priorities for different services. Important conclusions are also drawn to tune network parameters in order to improve the performance and reliability for high priority services. Simulations are performed in Matlab.

The U.S. FCC has allocated seven 10 MHz channels for DSRC: one control channel (CCH) and six service channels (SCHs). At the early stage of DSRC deployment, a vehicle may have only a single-radio DSRC device installed. To support concurrent applications on different channels, such a single-radio device can switch between different channels, one channel at a time, to access safety messages (*e.g.*, BSMs) on the CCH and other services on the SCHs. Therefore, the IEEE 1609.4 multi-channel operation is considered in Chapter 6 to evaluate the performance and reliability of the BSMs transmission on the CCH. The impacts of various factors such as concurrent transmission, hidden terminals problem, channel fading with path loss and channel switching mechanism are evaluated. Simulations are developed in NS2 to validate the accuracy and efficiency of the proposed analytic model.

Among the six service channels, the Channel 172 may be reserved for life critical safety applications with no time division [45]. This implied that a vehicle interested in both safety and non-safety applications requires two DSRC radios: one tuned to Channel

172 all the time, and the other participates in IEEE 1609.4 channel switching [45]. Since ESMs are life-critical messages, they are most likely to be transmitted on Channel 172. In addition, since some event-driven safety applications (*e.g.*, post-crash notification, road hazard warning) may require longer transmission distance than the one-hop communication range, multi-hop dissemination of ESMs is necessary. Hence, we introduce an accurate analytic model in Chapter 7 to evaluate multi-hop propagation of ESMs. Extensive Matlab simulations are performed. Important conclusions are obtained to provide deeper understandings of the performance and reliability of the ESMs transmission behavior.

The analytic models developed in Chapter 3-7 are all concentrated on 1-D highway traffic to simplify the model. Until now, there is no analytic model on 2-D evaluation. Nevertheless, very few of network scenarios in real applications can be abstracted as 1-D traffic. Therefore, in Chapter 8, we first introduce an analytic model on the performance and reliability evaluation of 2-D traffic at open field (*i.e.*, battle field) to capture more realistic message transmission behaviors. Simulations in NS2 are carried out and the numerical results are compared with the analytic-numerical results under a large range of network parameter settings.

Chapter 9 summarizes this dissertation and describes future research work on this topic.

Table 1.1 summarizes and compares the work presented in each chapter.

Table 1.1: Summary of chapters

Chapter	Message Type	Multiple Service?	Channel Switch?	Multi-hop?	2-D?	Fixed-point?	Simulation
3	BSM, ESM	No	No	No	No	Yes	Matlab, NS2
4	BSM	No	No	No	No	Yes	Matlab
5	BSM, ESM	Yes	No	No	No	Yes	Matlab
6	BSM	No	Yes	No	No	Yes	NS2
7	ESM	No	No	Yes	No	No	Matlab
8	BSM, ESM	No	No	No	Yes	Yes	NS2

2. Background

In this chapter, we briefly introduce the background on DSRC-related topics (including DCF access mechanism) and stochastic modeling methods (including Markov models, semi-Markov models and queuing models) used in this dissertation.

2.1 DSRC-related background

This section presents essential background of DSRC for analytic modeling of safety communication in VANETs.

2.1.1 MAC Layer Protocol Description

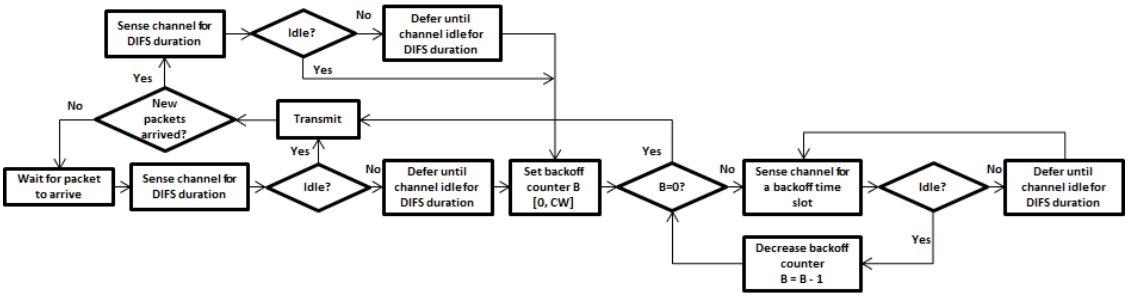

Figure 2.1: Flow chart of DCF function

To model and assess the performance of safety message broadcasting, MAC layer behavior specified by IEEE 802.11p has to be accurately evaluated. Hence, we briefly describe the MAC layer channel access for safety message broadcasting in this section.

From [44], we know that the DSRC adopts IEEE 802.11 MAC layer specification based on the carrier sense multiple access with collision avoidance (CSMA/CA) with minor modifications. In the 802.11 MAC layer protocol [11], distributed coordination function (DCF) is the primary medium access control technique for broadcast services.

Fig. 2.1 describes in detail the basic access mechanism of DCF for broadcast in the context of the safety communication. Enhanced Distributed Channel Access (EDCA) mechanism for multiple services with priorities specified in IEEE 802.11p [44] complies with the DCF function if only one type of service is considered in the channel.

According to Fig. 2.1, each vehicle in the network can generate messages and compete for the channel resource to transmit the message. If a vehicle does not have any message to transmit, it will wait for a packet to be generated. Then, for a newly generated packet, the vehicle senses the channel activity before it starts to transmit the packet. If the channel is sensed idle for a time period of distributed inter-frame space (*DIFS*), the packet can be directly transmitted. Otherwise, the vehicle continues to monitor the channel until channel is detected to be idle for *DIFS* time period. Subsequently, according to the collision avoidance feature of the protocol, the vehicle goes through the backoff process before transmitting the packet. It generates an initial random backoff counter from a uniform probability mass function (pmf) over the range [0, *CW*], where *CW* represents the contention window. The backoff time counter is decreased by one if the channel is sensed idle for a time slot of duration σ. Otherwise, the counter is *frozen* and reactivated when the channel is sensed idle again for more than *DIFS* duration. The packet is transmitted as soon as the backoff counter reaches zero. After this packet is transmitted, if there is no packet left in this vehicle, the process will start over again and the vehicle will wait for a new packet to be generated. Otherwise, if

there are packets left, the vehicle repeats the procedure starting with sensing the channel for *DIFS* duration and goes through the backoff procedure before transmitting the next packet. According to the protocol, a vehicle must go through the backoff process between two consecutive packet transmissions even if the channel is sensed idle for the duration of *DIFS* time for the second packet.

2.2 Modeling Methods

To evaluate the performance and reliability of safety communication in VANETs, state-space stochastic models are used in this dissertation to characterize the safety message broadcasting behavior. Compared to non-state-space models, state-space models can capture more complex dependencies in the system under consideration. This section introduces some commonly used state-space models including Markov models and semi-Markov models.

2.2.1 Markov Models

The stochastic process for Markov models is whose dynamic behavior for future development depends only on the current state and not on how the process arrived in that state, which is well known as Markov property. The formal definition for Markov process is:

Definition: A stochastic process $\{X(t) \mid t \geq 0\}$ is a **Markov chain** if for any $t_0 < t_1 < \ldots < t_n < t$, the conditional probability mass function (pmf) of $X(t)$ satisfies:

$$P\left(X(t)=x \mid X(t_n)=x_n, X(t_{n-1})=x_{n-1}, \ldots, X(t_0)=x_0\right) = P\left(X(t)=x \mid X(t_n)=x_n\right) \tag{2.1}$$

If the state space I is discrete as above, the Markov process is known as a **Markov chain**. If the parameter space T is also discrete, then we have a **discrete-time Markov chain** (DTMC). If the parameter space T is continuous, then we have a **continuous-time Markov chain** (CTMC). The Markov chain $\{X(t) \mid t \geq 0\}$ is said to be (time-) **homogeneous** if the state transition probability depends only on the difference of the two time epochs that we are considering. Otherwise, the Markov chain is a **non-homogeneous** Markov chain. Henceforth, we only consider the homogeneous case.

The transient behavior of a CTMC satisfies the **Chapman-Kolmogorov** equation in matrix form as follows:

$$\frac{d\boldsymbol{\pi}(t)}{dt} = \boldsymbol{\pi}(t)Q \tag{2.2}$$

where $\boldsymbol{\pi}(t) = [\pi_1(t), \pi_2(t), \ldots, \pi_n(t)]$ is the state probability vector, and n is the number of states in the CTMC. $Q = [q_{ij}]_{n \times n}$ is the infinitesimal generator matrix, where q_{ij} $(i \neq j)$ is the transition rate from state i to state j, and $q_{ii} = -\sum_{i \neq j} q_{ij}$. In steady-state, Eq. (2.2) becomes:

$$\boldsymbol{\pi}Q = 0 \tag{2.3}$$

For a DTMC, the state probability vector after n-step transition is given by:

$$\mathbf{p}(n) = \mathbf{p}(0) \cdot P^n \tag{2.4}$$

where $\mathbf{p}(0) = [p_1(0), p_2(0), \ldots, p_n(0)]$ is the initial state probability vector, and $P = [p_{ij}]_{n \times n}$ is the one-step transition probability matrix (p_{ij} is the transition probability from state i to state j). In steady-state, denote $\mathbf{v} = \lim_{n \to \infty} \mathbf{p}(n)$, then Eq. (2.4) becomes:

$$\mathbf{v} = \mathbf{v} \cdot P \tag{2.5}$$

2.2.2 Semi-Markov Process Model

Semi-Markov process (SMP) model is a generalization of both continuous and discrete time Markov chains which permit arbitrary sojourn time distribution function, possibly depending on both the current state and the state to be visited next [116]. For a better understanding, let us consider a stochastic process as follows [115]. First construct a k-state discrete-time Markov chain (DTMC) with state transition probability matrix $\boldsymbol{P} = [p_{ij}]$; next construct a process in continuous time by marking the time spent in a transition from state i to state j have a distribution function $F_{ij}(t)$ such that times are mutually independent; at the end of the interval, we have a point event of type j. Such a stochastic process is called semi-Markov process, which is a generalization of both continuous and discrete time Markov processes with countable state spaces.

A descriptive definition of SMP [115] is that it is a stochastic process which moves from one state to another state among a countable number of states with the successive states visited forming a discrete-time Markov chain, and that the process stays in a given state for a random amount of time, the distribution function of which

depends on this state as well as the one to be visited next but does not depend on which states the system had been in before it got there.

A formal definition of SMP [116] is described as follows. A SMP is the process $Y=\{Y_t;\ t\geq 0\}$ defined by:

$$Y_t = X_{N(t)} = X_n, \quad if\ S_n \leq t < S_{n+1} \tag{2.6}$$

for $t\geq 0$, where $N(t)$ is the counting process. From the SMP definition, it should be observed that the process only changes state (possibly back to the same state) at the Markov regeneration epochs S_n. To analyze the steady-state behavior or to calculate some expected values of a SMP model, there exists a method called the *two-stage* method. It describes an SMP model using the matrix $\boldsymbol{P}$ and the vector $\boldsymbol{H}(t)$, where $\boldsymbol{P} = [p_{ij}]$ is the one-step transition probability matrix for the embedded Markov chain (EMC) of the SMP model, and $\boldsymbol{H}(t)=[H_i(t)]$ with $i=1,\ldots,n$, is the sojourn time distribution in state i. Such a method considers SMP transitions as taking place in two stages:

1) In the first stage, the system stays in state i for some amount of time, the mean sojourn time in state i is:

$$h_i = \int_0^\infty \left(1 - H_i(t)\right) dt \tag{2.7}$$

2) In the second stage, the system moves to state j with probability p_{ij}.

When this *two-stage* method is applied to the steady-state analysis of SMP model, we first calculate the steady-state probability vector of the EMC using Eq. (2.5). Given the

mean sojourn time vector $\boldsymbol{h}$=[h_1, h_2,…, h_n], the steady-state probability vector $\boldsymbol{\pi}$=[π_1, π_2,…, π_n] of the SMP can be written as:

$$\pi_i = \frac{v_i h_i}{\sum_{k=0}^{n} v_k h_k} \tag{2.8}$$

which is the ratio between the average time spent in state i ($v_i h_i$) over the total average time spent ($\sum_k v_k h_k$) over all states.

2.2.3 Queuing Models

A queuing system consists of one or more stations (servers) that provide services to arriving customers (jobs). Customers who arrive to find all servers busy generally join one or more queues (waiting lines) in front of the servers. The queuing system can be characterized by three important components: arrival process, service process, and the number of servers. Assume that successive inter-arrival times Y_1, Y_2, …, between jobs are independent identically distributed random variables having a distribution F_Y. Similarly, the service times S_1, S_2, …, are assumed to be independent identically distributed random variables having a distribution F_S. Let m denote the number of servers in the system. Therefore, we can use the notation F_Y/ F_S/m to describe the queuing system. The following symbols are used to denote the specific types of inter-arrival times and service time distributions [9]:

- M: (for memoryless) for the exponential distribution
- D: for a deterministic or constant inter-arrival or service time

- E_k: for a k-stage Erlang distribution
- H_k: for a k-stage hyperexponential distribution
- G: for a general distribution
- GI: for general independent inter-arrival times

Based on the above convention, we can easily interpret the queuing system. The most frequent example of a queuing system is $M/M/1$ queue, which stands for a single-server queue with exponentially distributed inter-arrival times and exponentially distributed service time. In this dissertation, $M/G/1$ queue and $GI/G/1$ queue notions are used. $M/G/1$ queue represents a single-server queue with exponentially distributed inter-arrival times and an arbitrary service time distribution, and $GI/G/1$ queue represents a single-server queue with general independent inter-arrival times and an arbitrary service time distribution. If a queuing system has limited buffer space so that at most n jobs can be in the system, such a system can be denoted as $F_Y/ F_S/m/n$ using this *Kendall* notation. Therefore, $D/G/1/1$ queue system presented in Section 4.1 denote a single-server queue with deterministic inter-arrival times distribution, general service times distribution, and the number of jobs in the system is at most 1. Besides the nature of the inter-arrival time and service time distribution, queue scheduling discipline that describes how the server is to be allocated to the jobs waiting for service also needs to be specified. In this dissertation, two scheduling disciplines are used: First Come First Served (FCFS) and Last Come First Served (LCFS).

2.2.4 Fixed-point Iteration Method

In numerical analysis, fixed-point iteration is a method used to compute fixed points of iterated functions. More specifically, a solution to the equation $f(x)=x$ is referred to as a fixed point of the function f. Geometrically, the fixed points of a function $f(x)$ are the point(s) of intersection of the curve $y=f(x)$ and the line $y=x$. Given a point x_0 in the domain of f, successive substitution $x_{n+1} = f(x_n)$, $n=0,1,2,\ldots$ is commonly used to determine the fixed point. The sequence x_0, x_1, x_2, …, is expected to converge to a point x. The proofs for the existence, uniqueness and convergence of the fixed-point iteration process are provided in Chapter 3.

3. Broadcast Safety Messages Evaluation

3.1 Motivation

In the DSRC based vehicular ad hoc networks (VANETs), the transportation safety is one of the most crucial features that needs to be addressed. Safety applications usually demand direct vehicle-to-vehicle ad hoc communication due to a highly dynamic network topology and strict delay requirements. Such direct safety communication will involve a broadcast service because safety information can be beneficial to all vehicles around a sender. Broadcasting safety messages is one of the fundamental services in DSRC that is being standardized as IEEE 802.11p.

In the literature, unicast for IEEE 802.11 has been extensively investigated. Bianchi [27] proposed a simple yet accurate discrete-time Markov chain (DTMC) model to evaluate the performance of unicast mechanism under saturation conditions. His paper has inspired many other researchers to develop analytic models of unicast based on DTMC. For example, multiple types of safety messages are evaluated in [28][29] under saturation conditions. Bianchi's work was later extended to the unsaturated case in [30].

Unique characteristics of the broadcast make its analysis different from that of unicast. First, unicast can have handshake between the sender and the receiver, which provides feedback to the sender for the possible need for retransmission to enhance reliability. By contrast, broadcasting sender cannot obtain feedback information from the

receivers and hence it will generally be only broadcast once. Second, the hidden terminal area in broadcast can be considerably larger than that in unicast, which makes broadcast very sensitive to hidden terminals. Third, besides throughput and packet transmission delay, distinctly different output measures need to be utilized to characterize broadcast reliability as compared with unicast. Therefore, the analysis methods that have been used for unicast cannot be extended to broadcast in a straightforward manner.

Performance of vehicular safety communication in DSRC system has been studied in [2][3][4][5]. Two important performance metrics: packet delivery ratio (PDR) and packet reception rate (PRR) were introduced respectively in [7] and [3] to quantify the performance of safety message broadcast in DSRC based VANETs. However, the evaluations are mainly based on simulations or experiments. Recently, a few analytic models have been developed to characterize and evaluate the broadcast performance. In [23], an analytic model based on DTMC was constructed to characterize the operation of the IEEE 802.11 MAC backoff counter for broadcast, and closed form solution is obtained for the PDR of wireless LAN. However, saturation assumption is made in this paper, which is not a good approximation for a real situation. Efficiency and reliability of beacon message broadcast in DSRC VANETs was investigated in [24] considering channel fading as the only source of broadcast failures under the saturation condition without accounting for the hidden terminal problem. A DTMC model interacting with an M/G/1 queue was developed in [6][7][8] to analyze the performance of the DSRC

broadcast services incorporating the backoff counter process, hidden terminals and unsaturated message generation. Based on [7], a more precise model utilizing DTMC was constructed in [25] to evaluate the transmission delay and PDR of 1-D VANET, and the performance for protocols with and without broadcast retransmissions was compared. Channel switching in current version of IEEE 802.11p was considered and its effects on the VANET performance were evaluated in [26], whereas the hidden terminal effect and unsaturation condition are omitted. [31][32][33] considered multiple types of safety message broadcast using EDCA mechanism. However, most previous research was based on Bianchi's DTMC (*i.e.*, per-slot statistics) model [27] and ignored important aspects of continuous time system behavior leading to approximations. More specifically, due to the characteristic of such discrete models, backoff counter freezing behavior is not accurately captured. Lee [38] considered such freezing process by adding sub-Markov chain for multiple services using EDCA. However, the backoff counter freezing time triggered by the busy medium (*i.e.*, waiting for the packet in the channel to finish transmission) was still not considered. In a recent paper by Tinnirello and Bianchi [37], an analytic model not based on the per-slot statistics was proposed through a fixed-point computation of the residual backoff counter distribution occurring after a generic transmission attempt. However, this is only for the saturation condition.

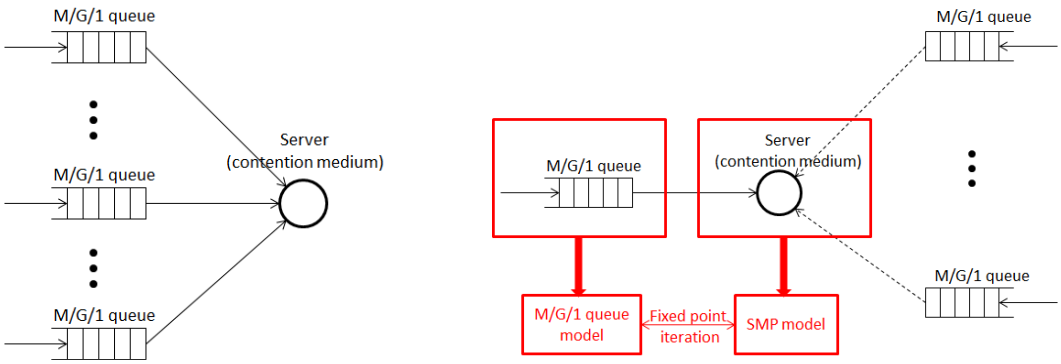

(a) The overall model (b) Models from one tagged vehicle's perspective

Figure 3.1: Models capturing interactions between vehicles

In this chapter of this thesis, we provide an accurate analytic model for the performance evaluation of one-hop direct broadcast safety message in the control channel of DSRC. The generation and service of safety messages in each vehicle is modeled by a generalized M/G/1 queue, where two classes of service are considered based on Welch's method [13]. The overall model is a set of interacting M/G/1 queues, one queue for each vehicle, as shown in Fig. 3.1(a). The interaction is that the server is shared as it is the contention medium/channel for the safety message transmissions. To make the model scalable, we use semi-Markov process (SMP) [9] model to capture the shared server's behavior from a single tagged vehicle's perspective, where the medium/channel contention and backoff behavior for this vehicle and the influence from other vehicles are considered as shown in Fig. 3.1(b). Different from the previous DTMC models capturing the shared server's discrete time behavior, this SMP model directly incorporates the unsaturation condition of the queue in a continuous time fashion. It

interacts with the tagged vehicle's M/G/1 queue through fixed-point iteration as shown in Fig. 3.1(b).

In this chapter, we concentrate on the study of fundamental performance issues of IEEE 802.11 based broadcast in DSRC vehicular environment. For simplicity of analysis, our proposed interacting stochastic model is for one type of safety service in a single channel. However, our model can be easily extended to multiple types of safety messages such as EDCA and multi-channel services in current or future IEEE 802.11p.

The major contributions made in this chapter are three-fold. First, a semi-Markov process model is developed to characterize MAC behavior of IEEE 802.11p based network with unsaturated message generation and hidden terminals in the continuous time, which is more general and precise compared with the existing DTMC based models. Second, in order to solve the SMP model, the service time for packets generated from the tagged vehicle is divided into two classes, (i) packets arriving when the tagged vehicle's queue is empty and (ii) packets arriving when the tagged vehicle's queue is not empty. Based on Welch's method [13] with two classes of arrivals in an M/G/1 queue, more accurate results can be obtained. Moreover, the proofs for the existence, uniqueness and convergence [14][15] of the fixed-point iteration [10] between the M/G/1 queue and the SMP model are provided. Third, based on the solution to the interacting SMP and M/G/1 queuing model, expressions for the key performance indices for the DSRC vehicular safety communication are derived. These metrics include the mean

transmission delay, packet delivery ratio (PDR) and packet reception ratio (PRR). The analytic numeric results are verified by simulations to show the errors caused by the decomposition approximations are small. The proposed model is compared with the analytic models published earlier in [7][39]. The numerical results show that the new model is more accurate.

3.2 System Assumptions

Several assumptions are made in the broadcast system to produce a simplified yet a high fidelity model.

a. The vehicular ad hoc network is considered to be one-dimensional (1-D). The number of vehicles in a line is Poisson distributed with parameter β (vehicle density), *i.e.*, the probability $P(i, l)$ of finding i vehicles in a length of l is given by:

$$P(i,l) = \frac{(\beta l)^i}{i!} e^{-\beta l} \tag{3.1}$$

The 2-D case is considered in Chapter 8 of this thesis.

b. All vehicles have the same transmission range, receiving range and carrier sensing range R.

c. Only one type of safety message in the control channel is considered.

d. Each vehicle is assumed to generate packets as a Poisson stream with rate λ (in packets per second).

e. Each vehicle has an infinite queue to store the packets at the MAC layer. Hence, each vehicle can be modeled as an M/G/1 queue.

f. Channel shadowing or fading, vehicle mobility and capture effect of transmissions are not considered in this chapter.

For assumption a, the 1-D VANET model is a good approximation of ad hoc networks on highways when the distances between lanes on the highway are negligible compared with the length of the highway. In addition, recent statistical analysis of empirical data collected from real world scenarios [34][35] show that exponential model is a good fit for sparse highway vehicle traffic in terms of inter-vehicle distance and inter-contact time distribution, which validates the reasonability of assumptions a and d. Heavy traffic scenarios where exponentially distributed inter-vehicle distance does not fit will be considered in our future work. For assumption b, we currently set three communication ranges the same values to simplify the analysis. Extension of the model to more general case with different communication ranges is straightforward with an approach similar to the one in [36]. Assumption c can be relaxed by extending our model to multiple types of services as described in the Section 3.6. The queuing model in assumption e is a reasonable approach as long as the channel service rate is substantially greater than message arrival rate. Therefore, an infinite queue is a reasonable assumption though it can be relaxed easily. . Assumption f is made because we only concentrate on the impact of packet collisions and the hidden terminal problem on the performance in this chapter. In fact, it has been proven in [40][41] that high mobility of vehicles (up to 120 *mph*) has a very minor impact on the performance of the direct

message broadcast network with high data rate (*e.g.*, ≥ 12 *Mbps*). Channel shadowing/fading will be considered in our future research.

3.3 Analytic Models

Due to the contention medium, the overall problem can be seen as a set of interacting M/G/1 queues. We simplify the problem in this chapter by developing an SMP model for the tagged vehicle that does not directly keep track of the queued requests but captures the channel contention and backoff behavior. This SMP model and the tagged vehicle's M/G/1 queue interact with each other and hence we set up the problems as a fixed-point iteration and solve using successive substitution.

3.3.1 SMP Model

The behavior of a tagged vehicle for packet transmission can be characterized using the SMP model in Fig. 3.2. The tagged vehicle is in *idle* state if there is no packet in its queue. After a packet is generated, the vehicle senses channel activity for *DIFS* time period. If the channel is detected not busy during this period (with probability $1-q_b$), the vehicle goes from *idle* state to *XMT* state, which means that a packet is transmitting. Otherwise, the vehicle will randomly choose a backoff counter in the range [0, W_0-1], where W_0 is the backoff window size. The backoff counter will be decreased by one if the channel is detected to be idle for a time slot of duration σ (with probability $1-p_b$), which is captured by the transition from state W_0-i to state W_0-i-1. If the channel is busy during a backoff time slot σ (*i.e.*, another vehicle is transmitting a packet), the backoff counter of

the tagged vehicle will be suspended and deferred for the duration of packet transmission time T, which is captured by the transition from state W_0-i to $D_{W0\text{-}i\text{-}1}$ with probability p_b. When the backoff counter reaches zero, the packet will directly be transmitted (an SMP transition occurs from state 0 to state *XMT* with probability one). In *XMT* state, a packet is transmitting. After the packet transmission, if there is no packet left in the queue of the tagged vehicle (with probability 1-ρ), the vehicle will go from *XMT* to *idle* state and wait for a new incoming packet. If there are packets left in the queue after a packet transmission (with probability ρ), the vehicle will sense the channel again for *DIFS* time and then randomly choose a backoff counter before transmitting the next packet.

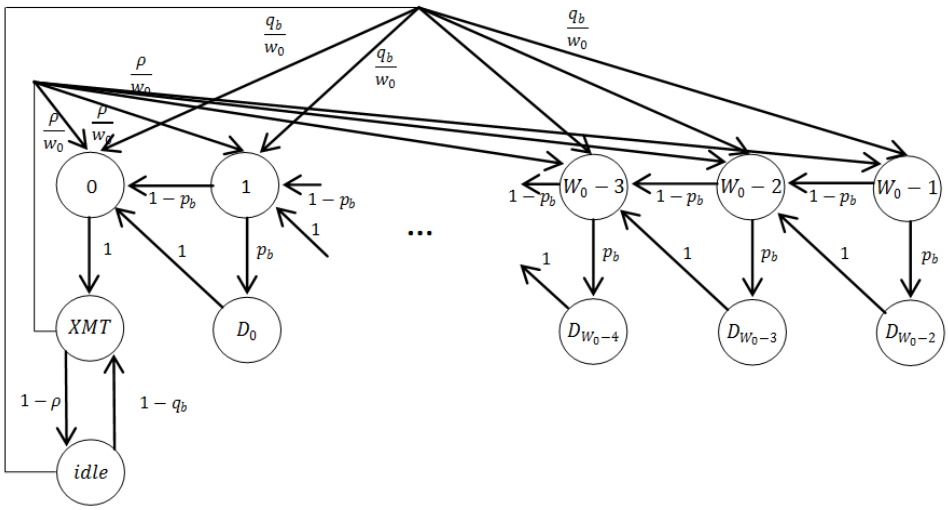

Figure 3.2: SMP model for 802.11p broadcast

Next, the analytic method is presented to solve this SMP model to obtain the steady-state probability that a vehicle transmits, which will be used in the fixed-point iteration in Section 3.3.3.

Define the sojourn time in state j as T_j. The mean and variance of T_j in the SMP model are:

$$E\left[T_j\right]=\tau_j=\begin{cases}\sigma & j=0,1,2,\cdots,W_0-1\\ T & j=D_0,D_1,\cdots,D_{W_0-2}\\ T & j=XMT\\ \dfrac{1}{\lambda}+DIFS & j=idle\end{cases} \tag{3.2}$$

$$Var\left[T_j\right]=\theta_j^2=\begin{cases}0 & j=0,1,2,\cdots,W_0-1\\ \dfrac{Var[PA]}{R_d{}^2} & j=D_0,D_1,\cdots,D_{W_0-2}\\ \dfrac{Var[PA]}{R_d{}^2} & j=XMT\\ 1/\lambda^2 & j=idle\end{cases} \tag{3.3}$$

where $T=E[PA]/R_d+T_H+DIFS+\delta$. The mean and variance of the packet length are $E[PA]$ and $Var[PA]$ respectively. R_d presents the data rate. Hence, $E[PA]/R_d$ is the time to transmit the packet. T_H is the time to transmit the packet header including physical layer header and MAC layer header while δ is the propagation delay.

For the model in Fig. 3.2, the embedded DTMC is first solved for its steady-state probabilities [9]:

$$\begin{cases} v_j = (W_0 - j)\cdot v_{W_0-1} & j = 0,1,\cdots W_0 - 1 \\ v_{D_j} = (W_0 - j - 1)\cdot p_b \cdot v_{W_0-1} & j = 0,1,\cdots W_0 - 2 \\ v_{XMT} = \dfrac{W_0}{\rho + q_b(1-\rho)}\cdot v_{W_0-1} & \\ v_{idle} = \dfrac{(1-\rho)W_0}{\rho + q_b(1-\rho)}\cdot v_{W_0-1} & \end{cases} \tag{3.4}$$

$$v_{W_0-1} = \frac{2\left[\rho + q_b(1-\rho)\right]}{\left[W_0 + 1 + p_b(W_0 - 1)\right]\left[\rho + q_b(1-\rho)\right]\cdot W_0 + 2(2-\rho)W_0} \tag{3.5}$$

Taking account of the mean sojourn time in each state, the steady-state probabilities of the SMP are given by [22]:

$$\pi_i = \frac{v_i \tau_i}{\sum_j v_j \tau_j} \tag{3.6}$$

Therefore, the steady-state probability that a vehicle is in the *XMT* state is given by:

$$\pi_{XMT} = \frac{2T}{\left[\rho + q_b(1-\rho)\right]\left[(\sigma + p_b \cdot T)W_0 + (\sigma - p_b \cdot T)\right] + 2T + 2(1-\rho)(1/\lambda + DIFS)} \tag{3.7}$$

Although the sojourn time in *XMT* state is *T*, the real packet transmission only occupies a portion of this sojourn time, which is ($E[PA]/R_d+T_H+\delta$)=(*T-DIFS*). Hence, the probability that a vehicle transmits in steady state is π_{XMT}(*T-DIFS*)/*T*.

In Eq. (3.7), three unknown parameters are:

- ρ: the probability that there are packets in the queue of the tagged vehicle.
- p_b: the probability that the channel is detected busy in one time slot by the tagged vehicle.
- q_b: the probability that the channel is detected busy in *DIFS* time by the tagged vehicle.

In Section 3.3.3, we will see that p_b and q_b are functions of ρ, whereas ρ depends on the mean service time to transmit a packet. Therefore, the service time is derived first in the next subsection. Section 3.3.3 subsequently illustrates the relationships between these parameters, a fixed-point equation is set up and successive substitution is utilized to compute the numerical results for these parameters as well as the service time.

3.3.2 Service Time Computation

As mentioned above, each vehicle in the network can be modeled as an M/G/1 queue. The MAC layer service time is defined as the time interval from the time instant when a packet becomes the head of the queue and starts to contend for transmission, to the time instant when the packet is received.

The SMP model in Section 3.3.1 describes the behavior of a tagged vehicle continuously transmitting packets in its queue. In this section, the service time for any one packet in the queue needs to be derived. Therefore, the SMP model in Section 3.3.1 can be modified to contain an absorbing state as shown in Fig. 3.3. By properly assigning the initial probability vector, the time to reach the absorbing state will be the service time for a packet transmission.

The mean and variance of the service time conditioned on starting from state i (S_i) will be derived first based on the mean and variance of the sojourn time (T_j) and visit counts (X_{ij}) in each state.

Since the embedded DTMC contains an absorbing state, the transition probability matrix can be partitioned so that [9]:

$$P = \begin{bmatrix} Q & C \\ 0 & 1 \end{bmatrix} \tag{3.8}$$

where Q is a $2W_0$ by $2W_0$ sub-stochastic matrix describing the probabilities of transitions only among the transient states. The fundamental matrix of the embedded DTMC is:

$$M = (I - Q)^{-1} \tag{3.9}$$

Let X_{ij} be the random variable denoting the visit counts to state j before entering the absorbing state, given that embedded DTMC started in state i. The expected number of visits to state j starting from state i before absorption is given by the (i, j)th element of the fundamental matrix M. Hence,

$$E\left[X_{ij}\right] = m_{ij} \tag{3.10}$$

Due to the acyclic nature of the DTMC model in Fig. 3.3, the fundamental matrix can be easily obtained through the definition of X_{ij} instead of computing Eq. (3.9).

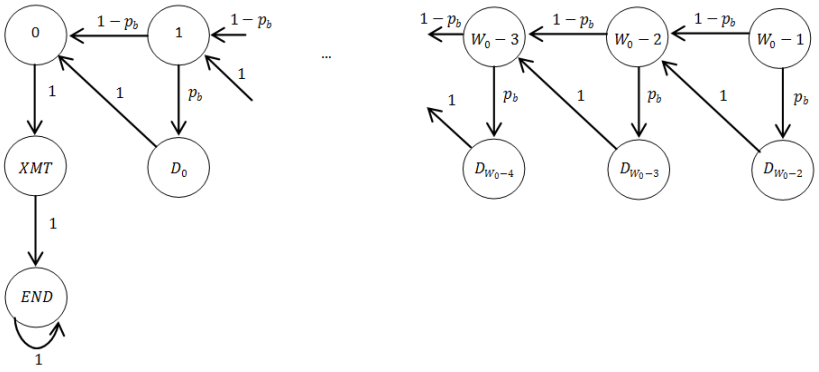

Figure 3.3: SMP model for service time computation

$$
M = \begin{array}{c} \\ 0 \\ 1 \\ 2 \\ \vdots \\ W_0-2 \\ W_0-1 \\ D_0 \\ D_1 \\ D_2 \\ \vdots \\ D_{W_0-2} \\ XMT \end{array}
\begin{array}{c}
\begin{array}{cccccccccccc} 0 & 1 & 2 & \cdots & W_0-2 & W_0-1 & D_0 & D_1 & D_2 & \cdots & D_{W_0-2} & XMT \end{array} \\
\begin{bmatrix}
1 & 0 & 0 & \cdots & 0 & 0 & 0 & 0 & 0 & \cdots & 0 & 1 \\
1 & 1 & 0 & \cdots & 0 & 0 & p_b & 0 & 0 & \cdots & 0 & 1 \\
1 & 1 & 1 & \cdots & 0 & 0 & p_b & p_b & 0 & \cdots & 0 & 1 \\
\vdots & \vdots & \vdots & \vdots & \vdots & \vdots & \vdots & \vdots & \vdots & \vdots & \vdots & \vdots \\
1 & 1 & 1 & \cdots & 1 & 0 & p_b & p_b & p_b & \cdots & 0 & 1 \\
1 & 1 & 1 & \cdots & 1 & 1 & p_b & p_b & p_b & \cdots & p_b & 1 \\
1 & 0 & 0 & \cdots & 0 & 0 & 1 & 0 & 0 & \cdots & 0 & 1 \\
1 & 1 & 0 & \cdots & 0 & 0 & p_b & 1 & 0 & \cdots & 0 & 1 \\
1 & 1 & 1 & \cdots & 0 & 0 & p_b & p_b & 1 & \cdots & 0 & 1 \\
\vdots & \vdots & \vdots & \vdots & \vdots & \vdots & \vdots & \vdots & \vdots & \vdots & \vdots & \vdots \\
1 & 1 & 1 & \cdots & 1 & 0 & p_b & p_b & p_b & \cdots & 1 & 1 \\
0 & 0 & 0 & \cdots & 0 & 0 & 0 & 0 & 0 & \cdots & 0 & 1
\end{bmatrix}
\end{array}
\tag{3.11}
$$

Furthermore, the variance of the number of visits can also be derived using the fundamental matrix. Define $MD=[md_{ij}]$ by:

$$
md_{ij} = \begin{cases} m_{ij} & if \quad i = j \\ 0 & otherwise \end{cases} \tag{3.12}
$$

Define $M_2=[m_{ij}^2]$. Hence, the variance of the visit counts is [17][114]:

$$
\sigma^2 = M\left(2M_D - I\right) - M_2 \tag{3.13}
$$

The service time for a packet transmission starting from state i is given by:

$$
S_i = \sum_j T_j \cdot X_{ij} \tag{3.14}
$$

$$
\begin{aligned}
E\left[S_i\right] &= E\left[\sum_j T_j \cdot X_{ij}\right] = \sum_j E\left[T_j \cdot X_{ij}\right] = \sum_j E\left[T_j\right] \cdot E\left[X_{ij}\right] = \sum_j \tau_j \cdot m_{ij} \\
&= \begin{cases} (i+1)\sigma + i \cdot p_b \cdot T + T & for \quad i = 0,1,\cdots,W_0-1 \\ T & for \quad i = XMT \end{cases} \\
j &\in \left\{0,1\cdots,W_0-1,D_0,D_1,\cdots,D_{W_0-2},XMT\right\}
\end{aligned} \tag{3.15}
$$

Since the sojourn time in state 0 is zero in the protocol instead of σ as specified in the model, we adjust the mean of S_i starting from i=0,1,…, W_0-1 by decreasing by σ in the results. Hence:

$$E[S_i] = \begin{cases} i \cdot \sigma + i \cdot p_b \cdot T + T & for \quad i = 0,1,\cdots,W_0 - 1 \\ T & for \quad i = XMT \end{cases} \tag{3.16}$$

The variance of S_i is given by Eq. (3.17).

$$\begin{aligned} & Var[S_i] = Var\left[\sum_j T_j \cdot X_{ij}\right] = \sum_j Var\left[T_j \cdot X_{ij}\right] \\ & = \sum_j \left\{ Var\left[T_j\right] \cdot E\left[X_{ij}\right] + \left(E\left[T_j\right]\right)^2 \cdot Var\left[X_{ij}\right] \right\} \\ & = \sum_j \left(\theta_j^2 \cdot m_{ij} + \tau_j^2 \cdot \sigma_{ij}^2\right) \\ & = \begin{cases} i\left\{\frac{Var[PA]}{R_d{}^2} \cdot p_b + T^2 \cdot p_b \cdot (1 - p_b)\right\} + \frac{Var[PA]}{R_d{}^2} & for \quad i = 0,1,\cdots,W_0 - 1 \\ \frac{Var[PA]}{R_d{}^2} & for \quad i = XMT \end{cases} \\ & j \in \left\{0,1\cdots,W_0 - 1, D_0, D_1, \cdots, D_{W_0-2}, XMT\right\} \end{aligned} \tag{3.17}$$

Based on the mean and variance of the conditional service time starting from state i (S_i) obtained above, we will compute the mean of un-conditional service time next to be used in Welch's method. To compute the mean service time, we separate the service time distribution into two classes, (i) for the packet arrivals when the tagged vehicle's queue is empty; (ii) for the packet arrivals when the tagged vehicle's queue is not empty. For the packet that arrives when the tagged vehicle's queue is empty, the service time is given by:

$$S_e = \begin{cases} S_0 & w.p. & q_{e,0} = q_b / W_0 \\ S_1 & w.p. & q_{e,1} = q_b / W_0 \\ \quad \vdots & & \\ S_{W_0-1} & w.p. & q_{e,W_0-1} = q_b / W_0 \\ S_{XMT} & w.p. & q_{e,XMT} = 1 - q_b \end{cases} \tag{3.18}$$

The mean and variance of the service time for the packet arrivals when the tagged vehicle's queue is empty are:

$$\beta_e = E[S_e] = \sum_i E[S_i] \cdot q_{e,i} = \frac{(W_0 - 1)(\sigma + p_b \cdot T) \cdot q_b}{2} + T \tag{3.19}$$

$$\begin{aligned} \sigma_e^2 &= Var[S_e] = E\left[S_e^2\right] - \left(E[S_e]\right)^2 = \sum_i E\left[S_i^2\right] \cdot q_{e,i} - \left(E[S_e]\right)^2 \\ &= \sum_i \left\{ Var[S_i] + \left(E[S_i]\right)^2 \right\} \cdot q_{e,i} - \left(E[S_e]\right)^2 \\ &= \frac{(W_0 - 1)(2W_0 - 1)}{6} (\sigma + p_b \cdot T)^2 \cdot q_b \\ &\quad + \frac{W_0 - 1}{2} \cdot \left\{ \frac{Var[PA]}{R_d^{\,2}} \cdot p_b + T^2 p_b (1 - p_b) + 2T(\sigma + p_b \cdot T) \right\} \cdot q_b \\ &\quad + \frac{Var[PA]}{R_d^{\,2}} + T^2 - \left(E[S_e]\right)^2 \\ i &\in \{0, 1, \cdots, W_0 - 1, XMT\} \end{aligned} \tag{3.20}$$

Similarly, for the packet that arrives when the tagged vehicle's queue is not empty, the service time is given by:

$$S_b = \begin{cases} S_0 & w.p. & q_{b,0} = 1/W_0 \\ S_1 & w.p. & q_{b,1} = 1/W_0 \\ \quad \vdots & & \\ S_{W_0-1} & w.p. & q_{b,W_0-1} = 1/W_0 \end{cases} \tag{3.21}$$

The mean and variance of the service time for such packets are:

$$\beta_b = E[S_b] = \sum_i E[S_i] \cdot q_{b,i} = \frac{(W_0 - 1)(\sigma + p_b \cdot T)}{2} + T \tag{3.22}$$

$$
\begin{aligned}
\sigma_b^2 &= Var[S_b] = E\left[S_b^2\right] - \left(E[S_b]\right)^2 = \sum_i E\left[S_i^2\right] \cdot q_{b,i} - \left(E[S_b]\right)^2 \\
&= \sum_i \left\{ Var[S_i] + \left(E[S_i]\right)^2 \right\} \cdot q_{b,i} - \left(E[S_b]\right)^2 \\
&= \frac{(W_0 - 1)(2W_0 - 1)}{6} \left(\sigma + p_b \cdot T\right)^2 \\
&\quad + \frac{W_0 - 1}{2} \cdot \left\{ \frac{Var[PA]}{R_d{}^2} \cdot p_b + T^2 p_b (1 - p_b) + 2T\left(\sigma + p_b \cdot T\right) \right\} \\
&\quad + \frac{Var[PA]}{R_d{}^2} + T^2 - \left(E[S_b]\right)^2 \\
i &\in \{0, 1, \cdots, W_0 - 1\}
\end{aligned}
\tag{3.23}
$$

By utilizing Welch's methods [13], the mean service time for a packet un-conditioning on the state of the tagged vehicle's queue is:

$$
E[S] = \frac{\beta_e}{1 - \lambda(\beta_b - \beta_e)} \tag{3.24}
$$

3.3.3 Fixed-point Equation

In the previous section, the mean service time is shown to depend on two unknown parameters p_b and q_b, whereas channel busy probabilities p_b and q_b depend on the channel utilization ρ of the M/G/1 queue in every vehicle. Therefore, relationships between ρ, p_b and q_b are determined first in this section, and then the fixed-point equation is established which is solved by successive substitution obtain the final solution.

Let N_{cs} denote the average number of vehicles in carrier sensing range of the tagged vehicle, and let N_{tr} denote the average number of vehicles in transmission range of the tagged vehicle. Hence, without loss of generality, we have:

$$N_{cs} = N_{tr} = 2\beta R \tag{3.25}$$

The average number of vehicles in potential hidden area is:

$$N_{ph} = 4\beta R - N_{cs} = 2\beta R \tag{3.26}$$

From the tagged vehicle's point of view, p_b is the probability that it senses channel busy during one time slot in the backoff process. Since the channel is detected busy if there is at least one neighbor (*i.e.*, a vehicle in the transmission range of the tagged vehicle) transmitting in a backoff time slot of the tagged vehicle, we have:

$$p_b = 1 - \sum_{i=0}^{\infty} (1 - P_{XMT})^i \frac{(N_{tr})^i}{i!} e^{-N_{tr}} = 1 - e^{-N_{tr} \cdot P_{XMT}} \tag{3.27}$$

where P_{XMT} is the probability that a neighbor is transmitting in a backoff time slot of the tagged vehicle, to be derived next.

Eq. (3.7) shows that the probability that a vehicle transmits a packet in steady state is $\pi_{XMT}(T\text{-}DIFS)/T$. In addition, the time to transmit a packet is $T\text{-}DIFS$. Therefore, we can abstractly define the total time to be T_{total} as shown in Fig. 3.4. Hence, $\pi_{XMT}(T\text{-}DIFS)/T = (T\text{-}DIFS)/T_{total}$.

Suppose a neighbor of the tagged vehicle transmits a packet as shown in Fig. 3.4 in time duration T_{total}, a backoff time slot of the tagged vehicle can occupy any one time slot within T_{total}.

For the first backoff time slot of the tagged vehicle, the time duration that can capture the transmission of the neighbor is $T\text{-}DIFS+2\sigma$. One extra time slot σ is the one just before transmission and another is the one just after transmission, which can capture

the starting time instant and ending time instant of the packet transmission. Therefore, the probability that a neighbor's transmission is detected in the first backoff time slot of the tagged vehicle is $\pi_{XMT}(T\text{-}DIFS+2\sigma)/T$.

For a backoff time slot that is not the first backoff time slot of the tagged vehicle, the time duration that captures the transmission of the neighbor is 2σ, which captures the starting time instant of the transmission. This is because when the neighbor's transmission is detected in the first backoff time slot by the tagged vehicle, the backoff

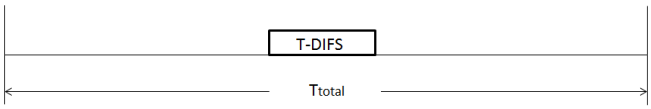

Figure 3.4: Abstraction of the packet transmission time

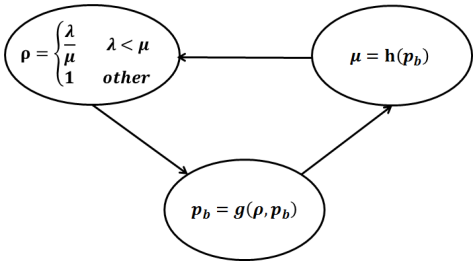

Figure 3.5: Import graph for fixed point iteration

counter will suspend and wait until the end of this transmission for further decrement. Therefore, if the first backoff time slot detects the transmission, there is no chance for the later backoff time slots to detect the same transmission. As a result, the non-first backoff time slot can only detect the transmission when the starting point of the transmission falls within this time slot. Therefore, the probability that a neighbor's transmission is detected in non-first backoff time slot of the tagged vehicle is $\pi_{XMT}\cdot 2\sigma/T$.

Since the probability that a backoff time slot is the first backoff time slot is $1/W_0$ and non-first backoff time slot is $(1-1/W_0)$, the probability that a neighbor's transmission is detected by a backoff time slot of the tagged vehicle is:

$$P_{XMT} = \frac{1}{W_0} \cdot \frac{T - DIFS + 2\sigma}{T} \pi_{XMT} + \left(1 - \frac{1}{W_0}\right) \cdot \frac{2\sigma}{T} \pi_{XMT} \tag{3.28}$$

Next, q_b denotes the probability that the channel is detected busy by the tagged vehicle in the *DIFS* duration. Therefore, we can similarly define Q_{XMT} to be the probability that a neighbor's transmission is detected in the *DIFS* duration by the tagged vehicle.

$$Q_{XMT} = \frac{T - DIFS + 2DIFS}{T} \pi_{XMT} = \frac{T + DIFS}{T} \pi_{XMT} \tag{3.29}$$

Hence, q_b is given by:

$$q_b = 1 - \sum_{i=0}^{\infty} (1 - Q_{XMT})^i \frac{(N_{tr})^i}{i!} e^{-N_{tr}} = 1 - e^{-N_{tr} \cdot Q_{XMT}} \tag{3.30}$$

Based on Eqs. (3.27)-(3.30), q_b is expressed in terms of p_b to simplify the iteration algorithm:

$$q_b = 1 - (1 - p_b)^{\frac{(T + DIFS)W_0}{T - DIFS + 2\sigma W_0}} \tag{3.31}$$

From the above analysis of the relationship between two parameters ρ and p_b (q_b can be expressed in terms of p_b), we notice that p_b depends on ρ and p_b itself. Hence, we denote $p_b = g(\rho, p_b)$ and the reciprocal of mean service time for M/G/1 queue to be $\mu = h(p_b)$. We thus have a fixed point problem consisting of equation $\rho = \min(\lambda/\mu, 1)$, $p_b = g(\rho, p_b)$ and

$\mu=h(p_b)$. The import graph [16] of this system of equations is shown in Fig. 3.5. We use successive substitution to obtain a solution to the fixed-point.

Fixed-point iteration algorithm:

Step 1: Initialize ρ=1, which is the saturation condition;

Step 2: With ρ, solve p_b according to Eqs. (3.27)(3.28)(3.7)(3.31);

Step 3: With p_b, calculate service rate $\mu=1/E[S]$ according to Eq. (3.24);

Step 4: If $\lambda<\mu$, $\rho=\lambda/\mu$; otherwise, set ρ=1;

Step 5: If ρ converges, then stop the iteration algorithm; otherwise, go to step 2 with the updated ρ.

By utilizing the fixed-point iteration algorithm, the parameters ρ, p_b, q_b, π_{XMT} as well as the mean and the variance of the service time can be determined, which are used for the performance indices computation in the next section. The proofs for the existence, uniqueness and convergence of the fixed-point iteration are given in the next subsection.

3.3.4 Existence, Uniqueness and Convergence of Fixed-point Iteration

In this section, we provide the proofs for the existence, uniqueness and convergence [14][15] of the fixed point mentioned in Section 3.3.3. Since ρ depends on the service time; the service time depends on p_b; p_b depends on ρ; hence, we have the fixed point equation:

$$\rho = f(\rho) \tag{3.32}$$

$$f(\rho) = \min\left(1, \frac{\lambda}{\mu(\rho)}\right) \tag{3.33}$$

3.3.4.1 Existence

In In this section, *Brouwer*'s fixed-point theorem will be used to prove that $\rho=f(\rho)$ has a solution [14][18]. *Brouwer*'s fixed-point theorem states that if there exists a compact, convex set C and there exists a continuous function f, such that if $y \in C$, then $f(y) \in C$, then there exists a solution to the equation $f(y)=y$.

Since ρ is the probability that there are packets ready to transmit, $\rho \in [0,1]$. Therefore, we define $C=[0,1]$.

According to *Heine-Borel* theorem [19], for a subset S of Euclidean space R^n, if S is closed and bounded, S is a compact set. Therefore, $C=[0,1]$ is a compact set. C is a convex set [19] if $\lambda x+(1-\lambda)y \in C$ whenever $x \in C$, $y \in C$ and $\lambda \in [0,1]$. Consider: $z=\lambda x+(1-\lambda)y$. $z \geq 0$ because $\lambda \geq 0$, $x \geq 0$, $(1-\lambda) \geq 0$, and $y \geq 0$. Since z is maximized when $x=y=1$ (since $\lambda \geq 0$ and $(1-\lambda) \geq 0$) to its maximum value 1, $z \leq 1$. Hence, C is a convex set.

Consider the function f over C. By definition, $f(\rho)=\min(1,\lambda/\mu(\rho))$, λ is positive. If $\rho \in [0,1]$, then $p_b \in [0,1]$, $\mu>0$ (according to the equations for $p_b(\rho)$ and $\mu(\rho)$); hence, $f(\rho)=\min(1,\lambda/\mu(\rho) \in [0,1]$. f is a continuous function if for each point $\hat{\rho} \in C$,

$$\lim_{\rho \to \hat{\rho}} f(\rho) = f(\hat{\rho})$$

By definition,

$$\lim_{\rho \to \hat{\rho}} f(\rho) = \lim_{\rho \to \hat{\rho}} \left\{ \min\left(1, \frac{\lambda}{\mu(\rho)}\right) \right\}$$

Since $\mu(\rho)$ is a continuous function of p_b and $p_b(\rho)$ is a continuous function regarding to ρ, hence $f(\rho)$ is a continuous function regarding to ρ. In conclusion, there exists a solution in C=[0,1] for $\rho=f(\rho)$.

3.3.4.2 Uniqueness

We can prove that $f(\rho)$ is a monotonic increasing function of ρ on [0,1] and hence there will be a unique solution [15][20].

Based on Eqs. (3.27)(3.28)(3.7)(3.31), p_b can be rewritten as:

$$p_b = 1 - e^{\frac{-2N_{tr}(T-DIFS+2\sigma W_0)/W_0}{\left\{\rho+\left[1-(1-p_b)^{\frac{(T+DIFS)W_0}{T-DIFS+2\sigma W_0}}\right](1-\rho)\right\}\left[(\sigma+p_b\cdot T)W_0+(\sigma-p_b\cdot T)\right]+2T+2(1-\rho)\left(\frac{1}{\lambda}+DIFS\right)}} \tag{3.34}$$

In Eq. (3.34),

$$\rho+\left[1-(1-p_b)^{\frac{(T+DIFS)W_0}{T-DIFS+2\sigma W_0}}\right](1-\rho)\le 1$$

In addition, since $p_b \le 1$,

$$\left\{\rho+\left[1-(1-p_b)^{\frac{(T+DIFS)W_0}{T-DIFS+2\sigma W_0}}\right](1-\rho)\right\}\left[(\sigma+p_b\cdot T)W_0+(\sigma-p_b\cdot T)\right]\le(\sigma+T)(W_0-1)+2\sigma$$

Since the safety message for each vehicle is generated occasionally, ρ is relatively small. Furthermore, we make a reasonable assumption that $1/\lambda+DIFS>>(\sigma+T)(W_0-1)$, *i.e.*, the mean packet arrival time $1/\lambda$ plus the *DIFS* channel sensing time is much larger than the maximum time duration of the backoff procedure $(\sigma+T)(W_0-1)$. Therefore, p_b can be simplified as:

$$p_b \approx 1 - \mathrm{e}^{\frac{-N_{tr}(T-DIFS+2\sigma W_0)/W_0}{\sigma+T+(1-\rho)\left(\frac{1}{\lambda}+DIFS\right)}} \tag{3.35}$$

According to Eq. (3.35), if ρ increases, p_b will increase given the condition that $1/\lambda+DIFS>>(\sigma+T)(W_0-1)$. Hence, μ will decrease, and then, $f(\rho)=\min(1,\lambda/\mu(\rho))$ will accordingly increase. Hence, $f(\rho)$ is a monotone increasing function of ρ on [0,1].

Moreover, $f(\rho)=\min(1,\lambda/\mu(\rho))>0$, $f(1)$ is also a value between 0 and 1. Therefore, the solution of $\rho=f(\rho)$ on [0,1] is unique.

3.3.4.3 Convergence

According to the fixed-point theorem: Let (X, d) be a complete metric space and f: $X->X$ be a map such that

$$d\left(f\left(x\right), f\left(x'\right)\right) \le kd\left(x, x'\right) \tag{3.36}$$

for some $0\le k<1$ and all x and x' in X. Then f has a unique fixed point in X. Moreover, for any x_0 in X, the sequence of iterates x_0, $f(x_0)$, $f(f(x_0))$,… converges to the fixed point of f.

Therefore, we need to find a value of k ($0\le k<1$) to satisfy Eq. (3.36) to prove that the fixed point converges.

According to *Lagrange* mean value theorem, if a function $f(x)$ is continuous on the closed interval $[a, b]$ and differentiable within this range, then there exists x_0, $a<x_0<b$, such that $f(b)-f(a)=f'(x_0)(b-a)$. Therefore, if we can find the upper bound of $f'(x_0)$, and prove $0\le f'(x_0)<1$, we can prove the convergence of the fixed point.

Since $f(\rho)=\min(1,\lambda/\mu(\rho))$ in our model, to make $f(\rho)$ differentiable in range [0,1], we need to make sure $\lambda<\mu(\rho)$ for $\rho\in[0,1]$, hence:

$$\begin{aligned} f(\rho) &= \frac{\lambda}{\mu(\rho)} = \frac{\lambda\beta_e}{1-\lambda(\beta_b-\beta_e)} \\ &= \frac{\lambda\left[(W_0-1)(\sigma+p_b\cdot T)\cdot q_b+2T\right]}{2-\lambda(W_0-1)(\sigma+p_b\cdot T)\cdot(1-q_b)} \\ &= \frac{\lambda\left\{(W_0-1)(\sigma+p_b\cdot T)\cdot\left[1-(1-p_b)^{\frac{(T+DIFS)W_0}{T-DIFS+2\sigma W_0}}\right]+2T\right\}}{2-\lambda(W_0-1)(\sigma+p_b\cdot T)\cdot(1-p_b)^{\frac{(T+DIFS)W_0}{T-DIFS+2\sigma W_0}}} \\ &= \frac{A}{B} \end{aligned} \tag{3.37}$$

where

$$A=\lambda\left\{(W_0-1)(\sigma+p_b\cdot T)\cdot\left[1-(1-p_b)^{\frac{(T+DIFS)W_0}{T-DIFS+2\sigma W_0}}\right]+2T\right\}$$

$$B=2-\lambda(W_0-1)(\sigma+p_b\cdot T)\cdot(1-p_b)^{\frac{(T+DIFS)W_0}{T-DIFS+2\sigma W_0}}$$

Thus,

$$\frac{df(\rho)}{d\rho}=\frac{df(\rho)}{dp_b}\cdot\frac{dp_b}{d\rho}=\frac{\frac{dA}{dp_b}\cdot B-\frac{dB}{dp_b}\cdot A}{B^2}\cdot\frac{dp_b}{d\rho}$$

$$\frac{dA}{dp_b}=\lambda(W_0-1)\left\{T\left[1-(1-p_b)^{\frac{(T+DIFS)W_0}{T-DIFS+2\sigma W_0}}\right]+(\sigma+p_b\cdot T)\frac{(T+DIFS)W_0}{T-DIFS+2\sigma W_0}(1-p_b)^{\frac{(T+DIFS)W_0}{T-DIFS+2\sigma W_0}-1}\right\} \tag{3.38}$$

$$\frac{dB}{dp_b}=-\lambda(W_0-1)\left\{T(1-p_b)^{\frac{(T+DIFS)W_0}{T-DIFS+2\sigma W_0}}-(\sigma+p_b\cdot T)\frac{(T+DIFS)W_0}{T-DIFS+2\sigma W_0}(1-p_b)^{\frac{(T+DIFS)W_0}{T-DIFS+2\sigma W_0}-1}\right\}$$

Since $p_b\in[0,1]$, $(dA/dp_b\cdot B-dB/dp_b\cdot A)/B^2$ is bounded according to Eq. (3.38). Denote the upper bound as U_1.

According to the theorem on differentiability, since $dp_b/d\rho$ is differentiable, then $dp_b/d\rho$ is continuous [19]. Furthermore, according to the boundedness theorem [21], since $dp_b/d\rho$ is continuous on the compact space [0,1], there exists a real number U_2 such that $dp_b/d\rho <= U_2$.

Therefore,

$$\frac{df(\rho)}{d\rho} = \frac{\frac{dA}{dp_b}\cdot B - \frac{dB}{dp_b}\cdot A}{B^2}\cdot\frac{dp_b}{d\rho} \le U_1 \cdot U_2 = k \tag{3.39}$$

Hence, if we choose reasonable parameters for λ, W_0, T, $DIFS$, σ to satisfy $0 \le k < 1$, then k will be the *Lipschitz* constant of f and successive iterates x_0, $f(x_0)$, $f(f(x_0))$,… will converge to the fixed point of f.

3.4 Performance Indices

3.4.1 Mean Transmission Delay

According to the Welch's method [13], the steady-state expected number of packets in the tagged vehicle's queue (including the packet in the head of the queue that is under service) is:

$$E[Q] = \frac{\lambda\beta_e}{1-\lambda(\beta_b-\beta_e)} + \frac{\lambda^2}{2}\cdot\frac{\left(\sigma_e^2+\beta_e^2-\sigma_b^2-\beta_b^2\right)}{1-\lambda(\beta_b-\beta_e)} + \frac{\lambda^2}{2}\cdot\frac{\sigma_b^2+\beta_b^2}{1-\lambda\beta_b} \tag{3.40}$$

Using Little's law, the mean delay for a packet transmission is:

$$E[D] = \frac{E[Q]}{\lambda} \tag{3.41}$$

3.4.2 Packet Delivery Ratio

The PDR is defined as [5][7]: given a broadcast packet sent by the tagged vehicle, the probability that all vehicles in its transmission range receive the packet successfully. Taking account of hidden terminals, we have:

$$PDR = P(N_{cs})\,P(N_{ph}) \tag{3.42}$$

where $P(N_{cs})$ is the probability that no vehicles in the transmission range of the tagged vehicle transmits when the tagged vehicle starts transmission, and $P(N_{ph})$ is the probability that no transmissions from the vehicles in the potential hidden terminal area collide with the broadcast packet from the tagged vehicle.

$P(N_{cs})$ can also be interpreted as the non-concurrent transmission probability, *i.e.*, two packets do not start transmission at the same time. Since DCF employs a discrete-time backoff scheme, if the backoff process is involved, a vehicle is only allowed to transmit at the beginning of each slot time after an idle *DIFS* time duration. Therefore, if the tagged vehicle has not gone through the backoff process before transmitting the packet (with probability $(1-\rho)(1-q_b)$), the concurrent transmission will not occur. Otherwise, the packet transmission is synchronized to the beginning of a slot time, and concurrent transmission may occur if other vehicles' transmission is also synchronized by the backoff process. From the model, we know that the probability that a neighbor starts to transmit a packet at the beginning of the same time slot with the tagged vehicle is $\pi_0 = \pi_{XMT} \bullet \sigma/T$. This is because the sojourn time in state 0 is one time slot σ as shown in

the SMP model, hence, π_0 is the probability that a vehicle starts to transmit in the beginning of a time slot immediately after the backoff process. Hence, $P(N_{cs})$ is:

$$\begin{aligned} P(N_{cs}) &= \left[1-(1-\rho)(1-q_b)\right]\cdot\left[\sum_{i=0}^{\infty}(1-\pi_0)^i\frac{(N_{cs}-1)^i}{i!}e^{-(N_{cs}-1)}\right]+(1-\rho)(1-q_b) \\ &= \left[1-(1-\rho)(1-q_b)\right]\cdot e^{-(N_{cs}-1)\pi_0}+(1-\rho)(1-q_b) \end{aligned} \tag{3.43}$$

Since the transmission time for a packet is $T\text{-}DIFS=E[PA]/R_d+T_H+\delta$, the event that a transmission from hidden terminals collides with the tagged vehicle's transmission only happens when hidden terminals start to transmit during the vulnerable period $2(T\text{-}DIFS)=2(E[PA]/R_d+T_H+\delta)$ [7]. Using $\pi_{XMT}=T/T_{total}$ as an abstraction of the steady state behavior shown in Fig. 3.4, the probability that a vehicle starts to transmit during the vulnerable period of hidden terminal transmissions [7] is:

$$\frac{2(T-DIFS)}{Ttotal}=\pi_{XMT}\frac{2(T-DIFS)}{T} \tag{3.44}$$

Therefore,

$$P(N_{ph})=\sum_{i=0}^{\infty}\left(1-\pi_{XMT}\cdot\frac{2(T-DIFS)}{T}\right)^i\frac{(N_{ph})^i}{i!}e^{-N_{ph}}=e^{\frac{-2(T-DIFS)\cdot N_{ph}\cdot\pi_{XMT}}{T}} \tag{3.45}$$

Hence, based on Eqs. (3.42)(3.43)(3.45), the PDR can be computed. From the analytic-numerical results demonstrated in Section 3.5, we can see that the hidden terminals problem has more impact than concurrent transmissions on the PDR.

3.4.3 Packet Reception Ratio

Packet reception ratio (PRR) is defined as the percentage of nodes that successfully receive a packet from the tagged node among the receivers being investigated at the moment that the packet is sent out [7].

Similar to the computation for PDR, we consider both the concurrent transmission and hidden terminal effects while computing PRR. Therefore,

$$PRR = PRR_{cc} PRR_{ht} \tag{3.46}$$

The impact of the concurrent transmission and hidden terminals will be evaluated in the following two sections.

a. Impact of concurrent transmission

Transmissions from nodes within a distance R away from the tagged node in the meantime at which the tagged node transmits may cause collisions. When the tagged node starts transmission in the beginning of a slot time, collisions will take place if any node in the transmission range of the tagged node starts transmission in the beginning of the same time slot. As shown in Fig. 3.6, any node transmitting on the right hand side of the tagged node (*i.e.*, node in $L_1=\{x \mid x \in [0, R]\}$) will result in failure of all nodes in L_1 receiving the broadcast packet. Hence, ratio of successfully receiving nodes in the range L_1 can be expressed as:

$$PRR_{cc}^{1} = \sum_{i=0}^{\infty} (1-\pi_0)^i \frac{(\beta R)^i}{i!} e^{-\beta R} = e^{-\beta R \pi_0} \tag{3.47}$$

On the other hand, transmissions from any node on the left hand side of the tagged node (*i.e.*, node in $L_2=\{x \mid x \in [-R, 0]\}$) will only result in failure of some of the nodes receiving the broadcast packet in L_1. Similar to analysis of the hidden terminal impact, the ratio of successful receiving nodes due to any transmission in L_2 depends on the position of the closest node transmitting in L_2 to the tagged node. Denote Y as a random variable that represents the distance from the closest node transmitting in L_2 (*B* in Fig. 3.6) to the outer boundary of range L_2. Let R_t be the range where no station transmits, so that

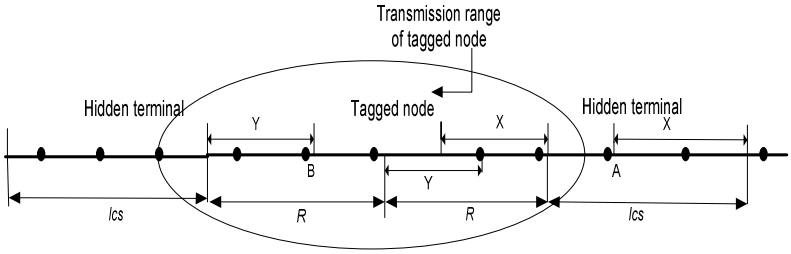

Figure 3.6: PRR computation

$$P(Y \le y) = \sum_{k=0}^{\infty} \left[P(\text{none of } k \text{ nodes in } R_t \text{ transmits in a slot}) \right] \tag{3.48}$$

$R_t=\{x \mid x \in [-R+y,0]]$. Then the CDF for Y is: Eq. (3.48) is the probability that the closest interfering node in L_2 is at least $(R-y)$ away from the transmitter; *i.e.*, the probability that no nodes within R_t transmit in the meantime the tagged node starts to transmit. Hence, we have:

$$P(Y \le y) = \sum_{k=0}^{\infty} (1-\pi_0)^k \frac{(\beta(R-y))^k}{k!} e^{-\beta(R-y)} = e^{-\beta(R-y)\pi_0} \tag{3.49}$$

Thus, the expected number of failed nodes in L_1 due to concurrent transmission of nodes in L_2 can be expressed as:

$$NF_h = \int_0^R \beta y P(y \le Y \le y + dy) = \int_0^R \beta^2 y \pi_0 e^{-\beta(R-y)\pi_0} dy = \beta R - \frac{1}{\pi_0}\left(1 - e^{-\beta\pi_0 R}\right) \tag{3.50}$$

Therefore, the percentage of receivers in L_1 that are free from collisions caused by the concurrent transmissions of nodes in the range L_2 is:

$$PRR_{cc}^2 = \frac{\beta R - NF_h}{\beta R} = \frac{1}{\beta R \pi_0}(1 - e^{-\beta R \pi_0}) \tag{3.51}$$

Define PRR_{cc} as the percentage of receivers in L_1 that are free from collisions caused by the concurrent transmissions of nodes in the range $\{x \mid x \in [-R, R]\}$. If the tagged vehicle transmits the packet without going through the backoff process, with probability $(1-\rho)(1-q_b)$, concurrent transmission will not occur. Otherwise, concurrent transmissions may occur. Therefore,

$$\begin{aligned} PRR_{cc} &= PRR_{cc}^1 \cdot PRR_{cc}^2 \cdot \left[1 - (1-\rho)(1-q_b)\right] + (1-\rho)(1-q_b) \\ &= \frac{e^{-\beta R \pi_0}}{\beta R \pi_0}(1 - e^{-\beta R \pi_0})\left[1 - (1-\rho)(1-q_b)\right] + (1-\rho)(1-q_b) \end{aligned} \tag{3.52}$$

b. Impact of hidden terminals

We observe that the ratio of receivers affected by the hidden terminals only depends on the position of the hidden node (referred as hidden crucial node) that has the closest distance to boundary of the transmitter's sensing range among all the transmitting nodes in the potential hidden terminal area. Denote X as a random variable that represents the distance from the hidden crucial node (A in Fig. 3.6) to the outer

boundary of $\{x \mid x \in [0, 2R]\}$. Let R_s be the range in the potential hidden terminal area, where no node transmits, such that $R_s=\{x \mid x \in [l_{cs}, 2R-x]\}$, where $l_{cs}=N_{cs}/(2\beta)$ is carrier sensing range of a node in the network.

Then the cumulative distribution function (CDF) for X is:

$$\begin{aligned} P(X \le x) &= \sum_{k=0}^{\infty}\left[P(\text{none of } k \text{ nodes in } R_s \text{ transmits during tagged node's transmission })\right] \\ &= \sum_{k=0}^{\infty}\left(1-\pi_{XMT}\cdot\frac{2(T-DIFS)}{T}\right)^k \frac{\left[\beta(2R-l_{cs}-x)\right]^k}{i!}\exp\left(-\beta(2R-l_{cs}-x)\right) \\ &= \exp\left(-\frac{2\pi_{XMT}\beta(T-DIFS)(2R-l_{cs}-x)}{T}\right) \\ &= \exp\left(-C(2R-l_{cs}-x)\right) \end{aligned} \tag{3.53}$$

where $C=2\pi_{XMT}\beta(T\text{-}DIFS)/T$. Thus, the expected number of failed nodes in [0, R] due to the hidden terminal problem can be expressed as:

$$\begin{aligned} NF_h &= \int_0^{2R-l_{cs}} \beta x f_X(x)dx \\ &= \int_0^{2R-l_{cs}} \beta x d\left\{P(X \le x)\right\} = \beta(2R-l_{cs}) - \frac{\beta}{C}\left[1-\exp\left(-c(2R-l_{cs})\right)\right] \end{aligned} \tag{3.54}$$

Therefore, the percentage of receivers that are free from collisions caused by hidden terminal problem is:

$$PRR_{ht} = \frac{\beta R - NF_h}{\beta R} = \frac{l_{cs}-R}{R} + \frac{1}{RC}\left[1-\exp\left(-C(2R-l_{cs})\right)\right] \tag{3.55}$$

Hence, based on Eqs. (3.46)(3.52)(3.55), the PRR can be computed. Similar to the case of the PDR, the hidden terminals problem also has more impact than concurrent transmissions on the PRR, as shown in Section 3.5.

3.5 Numerical and Simulation Results

The computation for analytic models and corresponding simulations are conducted in Matlab. Note that the analytic model consists of decomposition and fixed-point iteration while the simulative solution does not. All other assumptions are the same in the simulation and analytic models. The results show the high accuracy of our decomposition-based analytic approximation. We consider a freeway system where the number of vehicles is Poisson distributed. Each vehicle on the road is equipped with DSRC wireless capability. The control channel of DSRC is exclusively used for safety related broadcast communication. Table 3.1 shows the parameters used in this work, which reflect typical DSRC network settings in [1]. In addition, the variables in Table 3.1 such as the packet arrival rate and the average packet length are chosen according to [42] to satisfy the maximum channel utilization limitation of IEEE 802.11, which is required to be 54%-66% in the absence of hidden terminals. For unrealistic situations that exceed such limits, our proposed model in this work may not apply. Under such channel saturation conditions, other models have been developed earlier [23][43].

Table 3.1: DSRC communication parameter

Parameters	Values	Parameters	Values
Tx range R	500 m	Propagation delay δ	0 μs
Average Packet Length $E[PA]$	variable	Variance of Packet Length $Var[PA]$	0
PHY preamble	40 μs	PLCP header	4 μs
MAC header	272 $bits$	CWMin W_0-1	15
Packet arrival rate λ	variable	Vehicle density β	variable
Slot time σ	16 μs	DIFS	64 μs

3.5.1 Numerical Vs. Simulation Results

Figures 7-9 present the numerical results of the proposed model including mean transmission delay, PDR and PRR respectively, vs. the vehicle density β (# vehicles per meter), data rate R_d (*Mbps*), packet arrival rate λ (# packets per second) and average packet length $E[PA]$ (*byte*).

The simulation results for 95% confidence intervals are also presented in the figures. Figures 3.7-3.9 show that the analytic results from the model have nice match with the simulation results. Another observation from Fig. 3.7 is that high data rate and shorter packet length facilitate the decrease of the mean transmission delay. The PDR decreases fast as the density β increases as shown in Fig. 3.8 comparing to PRR as shown in Fig. 3.9. Similar to the mean delay, PDRs and PRRs also benefit from high data rate and short packet length. Comparing Fig. 3.8 with Fig. 3.9, we can observe that, given same network parameters, PDRs are less than PRRs. This is because that PDRs count the number of packets that are successfully received by all intended receivers, while *PRR*s count the percentage (or probability) of the intended receivers that successfully receive a packet from a sender.

3.5.2 Comparison with Previous Models

In this section, in order to show that our proposed model is more precise and general, we compare a few analytic and simulation results from the proposed model with the analytic results from previous models. The model in [7], denoted as Model 1, is

used for the mean delay and PDR comparison. The model in [39], denoted as Model 2, is used for PRR (although referred as PDR in Eq. 19 of the work) comparison. Figures 10-12 present the mean transmission delay, PDR and PRR respectively for these models along with the simulation results for 95% confidence intervals.

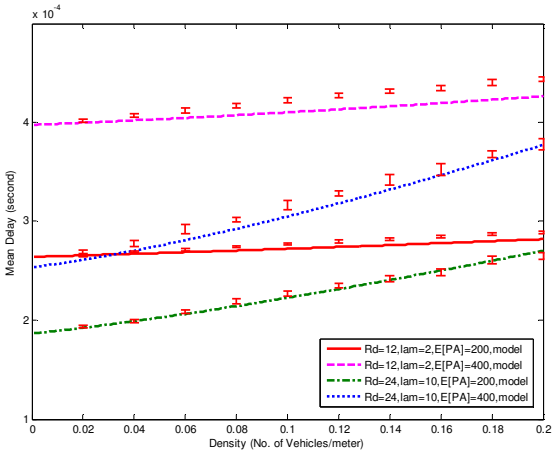

Figure 3.7: Mean delay

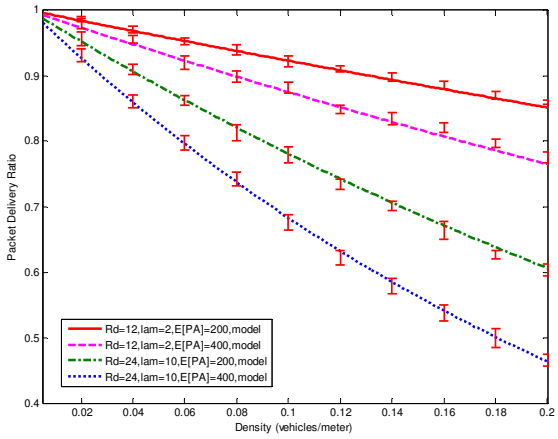

Figure 3.8: PDR

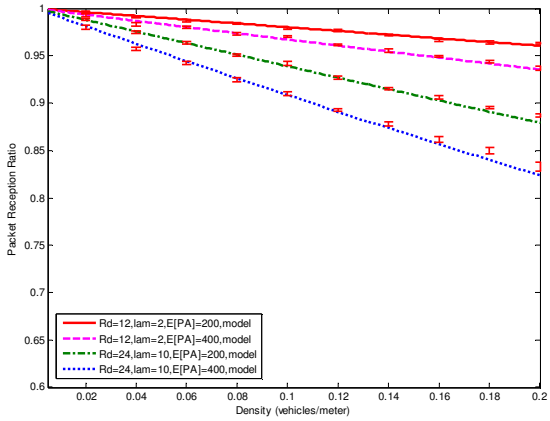

Figure 3.9: PRR

Fig. 3.10 shows that, for the same input parameters, the new model obtains lower mean delay than the model in [7]. This is mainly since the new SMP model considers the

fact that a packet can be directly transmitted without undergoing backoff process, which was ignored in [7]. In addition, the PDR results in Fig. 3.11 also show that new model has better match with simulations than Model 1. The PRR computation method in Eq. 19 in [39] (*i.e.*, Model 2) is shown as below (A few symbol adjustments are made according to our definitions in this work):

$$PRR = \frac{1-\pi_0}{2\beta R \cdot \pi_{XMT} \cdot \frac{T-DIFS}{T}} \cdot \exp(-2\beta R \pi_0) \cdot \left[1-\exp\left(-2\beta R \cdot \pi_{XMT} \cdot \frac{T-DIFS}{T}\right)\right] \tag{3.56}$$

The PRR results comparison is illustrated in Fig. 3.12 and the proposed new model shows better match than Model 2.

For better illustration, the relative errors of these models with simulation results are presented in Table 3.2-3.4, with input parameters R_d=24 *Mbps*, λ=10 packets/second, $E[PA]$=200 bytes. Table 3.2 shows that the packet mean transmission delay obtained from our proposed new model matches very well with the simulation (relative error is less than 2%), whereas the Model 1 without considering the packet transmission not undergoing backoff procedure deviates from the simulation results significantly (relative error is more than 48%). Table 3.3 also shows that the PDRs obtained from the new model (relative error is less than 2%) match better with the simulation than Model 1(relative error is less than 8%). Table 3.4 shows that the PRRs from the new model (relative error is less than 1%) match better than Model 2 (relative error is less than 2%).

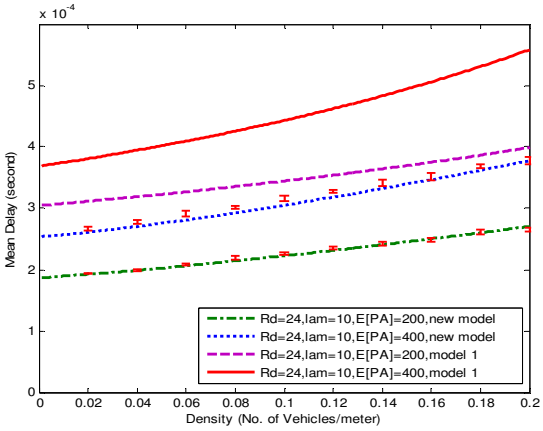

Figure 3.10: Mean delay comparison

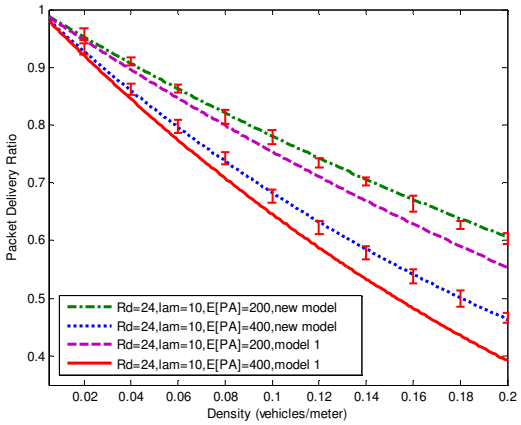

Figure 3.11: PDR comparison

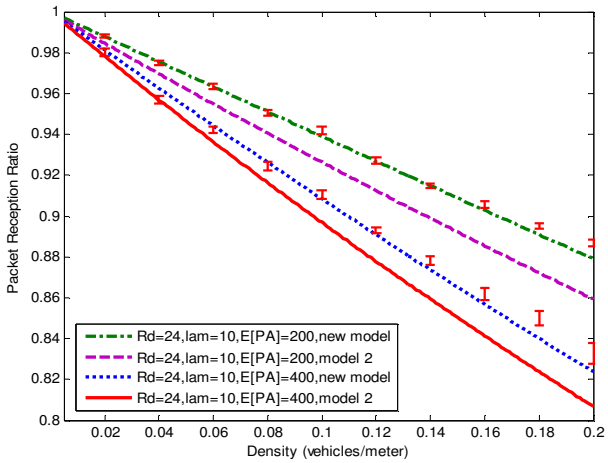

Figure 3.12: PRR comparison

Table 3.2: Mean delay *E*[*D*] comparisons

Density	0.02	0.06	0.1	0.14	0.18	0.2
Simulation(*ms*)	0.1938	0.2090	0.2265	0.2422	0.2608	0.2651
Model 1(*ms*)	0.3114	0.3269	0.3444	0.3642	0.3866	0.3989
new model(*ms*)	0.1924	0.2064	0.2227	0.2407	0.2602	0.2703

Table 3.3: PDR comparison

Density	0.02	0.06	0.1	0.14	0.18	0.2
Simulation	0.9568	0.8622	0.7788	0.7018	0.6271	0.6032
Model 1	0.9469	0.8465	0.7539	0.6687	0.5905	0.5540
new model	0.9523	0.8628	0.7809	0.7062	0.6381	0.6065

Table 3.4: PRR comparison

Density	0.02	0.06	0.1	0.14	0.18	0.2
Simulation	0.9888	0.9646	0.9440	0.9160	0.8963	0.8884
Model 2	0.9846	0.9549	0.9264	0.8988	0.8723	0.8594
new model	0.9878	0.9633	0.9389	0.9148	0.8909	0.8791

3.5.3 Impact Comparison between Concurrent Transmission and Hidden Terminals

As per Sections 3.4.2 and 3.4.3, the PDR and PRR are influenced by both concurrent transmission and hidden terminals. In order to determine which factor is more critical for DSRC safety message transmission, we conduct the impact comparison between the concurrent transmission and hidden terminals in this section. Fig. 3.13 presents the PDR according to Eq. (3.42), where $P(N_{cs})$ incorporates the impact of concurrent transmission and $P(N_{ph})$ incorporates the impact of hidden terminals. Similarly, Fig. 3.14 presents the PRR according to Eq. (3.46), where PRR_{cc} incorporates the impact of concurrent transmission and PRR_{ht} incorporates the impact of hidden terminals. As shown in these figures, the PDR and PRR are dominated by the hidden terminals problem, whereas the concurrent transmission has little influence on the PDR

and PRR. Therefore, to improve the performance of DSRC based safety message transmission, the most crucial thing is to reduce the impact of hidden terminals.

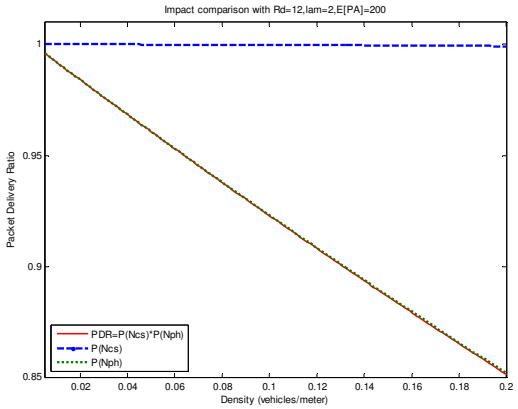

Figure 3.13: Impact on PDR

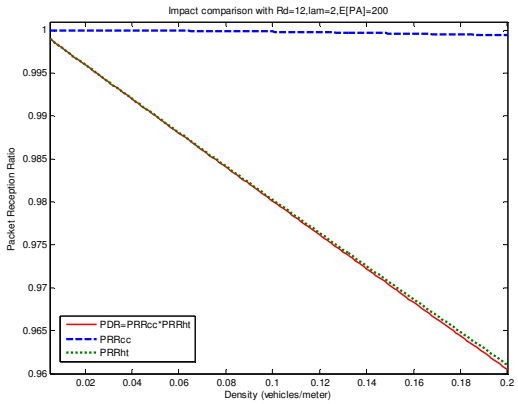

Figure 3.14: Impact on PRR

3.6 Conclusions and Future Work

In this work, a more general and accurate analytic model using SMP interacting with an M/G/1 queue has been developed to characterize the behavior of DSRC for highway safety communications. New proposed SMP model also facilitates the accurate evaluation of hidden terminal impact that is one of major factors for degradation of the reliability, which has not been properly or precisely addressed in the previous work. Both PDR and PRR, very important reliability metrics for DSRC safety-related services, are analytically derived using the new model structure. The model is cross validated against simulations. Moreover, the analysis with different input parameters is used to suggest better parameter settings that will improve the performance by decreasing the mean delay, increasing PDR and PRR. Above all, the proposed model will be beneficial

to the analysis, design, and network parameter optimization for required performance and reliability of DSRC VANET for safety-related services. Based on the proposed model, more practical models for more applications can be developed.

In the future, the assumptions made in Section 3.2 will be gradually relaxed to reflect the real world scenario. The analytic model will be extended to incorporate different packet arrival processes such as Markov modulated Poisson process (MMPP), Markovian arrival process (MAP) instead of Poisson arrivals. Different types of safety messages over the control channel will be considered. In a tagged vehicle, we can use different queues to store different types of messages and construct separate SMP models for each type of safety message service. These separated SMP models will interact with each other and also with their own corresponding M/G/1 queue. Fixed-point iteration will then be used to obtain the converged solution. Therefore, the extension of our model for multiple services is quite straightforward. Moreover, channel shadowing/fading, capturing effect and vehicle mobility will be incorporated. 1-D highway will be extended to 2-D case to model the intersecting roads, parallel lines in highways, square grid for downtown area, etc. Besides one-hop direct broadcast transmission strategy, multi-hop and multi-cycle transmission strategy will also be considered in future.

4. Periodic Beacon Messages Evaluation

4.1 Motivation

Transportation safety is one of the most critical features addressed in Intelligent Transportation System (ITS) [44]. In wireless vehicular communications, various safety applications such as collision avoidance and safety warnings are expected to be enabled to prevent and reduce traffic accidents. To support these safety applications, periodic beacon message, *i.e.*, basic safety message (BSM) [45][46], is widely used in dedicated short range communications (DSRC). Beacon message contains information related to the state of vehicle (*e.g.*, position, velocity and direction) and such messages are periodically exchanged with nearby vehicles in a broadcast fashion. Based on such information, various safety applications are able to assist drivers to take appropriate actions to prevent collisions when emergencies occur (*e.g.*, rear-end collision warning, slow vehicle indication, *etc*.). Hence, beacon messages are required to be transmitted both in a timely and reliable manner to ensure the quality of service (QoS) for various applications.

The MAC-level performance of the beacon message dissemination in DSRC system has been studied in [47][48][49] based on discrete event simulations. Analytic models are more suited in comparing design alternatives and exploring a large parameter space. Several analytic models are developed in [8][50][51] to characterize the MAC layer behavior of beacon message transmission and important performance

metrics are evaluated. However, Ma [8] used Poisson arrivals to approximate the periodic generations of beacon messages (*i.e.*, routine message), which leads to inaccuracies. Vinel [50] considered the deterministic behavior of beacon generations by modeling each vehicle as a D/M/1 queuing system. Infinite queue size is assumed by them where out-dated information replacement is not considered. Bastani [51] accounted for the periodic nature of beacon message generations and new message canceling out old message phenomena, which is more reasonable and practical. However, their model does not accurately capture the periodic beacon message generation since it separates the periodic message generation from the message channel contention and transmission behavior, although these behaviors are closely correlated. According to [46], beacon messages are periodically generated to broadcast vehicle's status information. However, for the model presented in [51], the time interval between the previous message finishing its transmission and the generation of the next message is fixed beaconing period, which implies that the message generation is no longer periodic since a message transmission time varies according to the channel's status. Hence, model in [51] cannot precisely capture the periodic beacon message generations. In addition, all the above models are based on discrete-time Markov chain (DTMC) and ignore the continuous time system behavior, which leads to approximations.

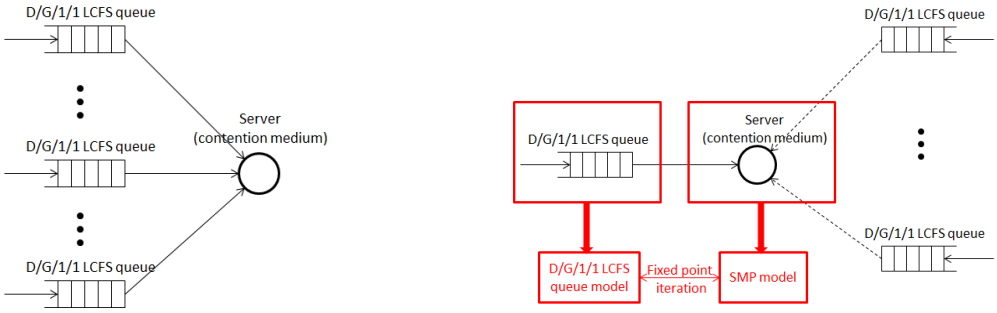

(a) Interactions between vehicles (b) Models from one tagged vehicle's perspective

Figure 4.1: Model capturing interactions between vehicles

In this chapter, we extend the work in [12][52] and develop a detailed and accurate interacting semi-Markov Process (SMP) model [9] to incorporate periodic generations as well as out-dated information replacement behavior for beacon messages. Compared to the M/G/1 FCFS (first come first served) queuing model in our previous work [52] in chapter 2, the generation and service of beacon messages in each vehicle in this chapter is modeled by a D/G/1/1 LCFS (last come first served) queue with preemption as shown in Fig. 4.1(a). In this notation, "D" represents that the message inter-arrival time is deterministic. "G" represents that the service time has an arbitrary distribution. The first "1" represents that there is only one server. The second "1" represents that the queue size is one (*i.e.*, no queuing). This queue is a LCFS preemption queue because out-dated beacon message will be replaced by the next message to ensure that the message to be sent in a vehicle is always up to date. Therefore, the overall model is a set of interacting D/G/1/1 LCFS queues, one for each vehicle. The interaction is that the server is shared as it is the contention medium/channel. To develop a tractable

analytic approximation, we use a semi-Markov process model to capture the shared server's behavior from one tagged vehicle's perspective, which incorporates the behavior of this tagged vehicle and the influences from other vehicles as shown in Fig. 4.1(b). This SMP model is accurate and comprehensive since it closely follows the operational flow specified by DCF in IEEE 802.11p shown in Fig. 2.1. In addition, SMP model with absorbing state is constructed to derive the message service time distribution via *Laplace–Stieltjes* transform (LST). Due to the interactions between the SMP models of different vehicles, fixed-point iteration [10][10] method is utilized to obtain the converged solution in steady state. MAC-level performance metrics including mean delay, packet delivery ratio (PDR), packet reception ratio (PRR) and normalized channel throughput are derived. The proposed approximation is verified through extensive simulations and compared with previous models for Poisson packet arrivals and with infinite queue scenarios (*i.e.*, M/G/1 FCFS queue) [52] and Bastani's model in [51].

Even though the MAC-level performance metrics play an important role for understanding the packet transmission behavior and evaluating the efficiency of a protocol, the application-level performance metrics are also essential to be addressed to ensure the QoS of safety and non-safety applications because performance requirements are typically given in terms of application-level metrics as opposed to packet-level metrics. Efforts have been made in previous work [53][54][55] to characterize the

application-level performance metrics for specifying the application performance requirements. Bai et al. [53] characterized Region of Interest (ROI) of VANET applications into three qualitative levels: long, medium and short. In addition, the application-level latency and application-level T-window reliability (TWR) (*i.e.*, the probability to successfully receive at least one packet during tolerance time window T) were also proposed in [53] to guide performance requirements in terms of application-level metrics. An et al. [54] proposed that the application requirements can be specified as awareness range and awareness probability. The awareness probability generalized the idea of TWR as the probability to successfully receive at least n packets in the tolerance time window T. Awareness range is defined as the maximum distance at which the awareness probability is greater than or equal to a certain threshold. The authors in [55] defined the invisible neighbor problem and proposed to minimize the total number of invisible neighbors over a certain time window to ensure the QoS of the vehicle's safety applications.

In this chapter, we adopt the definitions of Region of Interest, application-level latency, T-window reliability, awareness probability and invisible neighbors from previous work to characterize the application performance requirements. The corresponding analytic results are derived based on the newly proposed interacting SMP model for periodic beacon messages. Based on such analytic models for application-level performance metrics, we provide insights on network parameter

settings to satisfy performance requirements for various applications. Furthermore, three typical safety applications including slow vehicle indication, emergency vehicle warning and rear-end collision warning are analyzed to assess whether their performance requirement can be satisfied or not under a given DSRC network parameters setting.

The key contributions of this chapter are six-fold: 1) Periodic beacon message generation and out-dated message replacement behavior are incorporated into a detailed and accurate analytic model, which closely follows the operational flow specified by DCF in IEEE 802.11p; 2) Beacon message service time distribution is first derived using *Laplace–Stieltjes* transform, based on which the mean service time is computed; 3) Normalized channel throughput is derived for better understanding of channel conditions under various input parameters; 4) Analytic results for a vehicle with periodic beacon message generation and out-dated message replacement (*i.e.*, D/G/1/1 LCFS queue) are compared to those for a vehicle model in [52] with Poisson message arrivals and an infinite queue (*i.e.*, M/G/1 FCFS queue) and Bastani' model [51]; 5) Application-level performance metrics including application-level latency, T-window reliability, awareness probability, and the average number of invisible neighbors are derived based on the newly proposed interacting SMP model; 6) Three typical safety-applications are evaluated to assess whether their performance requirement can be met or not under a given DSRC network parameters setting.

4.2 System Assumptions

Several assumptions are made in the broadcast system to produce analytically tractable yet a high fidelity model. The vehicular ad hoc network is considered to be one-dimensional (1-D) for traffic on highway [9]. The number of vehicles in a line is assumed to be Poisson distributed with parameter β (vehicle density), *i.e.*, the probability $P(i, l)$ of finding i vehicles in a lane of length l is given by Eq. (3.1). In addition, we assume all vehicles have the same transmission range, receiving range and carrier sensing range R to simplify the analysis. Furthermore, an out-dated beacon message is replaced by the new message. In other words, if the previous message has not been transmitted when the new message is generated in a vehicle, the previous message will be replaced by the next packet. This assumption is made since a beacon message contains information such as the position, the velocity and the direction, *etc.*, that needs to be updated periodically. Therefore, different from event-driven safety messages that are too important to be replaced, no queueing of messages is needed for the periodic beacon messages. Channel shadowing or fading, vehicle mobility and capture effect of transmissions are not considered in this chapter. One more assumption is that only beacon message service in the control channel (CCH) is considered in the model.

4.3 Analytic Models

4.3.1 Overall Model

The overall system behavior is that of multiple vehicles competing for the channel resource to transmit their own beacon messages over the CCH. Due to such interactions between vehicles, the whole system can be captured by a Generalized Semi-Markov Processes (GSMP) [56][57], which is a set of interacting semi-Markov processes. Even assuming that all sojourn times are exponentially distributed, a single GSMP model to analyze system behavior faces state explosion problem when the number of vehicles is large. For example, suppose there are 100 vehicles in the system to be analyzed, and each vehicle's maximal backoff counter is 15, the GSMP model will contain at least 15^{100} states (can be more due to channel sensing and backoff frozen states) to capture the whole system behavior. First, there is no known analytic solution to a GSMP; it can be either solved using discrete-event simulation or phase-type expansion for all non-exponential distributions need to be carried out, in which case the state space will get even bigger. We use model decomposition to develop a tractable analytic model of such a complex system, denoted as ISP (Interacting Stochastic Processes). This newly proposed ISP model and GSMP model are both based on a set of interacting semi-Markov processes. The distinction is that: in GSMP model, the interactions are at the level of events while for the ISP model, solutions of one SMP

provide parameters to the others. This decomposition is what makes our proposed ISP approach analytically tractable while GSMP is not.

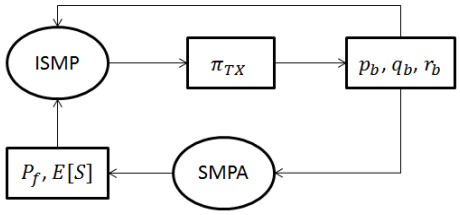

Figure 4.2: Import graph for the overall method

In this chapter, we decompose the overall model of the whole system and develop a detailed SMP model in Section 4.3.2 that directly captures the channel contention and backoff behavior from a single vehicle's perspective. The influences from other vehicles are incorporated into this single vehicle SMP model through four model parameters (P_f, p_b, q_b, r_b in Fig. 4.3) remaining to be determined. By solving the SMP model, we can obtain the fully symbolic solution for the steady-state probability that a single vehicle transmits. Based on a single vehicle's behavior, three model parameters (p_b, q_b, r_b in Fig. 4.3) that capture the degree of channel contention from multiple vehicles are derived. The one remaining model parameter (P_f in Fig. 4.3) is related to the out-dated message replacement behavior, and hence the message service time distribution needs to be derived first to determine whether a message will be replaced by the next one or not. We propose *Laplace–Stieltjes* transform method over a modified SMP model in Section 4.3.3 to derive a formula for this service time distribution and subsequently derive the related model parameter. Since these four model parameters are inter-

dependent on each other, fixed-point iteration method is used to obtain converged numerical solutions in Section 4.3.4. The import graph [16] for such overall method is shown in Fig. 4.2. Let the SMP model in Section 4.3.2 be denoted by ISMP (Irreducible SMP) and the modified SMP model with absorbing state in Section 4.3.3 be denoted by SMPA. The results produced by these models are presented within rectangles in Fig. 4.2.

4.3.2 SMP Model

The behavior of a tagged vehicle is characterized using the irreducible SMP model in Fig. 4.3. The channel sensing, backoff and transmission behavior matches well with the flow chart shown in Fig. 2.1. The tagged vehicle is in *idle* state if there is no packet. After a packet is generated, the vehicle senses channel activity for *DIFS* time period, which is represented by state CS_1. If the channel is detected not busy during this period (with probability $1-q_b$), the vehicle goes from *idle* state to *TX* state, which means that a packet is transmitting. Otherwise, the vehicle will defer until channel is idle for *DIFS* duration represented by state D_{CS}. Such deference behavior for the tagged vehicle includes two parts: waiting for the current packet in the channel finishing transmission and waiting for subsequent transmissions if any from other neighbors within its receiving range. The self-loop for state D_{CS} represents the phenomena in Fig. 4.6 that the tagged vehicle (vehicle *B*) waits for the current packet (from vehicle *A*) in the channel finishing transmission, and then senses the channel for *DIFS* time, which captures the transmission from another vehicle (vehicle *C*) and leads to further deference. The

probability that the tagged vehicle detects another neighbor's transmission during *DIFS* time is denoted as r_b. If no other neighbors' transmission is detected, the tagged vehicle will start backoff procedure and randomly choose a backoff counter in the range [0, *W*-1], where *W*=*CW*+1 is the backoff window size. The backoff counter will be decreased by one if the channel is detected to be idle for a time slot of duration σ (with probability 1-p_b), which is captured by the transition from state *W*-*i* to state *W*-*i*-1. If the channel is busy during a backoff time slot of duration σ (*i.e.*, another vehicle starts to transmit a packet during this time slot), the backoff counter of the tagged vehicle will be suspended, which represented by the transition from state *W*-*i* to D_{W-i-1} with probability p_b. Similar to state D_{CS}, state D_{W-i-1} also contains self-loop because other neighbors' transmission can lead to further deference of the tagged vehicle. When the backoff counter reaches zero, the packet will directly be transmitted (an SMP transition occurs from state 0 to state *TX* with probability one). In *TX* state, a packet is transmitting. To capture the out-dated packet replacement behavior, which can happen during any state except state *TX* and *idle*, we simplify the model by considering the replacement after state *TX*. If the current packet has not been replaced by the next packet (with probability 1-P_f), the SMP goes to state *idle*. Otherwise, this current packet is out-dated and replaced by the next incoming packet. Hence, the tagged vehicle starts the service for the next packet immediately and senses the channel for *DIFS* time (state CS_2) and goes through the backoff procedure before it transmits the next packet.

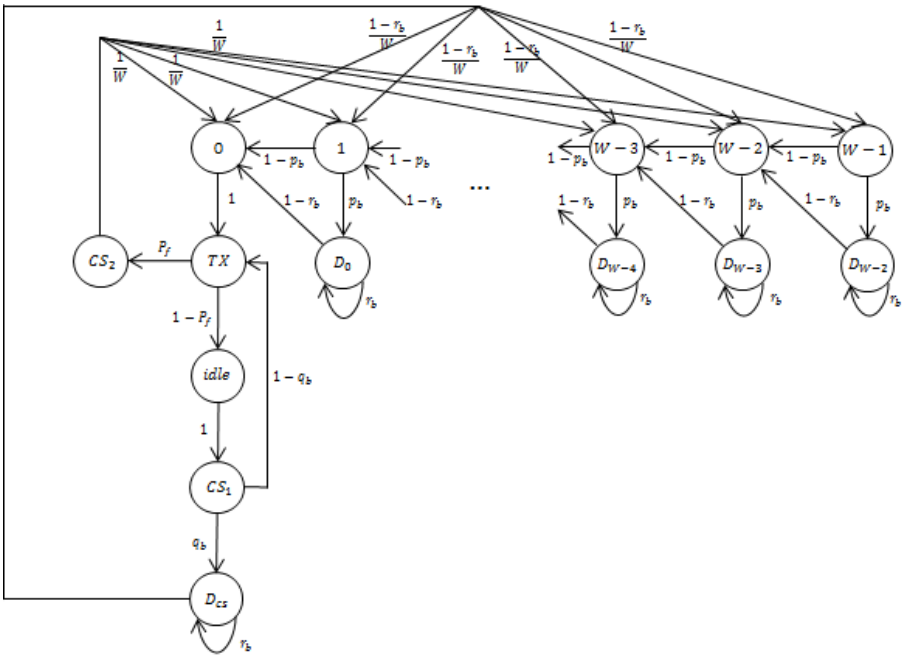

Figure 4.3: SMP model for 802.11p beacon broadcast

Compared to the SMP model in [52], the newly proposed SMP model captures more detailed DCF behavior for periodic beacon message transmission by adding more states and self-loop structure. In addition, out-dated message replacement behavior is incorporated into the model by the newly introduced model parameter P_f. Therefore, the sojourn times and steady-state solutions are totally different from that in [52] although similar computation procedure is used.

Define the sojourn time in state j as T_j. The mean and variance of T_j in the SMP model are:

$$E\left[T_j\right]=\tau_j=\begin{cases}A_1 & j=TX\\ A_2 & j=idle\\ A_3 & j=CS_1,CS_2\\ A_4 & j=D_{CS}\\ A_5 & j=D_0,D_1,\cdots,D_{W-2}\\ 0 & j=0\\ \sigma & j=1,2,\cdots,W-1\end{cases} \tag{4.1}$$

$$Var\left[T_j\right]=\theta_j^2=\begin{cases}0 & j\in U\\ B_1 & j=idle\end{cases} \tag{4.2}$$

where

$$\begin{cases}A_1=PL/R_d+T_H+\delta\\ A_2=\tau-E[S]\\ A_3=DIFS & B_1=Var[S]\\ A_4=(A_1+DIFS)/2\\ A_5=A_1+DIFS\end{cases}$$

$$U=\{TX,CS_1,CS_2,D_{CS},D_0,D_1,\cdots,D_{W-2},0,1,2,\cdots,W-1\}$$

PL represents the packet length. R_d presents the data rate. Hence, PL/R_d is the time to transmit the packet. T_H presents the time to transmit the packet header including physical layer header and MAC layer header. δ is the propagation delay. $E[S]$ and $Var[S]$ are the mean and variance of the overall message service time, which will be derived later. The sojourn time in state *idle* is the packet inter-arrival time excluding the packet service time.

As in [52], the embedded DTMC is first solved for its steady-state probabilities:

$$v_j = (W-j)\cdot v_{W-1} \qquad j = 0,1,\cdots W-1$$

$$v_{D_j} = \frac{(W-j-1)\cdot p_b}{1-r_b}\cdot v_{W-1} \qquad j = 0,1,\cdots W-2$$

$$v_{TX} = \frac{W}{P_f + q_b(1-P_f)}\cdot v_{W-1} \qquad v_{idle} = \frac{(1-P_f)W}{P_f + q_b(1-P_f)}\cdot v_{W-1}$$

$$v_{CS_1} = \frac{(1-P_f)W}{P_f + q_b(1-P_f)}\cdot v_{W-1} \qquad v_{CS_2} = \frac{P_f \cdot W}{P_f + q_b(1-P_f)}\cdot v_{W-1}$$

$$v_{D_{CS}} = \frac{q_b(1-P_f)W}{\left[P_f + q_b(1-P_f)\right](1-r_b)}\cdot v_{W-1}$$

$$v_{W-1} = \frac{2\left[P_f + q_b(1-P_f)\right](1-r_b)}{\left[(W+1)(1-r_b) + p_b(W-1)\right]\left[P_f + q_b(1-P_f)\right]\cdot W + 2\left[(3-P_f)(1-r_b) + q_b(1-P_f)\right]W}$$

Taking into account of the mean sojourn time in each state, the steady-state probabilities of the SMP are:

$$\pi_i = \frac{v_i \tau_i}{\sum_j v_j \tau_j} \tag{4.3}$$

Therefore, the steady-state probability that a vehicle is in the *TX* state is given by:

$$\pi_{TX} = \frac{2A_1}{\left[P_f + q_b(1-P_f)\right]\left(\sigma + \frac{p_b}{1-r_b}\cdot A_5\right)(W-1) + 2\left[A_1 + A_3 + (1-P_f)\left(A_2 + \frac{q_b}{1-r_b}\cdot A_4\right)\right]} \tag{4.4}$$

In Eq. (4.4), four unknown parameters are:

- P_f: the probability that the beacon message will be updated or replaced by the next beacon message.
- p_b: the probability that the channel is detected busy (transmitting messages from other vehicles) in one time slot by the tagged vehicle.

- q_b: the probability that the channel is detected busy (transmitting messages from other vehicles) in *DIFS* time by the tagged vehicle.
- r_b: the probability that the channel is detected busy for *DIFS* time by the tagged vehicle after another neighbor of the tagged vehicle finishes transmission.

In the following two subsections, these parameters will be derived. Due to the dependences between these parameters, fixed-point iteration algorithm will be utilized to obtain the converged solutions. Since P_f depends on the service time to transmit a packet, the service time is derived first in the next subsection in order to obtain P_f. Subsequently, the derivations of the other three parameters and the fixed-point iteration algorithm are presented in Section 4.3.4.

4.3.3 Service Time Computation

The MAC layer service time is defined as the time interval from the time instant when a packet starts to contend for transmission, until the time instant when the packet is received. The SMP model in Section 4.3.2 describes the behavior of a tagged vehicle continuously transmitting packets taking into account the replacement of out-dated packets. The SMP model of Fig. 4.3 is modified to contain an absorbing state as shown in Fig. 4.4 to capture the transmission of only one packet. Hence, the time to reach the absorbing state, denoted as *TA*, will be the service time for a packet transmission. Let the cumulative distribution function (*CDF*) for *TA* be denoted by $F_{TA}(t)$.

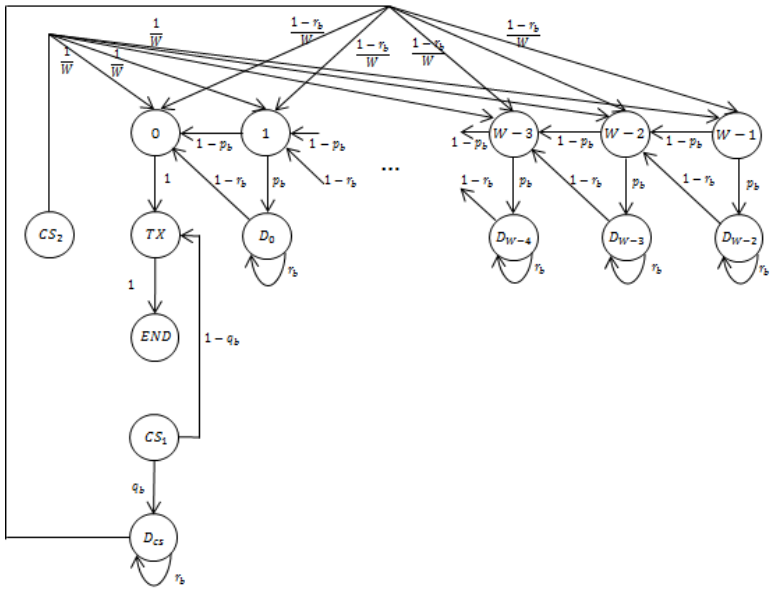

Figure 4.4: SMP model with an absorbing state

As mentioned earlier, P_f is the probability that a packet is updated or replaced by the next packet. Since the beacon packets are generated periodically at a fixed time interval τ, a packet is out-dated and will be replaced by the next packet only when its service time exceeds the message generation period τ. Therefore,

$$P_f = P(TA > \tau) = 1 - P(TA \le \tau) = 1 - F_{TA}(\tau) \tag{4.5}$$

According to Eq. (4.5), we need to derive the *CDF* of the service time first to compute P_f. We use the *Laplace* transform for obtaining *CDF* of *TA*. From Fig. 4.4, we notice that a packet can only start the transmission service from two different states (either CS_1 or CS_2) according to two different scenarios. If a new packet does not replace the previous packet (with probability 1-P_f), the packet will start service from state CS_1. Otherwise, if the packet replaces the previous packet (with probability P_f), the packet will start service

from state CS_2. Denote TA_{CS1} and TA_{CS2} to be the time to reach absorbing state *END* starting from state CS_1 or CS_2 respectively, and q_{CS1} and q_{CS2} to be the corresponding probabilities. Hence,

$$TA_j = \begin{cases} TA_{CS_1} & w.p. \quad q_{CS_1} = 1 - P_f \\ TA_{CS_2} & w.p. \quad q_{CS_2} = P_f \end{cases} \tag{4.6}$$

The service time for a packet transmission is then given by:

$$TA = \left(1 - P_f\right) \cdot TA_{CS_1} + P_f \cdot TA_{CS_2} \tag{4.7}$$

Since the sojourn time in each state is deterministic, their *Laplace–Stieltjes* transform (*LST*) can be easily determined:

$$L_{T_j}(s) = E\left[e^{-s \cdot T_j}\right] = \begin{cases} e^{-s \cdot A_1} & j = TX \\ e^{-s \cdot A_3} & j = CS_1, CS_2 \\ e^{-s \cdot A_4} & j = D_{CS} \\ e^{-s \cdot A_5} & j = D_0, D_1, \cdots D_{W-2} \\ 1 & j = 0 \\ e^{-s \cdot \sigma} & j = 1, \cdots W-1 \end{cases} \tag{4.8}$$

Therefore, the *LST* of TA_{CS1} and TA_{CS2} can be calculated from Fig. 4.4:

$$L_{TA_{CS_1}}(s) = e^{-s \cdot (A_1 + A_3)} \left\{ \begin{array}{l} \left(1 - q_b\right) + q_b \cdot e^{-s \cdot A_4} \sum_{k=0}^{\infty} \left(r_b \cdot e^{-s \cdot A_4}\right)^k \cdot \dfrac{\left(1 - r_b\right)}{W} \\ \cdot \sum_{i=0}^{W-1} \left[\left(1 - p_b\right) \cdot e^{-s \cdot \sigma} + p_b \cdot \left(1 - r_b\right) e^{-s \cdot (\sigma + A_5)} \sum_{k=0}^{\infty} \left(r_b \cdot e^{-s \cdot A_5}\right)^k \right]^i \end{array} \right\}$$

$$L_{TA_{CS_2}}(s) = e^{-s \cdot (A_1 + A_3)} \cdot \frac{1}{W} \cdot \sum_{i=0}^{W-1} \left[\left(1 - p_b\right) \cdot e^{-s \cdot \sigma} + p_b \cdot \left(1 - r_b\right) e^{-s \cdot (\sigma + A_5)} \sum_{k=0}^{\infty} \left(r_b \cdot e^{-s \cdot A_5}\right)^k \right]^i$$

From Eq. (4.7), we know that the *LST* of *TA* is:

$$L_{TA}(s) = \left(1 - P_f\right) \cdot L_{TA_{CS_1}}(s) + P_f \cdot L_{TA_{CS2}}(s) \tag{4.9}$$

Hence, the *Laplace* transform for $F_{TA}(t)$, denoted as $F^*(s)$ is:

$$F^*(s) = \frac{L_{TA}(s)}{s} = (1-P_f)\cdot\frac{L_{TA_{CS_1}}(s)}{s} + P_f\cdot\frac{L_{TA_{CS2}}(s)}{s} \tag{4.10}$$

Upon inversion of such a *Laplace* transform, the service time distribution, $F_{TA}(t)$, can be easily obtained:

$$F_{TA}(t) = L^{-1}\left(F^*(s)\right) = (1-P_f)\cdot L^{-1}\left(\frac{L_{TA_{CS_1}}(s)}{s}\right) + P_f\cdot L^{-1}\left(\frac{L_{TA_{CS2}}(s)}{s}\right) \tag{4.11}$$

Due to the packet replacement phenomena, if the service time of a packet exceeds the packet generation interval τ, the packet will be replaced by the next packet. Therefore, the service time for the replaced packet can be interpreted as τ. Thus, the service time distribution has to be adjusted to incorporate such packet replacement scenario:

$$F_{TA}(t) = \begin{cases} (1-P_f)\cdot L^{-1}\left(\frac{L_{TA_{CS_1}}(s)}{s}\right) + P_f\cdot L^{-1}\left(\frac{L_{TA_{CS2}}(s)}{s}\right) & t \le \tau \\ 1 & t > \tau \end{cases} \tag{4.12}$$

Since the sojourn time in every state of Fig. 4.4 is deterministic, we can easily conclude that the service time is a discrete variable. Therefore, the service time distribution in Eq. (4.12) is conceptually demonstrated in Fig. 4.5 for better comprehension. The minimal service time is A_1+A_3 with probability $p_0=(1-P_f)(1-q_b)+P_f/W$ from the symbolic solutions in Eq. (4.12).

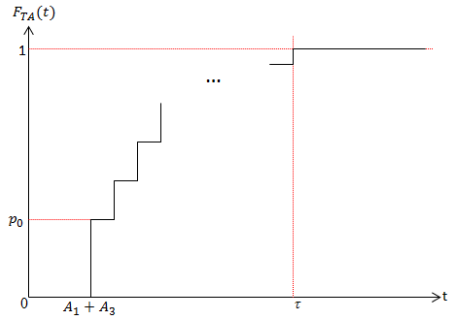

Figure 4.5: Conceptual service time distribution

After obtaining the service time distribution, the probability P_f that a packet is replaced by the next packet can be computed as in Eq. (4.5). To determine the sojourn time in *idle* state in Eq. (4.1), the mean service time also needs to be calculated as follows:

$$E[S] = E[TA] = \int_0^{\infty} R_{TA}(t)\,dt = \int_0^{\tau} \left[1 - F_{TA}(t)\right] dt \tag{4.13}$$

4.3.4 Fixed-point Iteration

As described in Section 4.3.2, four unknown model parameters need to be determined to obtain the system steady-state behavior (*i.e.*, a vehicle transmits in steady-state). In the previous section, P_f is shown to depend on the service time, which further depends on the other three model parameters p_b, q_b and r_b. In this section, the channel busy probabilities p_b, q_b and r_b are derived first, each of them is shown to depend on the other three parameters. Therefore, fixed-point iteration algorithm is used to obtain final solutions.

Let N_{cs} denote the average number of vehicles in the carrier sensing range of the tagged vehicle, and let N_{tr} denote the average number of vehicles in transmission range of the tagged vehicle. Hence, without loss of generality, we have:

$$N_{cs} = N_{tr} = 2\beta R \tag{4.14}$$

The average number of vehicles in potential hidden area is:

$$N_{ph} = 4\beta R - N_{cs} = 2\beta R \tag{4.15}$$

From the tagged vehicle's point of view, p_b is the probability that it senses channel busy during one backoff time slot. Through the SMP model in Fig. 4.3, we know that state $I \in \{0,1,\ldots,W\text{-}1\}$ stands for the backoff time slot. Furthermore, before the system enters one of these backoff time slots, the channel has been idle for either one time slot or *DIFS* time duration, which can be easily seen from the input transitions and states for state *I*. Therefore, to be more precise, p_b stands for the probability that the channel *becomes* busy (*i.e.*, goes from idle to busy) during one backoff time slot of the tagged vehicle. The probability that a vehicle starts to transmit during one time slot is given by π_1, which can be computed from Eq. (4.3), because the sojourn time in state 1 is one time slot. Furthermore, the channel becomes busy if there is at least one neighbor (*i.e.*, a vehicle in the transmission range of the tagged vehicle) that starts to transmit in a backoff time slot of the tagged vehicle. Thus, we have:

$$p_b = 1 - \sum_{i=0}^{\infty} (1-\pi_1)^i \frac{(N_{tr})^i}{i!} e^{-N_{tr}} = 1 - e^{-N_{tr}\cdot\pi_1} \tag{4.16}$$

Next, q_b denotes the probability that the channel is detected busy by the tagged vehicle in *DIFS* duration. Different from p_b derivation, the channel does not necessarily become busy during *DIFS* duration. In other words, the channel can becomes busy before *DIFS* duration, and only been detected busy during this *DIFS* duration. This is because the tagged vehicle is in state *idle* while waiting for a packet being generated and then it enters state CS_1 to sense the channel for *DIFS* duration, which implies that the channel could have become busy before such *DIFS* sensing time. As long as the channel busy status is captured by the *DIFS* channel sensing time, with probability q_b, the vehicle will enter state D_{CS} to defer transmission. Therefore, to be more precise, q_b stands for the probability that channel busy status is *captured* by *DIFS* duration. We can first define Q_{TX} to be the probability that a neighbor's transmission is captured in the *DIFS* duration by the tagged vehicle, hence:

$$Q_{TX} = \frac{A_1 + DIFS}{A_1} \pi_{TX} \tag{4.17}$$

Therefore, q_b is given by:

$$q_b = 1 - \sum_{i=0}^{\infty} (1 - Q_{TX})^i \frac{(N_{tr})^i}{i!} e^{-N_{tr}} = 1 - e^{-N_{tr} \cdot Q_{TX}} \tag{4.18}$$

Next we derive an expression for r_b. In Section 4.3.2, r_b presents the probability that the following phenomena occurs: the tagged vehicle (vehicle *B*) waits for the current packet (from vehicle *A*) in the channel to finish transmission, and then sense the channel for *DIFS* time, which captures the transmission from another vehicle (vehicle *C*) and

leads to further deference. As shown in Fig. 4.6, *A*, *B* and *C* present the vehicles on 1-D road. Two ovals present the transmission range of *A* and *B* respectively. For the tagged vehicle *B*, after it just received a packet from one of its neighbors *A*, it will sense the channel for *DIFS* time. During such *DIFS* time, only some of its neighbors are also in the

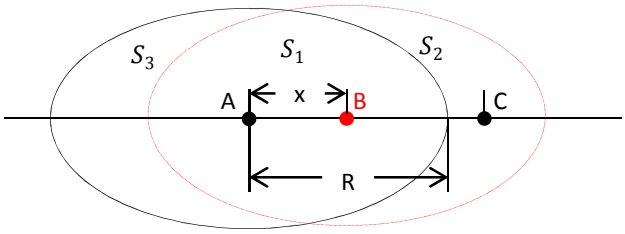

Figure 4.6: Channel sensing deference

DIFS channel sensing state (vehicles within S_1), whereas rest of its neighbors (vehicles within S_2, such as vehicle *C*) are not influenced by *A*'s transmission since they are outside *A*'s transmission range. Suppose the average number of these vehicles which are outside *A*'s transmission range but within *B*'s receiving range (*i.e.*, space S_2) is *N*. Therefore, in the tagged vehicle *B*'s *DIFS* sensing time, the probability that it receives a neighbors transmission is:

$$r_b = 1 - \sum_{i=0}^{\infty} (1 - Q_{TX})^i \frac{(N)^i}{i!} e^{-N} = 1 - e^{-N \cdot Q_{TX}} \tag{4.19}$$

where *N* is derived next. As shown in Fig. 4.6, let *x* denote the distance between vehicle A and B. Then, the 1-D distance in S_2 will also be *x*. Hence, the average number of vehicles in S_2 is given by:

$$N = \int_0^R \beta x \frac{1}{R} \cdot dx = \frac{\beta R}{2} = \frac{N_{tr}}{4} \tag{4.20}$$

Combining Eqs. (4.17)(4.19)(4.20), we obtain r_b.

From the above analysis, we know that the four parameters P_f, p_b, q_b and r_b are interdependent. Hence, the fixed-point iteration algorithm is utilized and outlined as follows to obtain the final converged solutions:

Step 1: Initialize P_f=0,p_b=0,q_b=0,r_b=0.

Step 2: With P_f, p_b, q_b, r_b, calculate new P_f, p_b, q_b, r_b according to Eqs. (4.5)(4.16)(4.18)(4.19).

Step 3: If P_f, p_b, q_b, r_b converge with the previous values, then stop the algorithm; otherwise, go to step 2 with the updated P_f, p_b, q_b, r_b.

Once the parameters P_f, p_b, q_b, r_b are determined using the above algorithm, they are used for the performance-indices computation in the next section.

4.4 Performance Indices

4.4.1 MAC-level Performance Metrics

4.4.1.1 Mean Transmission Delay

One of the most important performance indices is the mean transmission delay of the beacon message. Different from the mean service time that takes into account all of the packets generated, the mean transmission delay only accounts for the packets transmitted and exclude those that have been replaced. Let $E[D]$ be the mean transmission delay, that is also the mean service time of transmitted packets. Since the

service time for the packet that has been replaced is τ and the mean service time is given in Eq. (4.13), we have:

$$E[S] = (1 - P_f) \cdot E[D] + P_f \cdot \tau \tag{4.21}$$

Therefore, the mean transmission delay is:

$$E[D] = \frac{E[S] - P_f \cdot \tau}{1 - P_f} \tag{4.22}$$

4.4.1.2 Packet Delivery Ratio

The PDR [7] is the probability that all vehicles in the tagged vehicle's transmission range successfully receive the broadcast packet from the tagged vehicle. Using the approach in [52] in Chapter 2, we have:

$$PDR = P(N_{cs})\,P(N_{ph}) \tag{4.23}$$

Note that the formulas for $P(N_{cs})$ and $P(N_{ph})$ in [52] in Chapter 2 are adjusted according to the newly proposed model in this chapter. $P(N_{cs})$ can also be interpreted as the non-concurrent transmission probability, *i.e.*, two packets do not start transmission in the same time slot. Since the sojourn time in state 1 is one time slot, π_1 is equivalent to the probability that a vehicle starts to transmit in a time slot. Hence, $P(N_{cs})$ is given by:

$$P(N_{cs}) = \sum_{i=0}^{\infty} (1 - \pi_1)^i \frac{(N_{cs} - 1)^i}{i!} e^{-(N_{cs}-1)} = e^{-(N_{cs}-1)\pi_1} \tag{4.24}$$

The event that a transmission from hidden terminals collides with the tagged vehicle's transmission only happens when hidden terminals start to transmit during the vulnerable period of duration $2 \cdot A_1$ [7]. Therefore, the probability that a vehicle starts to

transmit during the vulnerable period of hidden terminal transmissions [7] is $2\cdot\pi_{TX}$, and hence:

$$P\left(N_{ph}\right)=\sum_{i=0}^{\infty}\left(1-2\cdot\pi_{TX}\right)^{i}\frac{\left(N_{ph}\right)^{i}}{i!}e^{-N_{ph}}=e^{-2\cdot N_{ph}\cdot\pi_{TX}} \tag{4.25}$$

4.4.1.3 Packet Reception Ratio

Packet reception ratio (PRR) is defined as the percentage of nodes that successfully receive a packet from the tagged node among the receivers being investigated at the moment that the packet is sent out [7]. Using an approach similar to that presented in [52] in Chapter 2, we adjusted and simplified the formulas according to the new model. Hence:

$$PRR = PRR_{cc}PRR_{ht} \tag{4.26}$$

where the impact of the concurrent transmission is:

$$PRR_{cc}=PRR_{cc}^{1}\cdot PRR_{cc}^{2}=\frac{e^{-\beta R\pi_1}}{\beta R\pi_1}(1-e^{-\beta R\pi_1}) \tag{4.27}$$

and the impact of the hidden terminal is:

$$PRR_{ht}=\frac{\beta R-NF_h}{\beta R}=\frac{l_{cs}-R}{R}+\frac{1}{RC}\left(1-e^{-C(2R-l_{cs})}\right) \tag{4.28}$$

with $C=2\beta\cdot\pi_{TX}$.

4.4.1.4 Normalized Channel Throughput

The normalized channel throughput is the ratio of the time used for successful transmitted packets and the entire time. From a channel's perspective, during one packet

generation interval τ, N_{tr} packets are generated in total for all vehicles sensing this channel, one packet from each vehicle. Hence, the normalized channel throughput can be easily computed as:

$$S = \frac{N_{tr}}{\tau} \cdot PDR \cdot PL \tag{4.29}$$

4.4.2 Application-level Performance Metrics

Besides MAC-level metrics, application-level performance metrics are also important to capture the performance of broadcast-based safety applications. Furthermore, the QoS requirements are typically expressed in terms of application-level performance metrics. Therefore, derivation of the application-level performance metrics is essential for QoS assessment of safety applications. To derive the application-level performance metrics, the evaluation of point-to-point reception probability needs to be conducted through coverage area computation for the impact of hidden terminal problem and concurrent transmissions. Therefore, the node reception probability is first computed, based on which the application-level performance metrics including T-window reliability, application-level delay, awareness probability and average number of invisible neighbors are derived.

4.4.2.1 Node Reception Probability

Given a transmitting node *O* placed at the origin (see Fig. 4.7), *U* is one of the receivers within transmission range *R* of node *O*. *U* is placed on 1-D line with certain distance to *O*, which is denoted as x ($0<x<R$). The probability that the node *U* receives

the broadcast message from the tagged node *O* successfully is the node reception probability (NRP) at distance *x*, which is denoted as $P_s(x)$.

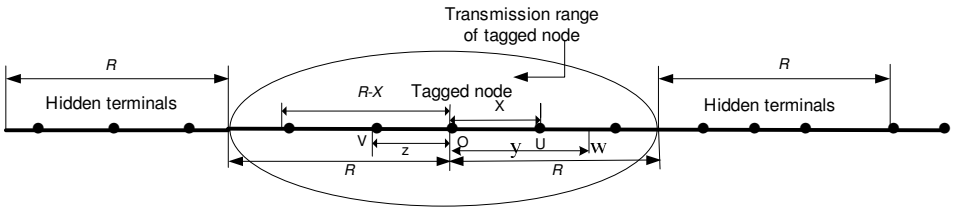

Figure 4.7: Node reception probability computation

There are two factors affecting the node reception probability: hidden terminal problems, collisions due to concurrent packet transmissions:

a. Impact of Hidden terminals

Based on the SMP model and its solution, we have the probability that node *U*'s reception of the broadcast message from node *O* is free from the hidden terminals:

$$P_H(x) = \sum_{i=0}^{\infty} (1-2\pi_{TX})^i \frac{(\beta x)^i}{i!} e^{-\beta x} = e^{-2\pi_{TX}\beta x} \tag{4.30}$$

b. Impact of concurrent collisions

In addition to collisions caused by the hidden nodes, transmissions from nodes within interference range from the tagged node in the meantime at which the tagged node transmits may also cause collisions. When the tagged node transmits in a slot time, collisions will take place if any node in the interference range of the tagged node transmits in the slot.

Given that as both *O* and *U* sense the channel idle, *O* will transmit within the duration of a slot. In order to prevent interference due to concurrent collisions to *U*'s

receiving the broadcast message sent by O, no transmission in [-(R-x), R] is allowed. The average number of nodes transmitting in the concurrent slot in area [0, x] is $\beta x\pi_1$.

Suppose node W is y away from O, $x<y<R$. The probability that concurrent transmission occurs resulting from node W is the probability that node W starts to transmit during the concurrent slot and all nodes in [R+x, R+y] are not in transmitting state, which is expressed as Eq. (4.31). The transmissions from nodes in [R, R+x] have been taken into account for the analysis of hidden terminals in Eq. (4.30), and hence, we do not need to consider such transmissions for concurrent transmission impact analysis.

$$P_s(y,x) = \pi_1 \sum_{i=0}^{\infty} (1-\pi_{TX})^i \frac{(\beta(y-x))^i}{i!} e^{-\beta(y-x)} = \pi_1 e^{-\beta\pi_{TX}(y-x)} \tag{4.31}$$

Hence, the average number of nodes that start transmission during the slot that collides with the transmission from O is:

$$\bar{n}_S = \beta \int_x^R P_s(y,x)dy = \beta \int_x^R \pi_1 e^{-\beta\pi_{TX}(y-x)} dy = \frac{\pi_1}{\pi_{TX}} (1-e^{-\beta\pi_{TX}(R-x)}) \tag{4.32}$$

Suppose node V is $|z|$ away from O, -(R-x)<z<0, the probability that the concurrent transmission occurs resulting from node V is the probability that node V starts to transmit during the concurrent slot and all nodes in [z-R, -R] are not in transmitting state, which is expressed as:

$$P_s'(z,x) = \pi_1 \sum_{i=0}^{\infty} (1-\pi_{TX})^i \frac{(\beta|z|)^i}{i!} e^{-\beta z} = \pi_1 e^{-\beta\pi_{TX}|z|} \tag{4.33}$$

Therefore, the average number of nodes located in area [-(R-x), 0] that start transmission during the concurrent slot that collides with the transmission from O is

$$\begin{aligned}\bar{n}_T &= \beta\int_{-(R-x)}^{0} P_s'(z,x)dz = \beta\int_{-(R-x)}^{0} \pi_1 e^{-\beta\pi_{TX}|z|}dz \\ &= \beta\int_{0}^{R-x} \pi_1 e^{-\beta\pi_{TX}z'}dz' = \frac{\pi_1}{\pi_{TX}}(1-e^{-\beta\pi_{TX}(R-x)})\end{aligned} \tag{4.34}$$

Hence, the total average number of nodes that may transmit concurrently is:

$$\bar{n}_\Sigma = \bar{n}_s + \bar{n}_T + \beta x\pi_1 \tag{4.35}$$

Therefore, given Poisson node distribution, the probability that no nodes within the reception range of *U* start transmission during the slot that collides with the transmission from *O* is:

$$P_{con}(x) = \frac{(\bar{n}_\Sigma)^0}{0!}\exp(-\bar{n}_\Sigma) = \exp(-\bar{n}_\Sigma) \tag{4.36}$$

Taking hidden terminal and possible packet collisions, the node reception probability that the node *U* receives the broadcast message from the tagged node *O* is:

$$P_s(x) = P_H(x)P_{con}(x) \tag{4.37}$$

4.4.2.2 T-window Reliability

Application-level T-window reliability is defined in [53] as the probability of successfully receiving at least one packet out of multiple packets from a broadcast vehicle at distance *x*, within a given time *T* (referred to as application tolerance window):

$$P_{app}(x,T) = 1-(1-P_s(x))^{\frac{T}{\tau}} \tag{4.38}$$

where τ is the beacon generation interval and $P_s(x)$ is the node reception probability given in Eq. (4.37).

4.4.2.3 Application-level Delay

Application-level latency [53] T_D is the duration between the time when a broadcast packet is generated at application layer of transmitting vehicle and the time at which the first successful packet is received by the application layer of receiving vehicle. Suppose the distance between the transmitting vehicle and the receiving vehicle is x, the average application-level delay is given by:

$$E_{T_D}(x) = \sum_{i=1}^{\infty} [(i-1)\tau + E[D]] P_s(x)(1-P_s(x))^{i-1} = E[D] + \tau\left(\frac{1}{P_s(x)} - 1\right) \tag{4.39}$$

where $E[D]$ is the mean transmission delay of the beacon message, which is given in Eq. (4.22).

4.4.2.4 Awareness Probability

The awareness probability [54] is the probability of successfully receiving at least n packets in the tolerance time window T.

$$P_A(x,n) = \sum_{k=n}^{\left\lfloor \frac{T}{\tau} \right\rfloor} \binom{\left\lfloor \frac{T}{\tau} \right\rfloor}{k} P_s(x)^k (1-P_s(x))^{\left\lfloor \frac{T}{\tau} \right\rfloor - k} \tag{4.40}$$

where x is the distance between the sender and receiver. It is noted that the awareness probability $P_A(x, n)$ becomes the application-level T-window Reliability $P_{app}(x, T)$ as n is equal to 1.

4.4.2.5 Average Number of Invisible Neighbors

Region of interest (ROI) has been proposed in [53] to present the size of the geographical region covered by entities participating in an application. For a safety application to work properly, a vehicle needs to be aware of the neighbors' status within ROI. Different applications may have different ROI. The invisible neighbor problem is defined in [55]: if vehicle A has not received any broadcast packet from vehicle B for a certain time interval, vehicle B is an invisible neighbor of A. Therefore, under the concept of ROI, the number of invisible neighbors needs to be under a certain constraint to satisfy the QoS of an application. We adopt this concept and newly define another application-level performance metric: average number of invisible neighbors within range x from the receiver after a tolerant time window T.

$$N_{invisible}(x) = 2\beta x\left(1-\int_0^x \frac{1}{x}\cdot P_{app}(s,T)ds\right) = 2\beta x - 2\beta\int_0^x P_{app}(s,T)ds \tag{4.41}$$

4.5 Numerical Results

Matlab is used for the computation of analytic models and simulations. The first subsection describes the simulation procedure. The second subsection compares the analytic results with the simulations, which show the high accuracy of our decomposition-based analytic approximation. The last subsection compares the model in [52] (Poisson arrival with infinite queue) and the model in [51] with the new proposed model (periodic arrival with packet replacement strategy).

4.5.1 Numerical Results for MAC-level Performance Metrics

4.5.1.1 Simulation Description

Discrete-event simulation is conducted in Matlab to assess the approximation error in the decomposition and fixed-point iteration used in solving the analytic model. Different from the decomposition method used for the analytic model, the simulation process simulates the overall system behavior of the GSMP model. To better illustrate the simulation procedure, a brief simulation flow chart is presented in Fig. 4.8. Note that this flow chart is drawn from the whole system's perspective, whereas each individual vehicle's behavior is consistent with the operation flow in Fig. 2.1. In Fig. 4.8, neighbors of the transmitting vehicle refer to the vehicles within the transmitting vehicle's transmission range. Possible backoff behavior of the neighbors is considered while deferring or resetting their next event time. This simulation procedure is performed multiple times based on independent replications, from which confidence intervals of the output measures are computed.

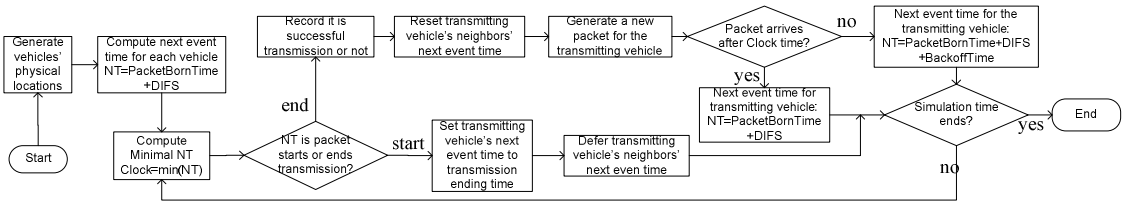

Figure 4.8: Simulation flow chart

4.5.1.2 Analytic Vs. Simulation Results

The same typical DSRC parameter settings as that in Table 3.1 in [52] are used for the proposed model. The numerical results from the analytic solution including mean transmission delay, PDR, PRR and normalized throughput are plotted in Figs. 4.9-4.12 respectively, vs. the vehicle density β (# vehicles per meter), data rate R_d (*Mbps*), packet generation interval τ (*second*) and packet length *PL* (*byte*).

We conducted 30 runs of simulation and each run last 5 seconds. Due to the Central Limit Theorem, normal distribution is assumed to compute confidence intervals for the population means of the output measures. Eq. (4.42) shows the 100(1-α)% confidence interval for population mean x, where x stands for the sample mean, σ for sample variance, n for sample size (*i.e.*, number of simulation runs) and z for critical value of normal distribution.

$$\bar{x} - z_{\alpha/2} \cdot \frac{\sigma}{\sqrt{n}} \le x \le \bar{x} + z_{\alpha/2} \cdot \frac{\sigma}{\sqrt{n}} \tag{4.42}$$

The simulation results for 95% confidence interval are also illustrated in Figs. 4.9-4.12 to compare with analytic-numerical results. The good match of the analytic and the simulation results verifies the accuracy of our proposed model. The packet replacement probability P_f is extremely low from our numerical analysis resulting from the fact that packet transmission delay is much smaller than the packet generation interval as shown in Fig. 4.9. Figs. 4.9-4.11 show that mean transmission delay, PDRs and PRRs benefit from high data rate and short packet length. Furthermore, PDRs are less than PRRs

given the same network parameters. Fig. 4.12 shows that normalized channel throughput increases as vehicle density increases resulting from more severe channel contentions. It may become saturated due to more severe packet collisions.

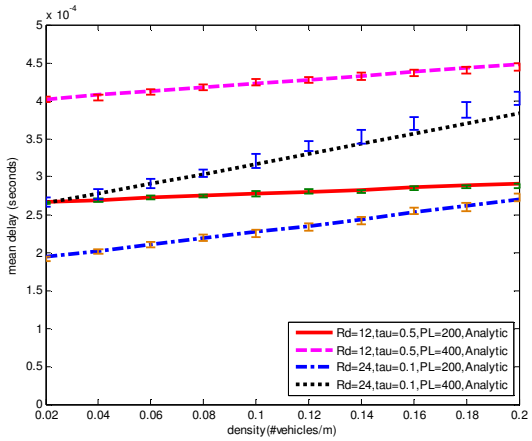

Figure 4.9: Mean transmission delay

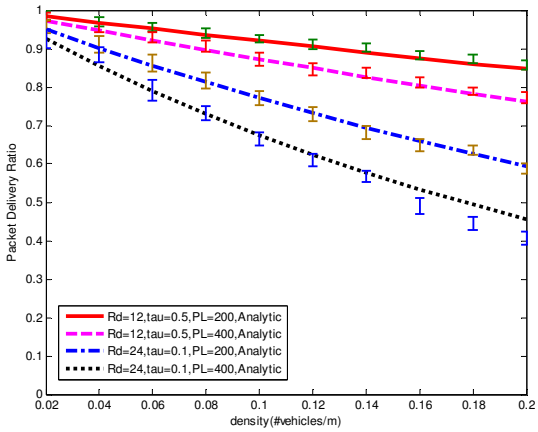

Figure 4.10: Packet delivery ratio

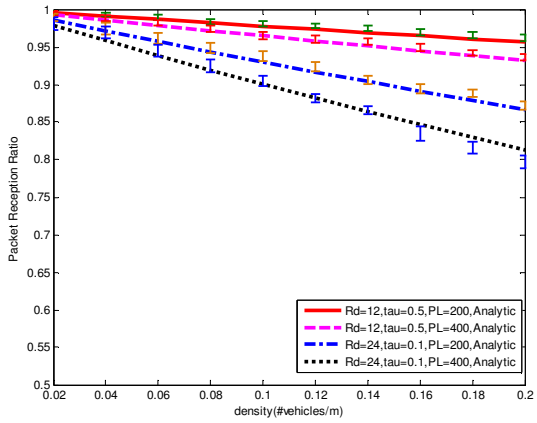

Figure 4.11: Packet reception ratio

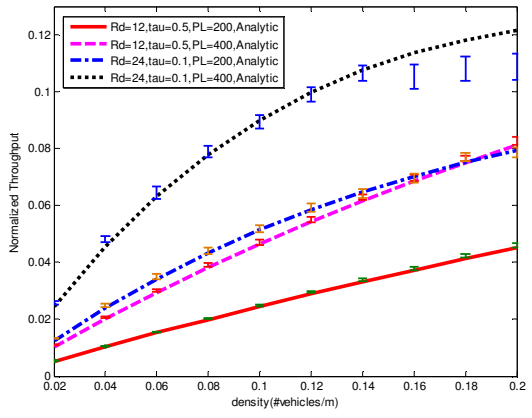

Figure 4.12: Normalized channel throughput

4.5.1.3 Compare with Previous Models

In this section, the model in [52] and the model in [51] are compared with our proposed model. These three models are comparable since all of them concentrate on

MAC layer behavior of safety message transmissions. However, the model in [52], denoted as model 1, assumes Poisson packet arrivals and that each vehicle has an infinite queue to store generated packets, which may be unrealistic for beacon messages. The proposed model, denoted as model 2, relaxes these assumptions and focuses on periodic message generation and no queue scenario (*i.e.*, out-dated message is replaced by the new message), which is more practical. Bastani's model proposed in [51] accounted for the periodic nature of beacon message generations and new message canceling out old message phenomena. However, their model does not accurately capture the periodic beacon message generation since it separates the periodic message generation from the message channel contention and transmission behavior, although these behaviors are closely correlated. Since the output measures computed in [51] are different from those we calculated in this chapter, Bastani's model is slightly modified, denoted as model 3, to obtain PDR for comparison. Eq. (11) in [51] for probability of successful transmission is modified to compute packet delivery ratio (PDR) of beacon message only as follows:

$$PDR = \left(1-\tau^b\right)^{N_{tr}-1+N_{ph}\frac{T_h^b}{p\cdot T_s^b+(1-p)\sigma}} \tag{4.43}$$

where

$$\tau^b = \frac{2}{W+1+2\tau/\sigma}; p = 1-\left(1-\tau^b\right)^{N_{tr}}; T_h^b = 2T_s^b; T_s^b = PL/R_d + T_H + \delta \tag{4.44}$$

Figs. 4.13-4.15 present the analytic-numerical results comparison of these three models. Notice that packet generation rate λ in model 1 is set to be equivalent to the reciprocal of

the packet generation interval τ in model 2 and model 3. The results show that the mean transmission delay obtained from model 2 is slightly higher than that from model 1, whereas the PDR and PRR are slightly lower than that from model 1. Taking into consideration the variations in the simulations results (*i.e.*, 95% confidence intervals) in Figs. 4.9-4.11, we can conclude that model 1 leads to similar results with model 2. In other words, Poisson arrival with infinite queue scenario can be used to approximate the periodic beacon message generation without any queue case. Such phenomena may result from the fact that the packet generation interval is much larger than the packet transmission delay, which further implies that a packet is out-dated and replaced by the next packet with a very low probability. Therefore, queue length does not have significant influence on packet transmissions. Fig. 4.14 also shows that PDR obtained from model 3 has a good match with model 1 and model 2 when the beacon message generation interval is longer. However, when the beacon message is generated more frequently, model 3 has much higher PDR than model 1 and model 2. Compared with the simulation results in Fig. 4.10, we conclude that model 3 is not as accurate as model 2 proposed in this chapter. The possible reason is already stated earlier.

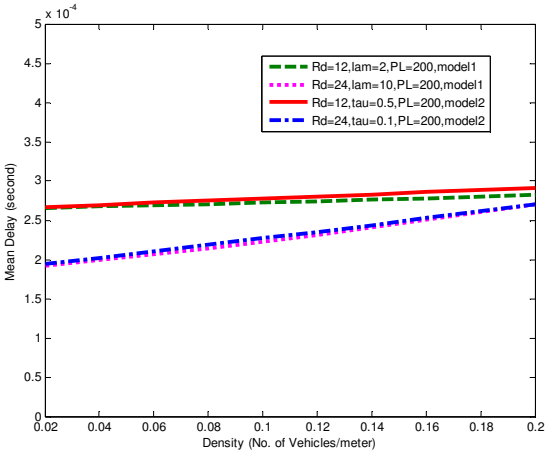

Figure 4.13: Comparison of mean delay

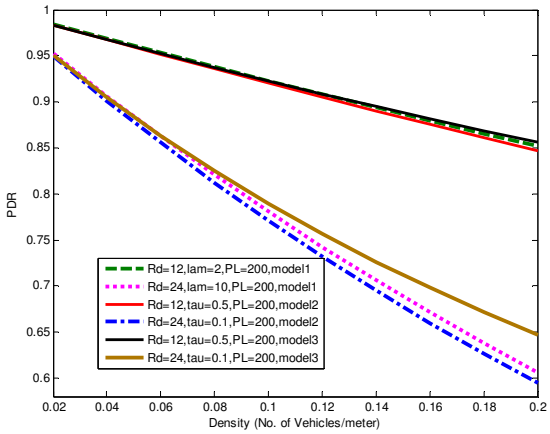

Figure 4.14: Comparison of PDR

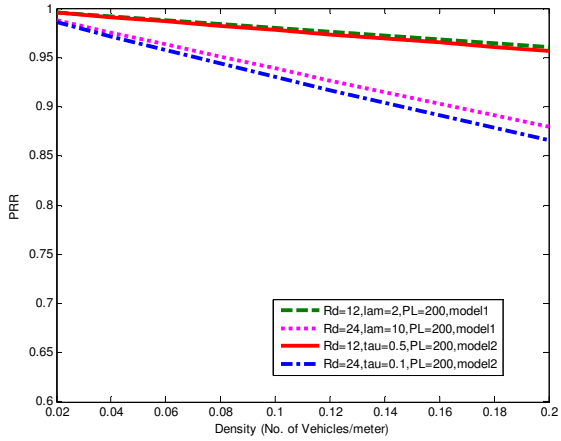

Figure 4.15: Comparison of PRR

4.5.2 Analytic-Numerical Results for Application-level Performance Metrics

4.5.2.1 Analytic-numerical Results for Fixed Network Parameters

Table 4.1: Network parameter settings

Parameters	Values	Parameters	Values
Transmission range R	500 m	Packet length PL	400 *bytes*
Time window T	1 s	Beacon message interval τ	0.1 s
Data rate R_d	24 *Mbps*	Vehicle density β	0.1 *vehicles/m*

In this section, the application-level performance metrics are evaluated for a given network parameter settings as shown in Table 4.1.

Fig. 4.16 shows that NRP decreases linearly with the distance from the sender. The awareness probability also decreases with the distance to the sender. Note that the Application-level T-window Reliability is equivalent to the awareness probability with packet requirement n=1. The application with stricter packets requirements has lower awareness probability. During the time window T=1s, there are 10 beacon packets sent out from the sender since the beacon message interval is 0.1s. If the packet requirement is less than or equals to 5 packets, the awareness obtained is larger than 99%, which can ensure the application works appropriate even though the NRP in the network layer is not very high. Otherwise, if the packet requirement is larger than 5 among 10 packets transmitted within 1 second, the application layer awareness probability may be even lower than the NRP in the network layer as seen from PA(n=8) case. Hence, for some applications that require more than 5 packets within T=1s, the reliability requirement may not be met.

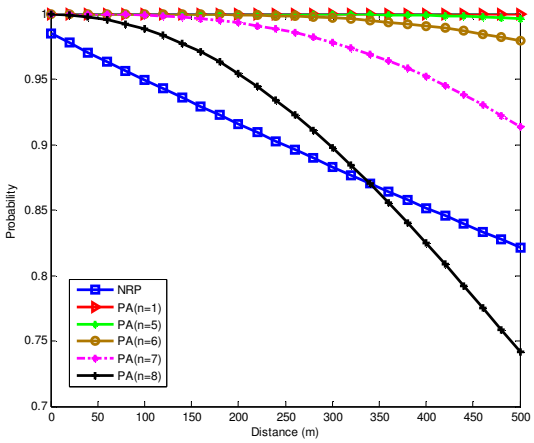

Figure 4.16: Node reception probability (NRP) and awareness probability (PA) with different packet requirement *n*

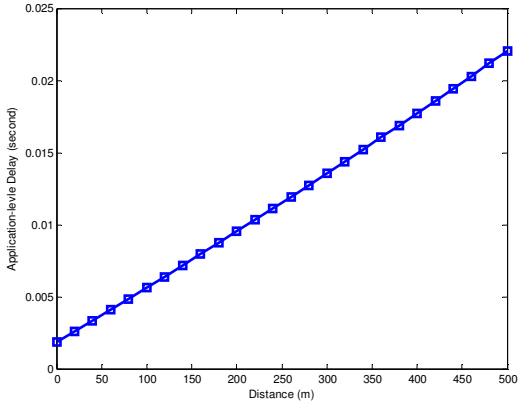

Figure 4.17: Application-level delay

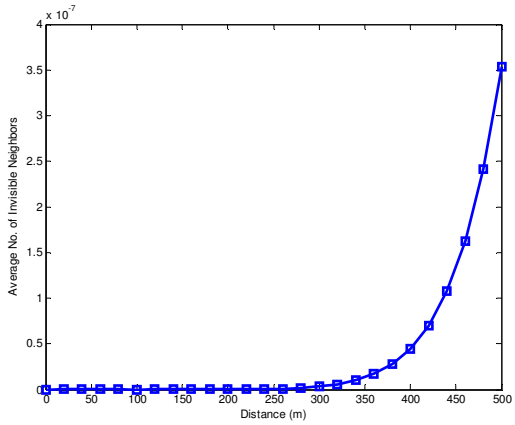

Figure 4.18: Average no. of invisible neighbors

Fig. 4.17 shows that the application-level delay increases almost linearly with the distance. Furthermore, compared to the MAC-level transmission delay in Fig. 4.9, the application-level delay is much higher, especially when the distance between the sender and receiver is large. Such phenomena results from the fact that NRP decreases linearly according to the distance. Fig. 4.18 shows that the number of invisible neighbors

increases fast when the distance exceeds 300m. However, the number of invisible neighbors is quite small (in the order of 1E-6), which means that the receiver can receive at least one packet from almost every neighbor within time window T=1s and hence all neighbors are visible to the receiver.

4.5.2.2 Analytic-numerical Results for Different Network Parameters

In order to evaluate the influences of different network parameters such as data rate, beacon message interval and packet length on the application-level metrics, we vary three input parameter value in Table 4.1 and analyze the output measures as shown in Figs. 4.19-4.22. The legend represents the data rate R_d (*Mbps*), beacon message interval τ (s) and data length PL (*bytes*), respectively.

Fig. 4.19 and Fig. 4.20 show that increasing the data rate helps increasing NRP and awareness probability (more obvious when the distance to the sender is large). Another important observation is that decreasing the beacon message interval (*i.e.*, messages are sent more frequently) will decrease the NRP, but increase awareness probability. This implies that even though more collisions occur in the MAC layer resulting from higher beacon message generation rate, we may still obtain satisfied QoS in the application layer. Furthermore, increasing the packet length leads to decreasing NRP and decreasing awareness probability. Therefore, we can improve the awareness probability by increasing the data rate, decreasing the data length or decreasing the

beacon message interval within the acceptable ranges for these parameters based on performance of IEEE 802.11p protocol.

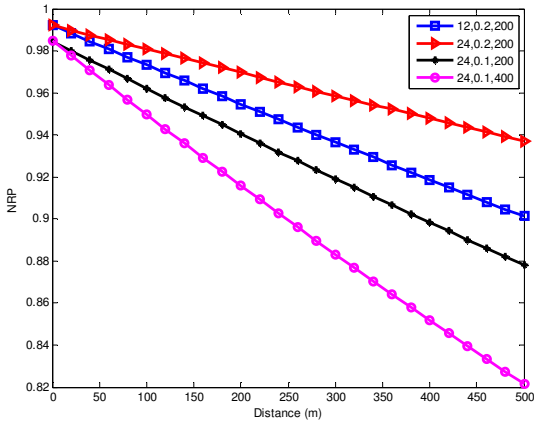

Figure 4.19: Node reception probability (NRP)

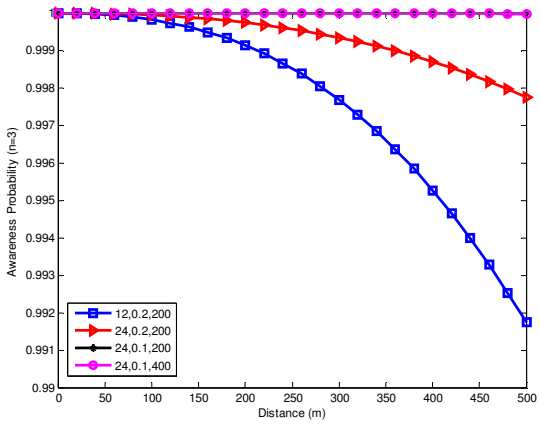

Figure 4.20: Awareness probability PA(n=3)

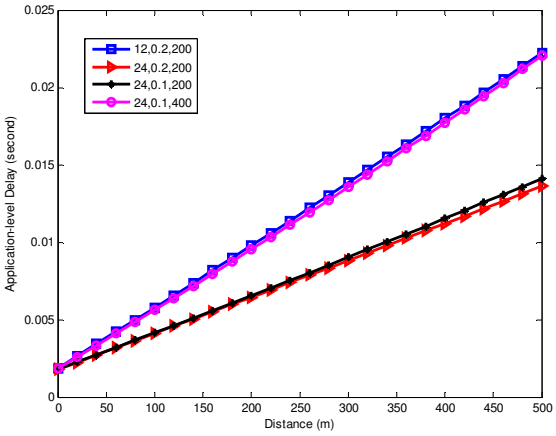

Figure 4.21: Application-layer delay

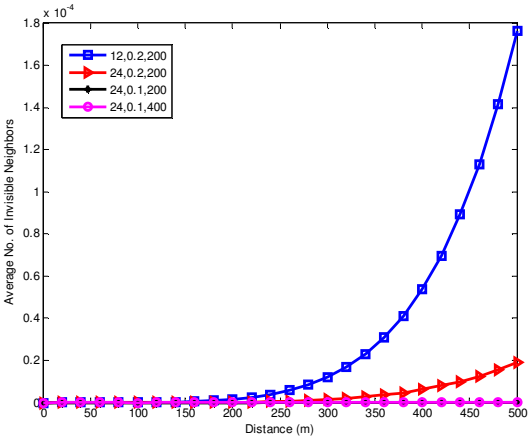

Figure 4.22: Number of invisible neighbors

Fig. 4.21 shows that increasing data rate or decreasing data length helps reducing the application-level delay. In addition, even though decreasing beacon message interval has significant impact on NRP and awareness probability (*i.e.*, decrease NRP whereas

increase awareness probability), it has little impact on the application-level delay. Therefore, to reduce the application-level delay, we can increase data rate or decrease the data length reasonably.

Fig. 4.22 shows that the number of invisible neighbors is relatively small for the given four sets of input parameters, which is in the order of 1E-4. We observe that the number of invisible neighbors has the inverse trend as the awareness probability. Hence, based on the observations for the awareness probability, we conclude that increasing data rate, decreasing data length or decreasing the beacon message interval helps reduce the number of invisible neighbors.

4.6 VANET Applications Evaluation

4.6.1 Application Requirements

In this chapter, we propose to specify the performance requirements for applications in terms of the following aspects to provide satisfied QoS:

- Range of interest (ROI) [53]: intended message delivery range R_I;
- Delay requirement: the time for a vehicle to receive beacon messages from any one of its neighbors within range R_I has to be less than D second;
- Awareness probability [54]: the probability that a vehicle successfully receives at least n packets from any one of its neighbors within range R_I in the tolerance time window T has to be larger than p_a;

- Average number of invisible neighbors [55]: the average number of invisible neighbors within range R_I in tolerance time window T has to be less than N;

Given the above application-level performance metrics, our proposed analytic models can be used to evaluate whether the given network parameters can satisfy the QoS requirement or not for an application. In addition, we can provide insights to tune the network parameters to meet the application requirements.

4.6.2 Case Studies for VANET Applications

Vehicles are able to track surrounding vehicles' status by their periodically broadcasted beacon messages containing position, velocity and acceleration. Many safety applications judge the risk based on such information and provide corresponding warnings to the driver to prevent potential accidents. In this section, three typical safety applications [58] are analyzed.

4.6.2.1 Emergency Vehicle Warning

Vehicles can receive route information of emergency vehicles (*e.g.*, police cars, ambulances, fire trucks *etc.*) from the beacon messages received. Hence, based on such information, emergency vehicle warning application [59] enables drivers to be aware of the emergency vehicle and take appropriate actions to reduce accidents and save time. Some reasonable assumptions are made for the performance requirements of the emergency vehicle warning application: The ROI is 500m [60]; Delay requirement is 1000ms [60]; Awareness probability that a vehicle successfully receives at least 1 packet

in the tolerance time window T=1s is larger than 99.9%; Average number of invisible neighbors is less than 1.

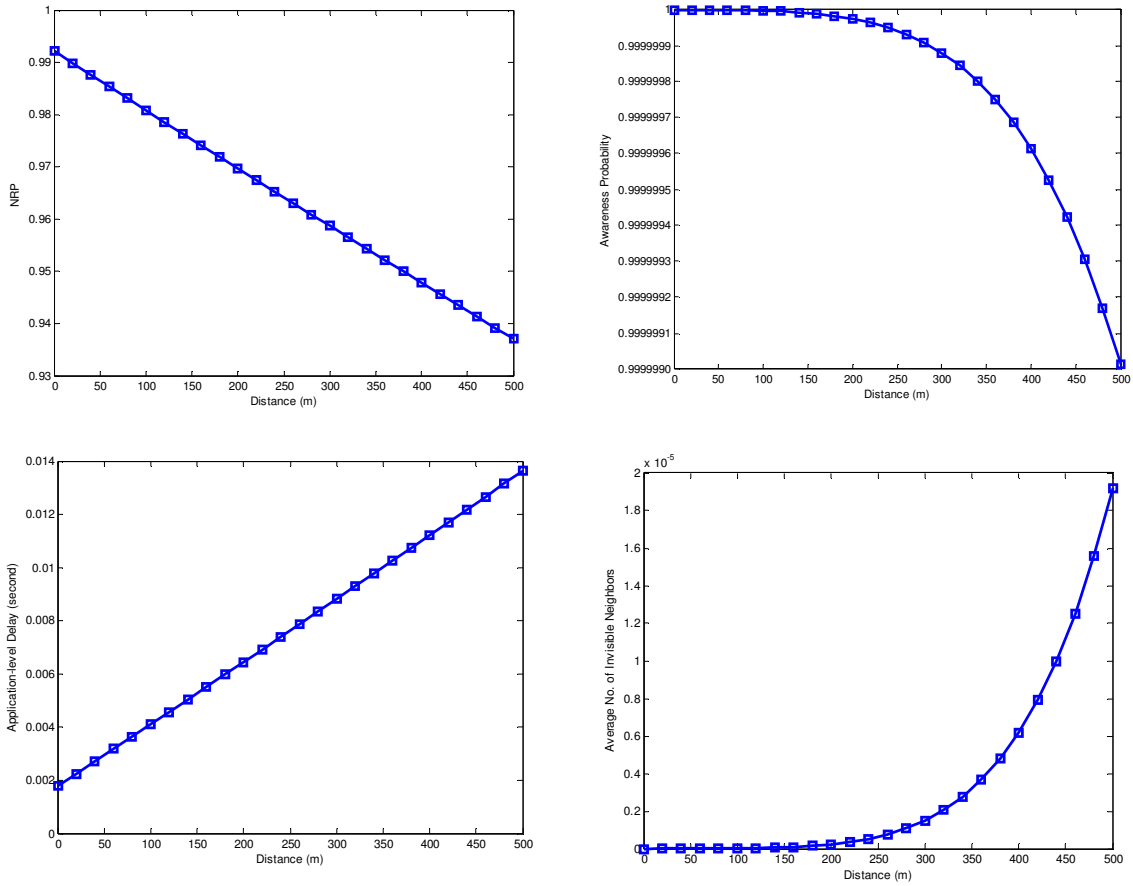

Figure 4.23: Emergency vehicle warning application-level metrics with parameters R_d=24, τ=0.2, PL=200

Fig. 4.23 shows that the application-level delay, awareness probability and average number of invisible neighbors requirement can all be satisfied with given input parameters R_d=24$Mbps$, τ=0.2s, PL=200$bytes$.

4.6.2.2 Slow Vehicle Indication

Slow vehicle indication application [58] is able to provide alerts to the driver about potential hazard if a slow vehicle is detected based on the beacon messages received. For the slow vehicle indication application to work properly, the vehicle has to receive beacon messages from the slow vehicle timely and reliably. This application may have stricter awareness requirements than the emergency vehicle warning application.

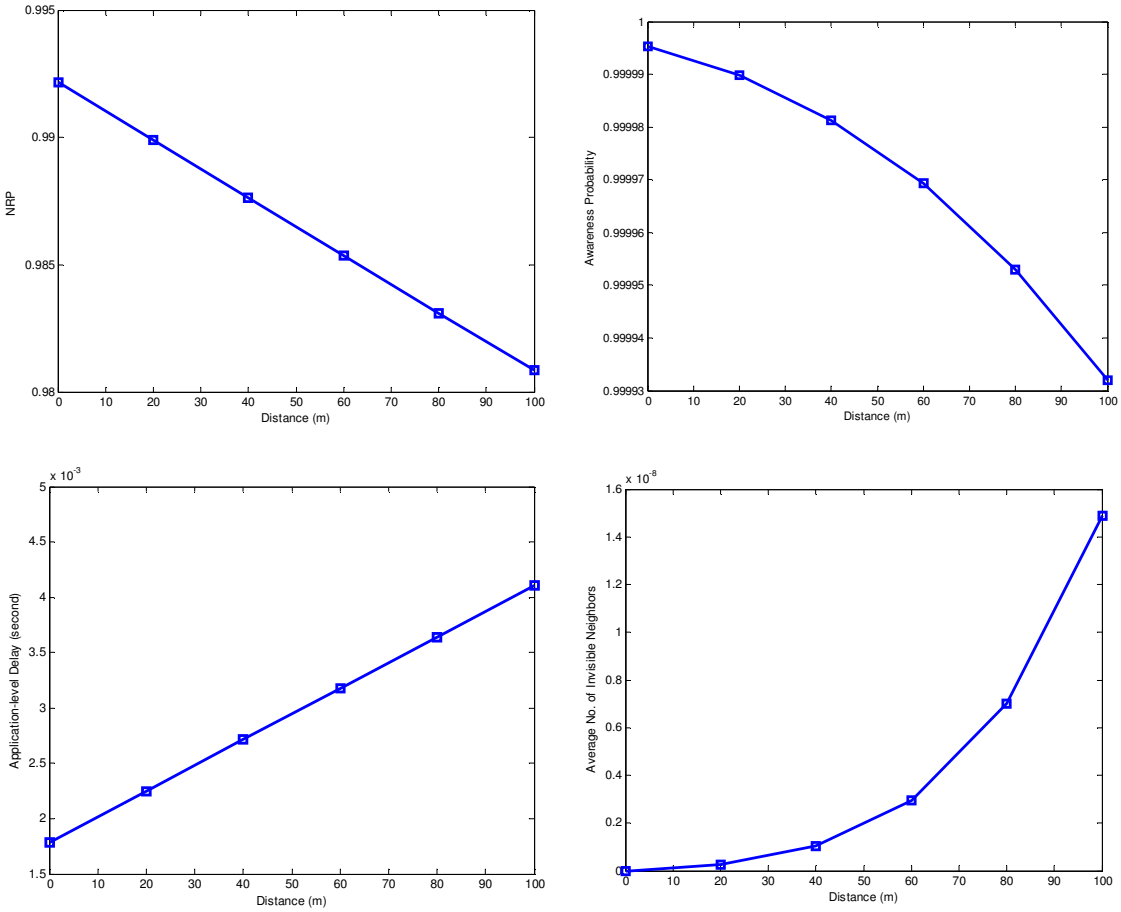

Figure 4.24: Slow vehicle indication application-level metrics with parameters R_d=24, τ=0.2, PL=200

The performance requirement assumptions can be made as follows: The ROI is 100*m*; Delay requirement is 50*ms*; Awareness probability that a vehicle successfully receives at least 3 out of 5 packets in the tolerance time window T=1*s* is larger than 99.9%; Average number of invisible neighbors is less than 1.

Fig. 3.24 shows that application-level delay, awareness probability and average number of invisible neighbors requirement can all be satisfied with given input parameters R_d =24*Mbps*, τ=0.2*s*, PL=200*bytes*.

4.6.2.3 Rear-end Collision Warning

Rear-end collision warning application should have stricter awareness requirements than the previous two applications since it is more critical for safety. Therefore, we suggest the performance requirements to be: The ROI is 50*m*; Delay requirement is 20*ms* [60]; Awareness probability that a vehicle successfully receives 4 out of 5 packets in the tolerance time window T=1*s* is larger than 99.9%; Average number of invisible neighbors is less than 1.

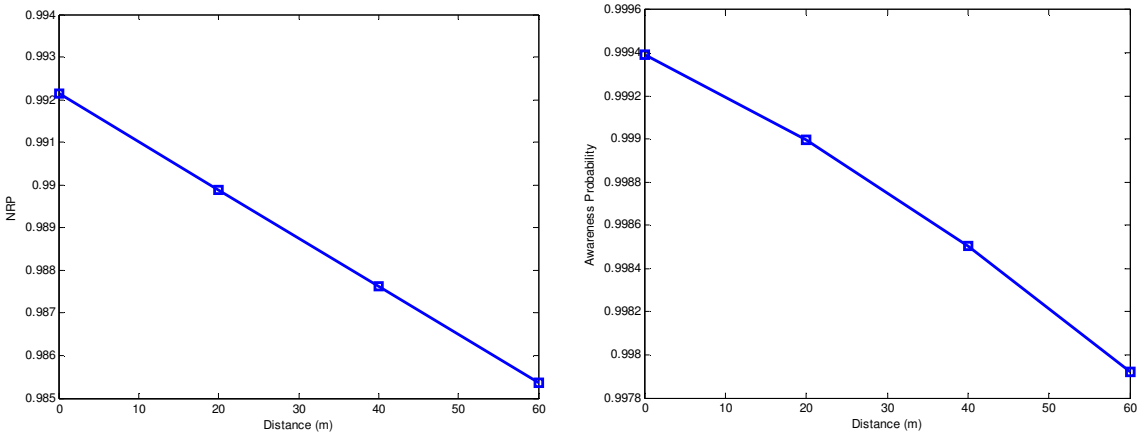

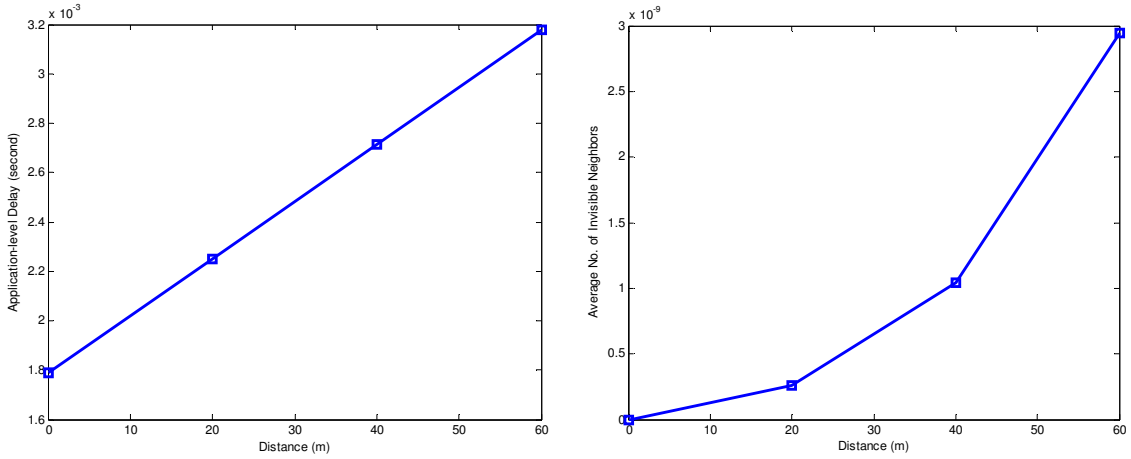

Figure 4.25: Rear-end collision avoidance application layer metrics with parameters R_d=24, τ=0.2, PL=200

Fig. 3.25 shows that the application-level delay and average number of invisible neighbors can satisfy the requirement given the input parameters. However, the awareness probability is lower than 99.9% when the distance to the sender is larger than 20m. Therefore, the rear-end collision avoidance application cannot provide the satisfactory QoS for the given input parameters. To meet the application requirement, based on the conclusions obtained in Section 4.5.2.2, we can improve the awareness probability by increasing the data rate, decreasing the data length or decreasing the beacon message interval.

4.7 Conclusions

In this chapter, an analytic model is developed to characterize the periodic beacon message dissemination in DSRC for highway safety communications. Instead of assuming Poisson arrivals and infinite queue as in most of the literature, the periodic

packet generation and out-dated information replacement are taken into consideration in the new proposed model. Important MAC-level performance indices such as the mean transmission delay, PDR, PRR and normalized channel utilization are analytically derived and computed. Detail simulations for the overall system in the MAC layer are conducted to verify the accuracy of the decomposed model. The model is also compared with previous model that assumed Poisson arrival and infinite queue and Bastani's model.

Besides MAC-level performance evaluation, application-level performance metrics including T-window reliability, application-level delay, awareness probability and average number of invisible neighbors are analytically derived based on the node reception probability. The analytic-numerical results are evaluated for application-level performance metrics under various network parameters. Such analysis can be very useful for tuning network parameters in order to obtain satisfied QoS for many safety applications. Three typical safety applications including emergency vehicle warning, slow vehicle indication and rear-end collision warning are assessed to check whether their performance requirements can be met for a given network parameter setting.

In the next chapter, we will take into account the channel switching behavior [26] between the control channel and service channels, where the control channel is used for beacon message and service channels are used for other types of messages. Furthermore, the assumptions in Section 4.2 will also be relaxed to reflect real world traffic scenarios.

For example, the MAC layer and application layer performance metrics will be analyzed incorporating fading channel. In addition to 1-D highway scenarios, 2-D models are also developed in Chapter 8.

5. Multiple Types of Services Evaluation

5.1 Motivation

According to the updated version of the DSRC standard [11], the DSRC physical layer follows the same frame structure, modulation scheme and training sequences specified by IEEE 802.11a physical layer standard with minor changes; MAC layer of the DSRC is equivalent to the Enhanced Distribution Coordination Access (EDCA) 802.11e that has four different access classes (ACs).

In the literature, unicast for IEEE 802.11 has been extensively investigated. Bianchi [27] proposed a simple yet accurate discrete-time Markov chain (DTMC) model to evaluate the MAC-layer performance of unicast mechanism under saturation conditions. His paper has inspired many other researchers to develop analytic models of unicast EDCA based on DTMC. The saturation performance for multiple types of services with priorities using EDCA mechanism has been studied in [81][82][83][84][38]. Many later work [85][86][87][88][89] extended to the unsaturation packet generation case, which reflects a more practical scenario. However, most previous researches are based on Bianchi's DTMC (*i.e.*, per-slot statistics) model [27] and ignore important aspects of continuous time system behavior leading to approximations. More specifically, due to the characteristic of such discrete model, backoff counter freezing behavior cannot be accurately captured. Lee [38] considered such freezing process by adding sub-Markov chain for multiple services using EDCA. However, the backoff

counter freezing time because of the busy medium (*i.e.*, waiting for the packet in the channel finishing transmission) is still not taken into account. In a recent paper by Tinnirello and Bianchi [37], an analytic model not based on the per-slot statistics was proposed through a fixed-point computation of the residual backoff counter distribution occurring after a generic transmission attempt. However, this is only for the saturation condition.

Recently, a few analytic models [33][90][91] are proposed to quantify the MAC-layer performance of multiple types of safety messages using broadcast EDCA over the control channel in DSRC based VANETs. Gallardo [33] used three DTMC models to capture the EDCA behavior for three types of messages for the performance evaluation. However, hidden terminal problem is not considered in this work and no simulation results are presented to verify the accuracy of the models. Hafeez [90] evaluated the broadcast performance of two types of safety messages under EDCA taking into consideration of interferences from hidden terminals. Nevertheless, the analytic model is also based on DTMC (per-slot analysis) and ignores the continuous time system behavior. More specifically, the backoff counter freezing process has not been accurately captured by the DTMC and the post backoff process is also not considered in this work. In addition, total reliability (*i.e.*, probability of successful reception) for packet transmission is computed instead of providing separate reliability for each type of services, which may not lead to comprehensive conclusions. Khabazian [91] proposed an

analytic model for the performance of multi-hop message dissemination with two classes of traffic. However, the detailed backoff process is not considered in the model and the channel service time is assumed to be exponential distributed, which may lead to approximations for the transmission delay computation.

In this chapter, we extend the work presented in Chapter 3 [12][52] for one type of services to three types of services using EDCA mechanism for one-hop direct broadcast over the control channel. We are interested in whether EDCA mechanism can provide service differentiations with respect to the performance and reliability. The generation and service of each type of safety messages in each vehicle is modeled by a generalized M/G/1 queue, where two classes of service are considered based on Welch's method [13]. The overall model is a set of interacting M/G/1 queues, three queues for each vehicle. The interaction is that the server is shared as it is the contention medium/channel for the safety message transmissions. To make the model scalable, we use semi-Markov process (SMP) model to capture the shared server's behavior for each service from a single tagged vehicle's perspective, where the medium/channel contention and backoff behavior for this type of service and the influence from the same vehicle and other vehicles are considered. Different from the previous DTMC models capturing the shared server's discrete time behavior, this SMP model directly incorporates the unsaturation condition of the queue in a continuous time fashion. It interacts with the tagged vehicle's M/G/1 queue through the fixed-point iteration.

The major contributions made in this research are five-fold. First, the proposed analytic models provide an accurate analysis for different types of broadcast services over DSRC channel using EDCA mechanism with unsaturated message generation and hidden terminals in the continuous time. Second, the service time for packets is divided into two classes (i) for the packet arrivals when the queue is empty; (ii) for the packet arrivals when the queue is not empty. Based on Welch's method with two classes of arrivals in an M/G/1 queue, more accurate results can be obtained. Third, based on the solution to the interacting SMP model and M/G/1 queuing model, expressions of MAC-layer performance metrics for DSRC vehicular safety communications are derived. These metrics include the mean and variance of the transmission delay, packet delivery ratio (PDR) and packet reception ratio (PRR). The analytic results are verified by simulations to show the errors in the approximations are small. Fourth, the MAC-layer performances for EDCA mechanism are evaluated according to various input parameters. The analysis shows that EDCA provides only latency differentiations but not reliability. Fifth, the M/G/1 queue is extended to GI/G/1 queue to incorporate more generalized packet arrival process. Whitt's method is used to compute the mean and variance of the waiting time for GI/G/1 queue instead.

This chapter is organized as follows. Section 5.2 briefly describes the system behavior in IEEE 802.11 MAC layer protocol and lists the assumptions made to produce a tractable model. Section 5.3 presents the analytic models and the fixed-point iteration.

MAC-layer performance indices including mean and variance of the transmission delay, PDR and PRR are derived in Section 5.4. The analytic and simulation results are compared in Section 5.5. Section 5.6 presents the extended analytic models to incorporate generalized distributed packet arrival process using GI/G/1 queue. A case study is constructed and evaluated in Section 5.7. Conclusions are presented in the last section.

5.2 System Description and Assumptions

As we know from [1], the DSRC MAC layer adopts IEEE 802.11 MAC layer specification with minor modifications. In the 802.11 MAC layer protocol [11], distributed coordination function (DCF) is the primary medium access control technique for broadcast services. IEEE 802.11p MAC layer utilizes the Enhanced Distribution Channel Access (EDCA) that has different access classes (*ACs*) with priorities to ensure quality of services (QoS). Each class has different backoff window size and Arbitration Inter Frame Space (AIFS) number to ensure less waiting time for high priority class.

In this dissertation, we consider the scenario that each vehicle in the network can occasionally generate three types of safety-related packets and compete for the channel resource to transmit the packet. These different types of services are referred as access categories (*ACs*). Each *AC* has a unique queue in each vehicle to store messages generated. Therefore, each vehicle has three queues to store different types of messages.

The packets from different *ACs* will contend internally and the winner will contend externally with other vehicles in the network for the channel use.

The basic channel contention behavior follows the basic *DCF* mechanism with different backoff window size and *AIFS* for different *ACs*. For a newly generated packet AC_i in a vehicle, the vehicle senses the channel activity before it starts to transmit the packet. If the channel is sensed idle for a time period of $AIFS_i$, the packet can be directly transmitted. Otherwise, the vehicle continues to monitor the channel until it is detected idle for $AIFS_i$ time period. Subsequently, according to the collision avoidance feature of the protocol, the vehicle generates an initial random backoff counter and goes through the backoff process before transmitting the packet. Moreover, a vehicle must go through the backoff process between two consecutive packet transmissions even if the channel is sensed idle for the duration of $AIFS_i$ time for the second packet. Therefore, a packet AC_i generated in a vehicle can directly transmit without undergoing the backoff process only when the following two conditions are satisfied:

- The packet is generated in a vehicle when the queue for AC_i is empty;
- The channel is sensed idle for $AIFS_i$ time starting from the time instant that the packet is generated.

Regarding the backoff process for a packet transmission, the initial backoff counter is chosen randomly from a uniform probability mass function (pmf) over the range [0, W_i-1], where W_i represents the backoff window size. The backoff time counter is decreased

by one if the channel is sensed idle for a time duration σ, which represents a time slot. The counter is frozen when channel is sensed busy and reactivated when the channel is sensed idle again for more than the $AIFS_i$ duration for AC_i. The packet is transmitted as soon as the backoff counter reaches zero.

Several assumptions similar to Chapter 3 are made in the broadcast system to produce a simplified yet a high fidelity model. The vehicular ad hoc network is considered to be one-dimensional (1-D). All vehicles have the same transmission range and receiving range R. Three types of safety messages in the control channel are considered. Each vehicle is assumed to generate AC_i packets as a Poisson stream with rate λ_i. Each vehicle has three infinite queues, one for each type of messages, to store the packets at the MAC layer. Hence, each type of messages can be modeled as an M/G/1 queue. Queue-length process is independent and identically distributed (i.i.d.). Channel shadowing or fading, vehicle mobility and capture effect of transmissions are not considered in this chapter.

5.3 Analytic Models

Due to the contention medium, the overall problem can be seen as a set of interacting M/G/1 queues. Similar to the method presented in Chapter 3, we simplify the problem in this chapter by developing an SMP model for each AC in the tagged vehicle that does not directly keep track of the queued requests but captures the channel contention and backoff behavior. This SMP model and the corresponding AC's M/G/1

queue interact with each other and hence we need to use fixed-point iteration to solve the overall model.

5.3.1 SMP Model for AC_i Service

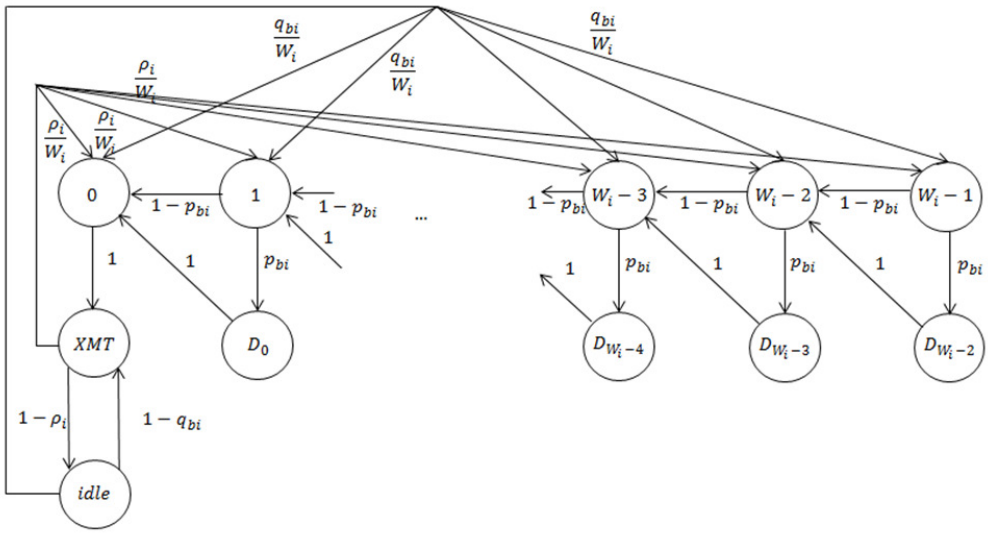

Figure 5.1: SMP model for AC_i message

The behavior of AC_i packet transmission can be characterized using the SMP model in Fig. 5.1. The AC_i is in *idle* state if there is no packet in its queue. After an AC_i packet is generated, the vehicle senses channel activity for $AIFS_i$ time period. If the channel is detected not busy during this period (with probability 1-q_{bi}, where q_{bi} represents the probability that the channel is detected busy in $AIFS_i$ time by AC_i), the AC_i goes from state *idle* to state *XMT*, which means that a AC_i packet is transmitting. Otherwise, the AC_i will randomly choose a backoff counter in the range [0, W_i-1]. The backoff counter will be decreased by one if the channel is detected to be idle for a time

slot of duration σ (with probability 1-p_{bi}, where p_{bi} represents the probability that the channel is detected busy in one time slot by AC_i), which is captured by the transition from state W_i-j to state W_i-j-1. If the channel is busy during a backoff time slot σ (*i.e.*, another vehicle is transmitting a packet), the backoff counter of the tagged vehicle will be suspended and deferred for the duration of packet transmission time TM_i, which presents the transition from state W_i-j to $D_{Wi\text{-}j\text{-}1}$ with probability p_{bi}. When the backoff counter reaches zero, the AC_i packet will directly be transmitted (an SMP transition occurs from state 0 to state *XMT* with probability one). In state *XMT*, a packet is transmitting. After the packet transmission, if there is no packet left in the queue for AC_i (with probability 1-ρ_i), the AC_i will go from state *XMT* to state *idle* and wait for a new incoming AC_i packet. If there are packets left in the queue after a packet transmission (with probability ρ_i), the vehicle will sense the channel again for $AIFS_i$ time and then randomly choose a backoff counter before transmitting the next AC_i packet.

Define the sojourn time in state j for AC_i as $T_{i,j}$. The mean and variance of $T_{i,j}$ are:

$$E\left[T_{i,j}\right]=\tau_{i,j}=\begin{cases}\sigma & j=0,1,\cdots W_i-1\\ TM_i=T_H+M_{PA}+\delta+AIFS_i & j=D_0,D_1,\cdots D_{W_i-2}\\ TD_i=T_H+PA_i/R_d+\delta+AIFS_i & j=XMT\\ 1/\lambda_i+AIFS_i & j=idle\end{cases} \tag{5.1}$$

$$Var\left[T_{i,j}\right]=\theta_{i,j}^2=\begin{cases}0 & j=0,1,\cdots W_i-1\\ 0 & j=D_0,D_1,\cdots D_{W_i-2},XMT\\ 1/\lambda_i^2 & j=idle\end{cases} \tag{5.2}$$

The AC_i packet length is PA_i. R_d presents the data rate. Hence, PA_i/R_d is the time to transmit the packet. T_H presents the time to transmit the packet header including physical layer header and MAC layer header. δ is the propagation delay.

$$AIFS_i = SIFS + AIFSN_i \cdot \sigma \qquad for \;\; i = 1,2,3 \tag{5.3}$$

The steady-state probability that a vehicle transmits an AC_i packet is:

$$EPA_i = \frac{TD_i - AIFS_i}{TD_i} \cdot \pi_{i,XMT} \tag{5.4}$$

where $\pi_{i,XMT}$ represents the steady-state probability that a vehicle is in state XMT for AC_i. TD_i - $AIFS_i$ is the real packet transmission time. Therefore, given a packet is transmitting through the control channel (any types of services is possible), the mean time to transmit this packet is:

$$M_{PA} = \frac{EPA_1 \cdot PA_1 + EPA_2 \cdot PA_2 + EPA_3 \cdot PA_3}{(EPA_1 + EPA_2 + EPA_3) \cdot R_d} \tag{5.5}$$

For the model in Fig. 5.1, the embedded DTMC is first solved for its steady-state probabilities [9][52]:

$$\begin{cases} v_{i,j} = (W_i - j) \cdot v_{i,W_i-1} & j = 0,1,\cdots W_i - 1 \\ v_{i,D_j} = (W_i - j - 1) \cdot p_{bi} \cdot v_{i,W_i-1} & j = 0,1,\cdots W_i - 2 \\ v_{i,XMT} = \dfrac{W_i}{\rho_i + q_{bi}(1-\rho_i)} \cdot v_{i,W_i-1} & \\ v_{i,idle} = \dfrac{(1-\rho_i)W_i}{\rho_i + q_{bi}(1-\rho_i)} \cdot v_{i,W_i-1} & \end{cases} \tag{5.6}$$

In the above equation,

$$v_{i,W_i-1} = \frac{2\left[\rho_i + q_{bi}(1-\rho_i)\right]}{\left[W_i + 1 + p_{bi}(W_i - 1)\right]\left[\rho_i + q_{bi}(1-\rho_i)\right] \cdot W_i + 2(1-\rho_i) \cdot W_i} \tag{5.7}$$

Taking account of the mean sojourn time in each state, the steady-state probabilities of the SMP are given by [22]:

$$\pi_i = \frac{v_i \tau_i}{\sum_j v_j \tau_j} \tag{5.8}$$

Therefore, the steady-state probability that an AC_i is in state XMT is given by:

$$\pi_{i,XMT} = \frac{2 \cdot TD_i}{\left[\rho_i + q_{bi}(1-\rho_i)\right]\left[(\sigma + p_{bi} \cdot TM_i)W_i + (\sigma - p_{bi} \cdot TM_i)\right] + 2 \cdot TD_i + 2(1-\rho_i)(1/\lambda_i + AIFS_i)} \tag{5.9}$$

Although the sojourn time in state XMT is TD_i, the real packet transmission only occupies a portion of this sojourn time, which is $PA_i/R_d+T_H+\delta=TD_i-AIFS_i$. Hence, the probability that a vehicle transmits in steady state is $\pi_{i,XMT}(TD_i-AIFS_i)/TD_i$, which is expressed in Eq. (5.4).

In Eq. (5.9), three unknown parameters are:

- ρ_i: the probability that there are AC_i packets in the queue of the tagged vehicle.
- p_{bi}: the probability that the channel is detected busy in one time slot by AC_i.
- q_{bi}: the probability that the channel is detected busy in $AIFS_i$ time by AC_i.

Since three types of AC_i are considered in this work, there are nine unknown parameters in total. These nine parameters are correlated with each other. This SMP model for ACi also interacts with the M/G/1 queue because parameter ρ_i depends on the mean service time to transmit an AC_i packet. Therefore, the service time is derived first in the next subsection. Section 5.3.3 subsequently illustrates the relationships between these

parameters and fixed-point iteration algorithm is utilized to compute the numerical results for these parameters as well as the service time.

5.3.2 Service Time Computation

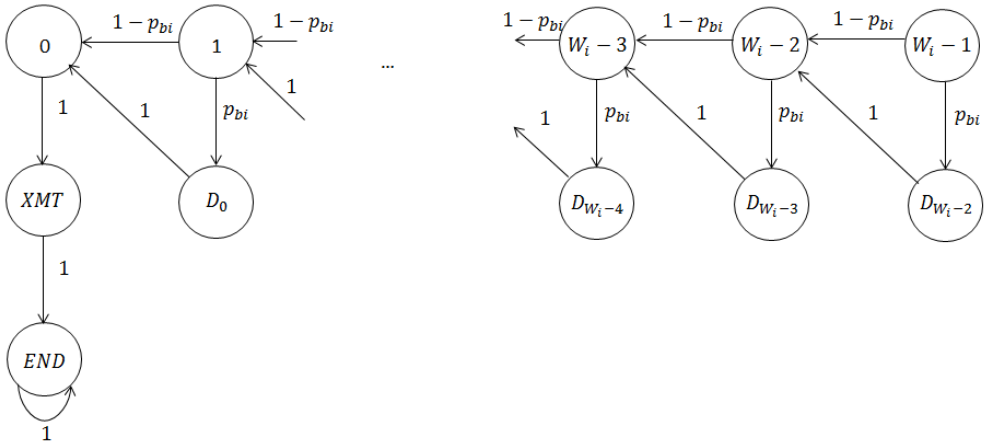

Figure 5.2: SMP model with absorbing state for service time computation

As mentioned above, each AC_i in a vehicle can be modeled as an M/G/1 queue. The MAC layer service time is defined as the time interval from the time instant when a packet becomes the head of the queue and starts to contend for transmission, to the time instant when the packet is received.

The SMP model in Section 5.3.1 describes the behavior of an AC_i continuously transmitting packets in its queue. In this section, the service time for any one AC_i packet in the queue needs to be derived. Therefore, the SMP model in Section 5.3.1 can be modified to contain an absorbing state as shown in Fig. 5.2. By properly allocating the initial probability, the time to reach the absorbing state will be the service time for an AC_i packet transmission.

Since the Markov chain contains an absorbing state, the transition probability matrix can be partitioned so that [9]:

$$P = \begin{bmatrix} Q & C \\ 0 & 1 \end{bmatrix} \tag{5.10}$$

where Q is a $2W_i$ by $2W_i$ sub-stochastic matrix describing the probabilities of transitions only among the transient states. The fundamental matrix is:

$$M = (I - Q)^{-1} \tag{5.11}$$

Let $X_{i,kj}$ be the random variable denoting the visit counts to state j before entering the absorbing state, given that embedded DTMC started in state k for AC_i. The expected number of visits to state j starting from state k before absorbing state is given by the (k,j)th element of the fundamental matrix M, hence:

$$E\left[X_{i,kj} \right] = m_{i,kj} \tag{5.12}$$

Due to the acyclic nature of the SMP model in Fig. 5.2, the fundamental matrix can be easily obtained through the definition of $X_{i,kj}$ instead of computing Eq. (5.11).

$$M_i=\left[m_{i,kj}\right]=\begin{array}{c} \\ 0 \\ 1 \\ 2 \\ \vdots \\ W_i-2 \\ W_i-1 \\ D_0 \\ D_1 \\ D_2 \\ \vdots \\ D_{W_i-2} \\ XMT \end{array}\begin{array}{c} \begin{array}{cccccccccccc} 0 & 1 & 2 & \cdots & W_i-2 & W_i-1 & D_0 & D_1 & D_2 & \cdots & D_{W_i-2} & XMT \end{array} \\ \begin{bmatrix} 1 & 0 & 0 & \cdots & 0 & 0 & 0 & 0 & 0 & \cdots & 0 & 1 \\ 1 & 1 & 0 & \cdots & 0 & 0 & p_{bi} & 0 & 0 & \cdots & 0 & 1 \\ 1 & 1 & 1 & \cdots & 0 & 0 & p_{bi} & p_{bi} & 0 & \cdots & 0 & 1 \\ \vdots & \vdots & \vdots & \vdots & \vdots & \vdots & \vdots & \vdots & \vdots & \vdots & \vdots & \vdots \\ 1 & 1 & 1 & \cdots & 1 & 0 & p_{bi} & p_{bi} & p_{bi} & \cdots & 0 & 1 \\ 1 & 1 & 1 & \cdots & 1 & 1 & p_{bi} & p_{bi} & p_{bi} & \cdots & p_{bi} & 1 \\ 1 & 0 & 0 & \cdots & 0 & 0 & 1 & 0 & 0 & \cdots & 0 & 1 \\ 1 & 1 & 0 & \cdots & 0 & 0 & p_{bi} & 1 & 0 & \cdots & 0 & 1 \\ 1 & 1 & 1 & \cdots & 0 & 0 & p_{bi} & p_{bi} & 1 & \cdots & 0 & 1 \\ \vdots & \vdots & \vdots & \vdots & \vdots & \vdots & \vdots & \vdots & \vdots & \vdots & \vdots & \vdots \\ 1 & 1 & 1 & \cdots & 1 & 0 & p_{bi} & p_{bi} & p_{bi} & \cdots & 1 & 1 \\ 0 & 0 & 0 & \cdots & 0 & 0 & 0 & 0 & 0 & \cdots & 0 & 1 \end{bmatrix} \end{array} \tag{5.13}$$

Furthermore, the variance of the number of visits can also be derived using the fundamental matrix. Define $M_{Di}=[md_{i,kj}]$ by:

$$md_{i,kj}=\begin{cases} m_{i,kj} & if \quad i=j \\ 0 & otherwise \end{cases} \tag{5.14}$$

Define $M_{2i}=[m_{i,kj}^2]$. Hence, the variance of the visit counts is [17]:

$$\sigma_i^2=M_i\left(2M_{Di}-I\right)-M_{2i} \tag{5.15}$$

The service time for a packet transmission starting from state i is given by:

$$S_{i,k}=\sum_j T_{i,j}\cdot X_{i,kj} \tag{5.16}$$

Therefore,

$$\begin{aligned} E\left[S_{i,k}\right]&=E\left[\sum_j T_{i,j}\cdot X_{i,kj}\right]=\sum_j E\left[T_{i,j}\cdot X_{i,kj}\right]=\sum_j E\left[T_{i,j}\right]\cdot E\left[X_{i,kj}\right]=\sum_j \tau_{i,j}\cdot m_{i,kj} \\ &=\begin{cases}(k+1)\sigma+k\cdot p_{bi}\cdot TM_i+TD_i & for \quad k=0,1,\cdots,W_0-1 \\ TD_i & for \quad k=XMT\end{cases} \end{aligned} \tag{5.17}$$

Since the sojourn time in state 0 is zero in the protocol instead of σ as specified in the model, we adjust the mean of $S_{i,k}$ starting from k=0,1,…, W_i-1 by decreasing σ in the results. Hence:

$$E\left[S_{i,k}\right]=\begin{cases} k\sigma+k\cdot p_{bi}\cdot TM_i+TD_i & for \quad k=0,1,\cdots,W_i-1 \\ TD_i & for \quad k=XMT \end{cases} \tag{5.18}$$

The variance of $S_{i,k}$ is given by:

$$\begin{aligned} Var\left[S_{i,k}\right] &= Var\left[\sum_j T_{i,j}\cdot X_{i,kj}\right]=\sum_j Var\left[T_{i,j}\cdot X_{i,kj}\right] \\ &= \sum_j \left\{Var\left[T_{i,j}\right]\cdot E\left[X_{i,kj}\right]+\left(E\left[T_{i,j}\right]\right)^2\cdot Var\left[X_{i,kj}\right]\right\} \\ &= \sum_j \left(\theta_{i,j}^2\cdot m_{i,kj}+\tau_{i,j}^2\cdot\sigma_{i,kj}^2\right) \\ &= \begin{cases} k\left\{TM_i^2\cdot p_{bi}\cdot\left(1-p_{bi}\right)\right\} & for \quad k=0,1,\cdots,W_i-1 \\ 0 & for \quad k=XMT \end{cases} \end{aligned} \tag{5.19}$$

To compute the mean service time, we separate the service time distribution into two classes, (i) for the packet arrivals when the AC_i queue is empty; (ii) for the packet arrivals when the AC_i queue is not empty.

For the packet that arrives when the tagged vehicle's queue is empty, the service time is given by:

$$S_{i,e}=\begin{cases} S_{i,0} & w.p. \quad q_{i,0,e}=q_{bi}/W_i \\ S_{i,1} & w.p. \quad q_{i,1,e}=q_{bi}/W_i \\ \quad\vdots & \\ S_{i,W_i-1} & w.p. \quad q_{i,W_i-1,e}=q_{bi}/W_i \\ S_{i,XMT} & w.p. \quad q_{i,XMT,e}=1-q_{bi} \end{cases} \tag{5.20}$$

If the channel is detected busy during $AIFS_i$ time, the AC_i has to wait until the end of the current packet transmission and then start backoff procedure. In our SMP

model, we have neglected such waiting time. Since such waiting time is relatively small comparing to the mean packet arrival time, it has little influence on the steady-state probability that a vehicle is in state *XMT*. Hence, *PDR* and *PRR* are not influenced by such waiting time, while it has influence on the mean transmission delay. Therefore, it is not necessary to represent this part as an additional state into the model. We only adjust the mean service time here to include this waiting time. When a packet transmission is detected by the tagged vehicle's $AIFS_i$ channel sensing time, the mean waiting time before the AC_i starts backoff procedure is half of the packet transmission. Therefore,

$$S_{i,e} = \begin{cases} S_{i,0} + \dfrac{TM_i - AIFS_i}{2} & w.p. \quad q_{i,0,e} = q_{bi} / W_i \\ S_{i,1} + \dfrac{TM_i - AIFS_i}{2} & w.p. \quad q_{i,1,e} = q_{bi} / W_i \\ \quad \vdots & \\ S_{i,W_i-1} + \dfrac{TM_i - AIFS_i}{2} & w.p. \quad q_{i,W_i-1,e} = q_{bi} / W_i \\ S_{i,XMT} & w.p. \quad q_{i,XMT,e} = 1 - q_{bi} \end{cases} \tag{5.21}$$

The mean and variance of the service time for the packet arrivals when the AC_i queue is empty are:

$$\begin{aligned} \beta_{i,e} &= E\left[S_{i,e}\right] = \sum_k E\left[S_{i,k}\right] \cdot q_{i,k,e} + \frac{q_{bi} \cdot \left(TM_i - AIFS_i\right)}{2} \\ &= \frac{\left(W_i - 1\right)\left(\sigma + p_{bi} \cdot TM_i\right) \cdot q_{bi}}{2} + TD_i + \frac{q_{bi} \cdot \left(TM_i - AIFS_i\right)}{2} \end{aligned} \tag{5.22}$$

$$\sigma_{i,e}^2 = Var\left[S_{i,e}\right] = E\left[S_{i,e}^2\right] - \left(E\left[S_{i,e}\right]\right)^2 = \sum_{k=0}^{W_i-1} E\left[\left(S_{i,k} + \frac{TM_i - AIFS_i}{2}\right)^2\right] \cdot q_{i,k,e} + E\left[S_{i,XMT}^2\right] \cdot q_{i,XMT,e} - \left(E\left[S_{i,e}\right]\right)^2$$

$$= \sum_{k=0}^{W_i-1}\left\{Var\left[S_{i,k}\right] + \left(E\left[S_{i,k} + \frac{TM_i - AIFS_i}{2}\right]\right)^2\right\} \cdot q_{i,k,e} + \left\{Var\left[S_{i,XMT}\right] + \left(E\left[S_{i,XMT}\right]\right)^2\right\} \cdot q_{i,XMT,e} - \left(E\left[S_{i,e}\right]\right)^2$$

$$= \left[\frac{(2W_i - 1)(\sigma + p_{bi} \cdot TM_i)^2}{6} + \frac{TM_i^2 \cdot p_{bi}(1 - p_{bi}) + 2 \cdot TD_i \cdot (\sigma + p_{bi} \cdot TM_i)}{2}\right] \cdot (W_i - 1) \cdot q_{bi} + TD_i^2 \tag{5.23}$$

$$+ \left[\frac{TM_i - AIFS_i}{2} + 2 \cdot TD_i + (W_i - 1)(\sigma + p_{bi} \cdot TM_i)\right] \frac{TM_i - AIFS_i}{2} \cdot q_{bi} - \left(E\left[S_{i,e}\right]\right)^2$$

$$i \in \{0, 1, \cdots, W_0 - 1, XMT\}$$

Similarly, for the packet that arrives when the AC_i queue is not empty, the service time is given by:

$$S_{i,b} = \begin{cases} S_{i,0} & w.p. \quad q_{i,0,b} = 1/W_i \\ S_{i,1} & w.p. \quad q_{i,1,b} = 1/W_i \\ \vdots & \\ S_{i,W_i-1} & w.p. \quad q_{i,W_i-1,b} = 1/W_i \end{cases} \tag{5.24}$$

The mean and variance of the service time for such packets:

$$\beta_{i,b} = E\left[S_{i,b}\right] = \frac{(W_i - 1)(\sigma + p_{bi} \cdot TM_i)}{2} + TD_i \tag{5.25}$$

$$\sigma_{i,b}^2 = Var\left[S_{i,b}\right] = E\left[S_{i,b}^2\right] - \left(E\left[S_{i,b}\right]\right)^2 = \sum_k E\left[S_{i,k}^2\right] \cdot q_{i,k,b} - \left(E\left[S_{i,b}\right]\right)^2$$

$$= \sum_k \left\{Var\left[S_{i,k}\right] + \left(E\left[S_{i,k}\right]\right)^2\right\} \cdot q_{i,k,b} - \left(E\left[S_{i,b}\right]\right)^2$$

$$= \frac{(W_i - 1)(2W_i - 1)}{6}(\sigma + p_{bi} \cdot TM_i)^2 + \frac{W_i - 1}{2} \cdot \left\{TM_i^2 \cdot p_{bi}(1 - p_{bi}) + 2 \cdot TD_i \cdot (\sigma + p_{bi} \cdot TM_i)\right\} \tag{5.26}$$

$$+ TD_i^2 - \left(E\left[S_{i,b}\right]\right)^2$$

By utilizing Welch's methods [13], the mean service time for a AC_i packet unconditioning on the state of the queue is:

$$E[S_i] = \frac{\beta_{i,e}}{1 - \lambda_i \left(\beta_{i,b} - \beta_{i,e} \right)} \tag{5.27}$$

5.3.3 Fixed-point Iteration

For the results obtained from SMP models above, we know that there are nine unknown parameters: ρ_1, ρ_2, ρ_3, p_{b1}, p_{b2}, p_{b3}, q_{b1}, q_{b2}, and q_{b3}. The mean service time for AC_i shown above depends on all these nine parameters. Therefore, channel utilization ρ_i of the M/G/1 queue in each vehicle depends on all nine unknown parameters. In this section, we determine how p_{bi} and q_{bi} depend on these nine parameters. Next, we can use the fixed point iteration to obtain the converged solution.

Let N_{cs} denote the average number of vehicles in carrier sensing range of the tagged vehicle, and let N_{tr} denote the average number of vehicles in transmission range of the tagged vehicle. Hence, without loss of generality, we have:

$$N_{cs} = N_{tr} = 2\beta R \tag{5.28}$$

The average number of vehicles in potential hidden area is:

$$N_{ph} = 4\beta R - N_{cs} = 2\beta R \tag{5.29}$$

From the tagged vehicle's point of view, p_{bi} is the probability that it senses channel busy during one time slot in the backoff process for AC_i service. The channel is detected busy can be due to two cases:

a. If this tagged vehicle is transmitting other types of message during this backoff slot, or

b. At least one neighbor (*i.e.*, a vehicle in the transmission range of the tagged vehicle) is transmitting any types of messages during this backoff slot. Therefore, we have:

$$
\begin{aligned}
p_{bi} &= 1-\left[\prod_{j=1,\, j\neq i}^{3}\left(1-P_{i,j,XMT}\right)\right]\cdot\left\{\sum_{k=0}^{\infty}\left[\left(1-P_{i,1,XMT}\right)\left(1-P_{i,2,XMT}\right)\left(1-P_{i,3,XMT}\right)\right]^{k}\frac{\left(N_{cs}-1\right)^{k}}{k!}e^{-\left(N_{cs}-1\right)}\right\} \\
&= 1-\left[\prod_{j=1,\, j\neq i}^{3}\left(1-P_{i,j,XMT}\right)\right]\cdot e^{-\left(N_{cs}-1\right)\cdot\left[1-\left(1-P_{i,1,XMT}\right)\left(1-P_{i,2,XMT}\right)\left(1-P_{i,3,XMT}\right)\right]}
\end{aligned}
\tag{5.30}
$$

where $P_{i,j,XMT}$ is the probability that AC_j message (either from a neighbor or the tagged vehicle itself) is transmitting in a backoff time slot of the tagged vehicle, which is attempting to transmit AC_i message.

For the first backoff time slot of the tagged vehicle, the time duration that can capture the transmission of the AC_j message is TD_j-$AIFS_j$+2σ. One extra time slot σ is the one just before transmission and another is the one just after transmission, which can capture the starting time instant and ending time instant of the packet transmission. Therefore, the probability that a neighbor's transmission is detected in the first backoff time slot of the tagged vehicle is $\pi_{i,XMT}(TD_j\text{-}AIFS_j+2\sigma)/\ TD_j$.

For a backoff time slot that is not the first backoff time slot of the tagged vehicle, the time duration that captures the transmission of the AC_j message is 2σ, which captures the starting time instant of the transmission. This is because when the AC_j message transmission is detected in the first backoff time slot by the tagged vehicle, the backoff counter will suspend and wait until the end of this transmission for further decrement. Therefore, if the first backoff time slot detects the transmission, there is no chance for the later backoff time slots to detect the same transmission. As a result, the non-first backoff time slot can only detect the transmission when the starting point of the

transmission falls within this time slot. Therefore, the probability that a AC_j message transmission is detected in non-first backoff time slot of the tagged vehicle is $\pi_{j,XMT} \times 2\sigma / TD_j$.

Since the probability that a backoff time slot is the first backoff time slot is $1/W_i$ and non-first backoff time slot is $(1-1/W_i)$, the probability that AC_j message transmission is detected by a backoff time slot of the AC_i is:

$$\begin{aligned} P_{i,j,XMT} &= \frac{1}{W_i} \cdot \left(\frac{TD_j - AIFS_j + 2\sigma}{TD_j} \pi_{j,XMT} \right) + \left(1 - \frac{1}{W_i} \right) \cdot \frac{2\sigma}{TD_j} \pi_{j,XMT} \\ &= \frac{TD_j - AIFS_j + 2\sigma W_i}{TD_j \cdot W_i} \pi_{j,XMT} \end{aligned} \tag{5.31}$$

Next, q_{bi} denotes the probability that the channel is detected busy by the tagged vehicle in the $AIFS_i$ duration. Therefore, we can similarly define $Q_{i,j,XMT}$ to be the probability that AC_j message transmission (either from a neighbor or the tagged vehicle itself) is detected in the $AIFS_i$ duration by the tagged vehicle, which is attempting to transmit AC_i message.

$$Q_{i,j,XMT} = \frac{TD_j - AIFS_j + 2 \cdot AIFS_i}{TD_j} \cdot \pi_{j,XMT} \tag{5.32}$$

Therefore,

$$\begin{aligned} q_{bi} &= 1 - \left[\prod_{j=1, j \neq i}^{3} \left(1 - Q_{i,j,XMT} \right) \right] \cdot \left\{ \sum_{k=0}^{\infty} \left[\left(1 - Q_{i,1,XMT} \right) \left(1 - Q_{i,2,XMT} \right) \left(1 - Q_{i,3,XMT} \right) \right]^k \frac{\left(N_{cs} - 1 \right)^k}{k!} e^{-\left(N_{cs} - 1 \right)} \right\} \\ &= 1 - \left[\prod_{j=1, j \neq i}^{3} \left(1 - Q_{i,j,XMT} \right) \right] \cdot e^{-\left(N_{cs} - 1 \right) \cdot \left[1 - \left(1 - Q_{i,1,XMT} \right) \left(1 - Q_{i,2,XMT} \right) \left(1 - Q_{i,3,XMT} \right) \right]} \end{aligned} \tag{5.33}$$

From the above analysis, we know that both p_{bi} and q_{bi} depend on all nine parameters ρ_1, ρ_2, ρ_3, p_{b1}, p_{b2}, p_{b3}, q_{b1}, q_{b2}, q_{b3}. Hence, we can use fixed-point iteration to obtain the converged solution for all nine parameters as below:

Step 1**:** Initialize $\rho_1=\rho_2=\rho_3=p_{b1}=p_{b2}=p_{b3}= q_{b1}=q_{b2}=q_{b3}=1$;

Step 2: Solve ρ_1, ρ_2, ρ_3, p_{b1}, p_{b2}, p_{b3}, q_{b1}, q_{b2}, q_{b3} according to $\rho_i=\lambda_i E[S_i]$ and Eqs. (5.27)(5.30)(5.33);

Step 3: If ρ_1, ρ_2, ρ_3, p_{b1}, p_{b2}, p_{b3}, q_{b1}, q_{b2}, q_{b3} converges, then stop the iteration algorithm; otherwise, go to step 2 with the updated ρ_1, ρ_2, ρ_3, p_{b1}, p_{b2}, p_{b3}, q_{b1}, q_{b2}, q_{b3}.

By utilizing the fixed-point iteration algorithm, the parameters ρ_1, ρ_2, ρ_3, p_{b1}, p_{b2}, p_{b3}, q_{b1}, q_{b2}, q_{b3} as well as the mean and the variance of the service time can be determined, which are used for the MAC-layer performance indices computation in the next section.

5.4 MAC-level Performance Metrics

5.4.1 Mean transmission delay

According to the *Welch*'s method [13], the steady-state expected number of packets in the tagged vehicle's queue (including the packet in the head of the queue that is under service) is:

$$E[Q_i]=\frac{\lambda_i\beta_{i,e}}{1-\lambda_i\left(\beta_{i,b}-\beta_{i,e}\right)}+\frac{\lambda_i^2}{2}\cdot\frac{\left(\sigma_{i,e}^2+\beta_{i,e}^2-\sigma_{i,b}^2-\beta_{i,b}^2\right)}{1-\lambda_i\left(\beta_{i,b}-\beta_{i,e}\right)}+\frac{\lambda_i^2}{2}\cdot\frac{\sigma_{i,b}^2+\beta_{i,b}^2}{1-\lambda_i\beta_{i,b}} \tag{5.34}$$

Using *Little*'s law, the mean delay for a AC_i packet transmission is:

$$E[D_i]=\frac{E[Q_i]}{\lambda_i} \tag{5.35}$$

5.4.2 Variance of the transmission delay

From the method proposed by *Welch* [13], we can get the *Laplace-Stieltjes* transform for the transmission delay:

$$\psi_i(s) = E\left[e^{-s\cdot D_i}\right] = \frac{1-\lambda\beta_{i,b}}{1-\lambda\left(\beta_{i,b}-\beta_{i,e}\right)}\cdot\frac{\lambda\left[\varphi_{i,e}(s)-\varphi_{i,b}(s)\right]-s\cdot\varphi_{i,e}(s)}{\lambda-s-\lambda\varphi_{i,b}(s)} \tag{5.36}$$

To obtain the variance of the transmission delay, we need to compute the second moment of the transmission delay first. This can be obtained from the derivatives of the *Laplace-Stielfjes* transform.

$$E\left[D_i^2\right] = \left.\frac{d^2\psi_i(s)}{ds^2}\right|_{s=0} = \psi_i''(s)\big|_{s=0} \tag{5.37}$$

Assume:

$$a = \lambda - s - \lambda\varphi_{i,b}(s)$$
$$b = \lambda\left[\varphi_{i,e}(s)-\varphi_{i,b}(s)\right]-s\cdot\varphi_{i,e}(s)$$

Hence,

$$\psi_i(s) = \frac{1-\lambda\beta_{i,b}}{1-\lambda\left(\beta_{i,b}-\beta_{i,e}\right)}\cdot\frac{b}{a}$$

Therefore, we get:

$$\psi_i'(s) = \frac{1-\lambda\beta_{i,b}}{1-\lambda\left(\beta_{i,b}-\beta_{i,e}\right)}\cdot\frac{b'a-a'b}{a^2}$$

$$\psi_i''(s)\big|_{s=0} = \frac{1-\lambda\beta_{i,b}}{1-\lambda\left(\beta_{i,b}-\beta_{i,e}\right)}\cdot\left\{\frac{b_i''a_i-a_i''b_i}{a_i^2}-\frac{2\left[a_i'b_i'a_i-\left(a_i'\right)^2b_i\right]}{a_i^3}\right\}\Bigg|_{s=0}$$

When s approaches 0, a_i, and b_i approach 0. Hence, we use *l'Hôpital'*s rule to obtain the results:

$$\left.\frac{b_i''a_i - a_i''b_i}{a_i^2}\right|_{s=0} = \left.\frac{b_i'''a_i' - a_i'''b_i'}{(a_i')^2}\right|_{s=0}$$

$$\left.\frac{2\left[a_i'b_i'a_i - (a_i')^2 b_i\right]}{a_i^3}\right|_{s=0} = \left.\frac{-2a_i'a_i'''b_i' + 3a_i''b_i''a_i' + 2(a_i')^2 b_i''' - 3(a_i'')^2 b_i' - a_i'b_i'a_i'''}{3(a_i')^3}\right|_{s=0}$$

where:

$$a_i'\big|_{s=0} = -1 - \lambda_i \cdot \varphi_{i,b}'(s)\big|_{s=0} \qquad a_i''\big|_{s=0} = -\lambda_i \cdot \varphi_{i,b}''(s)\big|_{s=0} \qquad a_i'''\big|_{s=0} = -\lambda_i \cdot \varphi_{i,b}'''(s)\big|_{s=0}$$

$$b_i'\big|_{s=0} = \lambda_i \cdot \left[\varphi_{i,e}'(s)\big|_{s=0} - \varphi_{i,b}'(s)\big|_{s=0}\right]$$

$$b_i''\big|_{s=0} = \lambda_i \cdot \left[\varphi_{i,e}''(s)\big|_{s=0} - \varphi_{i,b}''(s)\big|_{s=0}\right] - 2\varphi_{i,e}'(s)\big|_{s=0}$$

$$b_i'''\big|_{s=0} = \lambda_i \cdot \left[\varphi_{i,e}'''(s)\big|_{s=0} - \varphi_{i,b}'''(s)\big|_{s=0}\right] - 3\varphi_{i,e}'(s)\big|_{s=0}$$

$$\varphi_{i,e}'(s)\big|_{s=0} = -E\left[S_{i,e}\right] = -\beta_{i,e} \qquad \varphi_{i,b}'(s)\big|_{s=0} = -E\left[S_{i,b}\right] = -\beta_{i,b}$$

$$\varphi_{i,e}''(s)\big|_{s=0} = E\left[S_{i,e}^2\right] = \sigma_{i,e}^2 + \beta_{i,e}^2 \qquad \varphi_{i,b}''(s)\big|_{s=0} = E\left[S_{i,b}^2\right] = \sigma_{i,b}^2 + \beta_{i,b}^2$$

$$\varphi_{i,e}'''(s)\big|_{s=0} = -E\left[S_{i,e}^3\right] = -\gamma_{i,e} \qquad \varphi_{i,b}'''(s)\big|_{s=0} = -E\left[S_{i,b}^3\right] = -\gamma_{i,b}$$

In the above equations,

$$\begin{aligned}
\gamma_{i,e} = E\left[S_{i,e}^3\right] &= \sum_{k=0}^{W_i-1} E\left[\left(S_{i,k} + \frac{TM_i - AIFS_i}{2}\right)^3\right] \cdot q_{i,k,e} + E\left[S_{i,XMT}^3\right] \cdot q_{i,XMT,e} \\
&= \sum_k E\left[S_{i,k}^3\right] \cdot q_{i,k,e} + \left(\frac{TM_i - AIFS_i}{2}\right)^3 \cdot q_{bi} + \frac{3(TM_i - AIFS_i)}{2} \cdot \sum_{k=0}^{W_i-1} E\left[S_{i,k}^2\right] \cdot q_{i,k,e} \\
&\quad + \frac{3(TM_i - AIFS_i)^2}{4} \cdot \sum_{k=0}^{W_i-1} E\left[S_{i,k}\right] \cdot q_{i,k,e} \\
&= \sum_k E\left[S_{i,k}^3\right] \cdot q_{i,k,e} + \left(\frac{TM_i - AIFS_i}{2}\right)^3 \cdot q_{bi} + \frac{3(TM_i - AIFS_i)}{2} \cdot \sum_{k=0}^{W_i-1} \left\{Var\left[S_{i,k}\right] + \left(E\left[S_{i,k}\right]\right)^2\right\} \cdot q_{i,k,e} \\
&\quad + \frac{3(TM_i - AIFS_i)^2}{4} \cdot \sum_{k=0}^{W_i-1} E\left[S_{i,k}\right] \cdot q_{i,k,e}
\end{aligned}$$

$$\gamma_{i,b} = E\left[S_{i,b}^3\right] = \sum_k E\left[S_{i,k}^3\right] \cdot q_{i,k,b}$$

Furthermore,

$$\begin{aligned} E\left[S_{i,k}^3\right] &= E\left[\left(\sum_j T_{i,j} \cdot X_{i,kj}\right)^3\right] \\ &= \sum_j E\left[\left(T_{i,j} \cdot X_{i,kj}\right)^3\right] + 3 \cdot \sum_{\substack{j,l \\ l \neq j}} \left\{E\left[\left(T_{i,j} \cdot X_{i,kj}\right)^2\right] \cdot E\left[T_{i,l} \cdot X_{i,kl}\right]\right\} \\ &+6 \cdot \sum_{\substack{j,l,n \\ j \neq l \neq n}} E\left[T_{i,j} \cdot X_{i,kj}\right] E\left[T_{i,l} \cdot X_{i,kl}\right] E\left[T_{i,n} \cdot X_{i,kn}\right] \\ &= \sum_j \left(\tau_{i,j}^3 \cdot m_{i,kj}\right) + 3 \cdot \sum_{\substack{j,l \\ l \neq j}} \left\{\left[\theta_{i,j}^2 \cdot m_{i,kj} + \tau_{i,j}^2 \cdot \left(\sigma_{i,kj}^2 + m_{i,kj}^2\right)\right] \cdot \tau_{i,l} \cdot m_{i,kl}\right\} \\ &+6 \cdot \sum_{\substack{j,l,n \\ j \neq l \neq n}} \tau_{i,j} \cdot m_{i,kj} \cdot \tau_{i,l} \cdot m_{i,kl} \cdot \tau_{i,n} \cdot m_{i,kn} \end{aligned}$$

Therefore, based on Eqs. (5.35)(5.37), we can obtain the variance of the transmission delay:

$$Var\left[D_i\right] = E\left[D_i^2\right] - \left(E\left[D_i\right]\right)^2 \tag{5.38}$$

5.4.3 Packet Delivery Ratio (PDR)

The *PDR* is defined as [5][7]: given a broadcast packet sent by the tagged vehicle, the probability that all vehicles in its transmission range receive the packet successfully. Taking account of hidden terminals, we have *PDR* for AC_i message transmission:

$$PDR_i = P\left(N_{i,cs}\right) P\left(N_{i,ph}\right) \tag{5.39}$$

where $P(N_{i,cs})$ is the probability that no vehicles in the transmission range of the tagged vehicle transmits any types of messages when the tagged vehicle starts AC_i message transmission, and $P(N_{i,ph})$ is the probability that no transmissions from the vehicles in the

potential hidden terminal area collide with the broadcast AC_i packet from the tagged vehicle.

$P(N_{i,cs})$ can also be interpreted as the no-concurrent transmission probability, *i.e.*, two packets do not start transmission at the same time. Since EDCA employs a discrete-time backoff scheme, if the backoff process is involved, a vehicle is only allowed to transmit at the beginning of each slot time after an idle $AIFS_i$ time duration. Therefore, if the tagged vehicle has not gone through the backoff process before transmitting the AC_i packet (with probability $(1-\rho_i)(1-q_{bi})$), the concurrent transmission will not occur. Otherwise, the packet transmission is synchronized to the beginning of a slot time, and concurrent transmission may occur if other vehicles' transmission is also synchronized by the backoff process. From the model, we know that the probability that a neighbor or the tagged vehicle itself starts to transmit a AC_j packet at the beginning of the same time slot with the tagged vehicle is $\pi_{j,0}= \pi_{j,XMT}\times\sigma/TD_j$. This is because the sojourn time in state 0 is one time slot σ as shown in the SMP model, hence, $\pi_{j,0}$ is the probability that a vehicle starts to transmit AC_j packet in the beginning of a time slot immediately after the backoff process. Hence, $P(N_{i,cs})$ is:

$$\begin{aligned} P\left(N_{i,cs}\right) &= \left[1-\left(1-\rho_i\right)\left(1-q_{bi}\right)\right]\cdot\left[\prod_{j=1,\,j\neq i}^{3}\left(1-\pi_{j,0}\right)\right]\cdot\left\{\sum_{k=0}^{\infty}\left[\left(1-\pi_{1,0}\right)\left(1-\pi_{2,0}\right)\left(1-\pi_{3,0}\right)\right]^k\frac{\left(N_{cs}-1\right)^k}{k!}e^{-\left(N_{cs}-1\right)}\right\} \\ &\quad +\left(1-\rho_i\right)\left(1-q_{bi}\right) \\ &= \left[1-\left(1-\rho_i\right)\left(1-q_{bi}\right)\right]\cdot\left[\prod_{j=1,\,j\neq i}^{3}\left(1-\pi_{j,0}\right)\right]\cdot e^{-\left(N_{cs}-1\right)\cdot\left[1-\left(1-\pi_{1,0}\right)\left(1-\pi_{2,0}\right)\left(1-\pi_{3,0}\right)\right]}+\left(1-\rho_i\right)\left(1-q_{bi}\right) \end{aligned} \tag{5.40}$$

Since the transmission time for a packet is TD_j-$AIFS_j$=$E[PA_j]/R_d+T_H+\delta$, the event that a AC_j packet transmission from hidden terminals collides with the tagged vehicle's AC_i packet transmission only happens when hidden terminals start to transmit during the vulnerable period TD_j-$AIFS_j$+TD_i-$AIFS_i$. Therefore,

$$P\left(N_{i,ph}\right)=\sum_{k=0}^{\infty}\left[\prod_{j=1}^{3}\left(1-\pi_{j,XMT}\cdot\frac{TD_j-AIFS_j+TD_i-AIFS_i}{TD_j}\right)\right]^k\frac{\left(N_{ph}\right)^k}{k!}e^{-N_{ph}}$$
$$=e^{-N_{ph}\left[1-\prod_{j=1}^{3}\left(1-\pi_{j,XMT}\cdot\frac{TD_j-AIFS_j+TD_i-AIFS_i}{TD_j}\right)\right]} \tag{5.41}$$

Hence, the *PDR* can be computed. From the analytic results demonstrated in Section 5.5, we can see that the hidden terminals problem has more impact than concurrent transmissions on the *PDR*.

5.4.4 Packet Reception Ratio (PRR)

Packet reception ratio (*PRR*) is defined as the percentage of nodes that successfully receive a packet from the tagged node among the receivers being investigated at the moment that the packet is sent out [7]. Similar to the computation for *PDR*, we consider both the concurrent transmission and hidden terminal effects while computing *PRR*. Therefore, *PRR* for AC_i packet transmission is:

$$PRR_i = PRR_{i,cc}PRR_{i,ht} \tag{5.42}$$

The impact of the concurrent transmission and hidden terminals will be evaluated in the following two sections.

a. Impact of concurrent transmission

Transmissions from nodes within a distance R away from the tagged node in the meantime at which the tagged node transmits may cause collisions. When the tagged vehicle starts to transmit AC_i packet, no AC_j packet can be transmitted at the same time for the tagged vehicle. Therefore, the probability that there is no concurrent transmission from the tagged vehicle is:

$$PRR_{i,cc}^{1} = \prod_{j=1, j\neq i}^{3} (1-\pi_{j,0}) \tag{5.43}$$

AC_j packet transmissions from vehicles within a distance R away from the tagged vehicle in the meantime at which the tagged vehicle transmits AC_i packet may cause collisions. When the tagged node starts AC_i packet transmission in the beginning of a slot time, collisions will take place if any vehicle in the transmission range of the tagged vehicle starts AC_j packet transmission in the beginning of the same time slot. As shown in Fig. 3.6 in Chapter 3, any vehicles transmitting any types of messages on the right hand side of the tagged node on the origin (*i.e.*, node in [0, R]) will result in failure of all vehicles in [0, R] receiving the broadcast AC_i packet. Hence, ratio of successfully receiving vehicles in the range [0, R] can be expressed as:

$$\begin{aligned} PRR_{i,cc}^{2} &= \sum_{k=0}^{\infty} \left[(1-\pi_{1,0})(1-\pi_{2,0})(1-\pi_{3,0}) \right]^{k} \frac{(\beta R)^{k}}{k!} e^{-\beta R} \\ &= e^{-\beta R\left[1-(1-\pi_{1,0})(1-\pi_{2,0})(1-\pi_{3,0})\right]} \end{aligned} \tag{5.44}$$

On the other hand, transmissions from any vehicle on the left hand side of the tagged vehicle (*i.e.*, vehicle in [-R, 0]) will only result in failure of some of the vehicles receiving the broadcast AC_i packet in [0, R]. Similar to analysis of the hidden terminal

impact, the ratio of successful receiving nodes due to any transmission in [-*R*, 0] depends on the position of the closest vehicle transmitting in [-*R*, 0] to the tagged vehicle. Denote *Y* as a random variable that represents the distance from the closest vehicle transmitting in [-*R*, 0] (*B* in the above figure) to the outer boundary of range [-*R*, 0]. Let R_t be the range where no station transmits, so that R_t=[-*R*+*y*,0]. Then the *CDF* for *Y* is:

$$P(Y \le y) = \sum_{k=0}^{\infty} \left[P(\text{none of } k \text{ nodes in } R_t \text{ transmits in a slot}) \right] \tag{5.45}$$

It is the probability that the closest interfering node in [-*R*, 0] is at least (*R*-*y*) away from the transmitter; *i.e.*, the probability that no nodes within R_t transmit in the meantime the tagged node starts to transmit. Hence, we have:

$$P(Y \le y) = \sum_{k=0}^{\infty} \left[(1-\pi_{1,0})(1-\pi_{2,0})(1-\pi_{3,0}) \right]^k \frac{(\beta(R-y))^k}{k!} e^{-\beta(R-y)} = e^{-\beta(R-y)\left[1-(1-\pi_{1,0})(1-\pi_{2,0})(1-\pi_{3,0})\right]} \tag{5.46}$$

Thus, the expected number of failed nodes in [0, *R*] due to concurrent transmission of nodes in [-*R*, 0] can be expressed as:

$$\begin{aligned} NF_h &= \int_0^R \beta y P(y \le Y \le y+dy) \\ &= \int_0^R \beta^2 y \left[1-(1-\pi_{1,0})(1-\pi_{2,0})(1-\pi_{3,0}) \right] e^{-\beta(R-y)\left[1-(1-\pi_{1,0})(1-\pi_{2,0})(1-\pi_{3,0})\right]} dy \\ &= \beta R - \frac{1-e^{-\beta\left[1-(1-\pi_{1,0})(1-\pi_{2,0})(1-\pi_{3,0})\right]R}}{\left[1-(1-\pi_{1,0})(1-\pi_{2,0})(1-\pi_{3,0})\right]} \end{aligned} \tag{5.47}$$

Therefore, the percentage of receivers in [0, *R*] that are free from collisions caused by the concurrent transmissions of nodes in the range [-*R*, 0] is:

$$PRR_{i,cc}^3 = \frac{1-e^{-\beta R\left[1-(1-\pi_{1,0})(1-\pi_{2,0})(1-\pi_{3,0})\right]}}{\beta R\left[1-(1-\pi_{1,0})(1-\pi_{2,0})(1-\pi_{3,0})\right]} \tag{5.48}$$

Define $PRR_{i,cc}$ as the percentage of receivers in [0, R] that are free from collisions caused by the concurrent transmissions of vehicles in the range [-R, R]. If the tagged vehicle transmits the AC_i packet without going through the backoff process, with probability $(1-\rho_i)(1-q_{bi})$, concurrent transmission will not occur. Otherwise, concurrent transmissions may occur. Therefore,

$$\begin{aligned} PRR_{i,cc} &= \left[1-(1-\rho_i)(1-q_{bi})\right]\cdot PRR_{i,cc}^{1}\cdot PRR_{i,cc}^{2}\cdot PRR_{i,cc}^{3}+(1-\rho_i)(1-q_{bi}) \\ &= \left[1-(1-\rho_i)(1-q_{bi})\right]\cdot\left[\prod_{j=1,j\neq i}^{3}(1-\pi_{j,0})\right]\cdot\frac{e^{-\beta R\left[1-(1-\pi_{1,0})(1-\pi_{2,0})(1-\pi_{3,0})\right]}\left\{1-e^{-\beta R\left[1-(1-\pi_{1,0})(1-\pi_{2,0})(1-\pi_{3,0})\right]}\right\}}{\beta R\left[1-(1-\pi_{1,0})(1-\pi_{2,0})(1-\pi_{3,0})\right]} \\ &\quad +(1-\rho_i)(1-q_{bi}) \end{aligned} \tag{5.49}$$

b. Impact of hidden terminals

We observe that the ratio of receivers affected by the hidden terminals only depends on the position of the hidden node (referred as hidden crucial node) that has the closest distance to boundary of the transmitter's sensing range among all the transmitting nodes in the potential hidden terminal area. Denote X as a random variable that represents the distance from the hidden crucial node (A in Fig. 3.6 in Chapter 3) to the outer boundary of [0, 2R]. Let R_s be the range in the potential hidden terminal area, where no node transmits, such that R_s=[l_{cs}, 2R-x],where l_{cs}=N_{cs}/(2β) is carrier sensing range of a node in the network. Then the cumulative distribution function (CDF) for X is:

$$
\begin{aligned}
P(X \le x) &= \sum_{k=0}^{\infty}\left[P(\text{none of } k \text{ nodes in } R_s \text{ transmits during tagged node's transmission })\right] \\
&= \sum_{k=0}^{\infty}\left[\prod_{j=1}^{3}\left(1-\pi_{j,XMT}\cdot\frac{TD_j - AIFS_j + TD_i - AIFS_i}{TD_j}\right)\right]^k \frac{\left[\beta\left(2R-l_{cs}-x\right)\right]^k}{i!}e^{-\beta(2R-l_{cs}-x)} \\
&= e^{-C_i(2R-l_{cs}-x)}
\end{aligned}
\tag{5.50}
$$

where

$$
C_i = \beta\cdot\left[1-\prod_{j=1}^{3}\left(1-\pi_{j,XMT}\cdot\frac{TD_j - AIFS_j + TD_i - AIFS_i}{TD_j}\right)\right] \tag{5.51}
$$

Thus, the expected number of failed nodes in [0, R] due to the hidden terminal problem can be expressed as:

$$
\begin{aligned}
NF_h &= \int_0^{2R-l_{cs}} \beta x f_X(x)dx \\
&= \int_0^{2R-l_{cs}} \beta x d\left\{P(X \le x)\right\} = \beta\left(2R-l_{cs}\right) - \frac{\beta}{C_i}\left(1-e^{-c(2R-l_{cs})}\right)
\end{aligned}
\tag{5.52}
$$

Therefore, the percentage of receivers that are free from collisions caused by hidden terminal problem is:

$$
PRR_{i,ht} = \frac{\beta R - NF_h}{\beta R} = \frac{l_{cs}-R}{R} + \frac{1}{RC_i}\left(1-e^{-C_i(2R-l_{cs})}\right) \tag{5.53}
$$

Hence, based on Eqs. (5.42)(5.49)(5.53), the *PRR* can be computed. Similar to the case of the *PDR*, the hidden terminals problem also has more impact than concurrent transmissions on the *PRR*.

5.5 Numerical Results

The computation for analytic models and corresponding simulations are conducted in Matlab. Note that the analytic model consists of decomposition and fixed-

point iteration while the simulative solution does not. All other assumptions are the same in the simulation and analytic models. The results show the high accuracy of our decomposition-based analytic approximation. We consider a freeway system where the number of vehicles is Poisson distributed. Each vehicle on the road is equipped with DSRC wireless capability. The control channel of DSRC is exclusively used for safety related broadcast communication. Table 5.1 shows the parameters used in this chapter, which reflect typical DSRC network settings in [1]. Input parameters such as packet arrival rate, packet length, backoff window size, channel sensing time *AIFS* and carrier sensing range are variables since they may have different values according to different types of applications in practice. Therefore, we will evaluate the influence of these varied parameters on the output measures in this section. Based on the results, we may gain valuable insights about the parameters settings to satisfy service requirements with respect to latency and reliability.

Table 5.1: DSRC parameters for EDCA mechanism

Parameters	Values	Parameters	Values
Tx range R	500 m	Data rate R_d	24 $Mbps$
PHY preamble	40 μs	Vehicle density β	variable
PLCP header	4 μs	Packet arrival rate λ_i	variable
MAC header	272 $bits$	Packet Length PA_i	variable
Slot time σ	16 μs	CWMin W_i-1	variable
SIFS	32 μs	$AIFS_i$	variable
Propagation delay δ	0 μs	Carrier sensing range l_{cs}	variable

5.5.1 Influence of Packet Arrival Rate

For different applications in practice, the workloads may differ. Hence, we are interested in the following question: Will the application with smaller arrival rate has

higher reliability (*PDR* and *PRR*) than the application with larger arrival rate? Intuitively speaking, the message that rarely generated has less inference than message that frequently generated. However, this statement is proved to be wrong by our results presented next.

To evaluate the influence of the packet arrival rate, we set the input parameters values as in Table 5.2. The EDCA parameters including backoff window size and *AIFS* channel sensing time for different *ACs* are set to be different to provide service differentiations.

Table 5.2: Parameters for packet arrival rate influence evaluation

Parameters	Values for AC_1, AC_2, AC_3
Packet arrival rate λ_i (#/sec)	10, 5, 2
Packet Length PA_i (bytes)	200, 200, 200
CWMin W_i-1	7, 3, 3
$AIFSN_i$	6, 3, 2
Carrier sensing range l_{cs}	R=500m

The output measures including mean transmission delay, *PDR* and *PRR* are shown in Fig. 5.3.

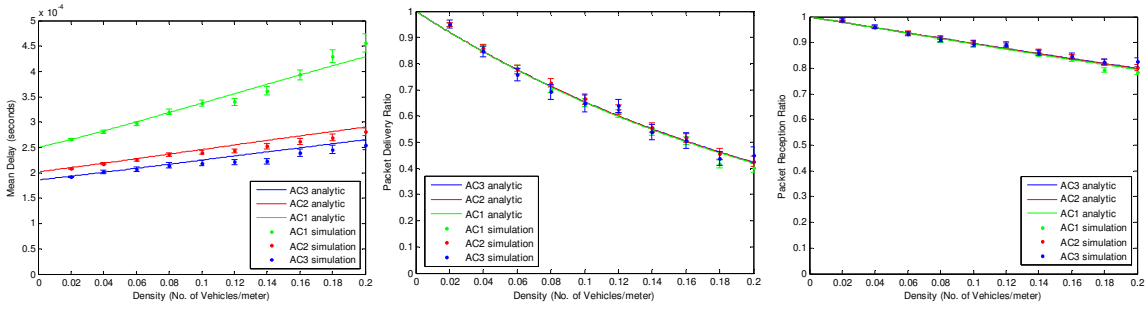

Figure 5.3: Influence of packet arrival rate

From the results above, we can see that mean delay, *PDR* and *PRR* from analytic model and simulation match very well, which validate the correctness of our proposed models. The delay is relatively small. In addition, when vehicle density increases, mean transmission delay increases, while *PDR* and *PRR* decrease. We can also observe that, given same network parameters, *PDRs* are less than *PRRs*. This is because that *PDRs* count the number of packets that are successfully received by all intended receivers, while *PRRs* count the percentage (or probability) of the intended receivers that successfully receive a packet from a sender. *PDR* and *PRR* are almost the same for three *ACs*, which means the arrival rate differentiation has little impact on *PDR* and *PRR*. In other words, the application that rarely generates messages has almost the same reliability with the application that frequently generates messages. The delay differentiations are mainly due to the EDCA parameters (backoff window size and *AIFS*). Hence, arrival rate has little impact to provide differentiations of transmission delay, *PDR* and *PRR* for different priority services. Our analytic results also show that *PDR* and *PRR* are influenced by the total arrival rate of three types of services but not the individual arrival rate.

5.5.2 Influence of Packet Length

Besides the arrival rates, we are also interested in how to choose the packet length for safety messages, which is addressed in this section.

Table 5.3: Parameters for packet length influence evaluation

Parameters	Values for AC_1, AC_2, AC_3
Packet arrival rate λ_i (#/sec)	2, 2, 2
Packet Length PA_i (bytes)	800, 400, 200
CWMin W_i-1	7, 3, 3
$AIFSN_i$	6, 3, 2
Carrier sensing range l_{cs}	R=500m

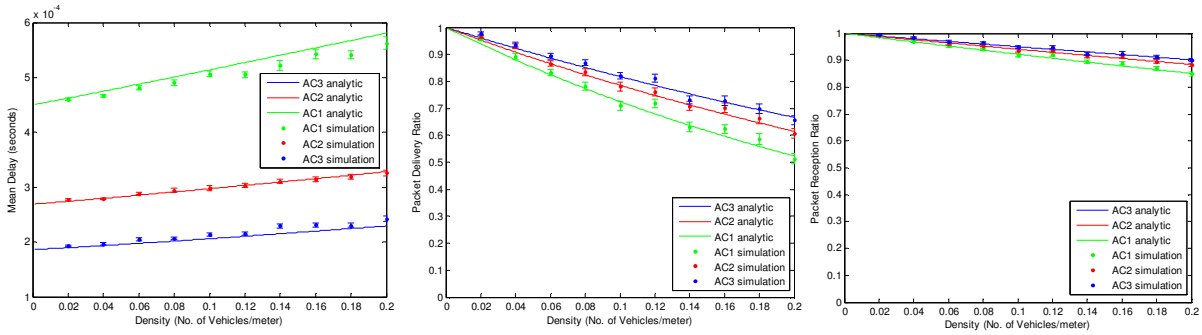

Figure 5.4: Influence of packet length

The input parameters are used as in Table 5.3. The results are shown as in Fig. 5.4. From the results above, we can see that mean delay, *PDR* and *PRR* from analytic model and simulation match very well. When vehicle density increases, mean transmission delay will increase, while *PDR* and *PRR* will decrease. *AC* with larger packet length will have higher mean transmission delay, lower *PDR* and lower *PRR*. Therefore, we have to choose short packet length to assure high reliability and small latency.

5.5.3 Influence of Backoff Window Size

EDCA mechanism has two important parameters to provide service differentiation: backoff window size and channel sensing time *AIFS*. Higher priority

services are allocated with smaller backoff window size and *AIFS*. Hence, whether higher priority service with smaller backoff window size has smaller latency and higher reliability is one of the major concerns. In order to evaluate the influence of the backoff window size on the output measures, we choose the following two sets of input parameters:

Table 5.4: D1 for backoff window size

Parameters	Values for AC_1, AC_2, AC_3
Packet arrival rate λ_i (#/sec)	2, 2, 2
Packet Length PA_i (bytes)	200, 200, 200
CWMin W_i-1	7, 3, 3
$AIFSN_i$	6, 3, 2
Carrier sensing range l_{cs}	R=500m

Table 5.5: D2 for backoff window size

Parameters	Values for AC_1, AC_2, AC_3
Packet arrival rate λ_i (#/sec)	2, 2, 2
Packet Length PA_i (bytes)	200, 200, 200
CWMin W_i-1	15, 7, 7
$AIFSN_i$	6, 3, 2
Carrier sensing range l_{cs}	R=500m

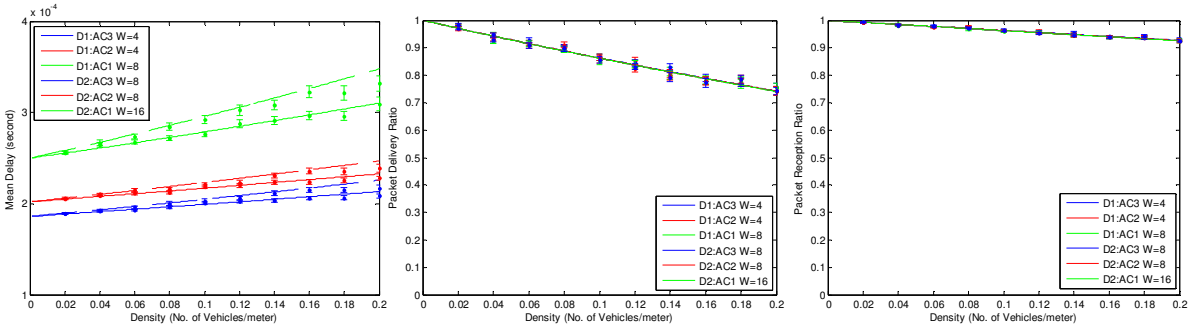

Figure 5.5: Influence of backoff window size

From the analytic results shown above, we can see that backoff window size only influences transmission delay, whereas has little influence on *PDR* and *PRR*. Therefore, smaller backoff window size only leads to smaller latency when vehicle density is relatively high but has little impact when vehicle density is small. In addition, smaller backoff window size does not assure the higher priority services to have higher reliability.

5.5.4 Influence of Channel Sensing Time

Table 5.6: D1 for channel sensing time

Parameters	Values for AC_1, AC_2, AC_3
Packet arrival rate λ_i (#/sec)	2, 2, 2
Packet Length PA_i (bytes)	200, 200, 200
CWMin W_i-1	7, 3, 3
$AIFSN_i$	6, 3, 2
Carrier sensing range l_{cs}	R=500m

Table 5.7: D2 for channel sensing time

Parameters	Values for AC_1, AC_2, AC_3
Packet arrival rate λ_i (#/sec)	2, 2, 2
Packet Length PA_i (bytes)	200, 200, 200
CWMin W_i-1	7, 3, 3
$AIFSN_i$	10, 8, 6
Carrier sensing range l_{cs}	R=500m

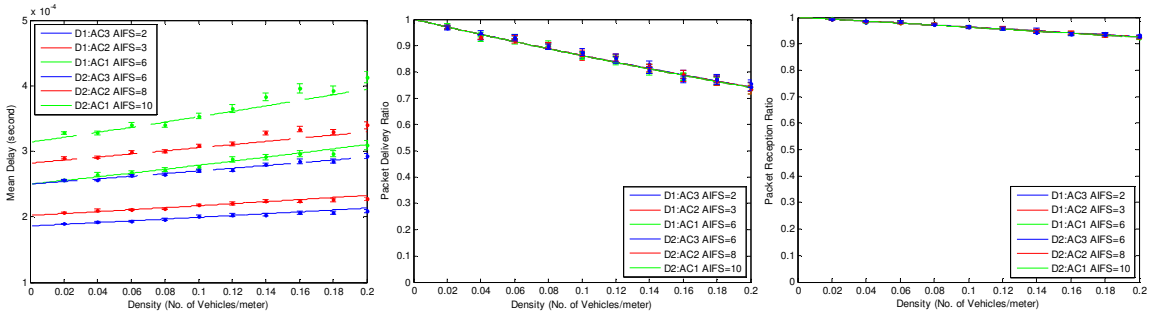

Figure 5.6: Influence of channel sensing time AIFS

As we mentioned above, besides backoff window size, another EDCA parameter is channel sensing time *AIFS*. Higher priority service is usually allocated shorter *AIFS* to ensure that it transmits before the lower priority services. Hence, whether higher priority service with shorter *AIFS* has smaller latency and higher reliability will be evaluated in this section. In order to evaluate the influence of the channel sensing time on the output measures, we choose the two sets of input parameters as shown in Table 5.6 and 5.7.

From the analytic results shown above, we can see that *AIFS* channel sensing time only influences transmission delay, whereas has little influence on *PDR* and *PRR*. Shorter *AIFS* ensures smaller latency but does not assure higher reliability for higher priority services.

5.5.5 Influence of Carrier Sensing Range

In practice, the carrier sensing range may differ for different types of devices. Since large carrier sensing range can reduce hidden terminal problem, we are interested in the significance of the carrier sensing range on the VANET safety communication

system's reliability. In order to evaluate the influence of carrier sensing range, we use two sets of input parameters:

Table 5.8: D1 for carrier sensing range

Parameters	Values for AC_1, AC_2, AC_3
Packet arrival rate λ_i (#/sec)	2, 2, 2
Packet Length PA_i (bytes)	200, 200, 200
CWMin W_i-1	7, 3, 3
$AIFSN_i$	6, 3, 2
Carrier sensing range l_{cs}	R=500m

Table 5.9: D2 for carrier sensing range

Parameters	Values for AC_1, AC_2, AC_3
Packet arrival rate λ_i (#/sec)	2, 2, 2
Packet Length PA_i (bytes)	200, 200, 200
CWMin W_i-1	7, 3, 3
$AIFSN_i$	10, 8, 6
Carrier sensing range l_{cs}	1.5R=750m

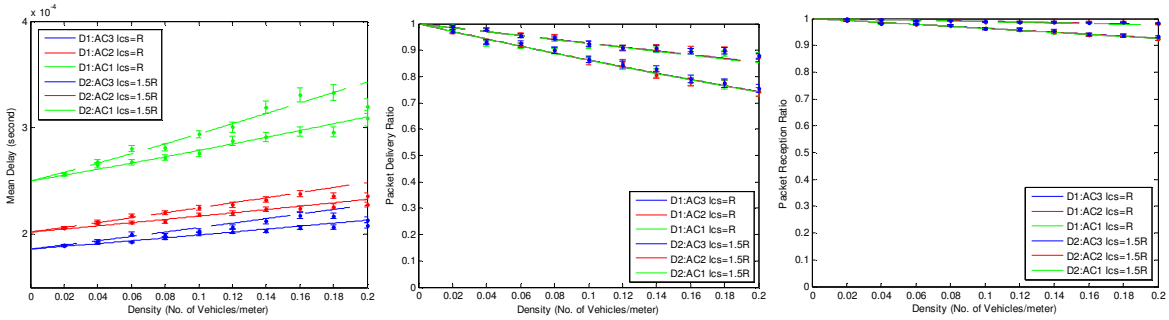

Figure 5.7: Influence of carrier sensing range

We observe that increasing carrier sensing range does not have significant influence on transmission delay, but can greatly improving *PDR* and *PRR*. This is because of the fact that larger carrier sensing range reduces the hidden terminal

problem, which dominates the transmission reliability as shown in Section 5.5.6. Therefore, we should use large carrier sensing range in practice to enhance the system reliability.

5.5.6 Hidden terminal Vs. Concurrent Transmission

From the analysis in Section 5.5.3-5.5.5, we conclude that EDCA parameters (backoff window size and channel sensing time *AIFS*) have little impact on reliability (*PDR* and *PRR*), whereas carrier sensing range has significant impact. Since EDCA parameters influence concurrent transmission and carrier sensing range is closely correlated with hidden terminal problem, we may make a hypothesis that concurrent transmission has less impact than hidden terminal problem with respect to reliability. This hypothesis will be verified by the analytic-numeric results for AC_1 service from the analytic model using parameters in Table 5.10. As shown in Fig. 5.8, the *PDR* and *PRR* are dominated by the hidden terminal problem's influence. The concurrent transmission has much less impact comparing to hidden terminal problem. This may be due to short packet length and relatively small arrival rate for safety messages.

Table 5.10: Parameters for reliability factors evaluation

Parameters	Values for AC_1, AC_2, AC_3
Packet arrival rate λ_i (#/sec)	2, 2, 2
Packet Length PA_i (bytes)	200, 200, 200
CWMin W_i-1	7, 3, 3
$AIFSN_i$	6, 3, 2
Carrier sensing range l_{cs}	$1.2R$=600m

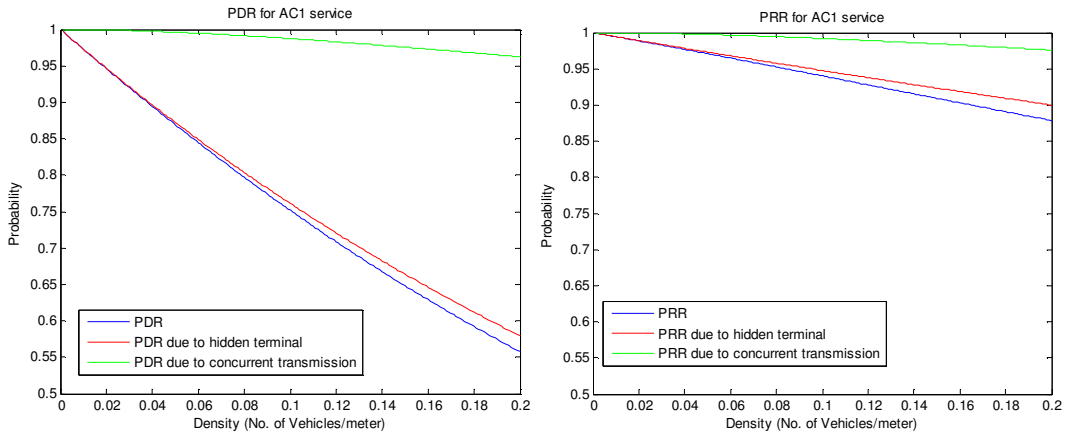

Figure 5.8: Hidden terminal Vs. concurrent transmission

5.5.7 One Vs. Multiple Types of Services

Since EDCA mechanism is supposed to provide service differentiations for different priority services, we want to compare the output measures for one type of service and multiple types of services using EDCA. Therefore, the following two set of parameters are used:

Table 5.11: Parameters for one type of service

Parameters	Values
Packet arrival rate λ (#/sec)	10
Packet Length PA (bytes)	200
CWMin W-1	3
$AIFSN$	3
Carrier sensing range l_{cs}	R=500m

Table 5.12: Parameters for multiple types of services using EDCA

Parameters	Values for AC_1, AC_2, AC_3
Packet arrival rate λ_i (#/sec)	4, 4, 2
Packet Length PA_i (bytes)	200, 200, 200
CWMin W_i-1	7, 3, 3
$AIFSN_i$	6, 3, 2
Carrier sensing range l_{cs}	R=500m

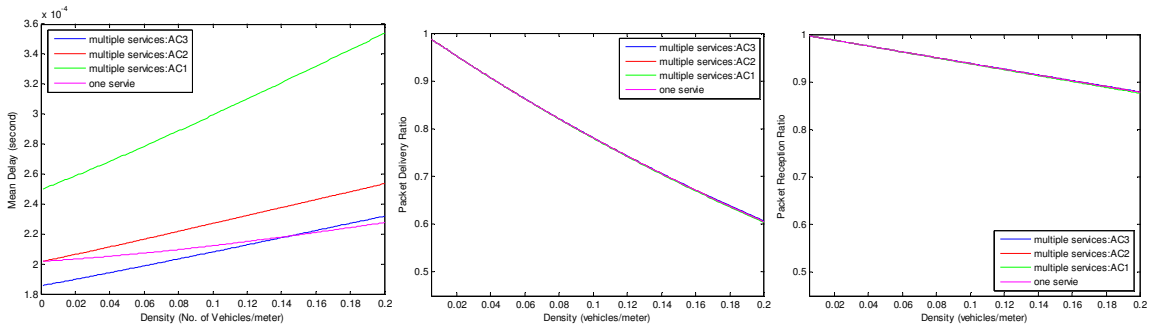

Figure 5.9: One Vs. multiple types of services

Fig. 5.9 shows analytic results for one type of service without priority and multiple services using EDCA mechanism to provide priority. One type of service uses most parameters the same as the second-highest priority service in multiple services. The packet arrival rate for one types of service is the same with the total arrival rate for multiple services. This is to ensure that for any vehicle, the packets generated are the same for one service and multiple services. We can conclude that EDCA mechanism for one-hop one-cycle packet transmission only helps to provide the transmission delay differentiations for different priority services, while not improving reliability of the packet transmission.

In addition, while most parameters, except arrival rate, are the same for one type of service and the second-highest priority service in multiple services type, the second-highest priority services' mean transmission delay increases faster than only one type of services. This is because there are three queues in each vehicle to store different priority services, whereas there is only one queue in each vehicle to store only one type of

service. Therefore, the competition is more severe for multiple services than only one type of service.

5.5.8 Preemptive Priority

Since EDCA mechanism for one-hop one-cycle safety communication does not help improving reliability of the packet transmission as shown in the previous section, other enhancement strategies need to be proposed and evaluated to improve reliability. One possible strategy is that we can set preemptive priority for the highest priority service by using the following input parameters:

Table 5.13: Parameters for preemptive priority

Parameters	Values for AC_1, AC_2, AC_3
Packet arrival rate λ_i (#/sec)	2, 2, 2
Packet Length PA_i (bytes)	200, 200, 200
CWMin W_i-1	7, 3, 0
$AIFSN_i$	6, 3, 1
Carrier sensing range l_{cs}	R=500m

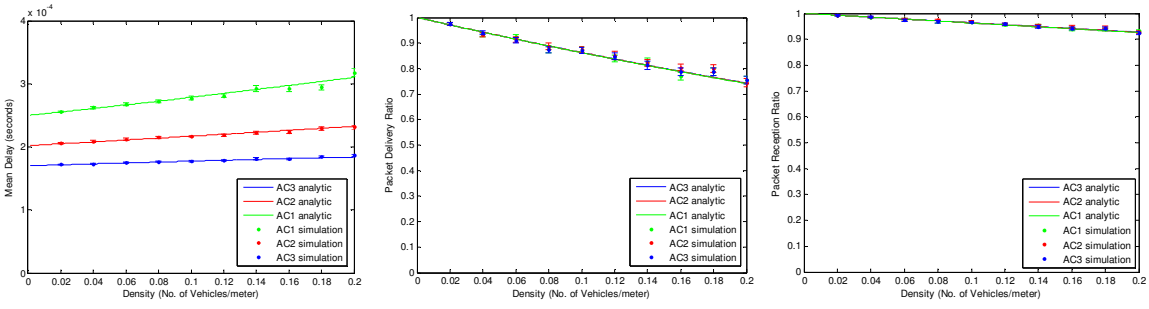

Figure 5.10: Preemptive priority results

The chosen input parameters ensure that for the highest priority service, it will transmit first when other types of services coexist at the same time because of its shortest

channel sensing time and no backoff process. From Fig. 5.10, we can see that preemptive priority only provides delay differentiations whereas not help improving *PDR* and *PRR*. Therefore, preemptive priority is not a good strategy to enhance reliability. This is because of the fact that preemptive priority only helps to reduce concurrent transmission and not influence hidden terminals problem, which dominates the reliability.

5.5.9 Strict Priority

Another possible strategy to enhance performance is utilizing strict priority [92]. Strict priority can be implemented by using distinct *AIFS* for different priority services. The lower priority service's channel sensing time *AIFS* should be larger than the *AIFS* plus the maximum backoff window size of the higher priority services.

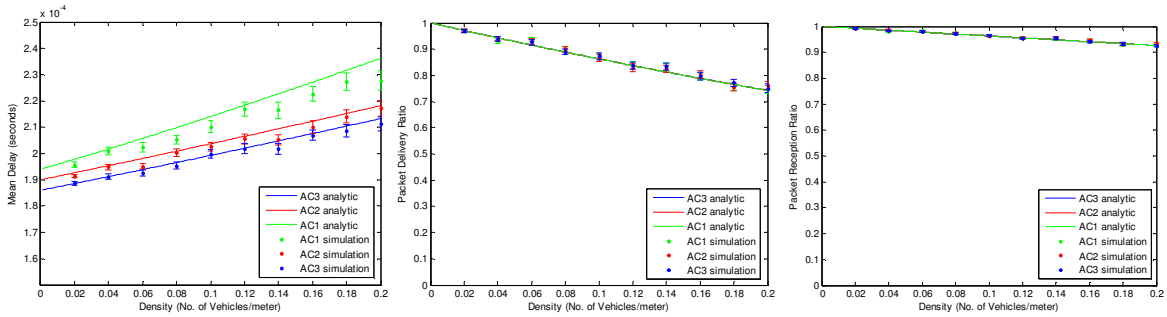

Figure 5.11: Strict priority results

From Fig. 5.11, we observe that strict priority also only provides delay differentiations whereas not help improving *PDR* and *PRR*. Therefore, strict priority is not a good strategy to enhance reliability. This is because of the fact that strict priority

only helps to reduce concurrent transmission and not influence hidden terminals problem, which dominates the reliability.

5.5.10 Variance of Transmission Delay

According to Section 5.4.2, we can obtain the analytic-numeric results for the variance of the transmission delay. The following input parameters are used:

Table 5.14: Parameters for variance computation

Parameters	Values for AC_1, AC_2, AC_3
Packet arrival rate λ_i (#/sec)	2, 2, 2
Packet Length PA_i (bytes)	200, 200, 200
CWMin W_i-1	7, 3, 3
$AIFSN_i$	6, 3, 2
Carrier sensing range l_{cs}	R=500m

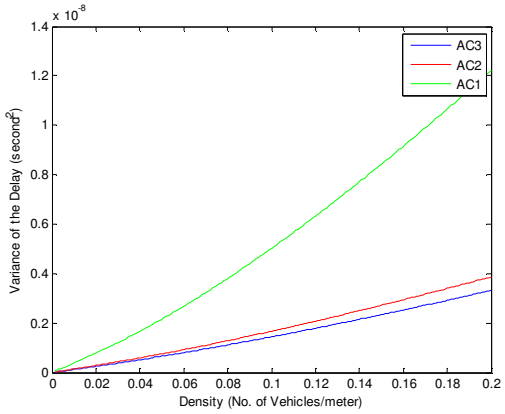

Figure 5.12: Variance of the transmission delay

From Fig. 5.12, we can see that the variance for the transmission delay is very small even when the vehicle density is high. Since we assume packet inter-arrival time is exponential distributed and set the packet arrival rate the same for three types of

services, the difference of the variance are mainly due to the EDCA parameters (backoff window size and *AIFS*).

5.6 GI/G/1 Queue Extension

In the previous analytic model, M/G/1 queue interacting with SMP model, we assume the packet inter-arrival time is exponential distribution. However, in real scenarios, the inter-arrival time can be more generally distributed. Therefore, we are interested in the packet transmissions when packet inter-arrival time is general independent distribution, which can be modeled as GI/G/1 queue instead. In this section, we assume only the mean and variance of the packet inter-arrival time are provided whereas its distribution is unknown. Therefore, the computation methods presented in Section 5.3 and Section 5.4 cannot be directly used. The corresponding modifications for the GI/G/1 queue interacting with SMP models are shown as follows.

5.6.1 SMP Model

The structure of the SMP model for the GI/G/1 queue case is the same as that for the M/G/1 queue. One exception is that the sojourn time in state *idle* will be different. Hence, the mean and variance of the sojourn time in each state is adjusted to:

$$E\left[T_{i,j}\right]=\tau_{i,j}=\begin{cases}\sigma & j=0,1,\cdots W_i-1\\ TM_i=T_H+M_{PA}+\delta+AIFS_i & j=D_0,D_1,\cdots D_{W_i-2}\\ TD_i=T_H+E\left[PA_i\right]/R_d+\delta+AIFS_i & j=XMT\\ E\left[A_i\right]+AIFS_i & j=idle\end{cases} \tag{5.54}$$

$$Var\left[T_{i,j}\right]=\theta_{i,j}^{2}=\begin{cases}0 & j=0,1,\cdots W_i-1\\ 0 & j=D_0,D_1,\cdots D_{W_i-2},XMT\\ Var\left[A_i\right] & j=idle\end{cases} \tag{5.55}$$

where $E[A_i]$ and $Var[A_i]$ represent the mean and variance of the packet inter-arrival time. Therefore, the steady-state probability that a vehicle is in state XMT is adjusted to:

$$\pi_{i,XMT}=\frac{2\cdot TD_i}{\left[\rho_i+q_{bi}\left(1-\rho_i\right)\right]\left[\left(\sigma+p_{bi}\cdot TM_i\right)W_i+\left(\sigma-p_{bi}\cdot TM_i\right)\right]+2\cdot TD_i+2\left(1-\rho_i\right)\left(E\left[A_i\right]+AIFS_i\right)} \tag{5.56}$$

5.6.2 Service Time Computation

Since the current queueing model is GI/G/1 instead of M/G/1, *Welch*'s method to compute the mean of the service time for M/G/1 queue does not apply. Therefore, we use direct initial probability allocation method in this section to compute the mean service time.

The mean and variance of the service time starting from state k for AC_i message ($S_{i,k}$) are the same with M/G/1 queuing model as shown in Section 5.3.2:

$$E\left[S_{i,k}\right]=\begin{cases}k\left(\sigma+p_{bi}\cdot TM_i\right)+TD_i & for\quad k=0,1,\cdots,W_i-1\\ TD_i & for\quad k=XMT\end{cases} \tag{5.57}$$

$$Var\left[S_{i,k}\right]=\begin{cases}k\left[TM_i^2\cdot p_{bi}\cdot\left(1-p_{bi}\right)\right] & for\quad k=0,1,\cdots,W_i-1\\ 0 & for\quad k=XMT\end{cases} \tag{5.58}$$

For a newly generated packet, if the channel is detected busy during $AIFS_i$ time, the tagged vehicle has to wait until the end of the current packet transmission and then start backoff procedure. In our SMP model, we have neglected such waiting time. Since such waiting time is relatively small comparing to the mean packet arrival time, it has

little influence on the steady-state probability that a vehicle is in state *XMT*. Hence, *PDR* and *PRR* are not influenced by such waiting time, while it has some influence on the mean transmission delay. Therefore, it is not necessary to represent this part as an additional state into the model. We only adjust the mean service time here to include this waiting time. When a packet transmission is detected by the tagged vehicle's $AIFS_i$ channel sensing time, the mean waiting time before the tagged vehicle starts backoff procedure is half of the packet transmission. Therefore, the service time for AC_i message will be:

$$S_i = \begin{cases} SI_{i,0} = S_{i,0} & w.p. \quad q_{i,0} = \rho_i / W_i \\ SI_{i,1} = S_{i,1} & w.p. \quad q_{i,1} = \rho_i / W_i \\ \quad \vdots & \\ SI_{i,W_i-1} = S_{i,W_i-1} & w.p. \quad q_{i,W_i-1} = \rho_i / W_i \\ SI_{i,W_i} = S_{i,0} + \dfrac{(TM_i - AIFS_i)}{2} & w.p. \quad q_{i,W_i} = (1-\rho_i) q_{bi} / W_i \\ SI_{i,W_i+1} = S_{i,1} + \dfrac{(TM_i - AIFS_i)}{2} & w.p. \quad q_{i,W_i+1} = (1-\rho_i) q_{bi} / W_i \\ \quad \vdots & \\ SI_{i,2W_i-1} = S_{i,W_i-1} + \dfrac{(TM_i - AIFS_i)}{2} & w.p. \quad q_{i,2W_i-1} = (1-\rho_i) q_{bi} / W_i \\ SI_{i,2W_i} = S_{i,XMT} & w.p. \quad q_{i,2W_i} = (1-\rho_i)(1-q_{bi}) \end{cases} \tag{5.59}$$

with

$$E\left[SI_{i,k}\right] = \begin{cases} k(\sigma + p_{bi} \cdot TM_i) + TD_i & for \quad k = 0,1,\cdots,W_i - 1 \\ (k - W_i)(\sigma + p_{bi} \cdot TM_i) + TD_i + \dfrac{(TM_i - AIFS_i)}{2} & for \quad k = W_i, W_i + 1, \cdots, 2W_i - 1 \\ TD_i & for \quad k = 2W_i \end{cases} \tag{5.60}$$

$$Var\left[SI_{i,k}\right]=\begin{cases} k\left[TM_i^2\cdot p_{bi}\cdot\left(1-p_{bi}\right)\right] & for \quad k=0,1,\cdots,W_i-1 \\ \left(k-W_i\right)\left[TM_i^2\cdot p_{bi}\cdot\left(1-p_{bi}\right)\right] & for \quad k=W_i,W_i+1,\cdots,2W_i-1 \\ 0 & for \quad k=2W_i \end{cases} \tag{5.61}$$

Hence, the mean and variance of the service time is given by:

$$E\left[S_i\right]=\sum_k E\left[SI_{i,k}\right]\cdot q_{i,k}=\frac{\left(\sigma+p_{bi}\cdot TM_i\right)\left[1-\left(1-\rho_i\right)\left(1-q_{bi}\right)\right]\left(W_i-1\right)}{2}+TD_i+\frac{\left(1-\rho_i\right)q_{bi}\cdot\left(TM_i-AIFS_i\right)}{2} \tag{5.62}$$

$$\begin{aligned} Var\left[S_i\right] &= E\left[S_i^2\right]-\left(E\left[S_i\right]\right)^2=\sum_{k=0}^{2W_i}E\left[SI_{i,k}^2\right]\cdot q_{i,k}-\left(E\left[S_i\right]\right)^2 \\ &= \sum_{k=0}^{2W_i}\left\{Var\left[SI_{i,k}\right]+\left(E\left[SI_{i,k}\right]\right)^2\right\}\cdot q_{i,k}-\left(E\left[S_i\right]\right)^2 \\ &= \left[\frac{\left(\sigma+p_{bi}\cdot TM_i\right)^2\left(2W_i-1\right)}{6}+\frac{TM_i^2p_{bi}\left(1-p_{bi}\right)+2\cdot TD_i\cdot\left(\sigma+p_{bi}\cdot TM_i\right)}{2}\right]\left(W_i-1\right)\left[1-\left(1-\rho_i\right)\left(1-q_{bi}\right)\right] \\ &+TD_i^2+\left[\frac{TM_i-AIFS_i}{2}+2\cdot TD_i+\left(\sigma+p_{bi}\cdot TM_i\right)\left(W_i-1\right)\right]\frac{TM_i-AIFS_i}{2}\left(1-\rho_i\right)q_{bi}-\left(E\left[S_i\right]\right)^2 \end{aligned} \tag{5.63}$$

5.6.3 Fixed-point Iteration

The fixed point iteration procedure is exactly the same as the M/G/1 queue interacting with SMP, except that:

$$\rho_i=\frac{E\left[S_i\right]}{E\left[A_i\right]} \tag{5.64}$$

5.6.4 MAC-level Performance Metrics

5.6.4.1 Mean Transmission Delay

Welch's method cannot be used for the mean delay computation. Therefore, we use the approximation formulas proposed by *Whitt* to compute the mean and variance of the queue waiting time for GI/G/1 queue instead:

$$E[W_i] \approx \psi_i \frac{c_{S_i}^2 + c_{A_i}^2}{2} E[W_i]_{M/M/1} = \psi_i \frac{c_{S_i}^2 + c_{A_i}^2}{2} \cdot \frac{\rho_i}{\mu_i (1-\rho_i)} = \psi_i \frac{\left(c_{S_i}^2 + c_{A_i}^2\right) \rho_i E[S_i]}{2(1-\rho_i)} \tag{5.65}$$

where

$$\psi_i = \begin{cases} \dfrac{4\left(c_{A_i}^2 - c_{S_i}^2\right) + c_{S_i}^2 \Psi\left(\dfrac{c_{A_i}^2 + c_{S_i}^2}{2}\right)}{4c_{A_i}^2 - 3c_{S_i}^2} & if \quad c_{A_i}^2 \geq c_{S_i}^2 \\ \dfrac{\left(c_{S_i}^2 - c_{A_i}^2\right) e^{\frac{-2(1-\rho_i)}{3\rho_i}} + \left(c_{S_i}^2 + 3c_{A_i}^2\right) \Psi\left(\dfrac{c_{A_i}^2 + c_{S_i}^2}{2}\right)}{2\left(c_{A_i}^2 + c_{S_i}^2\right)} & if \quad c_{A_i}^2 \leq c_{S_i}^2 \end{cases}$$

The function $\Psi(.)$ is defined as:

$$\Psi\left(c_i^2\right) = \begin{cases} 1 & if \quad c_i^2 \geq 1 \\ \left(0.5 + 0.5e^{\frac{-2(1-\rho_i)}{3\rho_i}}\right)^{2\left(1-c_i^2\right)} & if \quad 0 \leq c_i^2 \leq 1 \end{cases}$$

Hence, based on Eqs. (5.62)(5.65), the mean of the transmission delay for AC_i message is:

$$E[D_i] = E[W_i] + E[S_i] \tag{5.66}$$

5.6.4.2 Variance of Transmission Delay

To derive the variance of the transmission delay, we use the formulas proposed by *Whitt* for the squared coefficient of variation of the steady-state waiting time in a GI/G/m queue. For a GI/G/1 queue, the approximation reduces to:

$$c_{W_i}^2 \approx \frac{2\rho_i + \dfrac{4(1-\rho_i) d_{S_i}^3}{3\left(c_{S_i}^2 + 1\right)^2} - P(W_i > 0)}{P(W_i > 0)}$$

where

$$d_{S_i}^3 = \frac{E\left[S_i^{\,3}\right]}{\left(E\left[S_i\right]\right)^3}$$

$$\begin{aligned}
E\left[S_i^3\right] &= \sum_{k=0}^{2W_i} E\left[SI_{i,k}^3\right]\cdot q_{i,k} \\
&= \sum_{k=0}^{W_i-1} E\left[S_{i,k}{}^3\right]\cdot\frac{\rho_i}{W_i} + \sum_{k=W_i}^{2W_i-1} E\left[\left(S_{i,k-W_i}+\frac{TM_i-AIFS_i}{2}\right)^3\right]\cdot\frac{(1-\rho_i)q_{bi}}{W_i} + E\left[S_{i,XMT}{}^3\right]\cdot\frac{(1-\rho_i)(1-q_{bi})}{W_i} \\
&= \sum_{k=0}^{W_i-1} E\left[S_{i,k}^3\right]\cdot\frac{\left[1-(1-\rho_i)(1-q_{bi})\right]}{W_i} + E\left[S_{i,XMT}{}^3\right]\cdot\frac{(1-\rho_i)(1-q_{bi})}{W_i} + \left(\frac{TM_i-AIFS_i}{2}\right)^3\cdot(1-\rho_i)q_{bi} \\
&\quad + \frac{3(TM_i-AIFS_i)}{2}\cdot\sum_{k=0}^{W_i-1} E\left[S_{i,k}{}^2\right]\cdot\frac{(1-\rho_i)q_{bi}}{W_i} + \frac{3(TM_i-AIFS_i)^2}{4}\cdot\sum_{k=0}^{W_i-1} E\left[S_{i,k}\right]\cdot\frac{(1-\rho_i)q_{bi}}{W_i}
\end{aligned}$$

In the above equation,

$$\sum_{k=0}^{W_i-1} E\left[S_{i,k}\right] = \left\{\frac{(W_i-1)(\sigma+p_{bi}\cdot TM_i)}{2}+TD_i\right\}W_i$$

$$E\left[S_{i,k}{}^2\right] = Var\left[S_{i,k}\right]+\left(E\left[S_{i,k}\right]\right)^2$$

$$\sum_{k=0}^{W_i-1} E\left[S_{i,k}{}^2\right] = \left\{\frac{(W_i-1)(2W_i-1)(\sigma+p_{bi}\cdot TM_i)^2}{6}+TD_i^2+\frac{(W_i-1)\left[2\cdot TD_i\cdot(\sigma+p_{bi}\cdot TM_i)+TM_i{}^2 p_{bi}(1-p_{bi})\right]}{2}\right\}W_i$$

$$E\left[S_{i,k}^3\right] = E\left[\left(\sum_j T_{i,j}\cdot X_{i,kj}\right)^3\right]$$

$$= \sum_j E\left[\left(T_{i,j}\cdot X_{i,kj}\right)^3\right]+3\cdot\sum_{\substack{j,l\\ l\neq j}}\left\{E\left[\left(T_{i,j}\cdot X_{i,kj}\right)^2\right]\cdot E\left[T_{i,l}\cdot X_{i,kl}\right]\right\}+6\cdot\sum_{\substack{j,l,n\\ j\neq l\neq n}} E\left[T_{i,j}\cdot X_{i,kj}\right]E\left[T_{i,l}\cdot X_{i,kl}\right]E\left[T_{i,n}\cdot X_{i,kn}\right]$$

$$= \sum_j\left(\tau_{i,j}^3\cdot m_{i,kj}\right)+3\cdot\sum_{\substack{j,l\\ l\neq j}}\left\{\left[\theta_{i,j}^2\cdot m_{i,kj}+\tau_{i,j}^2\cdot\left(\sigma_{i,kj}^2+m_{i,kj}^2\right)\right]\cdot\tau_{i,l}\cdot m_{i,kl}\right\}+6\cdot\sum_{\substack{j,l,n\\ j\neq l\neq n}}\tau_{i,j}\cdot m_{i,kj}\cdot\tau_{i,l}\cdot m_{i,kl}\cdot\tau_{i,n}\cdot m_{i,kn}$$

Whitt also gives the following approximation for $P(W_i>0)$:

$$P(W_i>0)\approx\rho_i^2\pi_1+\left(1-\rho_i^2\right)\pi_2$$

where

$$\pi_1 = \min\left\{1, \rho_i \frac{1-\Phi\left(\frac{\left(1+c_{S_i}^2\right)(1-\rho_i)}{c_{A_i}^2+c_{S_i}^2}\right)}{1-\Phi(1-\rho_i)}\right\}$$

$$\pi_2 = \min\left\{1, \rho_i \frac{1-\Phi\left(2\left(1+c_{A_i}^2\right)(1-\rho_i)\right)}{1-\Phi(1-\rho_i)}\right\}$$

$\Phi(.)$ is the *pdf* for the standard normal distribution. Therefore, the variance of the queuing waiting time is given by:

$$Var[W_i] = c_{W_i}^2 \cdot \left(E[W_i]\right)^2 \tag{5.67}$$

Assuming the queue waiting time and service time are independent and based on Eqs. (5.63)(5.67), we can approximate the variance of the transmission delay as:

$$Var[D_i] \approx Var[W_i] + Var[S_i] \tag{5.68}$$

5.6.4.3 PDR

The *PDR* computation formula is the same as M/G/1 queue.

5.6.4.4 PRR

The *PDR* computation formula is the same as M/G/1 queue.

5.6.4.5 Numerical Results

To evaluate the correctness and accuracy of the method for GI/G/1 queue case, the parameters in Table 5.15 are used for the numeric results computation. The numeric results for the analytic model are shown in Fig. 5.13.

Table 5.15: Parameters for GI/G/1 queue

Parameters	Values for AC_1, AC_2, AC_3
Mean packet inter-arrival time $E[A_i]$ (sec)	0.5, 0.5, 0.5
Variance of packet inter-arrival time $Var[A_i]$ (sec^2)	0.25, 0.25, 0.25
Packet Length PA_i (bytes)	200, 200, 200
CWMin W_i-1	7, 3, 3
$AIFSN_i$	6, 3, 2
Carrier sensing range l_{cs}	R=500m

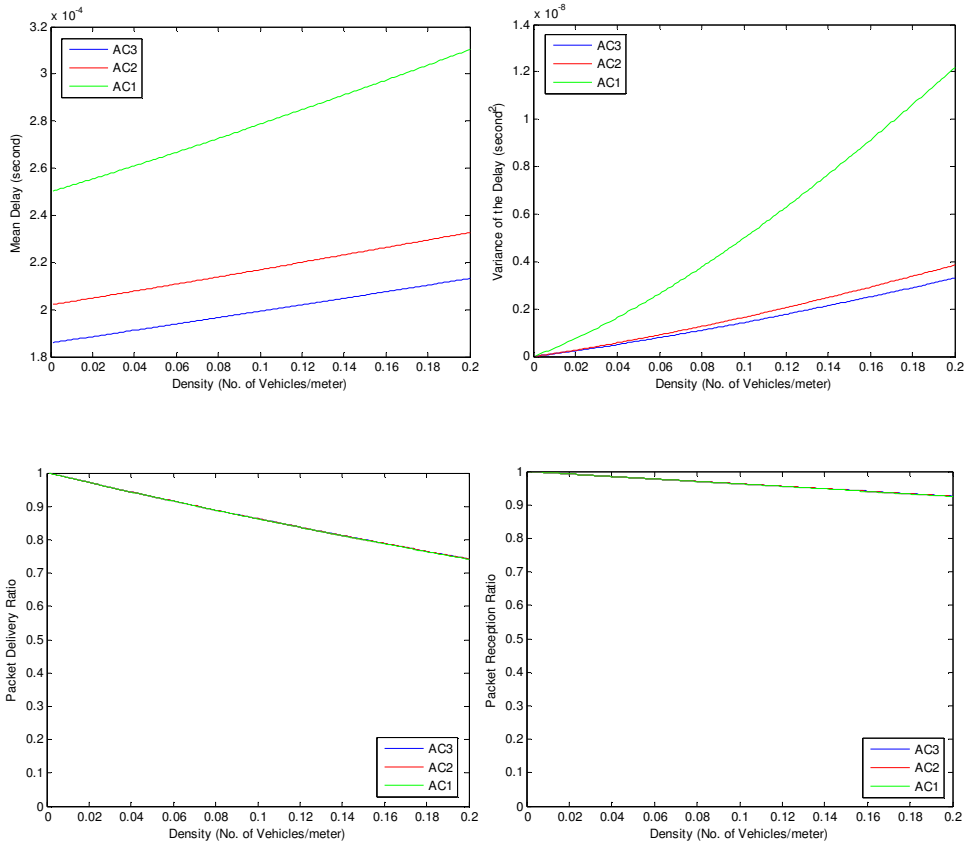

Figure 5.13: Output measures for GI/G/1 queue

Comparing to the M/G/1 queue case, we set the input parameters for M/G/1 queue as the counterpart of GI/G/1 queue, where the mean and variance of the packet inter-arrival time is the same as shown in Table 5.16.

Table 5.16: Parameters for GI/G/1 queue

Parameters	Values for AC_1, AC_2, AC_3
Packet arrival rate λ_i (#/sec)	2, 2, 2
Packet Length PA_i (bytes)	200, 200, 200
CWMin W_i-1	7, 3, 3
$AIFSN_i$	6, 3, 2
Carrier sensing range l_{cs}	R=500m

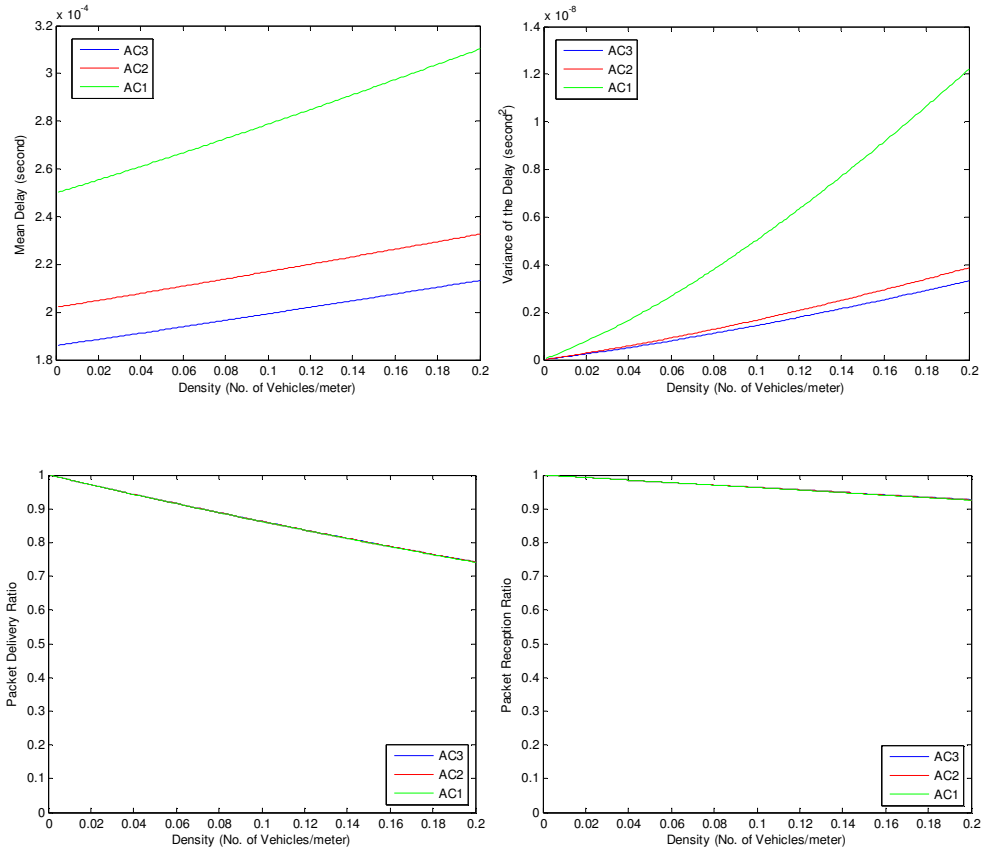

Figure 5.14: Output measures for M/G/1 queue

From the results, we observe that for GI/G/1 queue with the same mean and variance of the packet inter-arrival time as M/G/1 queue, they have almost the same output measures. Such close match validates the correctness and accuracy of our analytic model for the GI/G/1 queue case. In addition, from the numerical results, we conclude that the mean and variance of the transmission delay is dominated by the mean and variance of the service time respectively. Queueing waiting time occupies a very small portion of the transmission delay.

5.7 A Case Study

In this section, we apply our proposed model to a case study for Vehicle Safety Communications (VSC) vehicles to reflect MAC-layer performances in real scenarios. Since currently there is no standard on the applications that will be deployed in future and corresponding implementations (*i.e.*, channel allocation and priority setting), we propose the applications over the control channel with three priorities based on [53] as shown in Table 5.17. Important input parameters for VSC vehicles, including packet length and transmission range, are chosen from the testbed used in GM's EN-V concept vehicles. Electric Networked-Vehicles (EN-V) are capable of low-speed autonomous driving in both indoor and outdoor controlled environments. State-of-the-art DSRC-based V2X communication, GPS, in-vehicle vision and ultrasonic sensors were used in combination with GM R&D-developed motion control, dead reckoning, collision avoidance and platoon control algorithms and software to achieve the intended

autonomous driving capability. The other parameters for VSC vehicles are chosen in the way to reflect typical DSRC network settings in [1] and default EDCA parameter settings in [93] as shown in Table 5.18.

Table 5.17: Safety applications over the control channel

Access Category	Priority Level	Applications	Description	Arrival Rate
AC3	Highest	Emergency Electronic Brake Light	A vehicle braking hard broadcasts a warning message to approaching vehicles in its neighborhood for the duration of the event	5.6e-5~2.8e-4 packets/sec (every 1~5 hours a packet)
AC2	Second	Cooperative Collision Warning (CCW)	A vehicle actively monitors kinematics status messages from vehicles in its neighborhood to warn of potential collisions	2~10 packets/sec (every 0.1~0.5 sec a packet)
AC1	Lowest	Road Feature Notification (RFN)	A vehicle detecting a road feature (*e.g.*, road curve, hill, road grade) notifies approaching vehicles in its neighborhood	2.8e-4~5.6e-4 packets/sec (every 30~60 min a packet)

Table 5.18: Parameters setting for case study

Parameters	Values	Parameters	Values
Tx range R	300 m	Data rate R_d	24 *Mbps*
PHY preamble	40 μs	Vehicle density β	Variable
PLCP header	4 μs	Packet arrival rate λ_i	Variable
MAC header	272 bits	Packet Length PA_i (bytes)	[119, 102, 102]
Slot time σ	16 μs	CWMin W_i-1	[15, 7, 3]
SIFS	32 μs	$AIFS_i$	[6, 3, 2]
Propagation delay δ	0 μs	Carrier sensing range l_{cs}	1.2R=360m

Since the packet arrival rates for three types of services are variable within the range in Table 5.17, we evaluate the upper and lower bound respectively in the next step.

For the lower bound, the packet arrival rates are [λ_{AC1}, λ_{AC2}, λ_{AC3}]=[2.8e-4, 2, 5.6e-5]. Fig. 5.15 shows the output measures.

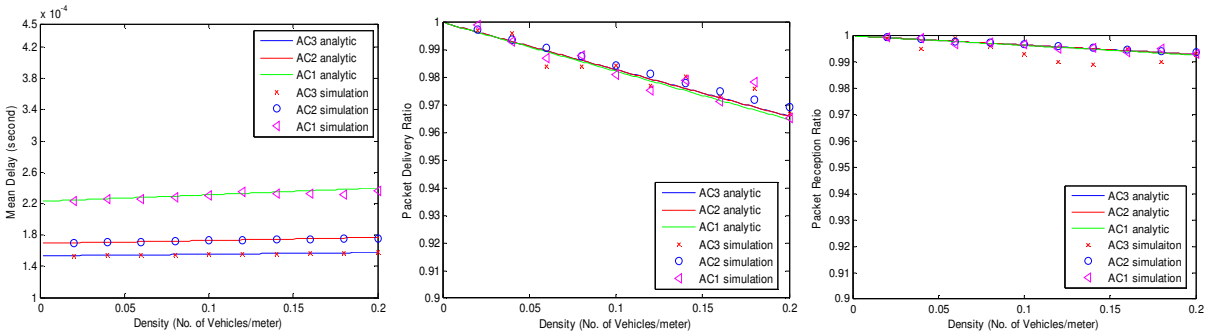

Figure 5.15: Applications with lower bound packet arrival rates

For the upper bound, the packet arrival rates are [λ_{AC1}, λ_{AC2}, λ_{AC3}]=[5.6e-4, 10, 2.8e-4]. Fig. 5.16 shows the output measures.

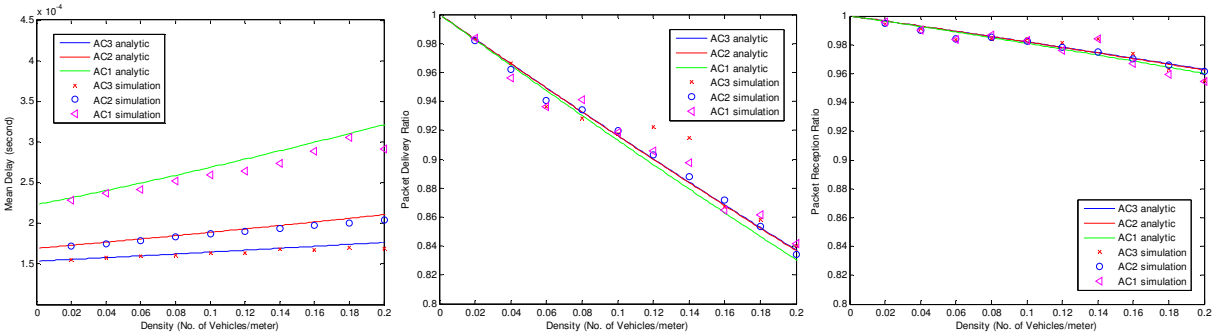

Figure 5.16: Applications with upper bound packet arrival rates

From the results, we can see that the analytic matches with the simulation very well. In addition, we observe that when the total packet arrival rate becomes large, the delay increases whereas the *PDR* and *PRR* decrease. The delay differentiations are mainly due to EDCA parameters (backoff window size and *AIFS*) as shown in Section 5.5. Furthermore, even though the packet length for AC_1 is different from the other two

types of services, the reliability does not show much difference because the difference on packet length is relatively small.

5.8 Conclusions

In this research, a more general and accurate analytic model using SMP interacting with an M/G/1 or GI/G/1 queue has been developed to characterize the behavior of DSRC for highway safety communications with multiple types of services with priority using EDCA mechanism. In a tagged vehicle, we use different queues to store different types of messages and construct separating SMP models for each type of safety message services. These separating SMP models interact with each other and also with their own corresponding M/G/1 queues. Fixed-point iteration is used to obtain the converged solution. New proposed analytic model also facilitates the accurate evaluation of hidden terminal impact that is one of major factors for degradation of the reliability, which has not been properly or precisely addressed in the previous work. Both *PDR* and *PRR*, the two very important reliability metrics for DSRC safety-related services, are analytically derived using the new model structure. The model is cross validated against simulations. Moreover, the analysis with different input parameters is used to suggest better parameter settings that will improve the MAC-layer performance by decreasing the mean delay, increasing *PDR* and *PRR*. A case study is conducted based on the testbed for GM's EN-V concept vehicles to provide insights for real scenarios.

From our analysis, several conclusions and observations are made. First, *PDR* and *PRR* are dominated by hidden terminal problem whereas concurrent transmission has little impact. In addition, higher priority service should choose shorter packet length, higher data rate and larger carrier sensing range to ensure high packet transmission reliability. Furthermore, the EDCA mechanism can only provide service differentiation in terms of transmission delay, but is not helpful to improve the reliability for higher priority services.

Above all, the proposed model and conclusions will be beneficial to the analysis, design, and network parameter optimization for required MAC-layer performance and reliability of DSRC VANET for multiple types of safety-related services. Based on the proposed model, more practical models for more applications can be developed in future.

6. Multi-channel Operation Evaluation

6.1 Motivation

Dedicated Short Range Communication (DSRC) band consists of seven channels, one control channel (CCH) and six service channels (SCHs). IEEE 1609.4 architecture [63] extends MAC layer operation and defines a channel switching protocol to enable a DSRC radio to operate efficiently on multiple DSRC channels. The default access mode in IEE 1609.4 is alternating access scheme in which the channel time is divided into synchronization periods with a fixed length of 100 *ms*, consisting of CCH and SCH intervals as shown in Fig. 1.1 in Chapter 1. All vehicles are assumed to have access to Universal Coordinated Time (UTC) (*e.g.*, achieved via GPS). During the CCH interval, all vehicles tune on the CCH frequency for safety-related and system management data exchange. During the SCH interval, vehicles switch to one of the SCH frequencies for safety or non-safety related services been provided. 4 *ms* guard time is set at the beginning of each interval to account for switching delay and time inaccuracy. Basic Safety Message (BSM) [45][46] is one type of messages broadcasted in CCH interval to announce the status information of a vehicle (*i.e.*, position, speed, direction) to its neighbors. Many safety applications rely on the timely and reliable transmissions of such information to provide satisfactory services.

The safety message dissemination on CCH has been extensively evaluated by either simulation or analytic model, but most of them have not considered the channel

switching for multi-channel operations and its impact on system performances. The performance of multi-channel operations for safety messages have been evaluated in [61][64][67]. Chen. [61] evaluated three access modes of the communication for a single radio and the one with optimized scheduling has shown to effectively avoid synchronization collisions associated with naïve use of channel switching access. Hong. [64] proposed three alternative approaches for V2V safety communications in a multi-channel environment for single-radio and multi-radio vehicle accommodation. Du. [67] assessed performance of periodic beacon message transmission in CCH intervals with respect to number of vehicles in the system. However, they are all based on simulations in either NS2 or NCTUns and only MAC-level performance metrics (*i.e.*, message reception probability, transmission delay) is evaluated. Few analytic models [26][65][66] have been proposed to characterize the MAC-level performance of safety messages broadcasting on CCH intervals. Campolo. [26] proposed a recursive method to assess the basic access mode for channel switching operation in which synchronization collisions remain a severe problem. In addition, hidden terminal problem, which is one of major factors for degradation of packet delivery reliability, is omitted in this work. Misic. [65] investigated the performance of a single-radio supporting several traffic combinations, each of which presents a mix of traffic classes, over control and service channels based on Markov chain. However, no simulation is conducted to validate the accuracy of their proposed model. Ghandour. [66] constructed analytic models for

upper-bound on the packet delivery delay of safety broadcast messages in multi-channel environment and validated through simulations in NS2. These work on analytic models only derived very few MAC-level performances (*i.e.*, transmission delay, packet reception probability) and channel fading effect has not been considered to characterize practical communication environment.

In this work, we develop a detailed analytic model based on SMP [9] to characterize both MAC and application-level performance of BSM dissemination in CCH interval for multi-channel operations in a single-radio device incorporating channel switching mechanism. Synchronization collisions [45] are avoided through optimized scheduling [61]. BSM service time distribution is derived using *Laplace-Stieltjes* transform based on the proposed SMP model. Next, fixed-point iteration method is used to obtain converged solutions. Based on the fixed-point solution, MAC and application-level performance metrics are derived. Channel fading with path loss is taken into account in such derivation. The analytic models are validated through simulations in NS2 to verify the accuracy of the proposed model. The model is also compared with previous models [68] to evaluate the effect of channel switching mechanism on the performance of message delivery probability.

The major contributions of this work are four-fold: 1) BSM broadcasting behavior in CCH interval incorporating channel switching mechanism is accurately captured by a detailed analytic model; 2) Important MAC and application-level performance metrics

are derived to evaluate the performance of message broadcasting; 3) Channel switching utilizing optimized scheduling is implemented in NS2 to validate the accuracy of the proposed models; 4) Concurrent transmissions, hidden terminal problem and channel fading effect are all taken into consideration for the performance assessment and their impact are evaluated.

6.2 System Assumptions

In this work, several assumptions are made. Similar to Chapters 3-5, we consider one-dimensional (1-D) for the traffic on highway and the number of vehicles in a line is Poisson distributed with parameter β (vehicle density). All vehicles have the same transmission range, receiving range and carrier sensing range R. To avoid the synchronized collisions, we utilize the optimized scheduling [61] to ensure that the BSM is en-queued at the MAC layer during a random time within the CCH interval only [45]. Suppose the basic BSM generation interval is τ, the message generation frequency after optimized scheduling is $T/(T_C \cdot \tau)$ (By default, sync period duration T=100 *ms*; CCH interval duration T_C=46 *ms*), where the message generated during non-CCH interval are ignored [61]. In addition, since the typical safety message generation rate is within [2, 10] packets/second, we only consider at most one message transmission from a vehicle during a CCH interval. Channel fading with path loss is considered in this work to reflect real traffic scenarios. Vehicle mobility is not considered.

6.3 Analytic Models

6.3.1 Overall Method Description

Similar to the approaches described in Chapter 3, we use model decomposition to develop a tractable analytic model to capture the interactions between multiple vehicles. First, a SMP model with an absorbing state (SMPA) in Section 6.3.2 is developed to capture the channel contention and backoff behavior for a packet transmission during a CCH interval. The influences from other vehicles are represented through three model parameters (p_b, q_b, r_b) remaining to be determined. Based on such SMPA model, service time distribution ($F_{TA}(t)$) for a packet transmission can be computed using *Laplace–Stieltjes* transform in Section 6.3.3. If the service time exceeds this CCH interval, then the message will be discarded. Therefore, the probability that a BSM is not discarded (P_{TX}) can be obtained based on the service time distribution computed earlier. SMPA model parameters p_b, q_b, r_b can be subsequently derived using P_{TX}. Due to the interaction between these four model parameters, fixed-point iteration can be used to obtain the final converged solutions presented in Section 6.3.4. The import graph for such overall method is shown in Fig. 6.1.

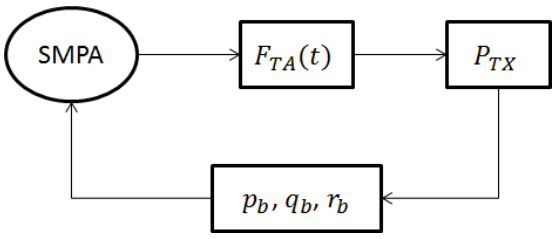

Figure 6.1: Import graph for the overall method

6.3.2 SMP Model

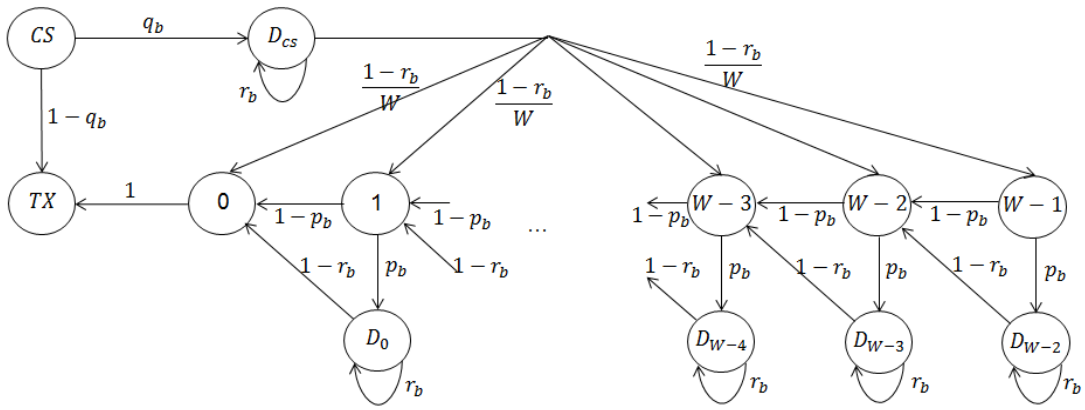

Figure 6.2: SMP model for a BSM transmission

The behavior for a BSM transmission from a tagged vehicle is captured by the SMP model with absorbing state in Fig. 6.2. Initially, the vehicle is in *CS* state, which just generated a packet and has to sense the channel for *DIFS* time duration. If there is no packet transmission in the channel (with probability 1-q_b), the vehicle immediately starts to transmit, going to state *TX*. Otherwise, the vehicle will defer until channel is idle for *DIFS* duration represented by state *Dcs*. Such deference behavior for the tagged vehicle includes two parts: waiting for the current packet in the channel finishing transmission and waiting for subsequent transmissions if any from other neighbors within its receiving range. The self-loop for state *Dcs* represents the phenomena in the Fig. 4.6 in Chapter 4 that the tagged vehicle (vehicle *B*) waits for the current packet (from vehicle *A*) in the channel finishing transmission, and then senses the channel for *DIFS* time, which captures the transmission from another vehicle (vehicle *C*) and leads to further

deference. The probability that the tagged vehicle detects another neighbor's transmission during DIFS time is denoted as r_b.

If no other neighbors' transmission is detected, the tagged vehicle will start backoff procedure and randomly choose a backoff counter in the range [0, W-1], where W=CW+1 is the backoff window size. The backoff counter will be decreased by one if the channel is detected to be idle for a time slot of duration σ (with probability 1-p_b), which is captured by the transition from state W-i to state W-i-1. If the channel is busy during a backoff time slot of duration σ (i.e., another vehicle starts to transmit a packet during this time slot), the backoff counter of the tagged vehicle will be suspended, which is represented by the transition from state W-i to $D_{W\text{-}i\text{-}1}$ with probability p_b. Similar to state D_{CS}, state $D_{W\text{-}i\text{-}1}$ also contains self-loop because other neighbors' transmission can lead to further deference of the tagged vehicle. When the backoff counter reaches zero, the packet will directly be transmitted (an SMP transition occurs from state 0 to state TX with probability one). In TX state, a packet is transmitting.

Compared to the SMP model presented in Chapter 2 and Chapter 3, which captures packets transmission from a tagged vehicle continuously over time, we directly construct this SMP model with absorbing state in this work because we have assumed that at most one packet will transmit from a vehicle during a CCH interval, which has limited time duration: 46 *ms*.

In this SMPA model, sojourn time in each state T_j are all deterministic:

$$T_j = \begin{cases} A_1 & j = \text{TX} \\ A_2 & j = \text{CS} \\ A_3 & j = D_{CS} \\ A_4 & j = D_0, D_1, \cdots, D_{W-2} \\ 0 & j = 0 \\ \sigma & j = 1, 2, \cdots, W-1 \end{cases} \tag{6.1}$$

where

$$\begin{cases} A_1 = PL / R_d + T_H + \delta \\ A_2 = DIFS \\ A_3 = (A_1 + DIFS)/2 \\ A_4 = A_1 + DIFS \end{cases}$$

PL represents the packet length. R_d presents the data rate. Hence, PL/R_d is the time to transmit the packet. T_H represents the time to transmit the packet header including physical layer header and MAC layer header. δ is the propagation delay.

6.3.3 Service Time Computation

Based on the SMPA model in Section 6.3.2, the time to reach the absorbing state, denoted as *TA*, will be the service time for a packet transmission. Let the cumulative distribution function (*CDF*) for *TA* be denoted by $F_{TA}(t)$. Since the sojourn time in each state is deterministic, their *Laplace–Stieltjes* transform (*LST*) can be easily determined:

$$L_{T_j}(s) = E\left[e^{-s \cdot T_j}\right] = \begin{cases} e^{-s \cdot A_1} & i = TX \\ e^{-s \cdot A_2} & i = CS \\ e^{-s \cdot A_3} & j = D_{CS} \\ e^{-s \cdot A_4} & j = D_0, D_1, \cdots D_{W-2} \\ 1 & j = 0 \\ e^{-s \cdot \sigma} & j = 1, \cdots W-1 \end{cases} \tag{6.2}$$

Hence, the LST of the time to reach the absorbing state *TA* is given by:

$$L_{TA}(s) = E\left[e^{-s\cdot TA}\right] = e^{-s\cdot(A_1+A_2)}\left\{\begin{array}{l}(1-q_b)+q_b\cdot e^{-s\cdot A_3}\sum_{k=0}^{\infty}\left(r_b\cdot e^{-s\cdot A_3}\right)^k\cdot\dfrac{(1-r_b)}{W} \\ \cdot\sum_{i=0}^{W-1}\left[(1-p_b)\cdot e^{-s\cdot\sigma}+p_b\cdot(1-r_b)e^{-s\cdot(\sigma+A_4)}\sum_{k=0}^{\infty}\left(r_b\cdot e^{-s\cdot A_4}\right)^k\right]^i\end{array}\right\} \quad (6.3)$$

Hence, the *Laplace* transform for $F_{TA}(t)$, denoted as $F^*(s)$ is:

$$F^*(s) = \frac{L_{TA}(s)}{s} \quad (6.4)$$

Upon inversion of such a *Laplace* transform, the service time distribution, $F_{TA}(t)$, can be easily obtained:

$$F_{TA}(t) = L^{-1}\left(F^*(s)\right) \quad (6.5)$$

Based on such service time distribution, the probability that a BSM message is not discarded when the CCH interval expires can be obtained. Since the arrival time for a BSM is uniformly distributed in a CCH interval, the conditional probability that a BSM is not discarded given that it arrives at time t_0 is $F_{TA}(T_C\text{-}t_0)$ (we assume that the CCH interval starts at time 0 and the duration for CCH interval is T_C). Therefore, the unconditional probability that a BSM is not discarded when the CCH interval expires is:

$$P_{TX} = \int_0^{T_c}\frac{1}{T_c}\cdot F_{TA}(T_c - t_0)\cdot dt_0 \quad (6.6)$$

6.3.4 Fixed-point Iteration

As described in Section 6.3.2 and Section 6.3.3, four unknown model parameters need to be determined to obtain the system steady-state behavior. In the previous section, P_{TX} is shown to depend on the service time distribution, which further depends

on the other three model parameters p_b, q_b and r_b. In this section, the channel busy probabilities p_b, q_b and r_b are derived first, each of them is shown to depend on the other three parameters. Therefore, fixed-point iteration algorithm is used to obtain final solutions.

p_b is the probability that the tagged vehicle detected other vehicles start to transmit within a backoff time slot during backoff procedure. Since P_{TX} represents the probability that a vehicle transmits one packet during CCH interval, we can abstract the packet transmission as Fig. 6.3.

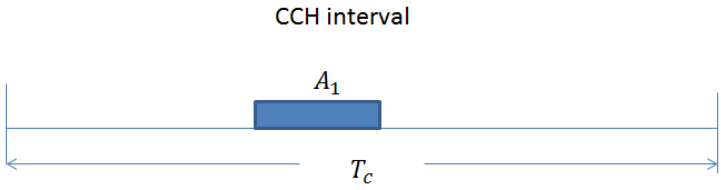

Figure 6.3: A BSM transmission during CCH interval

From Fig. 6.3, we know that the starting time instance of the packet transmission can only happen during T_C-A_1 interval. If one vehicle starts to transmit during one backoff time slot of the tagged vehicle, it will cause the tagged vehicle to freeze the backoff counter and wait for the packet finishes transmission. Hence, $P_{TX}\cdot\sigma/(T_C\text{-}A_1)$ means the probability that a vehicle transmits during one backoff time slot of the tagged vehicle. Hence,

$$p_b = 1-\sum_{i=0}^{\infty}(1-D_1)^{i\cdot\frac{T}{\tau}}\frac{N_{tr}^i}{i!}e^{-N_{tr}} = 1-e^{-N_{tr}\cdot\left[1-(1-D_1)^{\frac{T}{\tau}}\right]} \tag{6.7}$$

where

$$D_1 = \mathrm{P_{TX}} \cdot \frac{\sigma}{\mathrm{T}_c - A_1}$$

and N_{tr} is the average number of vehicles within the transmission range of the tagged vehicle given by Eq. (4.14).

In Eq. (6.7), T/τ represents the total number of packets generated within one sync period from one vehicle. Based on optimized scheduling [61], the packets generated within the SCH period will be scheduled uniformly to CCH interval. Hence, the packets generated from one vehicle will be T/τ within one CCH interval. Since we only consider the typical BSM generation rate 2~10Hz, then $0.2 \le T/\tau \le 1$. Therefore, the packets generated from one vehicle within a CCH interval will not be larger than 1. If there are i vehicles within the tagged vehicle's transmission range, the total number of packets generated from these i vehicles will be $i \cdot T/\tau$ within one CCH interval. In other words, we can also interpret $i \cdot T/\tau$ as the average number of vehicles that generate a packet within a CCH interval.

q_b denotes the probability that the tagged vehicle detects other vehicle's transmission within the channel sensing time *DIFS*. Fig. 6.4 shows that when a vehicle is transmitting, the tagged vehicle can detect this transmission during *DIFS* time if there is an overlap between *DIFS* and A_1. Hence, the starting point of *DIFS* can vary over range $DIFS+A_1$ to detect such transmission. Therefore, $P_{TX} \cdot (DIFS+A_1)/T_C$ represents the probability that a vehicle's transmission is detected in the tagged vehicle's *DIFS* channel sensing time.

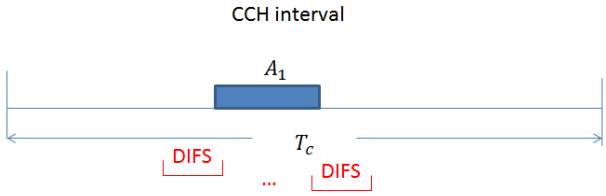

Figure 6.4: DIFS channel sensing during CCH interval

Therefore,

$$q_b = 1 - \sum_{i=0}^{\infty} (1-D_2)^{i \cdot \frac{T}{\tau}} \frac{N_{tr}^i}{i!} e^{-N_{tr}} = 1 - e^{-N_{tr} \cdot \left[1-(1-D_2)^{\frac{T}{\tau}}\right]} \tag{6.8}$$

where

$$D_2 = \mathrm{P_{TX}} \cdot \frac{DIFS + A_1}{\mathrm{T}_c}$$

Following the same concept and computation procedures for r_b in Chapter 4 Section 4.3.3, r_b is given by:

$$r_b = 1 - \sum_{i=0}^{\infty} (1-D_2)^{i \cdot \frac{T}{\tau}} \frac{(N)^i}{i!} e^{-N} = 1 - e^{-N \cdot \left[1-(1-D_2)^{\frac{T}{\tau}}\right]} \tag{6.9}$$

where

$$N = \int_0^R \beta x \frac{1}{R} \cdot dx = \frac{\beta R}{2} = \frac{N_{tr}}{4}$$

From the above analysis, we know that the four parameters P_{TX}, p_b, q_b and r_b are interdependent. Hence, the fixed-point iteration algorithm is utilized and outlined as follows to obtain the final converged solutions.

Step 1: Initialize P_{TX}=1,p_b=0,q_b=0,r_b=0.

Step 2: With P_{TX}, p_b, q_b, r_b, calculate new P_{TX}, p_b, q_b, r_b according to Eqs. (6.6)(6.7)(6.8)(6.9).

Step 3: If P_{TX}, p_b, q_b, r_b converge with the previous values, then stop the algorithm; otherwise, go to step 2 with the updated P_{TX}, p_b, q_b, r_b. Once the parameters P_{TX}, p_b, q_b, r_b are determined using the above algorithm, they are used for both MAC and application layer performance indices computation in the next section.

6.4 Performance Metrics

6.4.1 MAC-level Performance Metrics

6.4.1.1 Mean Transmission Delay

The mean transmission delay conditioning on a BSM arrives at t_0 is given by:

$$\int_0^{T_c - t_0} \left[1 - F_{TA}(t)\right] dt$$

Therefore, the un-conditioning mean transmission delay for a BSM is:

$$E[D] = \int_0^{T_c} \frac{1}{T_c} \left(\int_0^{T_c - t_0} \left[1 - F_{TA}(t)\right] dt \right) dt_0 \tag{6.10}$$

6.4.1.2 Node Reception Probability (NRP)

In Chapter 3, the reliability for a packet transmission (node reception probability, packet delivery ratio and packet reception ratio) has not taken into account of channel fading effects. In this Chapter, to model real traffic scenarios, we consider hidden terminal problem, concurrent transmissions and channel fading with path loss to obtain MAC layer packet transmission reliability metrics.

As shown in Fig. 4.7, we compute the node reception probability $P_s(x)$ that node *U* successfully receives the broadcast BSM from the tagged node *O*. Three factors

affecting the performance of the packet reception are considered: hidden terminal problems, collision due to concurrent transmissions, and channel fading.

a. Impact of hidden terminals

Based on the SMPA model and its solution, we have the probability that node *U*'s reception of the broadcast message from node *O* is free from the hidden terminals:

$$P_H(x) = \sum_{i=0}^{\infty} (1 - \mathrm{P_{TX}} \cdot \frac{2 \cdot A_1}{\mathrm{T}_c - A_1})^{i \cdot \frac{T}{\tau}} \frac{(\beta x)^i}{i!} e^{-\beta x} = e^{-\beta x \left[1 - \left(1 - \mathrm{P_{TX}} \cdot \frac{2 \cdot A_1}{\mathrm{T}_c - A_1} \right)^{\frac{T}{\tau}} \right]} \quad (6.11)$$

b. Impact of concurrent collisions

In addition to collisions caused by the hidden nodes, transmissions from nodes within interference range from the tagged node in the meantime at which the tagged node transmits may also cause collisions. If the tagged node has not gone through the backoff process before transmitting the packet, concurrent transmission will not occur (with probability 1-q_b). Otherwise, the packet transmission is synchronized to the beginning of a slot time and concurrent transmission may occur if other vehicles' transmission is also synchronized by the backoff process.

Given that as both *O* and *U* sense the channel idle, *O* will transmit within the duration of a slot. Suppose *O* has experienced backoff process. In order to prevent interference from concurrent collisions with *U*'s receiving the broadcast message sent by *O*, no transmission in [-(*R*-*x*), *R*] is allowed. The average number of nodes transmitting in the concurrent slot in area [0, *x*] is $\beta x P_{TX} \cdot \sigma / (T_c - A_1) \cdot T / \tau$. Suppose node *W* is *y* away from

O, *x*<*y*<*R*. The probability that node *W* starts transmitting during the slot is the probability that node *W* intends to transmit and all nodes in [*R*+*x*, *R*+*y*] are not in transmitting state, which is expressed as:

$$P_s(y,x) = D_1 \cdot \frac{T}{\tau} \sum_{i=0}^{\infty} (1-D_3)^{i\cdot\frac{T}{\tau}} \frac{(\beta(y-x))^i}{i!} e^{-\beta(y-x)} = D_1 \cdot \frac{T}{\tau} e^{-\beta(y-x)\left[1-(1-D_3)^{\frac{T}{\tau}}\right]} \tag{6.12}$$

where

$$D_3 = \mathrm{P_{TX}} \cdot \frac{A_1}{\mathrm{T}_c - A_1}$$

Hence, the average number of nodes that start transmission during the slot that collides with the transmission from *O* is:

$$\bar{n}_S = \beta \int_x^R P_s(y,x)dy = \beta \int_x^R D_1 \cdot \frac{T}{\tau} e^{-\beta(y-x)\left[1-(1-D_3)^{\frac{T}{\tau}}\right]} dy = \frac{D_1 \cdot \frac{T}{\tau}}{1-(1-D_3)^{\frac{T}{\tau}}} \left\{ 1 - e^{-\beta(R-x)\left[1-(1-D_3)^{\frac{T}{\tau}}\right]} \right\} \tag{6.13}$$

Suppose node *V* is |*z*| away from *O*, -(*R*-*x*)<*z*<0, the probability that the node *V* starts transmitting during the slot is the probability that node *V* intends to transmit and all nodes in [*z*-*R*, -*R*] are not in transmitting state, which is expressed as

$$P_s'(z,x) = D_1 \cdot \frac{T}{\tau} \sum_{i=0}^{\infty} (1-D_3)^{i\cdot\frac{T}{\tau}} \frac{(\beta|z|)^i}{i!} e^{-\beta|z|} = D_1 \cdot \frac{T}{\tau} e^{-\beta|z|\left[1-(1-D_3)^{\frac{T}{\tau}}\right]} \tag{6.14}$$

Therefore, the average number of nodes that start transmission during the slot that collides with the transmission from *O* is:

$$\bar{n}_T = \beta \int_{-(R-x)}^0 P_s'(z,x)dz = \beta \int_{-(R-x)}^0 D_1 \cdot \frac{T}{\tau} e^{-\beta|z|\left[1-(1-D_3)^{\frac{T}{\tau}}\right]} dz = \frac{D_1 \cdot \frac{T}{\tau}}{1-(1-D_3)^{\frac{T}{\tau}}} \left\{ 1 - e^{-\beta(R-x)\left[1-(1-D_3)^{\frac{T}{\tau}}\right]} \right\} \tag{6.15}$$

Hence, the total average number of nodes that may transmit concurrently is:

$$\bar{n}_{\Sigma} = \bar{n}_s + \bar{n}_T + \beta x \cdot D_1 \cdot \frac{T}{\tau} \tag{6.16}$$

Therefore, given Poisson node distribution, the probability that no nodes within the reception range of *U* start transmission during the slot that collides with the transmission from *O* is:

$$P_{con}(x) = q_b \cdot \left[\frac{(\bar{n}_{\Sigma})^0}{0!} \exp(-\bar{n}_{\Sigma}) \right] + (1 - q_b) = q_b \cdot \exp(-\bar{n}_{\Sigma}) + (1 - q_b) \tag{6.17}$$

c. Impact of channel fading with path loss

DSRC channel modeling involves two important aspects: large scale path loss and small scale fading. The former is used to determine the average received signal strength at a particular distance from the transmitter, whereas small scale fading generally involves the detailed modeling of multi-path fading statistics, power delay profile, and Doppler spectrum. The *Nakagami* distribution has been shown to fit the amplitude envelope of empirical data for DSRC channel well. The probability density function (PDF) of a signal amplitude *Y* in *Nakagami* fading can be expressed as:

$$f_Y(y) = \frac{2m^m y^{2m-1}}{\Gamma(m)\omega^m} \exp(-\frac{my^2}{\omega}),\ y \geq 0, \omega > 0, m \geq 1/2 \tag{6.18}$$

where *m* is the fading parameter, and ω is the average received power. The values of the two parameters are functions of distance to the sender. From empirical data obtained for vehicular environment in [40], the fading parameter *m* is approximated as 3 for low

values of d (d<50m) expecting line of sight conditions, 1.5 for middle range distances (50m≤d≤150m), and 1 (Rayleigh distribution) for distance higher than 150m.

The path loss model is represented by the following equation:

$$\frac{\omega(x_0)}{\omega(x)} = (\frac{x}{x_0})^{\gamma} \tag{6.19}$$

where $\omega(x_0)$ and $\omega(x)$ are the mean received power with distance to the sender x_0 and x, respectively, and γ is the path loss exponent. γ is usually empirically determined by field measurement. γ can be 2 for free space environment, 1.6~1.8 for indoor line of sight, and 2.7~5 for obstructed area or shadowed urban area. In this work, we use 2 as the value for γ.

According to PDF for signal amplitude Y, the PDF of the signal power Z=Y^2 is:

$$f_Z(z) = \frac{m^m}{\Gamma(m)\omega^m} z^{m-1} e^{-(mz/\omega)} \tag{6.20}$$

Therefore, the CDF of the signal power Z is:

$$F_Z(z) = \frac{m^m}{\Gamma(m)\omega^m} \int_0^z x^{m-1} e^{-(m/\omega)x} dx \tag{6.21}$$

Then, the probability that a message is successfully received in the absence of interferers deduces from the probability that the message's signal power is stronger than the power reception threshold p_{th}, that is:

$$\begin{aligned} P_F &= P_Z(Z > p_{th}) = 1 - F_Z(p_{th}) \\ &= 1 - \frac{m^m}{\Gamma(m)\omega^m} \int_0^{p_{th}} u^{m-1} e^{-(m/\omega)x} du \end{aligned} \tag{6.22}$$

p_{th} should, in average, be detected in a distance equal to the "intended" communication range R from the transmitter.

$$\frac{p_{th}}{\omega(x)} = \frac{\omega(R)}{\omega(x)} = \left(\frac{x}{R}\right)^{\gamma} \tag{6.23}$$

Therefore:

$$\omega(x) = p_{th}\left(\frac{\mathrm{R}}{x}\right)^{\gamma} \tag{6.24}$$

Hence, we obtain the expected probability of successfully receiving a message at distance x:

$$\begin{aligned} P_F(x) &= 1 - \frac{m^m}{\Gamma(m)\omega^m}\int_0^{p_{th}} u^{m-1} e^{-(m/\omega)u}\, du \\ &= 1 - \frac{\left(x^{\gamma} m\right)^m}{\Gamma(m)}\int_0^{1/R^{\gamma}} u^{m-1} e^{-x^{\gamma} m u}\, du \end{aligned} \tag{6.25}$$

Taking hidden terminal, possible packet collisions, and channel fading and path loss into account, the probability (or node reception probability) that the node *U* receives the broadcast message from the tagged node *O* is:

$$P_s(x) = P_H(x) P_{con}(x) P_F(x) \tag{6.26}$$

6.4.1.3 Packet Reception Ratio (PRR)

PRR over a coverage range with distance x is defined as, considering vehicles within the coverage range, the percentage of nodes that successfully receive a packet from the tagged node among all the receivers that are at the moment that the packet is sent out.

Assuming Poisson distribution of nodes along a 1-D line, the average number of nodes within an incremental distance dx should be βdx. Given the reception probability of each node $P_s(x)$, the average number of nodes in dx that successfully receive the broadcast message from the tagged node is $P_s(x)\beta dx$. For a coverage distance with range R from node O, PRR over a coverage range with distance x ($0<x\leq R$) found by integrating the probabilities that nodes with distance x to the source node O within an incremental range successfully receives the broadcast message from O. Therefore,

$$PRR(x) = \frac{\int_0^x \beta P_s(u)du}{\beta x} = \frac{1}{x}\int_0^x P_s(u)du; \qquad x \leq R \tag{6.27}$$

6.4.1.4 Packet Delivery Ratio (PDR)

PDR over a coverage range with distance x is defined as the probability that a broadcast packet from the tagged vehicle is successfully received by all vehicles within the coverage range. We need to derive PDR with respect to two aspects: the impact from concurrent transmission and hidden terminal problem together and the impact from channel fading.

a. Impact of hidden terminals and concurrent transmissions

Suppose there is no influence from channel fading, then only concurrent transmission and hidden terminals problem will lead to packet reception failure. Suppose there are n_1 vehicles locate on the left hand side of the tagged vehicle and n_2 vehicles locate on the right hand side within distance x. Then, if both the left most

vehicle and right most vehicle have successfully receive the packet from the tagged vehicle, then all vehicles within coverage range x of the tagged vehicle will successfully receive the packet. This is because both the left most vehicle and right most vehicle successfully receive the packet ensures that there is no concurrent transmission and hidden terminals' influence for all vehicles between them.

Let's consider vehicles on one hand side (left) of the tagged vehicle first. Given that there are n vehicles located on one hand side of the tagged vehicle within the coverage range x, the conditional joint *pdf* of the n vehicles' locations Y_1, Y_2, …, Y_n is given by [9]:

$$f\left[y_1, y_2, \cdots, y_n \mid N(x) = n\right] = \frac{n!}{x^n}, \qquad 0 \le y_1 \le y_2 \le \cdots \le y_n \le x \tag{6.28}$$

Therefore, the probability that the left most vehicle within coverage area x of the tagged vehicle receive the packet successfully is:

$$\begin{aligned}
PDR_1(x) &= \sum_{n=0}^{\infty}\left\{\int_{y_n=0}^{y_n=x}\cdots\int_{y_3=0}^{y_3=y_4}\int_{y_2=0}^{y_2=y_3}\int_{y_1=0}^{y_1=y_2} P_{con}(y_n)P_H(y_n) f\left[y_1, y_2, \cdots, y_n \mid N(x)=n\right] dy_1 dy_2 dy_3 \cdots dy_n\right\} \cdot P\left(N(x)=n\right) \\
&= \sum_{n=0}^{\infty}\left\{\int_{y_n=0}^{y_n=x}\cdots\int_{y_3=0}^{y_3=y_4}\int_{y_2=0}^{y_2=y_3}\int_{y_1=0}^{y_1=y_2} P_{con}(y_n)P_H(y_n)\cdot\frac{n!}{x^n}\cdot dy_1 dy_2 dy_3 \cdots dy_n\right\}\cdot\frac{(\beta x)^n}{n!}e^{-\beta x} \\
&= \sum_{n=0}^{\infty}\left\{\int_{y_n=0}^{y_n=x} P_{con}(y_n)P_H(y_n)\cdot\frac{n\cdot {y_n}^{n-1}}{x^n}\cdot dy_n\right\}\cdot\frac{(\beta x)^n}{n!}e^{-\beta x} \\
&= \sum_{n=0}^{\infty}\left\{\int_{y_n=0}^{y_n=x} P_{con}(y_n)P_H(y_n)\cdot {y_n}^{n-1}\cdot dy_n\right\}\cdot\frac{\beta^n}{(n-1)!}e^{-\beta x} \\
&= \sum_{n=0}^{\infty}\left\{\int_{y_n=0}^{y_n=x} P_{con}(y_n)P_H(y_n)\cdot(\beta y_n)^{n-1}\cdot dy_n\right\}\cdot\frac{\beta}{(n-1)!}e^{-\beta x}
\end{aligned} \tag{6.29}$$

b. Impact of channel fading with path loss

For channel fading's impact, we can assume impact of fading on different nodes is independent from each other. Hence,

$$
\begin{aligned}
PDR_2(x) &= \sum_{n=0}^{\infty}\left\{\int_{y_n=0}^{y_n=x}\cdots\int_{y_3=0}^{y_3=y_4}\int_{y_2=0}^{y_2=y_3}\int_{y_1=0}^{y_1=y_2}\left[\prod_{i=1}^{n}P_F(y_i)\right]f\left[y_1,y_2,\cdots,y_n \mid N(x)=n\right]dy_1dy_2dy_3\cdots dy_n\right\}\cdot P\left(N(x)=n\right) \\
&= \sum_{n=0}^{\infty}\left\{\int_{y_n=0}^{y_n=x}\cdots\int_{y_3=0}^{y_3=y_4}\int_{y_2=0}^{y_2=y_3}\int_{y_1=0}^{y_1=y_2}\left[\prod_{i=1}^{n}P_F(y_i)\right]\cdot\frac{n!}{x^n}\cdot dy_1dy_2dy_3\cdots dy_n\right\}\cdot\frac{(\beta x)^n}{n!}e^{-\beta x} \\
&= \sum_{n=0}^{\infty}\left\{\int_{y_n=0}^{y_n=x}\cdots\int_{y_3=0}^{y_3=y_4}\int_{y_2=0}^{y_2=y_3}\int_{y_1=0}^{y_1=y_2}\left[\prod_{i=1}^{n}P_F(y_i)\right]\cdot dy_1dy_2dy_3\cdots dy_n\right\}\cdot\frac{n!}{x^n}\cdot\frac{(\beta x)^n}{n!}e^{-\beta x} \\
&= \sum_{n=0}^{\infty}\left\{\int_{y_n=0}^{y_n=x}\cdots\int_{y_3=0}^{y_3=y_4}\int_{y_2=0}^{y_2=y_3}\int_{y_1=0}^{y_1=y_2}\left[\prod_{i=1}^{n}P_F(y_i)\right]\cdot dy_1dy_2dy_3\cdots dy_n\right\}\cdot\beta^n\cdot e^{-\beta x}
\end{aligned}
\tag{6.30}
$$

Therefore, taking into consideration of hidden terminal problem, concurrent transmissions and channel fading with path loss for vehicles on both sides of the tagged vehicle, packet delivery ratio is given by:

$$
PDR(x) = \left[PDR_1(x)\cdot PDR_2(x)\right]^2 \tag{6.31}
$$

6.4.2 Application-level Performance Metrics

6.4.2.1 Application-level Delay

Application-level delay is the duration between the time when a broadcast packet is generated at application layer of transmitting vehicle and the time at which the first successful packet is received by the application layer of receiving vehicle:

$$
E(T_D) = \sum_{i=1}^{\infty}\left[(i-1)\tau + E[D]\right]P_s(x)\left(1-P_s(x)\right)^{i-1} = E[D] + \tau\left[\frac{1}{P_s(x)} - 1\right] \tag{6.32}
$$

where x is the distance between the sender and receiver, $E[D]$ is the MAC-level mean transmission delay of the BSM given by Eq. (6.10) and $P_s(x)$ is the node reception probability given in Eq. (6.26).

6.4.2.2 T-window Reliability

Application-level T-window reliability is defined [53] in the probability of successfully receiving at least one packet out of multiple packets from a broadcast vehicle at distance x, within a given time T_{tol} (referred to as application tolerance window):

$$P_{app}(x,T_{tol}) = 1-(1-P_s(x))^{\frac{T_{tol}}{\tau}} \tag{6.33}$$

where τ is the beacon generation interval and $P_s(x)$ is the node reception probability given in Eq. (6.26).

6.4.2.3 Awareness Probability

The awareness probability [54] is the probability of successfully receiving at least n packets in the tolerance time window T.

$$P_A(x,n) = \sum_{k=n}^{\left\lfloor \frac{T_{tol}}{\tau} \right\rfloor} \binom{\left\lfloor \frac{T_{tol}}{\tau} \right\rfloor}{k} P_s(x)^k (1-P_s(x))^{\left\lfloor \frac{T_{tol}}{\tau} \right\rfloor - k} \tag{6.34}$$

It is noted that the awareness probability $P_A(x, n)$ becomes the application-level T-window Reliability $P_{app}(x, T_{tol})$ as n is equal to 1.

6.4.2.4 Average Number of Invisible Neighbors

The average number of invisible neighbor problem has been defined and described in detail in Section 4.4.2.5 in Chapter 4. Using the same concept, we have:

$$N_{invisible}(x) = 2\beta x(1-PRR(x)) = 2\beta x\left(1-\int_0^x \frac{1}{x}\cdot P_{app}(s,T_{tol})ds\right) = 2\beta x - 2\beta\int_0^x P_{app}(s,T_{tol})ds \tag{6.35}$$

6.5 Numerical Results

6.5.1 Simulation Description

The simulator used in this work is NS2 release version 2.35. Channel switching mechanism is not incorporated in this version; therefore, the NS2 source codes are modified to implement the channel switching behavior. We intend to evaluate the performance for broadcast BSM messages in the CCH while the radio is participating in IEEE 1609.4 compliant channel switching activities. Hence, based on the strategy in [61], the message generation frequency is adjusted to $100/(46\cdot\tau)$, and the messages generated during non-CCH intervals are ignored and not been broadcasted. In addition, unfinished packet receptions will be dropped when the CCH interval expires. This is implemented in PHY layer by setting an error flag for the MAC to declare CRC check failure.

6.5.2 Numerical Results

Table 6.1: Input parameter settings

Parameters	Values	Parameters	Values
Transmission range R	500 m	CCH interval T_c	46 ms
Slot time σ	16 us	Data rate R_d	24 $Mbps$
$DIFS$	64 us	Packet length PL	100 $bytes$
CW W-1	15	path loss exponent Υ	2
PHY preamble T_{H1}	40 μs	Fading Parameter m	3 for d<50m 1.5 for 50m≤d<150m 1 for d≥150m
MAC header T_{H2}	272 $bits$		
PLCP header T_{H3}	4 μs		
Sync period T	100 ms		

The MAC-level mean transmission delay under various network parameters is presented in Fig. 6.5 using parameters shown in Table 6.1. The time to transmit the header is: $T_H = T_{H1} + T_{H3}/R_d + T_{H3}$.

Fig. 6.5 shows that the MAC-level mean transmission delay matches very well with the simulation results under various vehicle density β (#vehicles/m) and message generation interval τ (s), which verified the accuracy of our proposed model. In addition, the MAC-level mean transmission delay is relatively small since the maximum delay is still less than 0.3 *ms* under typical network parameters that we choose.

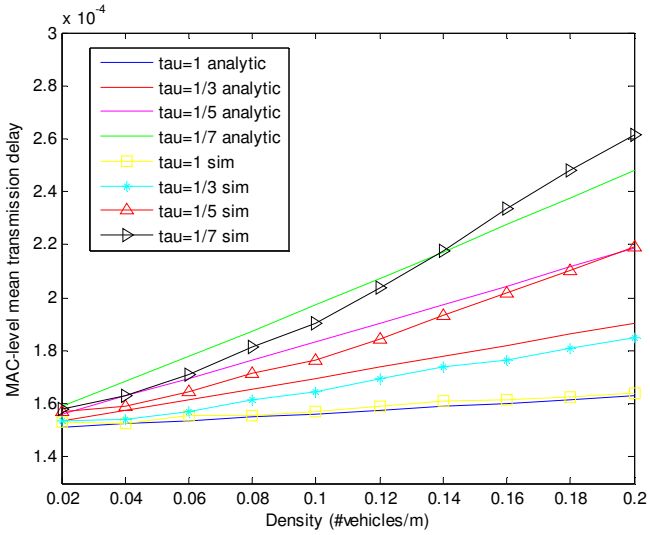

Figure 6.5: MAC-level mean transmission delay

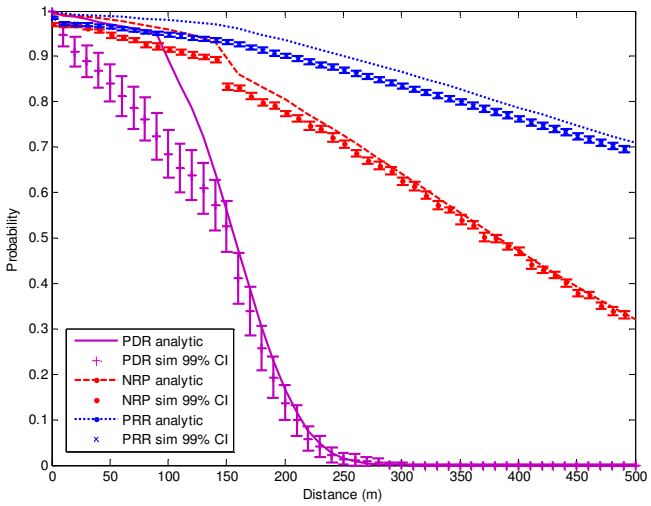

Figure 6.6: Packet transmission reliability

The other MAC-level performance indices except the mean transmission delay are functions of distance from the sender to receiver. Hence, we evaluate them according to distance under a specific vehicle density and message generation interval setting (β=0.1 *vehicles*/*m* and τ=1/7 *s*). The analytic-numerical results for *NRP*, *PRR* and *PDR* are obtained and compared with simulation results as shown in Fig. 6.6. We conducted 50 runs of simulation with each run lasting 1 second. Due to the Central Limit Theorem, 99% confidence intervals (CI) are computed based on normal distribution. The time taken to obtain such analytic-numerical results for *NRP*, *PRR* and *PDR* is around 5 minutes, whereas the simulation takes several hours to obtain the corresponding 99% CI. The results in Fig. 6.6 show that *NRP* has a good match with the simulation results, and the relative difference becomes smaller when the distance from the sender is longer. Analytic result for *PRR* is relatively higher than the simulation results with acceptable

accuracy. Such difference may result from the fact that the *NRP* for shorter distance is a little higher than the simulation results and $PRR(x)$ is derived from the integration of *NRP* over the range $[0, x]$. The result for *PDR* shows that *PDR* has a very good match with the simulation results when the distance from the sender is longer than 150 *m*, while the difference is relatively obvious when the distance is shorter than 150 *m*. This may also result from the fact that analytic model for *PDR* is derived from *NRP* which has bigger difference with the simulation results when the distance is shorter. In addition, due to the computational complexity for Eq. (6.30), we used polynomial approximation to approach the analytic results for $P_F(y_i)$, which has relatively larger difference with the exact analytic-numerical results when the distance is short. To sum up, the analytic models for MAC-level performance metrics have a good match with simulations with acceptable differences for shorter distances, which validate the accuracy of our model.

Moreover, we observe that as the distance becomes longer, the *NRP*, *PRR* and *PDR* decrease. For *NRP*, when the distance from the sender is longer, a receiver has lower probability to receive a broadcast packet resulting from the impact of concurrent transmission, hidden terminal problems and channel fading with path loss. Due to this fact, the percentage of receivers that successfully receive the packet over all receivers in the coverage area (*PRR*) also decreases as the coverage area becomes larger. For *PDR*, which represents the probability that all vehicles within a coverage area receive a

broadcast packet successfully, decreases dramatically with the distance. Fig. 6.6 shows that *PDR* drops to almost 0 when the coverage area is a half of the communication range.

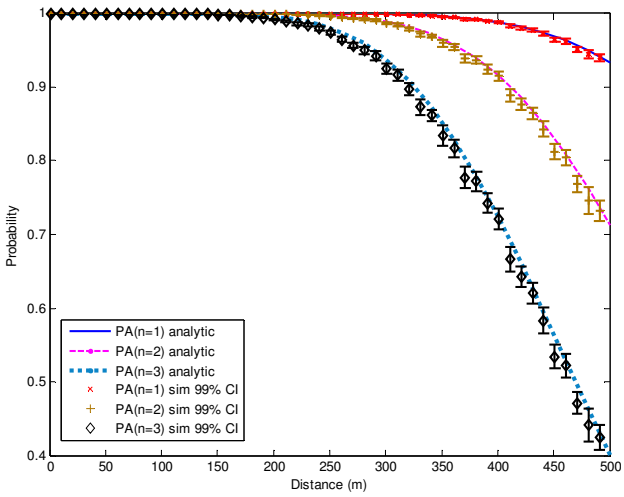

Figure 6.7: Awareness probability with different packet requirements

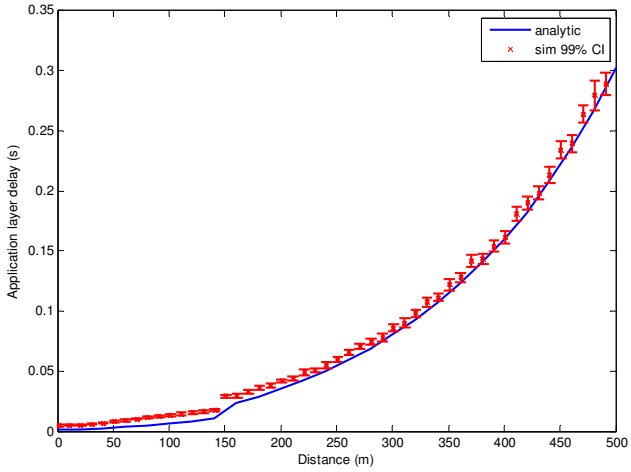

Figure 6.8: Application-level delay

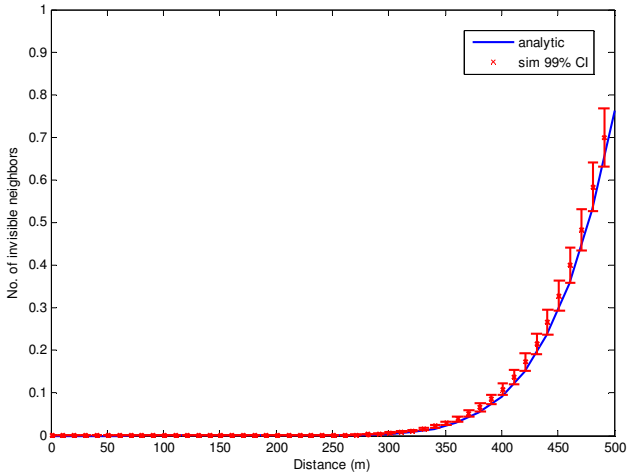

Figure 6.9: Average no. of invisible neighbors

Figs. 6.7-6.9 show the comparisons between analytic model and simulation for application-level performance and reliability metrics with tolerance window T_{tol}=1s. The results show that they have very good match over the whole communication range. In addition, we observe that the differences with simulation results when the distance is shorter for MAC-level performance and reliability metrics (*NRP*, *PRR* and *PDR*) have little impact on the accuracy of the application-level metrics. Therefore, this further validates the accuracy ofour proposed model for application-level performance and reliability metrics. Furthermore, Figs. 6.7-6.9 show that the application-level metrics varies dramatically when the distance from the sender is longer. T-window reliability and awareness probability decreases with the distance (Notice that T-window reliability is equivalent to the awareness probability with packet requirement n=1). In addition, we observe from Fig. 6.7 that as the packet requirement increases, the awareness probability decreases faster. Fig. 6.8 shows that the application-level delay increases faster with the

distance and is much higher than the MAC-level mean transmission delay in Fig. 6.6. Fig. 6.9 shows that the average number of invisible neighbors increases dramatically with the distance especially when the distance is longer.

6.5.3 Impacts of Channel Switching and Channel Fading

In our previous work in Chapter 2 and 3, we have shown that hidden terminal problem has much larger impact than concurrent transmission on packet reception probability (*PDR* and *PRR*). In this work, we have incorporated channel fading scenario. Hence, we will evaluate the impact of channel fading on the packet reception probabilities in this section. Channel fading has no impact on MAC-level mean transmission delay since we only account for the packets that have been successfully received. Other MAC-level and application-level performance metrics are derived based on *NRP*, and hence it is only necessary to evaluate the impact of channel fading on *NRP*. An analytic model is proposed and validated in Chapter 4 [68] for periodic beacon message broadcast over a single channel without considering channel switching mechanism and channel fading. Hence, to evaluate the influence of channel switching mechanism, we compare the models in Chapter 4 [68] to our newly models in this chapter. The message generation interval is set to be the same for these two models. The difference is that: the model in Chapter 4 [68] periodically broadcasts these messages, whereas the new model schedules the messages to be broadcast only during CCH intervals using optimized scheduling [61][94].

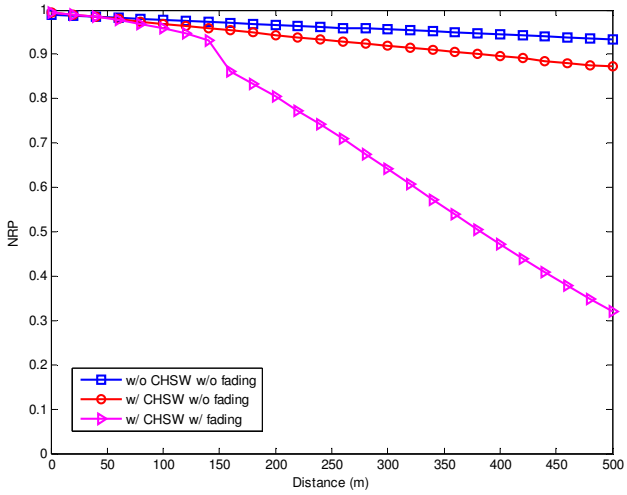

Figure 6.10: Impacts of channel switching and channel fading on *NRP*

Fig. 6.10 shows the analytic-numerical results for *NRP* under different scenarios: without channel switching and without channel fading (based on results from [68], referred as "w/o CHSW w/o fading"), with channel switching and without channel fading (exclude channel fading influence in Eq. (6.26), referred as "w/ CHSW w/o fading"), with channel switching and with channel fading (Eq. (6.26), referred as "w/ CHSW w/ fading").

We observe that incorporating channel switching mechanism degrades *NRP* linearly compared to non-channel switching mechanism. Such phenomena results from the fact that for the same number of packets generated, non-channel switching mechanism allocates packets to be transmitted over the whole time period, while channel switching mechanism schedules all packets transmitted CCH intervals only. Therefore, channel switching mechanism has more collisions in CCH intervals, which

leads to lower *NRP*. In addition, *NRP* under channel fading scenario is much lower than that without channel fading. Such difference becomes more obvious when the distance from the sender is longer. When the distance is less than 150 *m*, the difference is relatively small because the fading parameter *m* we used is larger for small distances. Therefore, we conclude that bigger fading parameter brings smaller fading to the communications, whereas smaller fading parameter has significant impact on degrading the *NRP*.

6.6 Conclusions

In this chapter, an analytic model is proposed to characterize the BSM message broadcasting in CCH interval for multi-channel operations. Optimized scheduling is assumed to avoid synchronization collisions presented in basic access mode for IEEE 802.11p and IEEE 1609.4. Channel fading with path loss is taken into account in this work to capture practical communication environment. MAC-level performance indices including mean transmission delay, *NRP*, *PDR*, *PRR* and application-level performance including T-window reliability, awareness probability, application-level delay and average number of invisible neighbors are derived. Simulation in NS2 incorporating channel switching mechanism is implemented for verification purposes. The good match between the analytic model and simulation results validate the accuracy of our proposed model.

In future, vehicle mobility will be considered to make the model more realistic. Even though it has been proven in [41][42] that high mobility of vehicles has very minor impact on the performance of the direct message broadcasting with high data rate, it may have great impact on application level performance metrics.

7. Multi-hop Dissemination Evaluation

7.1 Motivation

In the U.S., Dedicated Short Range Communication (DSRC) [1][45] spectrum consists of seven channels as shown in Fig. 1.1 to support both safety and non-safety applications in vehicular ad hoc networks (VANET). Channel 178 is the control channel (CCH), which is the default channel for safety communication. Periodic beacon message containing vehicle status information (*e.g.*, position, speed, direction) may be transmitted through this channel to enable various collision avoidance applications. In dense traffic scenarios, the periodic beacons may consume the entire channel bandwidth. Therefore, Channel 172 at one edge is preserved for low-latency, high availability vehicle to vehicle (V2V) critical safety communications. The event-driven safety message, which is broadcast in case of an emergency situation (*e.g.*, accidents, hard-braking, road hazard), is a type of safety critical message that is most likely to be transmitted through such a channel.

The one-hop direct message broadcasting can cover a short range due to radio's limited communication range (usually less than 1 km in DSRC). However, some event-driven safety applications may be required to cover longer distances than the communication range, such as in the post-crash notification or road hazard warning situations. Therefore, multi-hop message dissemination is necessary in such scenarios. For multi-hop broadcast scheme, the protocols proposed in the literature can be

categorized into several classes [80]: simple flooding, probability-based methods, area-based methods and neighbor knowledge method. Many techniques focus on minimizing the number of retransmissions while attempting to ensure that a broadcast packet is delivered to every vehicle within the intended coverage area. In this chapter, we adopt a robust relay selection strategy proposed in our previous work [73] for multi-hop propagation of event-driven safety message utilizing distance-based timers to choose farthest node as the relay.

Most of the previous work on this topic is based on simulations [98][99][100][101] to analyze the performance and reliability of multi-hop message dissemination. Several experimental studies [102][103][96] have been conducted to capture more practical network dynamics. Very few analytic models [73] have been proposed. However, many of the existing studies [73][98] assume a fixed one-hop message transmission reliability: when a vehicle broadcasts a message, all vehicles within the transmission range from the sender have the same probability of correctly receiving the message. Such an assumption fails to capture complex traffic scenarios such as fading channel, Doppler spectrum effect, etc. In addition, the simulation approach usually consumes long time and only a few metrics can be obtained within a reasonable length of time. Due to the high equipment cost, the experimental testbed usually only consists of very few vehicles (six in [102], and four in [103][96]). Even though some techniques are utilized to create a

large scale virtual communication network using a small number of vehicles, the resulting virtual network is still only capable of capturing sparse network scenarios.

In this chapter, we propose an accurate and efficient analytic model to evaluate the performance and reliability of multi-hop safety message dissemination. Since event-driven safety message is occasionally generated (only when an emergency event is detected), we can reasonably assume that during the lifetime of an event-driven safety message, no other event-driven safety message is generated. In other words, we concentrate on the performance and reliability of multi-hop delivery of a single event-driven safety message. Therefore, concurrent transmissions and hidden terminal problem do not exist in such a system that is under consideration. The main focus of this chapter is the impact of channel fading on the system performance and reliability.

The main contributions of this chapter are: 1) An accurate and efficient analytic model is developed to capture the channel fading's effect on multi-hop safety message dissemination; 2) Various performance and reliability metrics are derived to provide a deeper understanding of the message transmission behavior from different angles. 3) Extensive simulations are conducted to verify the accuracy of our proposed models.

This chapter is organized as follows. Section 7.2 briefly explains the system under investigation and model assumptions. Section 7.3 presents analytic models to evaluate various types of performance and reliability metrics. Analytic-numerical results are shown in Section 7.4 to compare with simulations. Section 7.5 shows the

simplification techniques for the analytic models proposed. Conclusions are in the last section.

7.2 System Description and Assumptions

Once an emergency message is generated, its header contains the information about the originating source node, the type of message and the message propagation direction. Based on this information, we propose and evaluate an efficient multi-hop broadcast scheme for the emergency notification services. We adopt a multi-hop relay scheme similar to the one proposed in our previous paper [73], which provides a reliable way to select a routing node to rebroadcast the emergency message. A vehicle will be selected to rebroadcast the message under the following conditions:

- the vehicle has successfully received the message;
- the vehicle's distance to the sender is the farthest among all one-hop vehicles that have received the message successfully.

The second condition is guaranteed by setting a deterministic timer in each vehicle that received the message. The timer is a function of the distance from the receiver to the sender x and is defined as follows:

$$t_{AD}(x) = \begin{cases} T_{\max}\left(1 - \frac{x}{R}\right) & if\ x \le R \\ 0 & if\ x > R \end{cases} \tag{7.1}$$

where T_{max} is chosen as the one-hop lifetime of the emergency message and R is the average transmission range of a node.

All vehicles that received the message will trigger the AD timer according to Eq. (7.1). The one whose AD timer expires first is chosen to rebroadcast the emergency message. If such rebroadcast message is received by some vehicles in the hop, they will cancel their AD timers and stop their attempts to relay the message. In case that the rebroadcast message from the selected node fails to reach some nodes in the hop due to fading channel condition, those candidate nodes keep counting down their AD timer until one of the candidates is selected as a new relaying node. This process continues until at least one rebroadcast is successful in the hop.

The proposed multi-hop scheme aims at a fast and reliable delivery of the emergency message. The AD timer strategy guarantees that the farthest node in the transmission direction has the highest priority to be selected as the relaying node so that the multi-hop coverage can be extended farthest as fast as possible. In addition, to achieve reliable delivery, the redundant relaying nodes are set in a ready mode through the distance based counters to cope with possible delivery failures of the rebroadcast message in the one hop.

The following assumptions are made in this chapter to produce a simplified yet high fidelity analytic model. The network is considered one-dimensional (1-D). The number of vehicles in a line is Poisson distributed with parameter λ (vehicle density). In addition, all vehicles are assumed to have the same transmission range, receiving range, and carrier sensing range R. Vehicle mobility is not taken into account in this chapter.

The 1-D VANET model is a good approximation of ad hoc networks on highway when the distances between lanes on the highway are negligible compared with the length of the highway. Furthermore, recent statistical analysis of empirical data collected from real-world scenarios [34][35] show that Poisson model is a good fit for sparse highway vehicle traffic in terms of inter vehicle distance. Heavy traffic scenarios where exponentially distributed inter vehicle distance does not fit will be considered in our future work. We have set the values of three communication ranges (transmission range, receiving range and carrier sensing range) the same to simplify the analysis. Extension of the model to more general cases with different values of communication ranges is straightforward [36].

7.3 Analytic Models

7.3.1 Channel Fading Model

In this chapter, we concentrate on the impact of channel fading on multi-hop safety message transmission. DSRC channel modeling involves two important aspects: large scale path loss and small scale fading. The former is used to determine the average received signal strength at a particular distance from the transmitter, whereas small scale fading generally involves the detailed modeling of multi-path fading statistics, power delay profile, and Doppler spectrum. The *Nakagami* distribution has been shown to fit the amplitude envelope of empirical data for DSRC channel well [94]. The

probability density function (pdf) of a signal amplitude Y in *Nakagami* fading can be expressed as:

$$f_Y(y) = \frac{2m^m y^{2m-1}}{\Gamma(m)\omega^m} \exp\left(-\frac{my^2}{\omega}\right), \; y \geq 0, \omega > 0, m \geq 1/2 \tag{7.2}$$

where m is the fading parameter, and ω is the average received power. The values of the two parameters are functions of distance to the sender.

The path loss model is represented by the following:

$$\frac{\omega(x_0)}{\omega(x)} = \left(\frac{x}{x_0}\right)^{\gamma} \tag{7.3}$$

where $\omega(x_0)$ and $\omega(x)$ are the mean received power at distance x_0 and x to the sender, respectively, and γ is the path loss exponent. γ is usually empirically determined by field measurement.

From the *pdf* of the signal amplitude Y, the *pdf* of the signal power $Z=Y^2$ is:

$$f_Z(z) = \frac{m^m}{\Gamma(m)\omega^m} z^{m-1} \exp\left(-\frac{mz}{\omega}\right) \tag{7.4}$$

Therefore, the CDF of the signal power Z is:

$$F_Z(z) = \frac{m^m}{\Gamma(m)\omega^m} \int_0^z x^{m-1} \exp\left(-\frac{mx}{\omega}\right) dx \tag{7.5}$$

Then, the probability that a message is successfully received in the absence of interference is deduced from the probability that the message's signal power is stronger than the power reception threshold p_{th}, that is:

$$P_s(x) = P(Z > p_{th}) = 1 - F_Z(p_{th}) \\ = 1 - \frac{m^m}{\Gamma(m)\omega^m} \int_0^{p_{th}} u^{m-1} \exp\left(-\frac{mx}{\omega}\right) du \tag{7.6}$$

p_{th} should, on the average, be detected in a distance equal to the *intended* communication range R from the transmitter:

$$\frac{p_{th}}{\omega(x)} = \frac{\omega(R)}{\omega(x)} = \left(\frac{x}{R}\right)^{\gamma} \tag{7.7}$$

Hence, we obtain the probability of successfully receiving a message at a distance x considering channel fading with path loss effects:

$$P_s(x) = 1 - \frac{m^m}{\Gamma(m)\omega^m} \int_0^{p_{th}} u^{m-1} \exp\left(-\frac{mu}{\omega}\right) du \\ = 1 - \frac{m^m}{\Gamma(m)} \int_0^{(x/R)^{\gamma}} z^{m-1} \mathrm{e}^{-mz} \, dz \tag{7.8}$$

7.3.2 Rebroadcast Probability

Due to the unfavorable characteristics of channel fading in DSRC, various performance metrics for multi-hop message delivery are impacted. One of the most important metrics is the rebroadcast probability. In order to better illustrate the rebroadcast behavior, we evaluate the rebroadcast probability from two perspectives: one from a broadcast message's perspective, and another from a receiver's perspective:

- Message-centric rebroadcast probability P_{rb} is defined as the probability that a message can be rebroadcast by a receiver within this hop given the message is broadcast within a hop.

- Receiver-centric rebroadcast probability $P_{rbA}(x)$ is defined as given a receiver located with distance x from the sender, the probability that this receiver can rebroadcast the safety message.

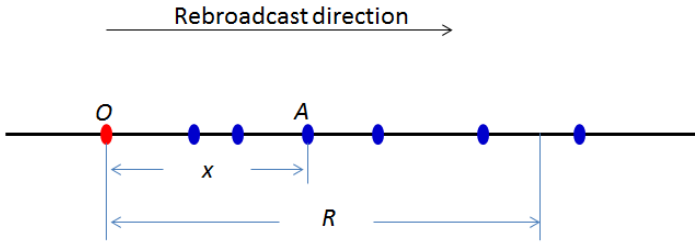

Figure 7.1: Message rebroadcast in a hop

7.3.2.1 Message-centric rebroadcast probability

As shown in the Fig. 7.1, sender O broadcasts a safety message to all one-hop receivers. This message can be rebroadcast if at least one one-hop receiver in the rebroadcast direction receives the message successfully.

Suppose that there are n vehicles located on the rebroadcast direction within O's transmission range R. According to Theorem 6.2 in [9], the conditional *pdf* of the n nodes' un-ordered locations $T_1, T_2, \ldots, T_n$ respectively is given by:

$$f_{T_i}\left[t_i \mid N(R)=n\right]=\frac{1}{R},\ \ x \le t_i \le R,\ i=1,2,...,n \tag{7.9}$$

We first calculate the conditional probability that a node with location $T_i=t_i$ fails to receive the signal as $1-P_s(t_i)$ and then uncondition by multiplying with the location density in Eq. (7.9) and integrating to obtain the probability that a single vehicle among these n nodes fails to receive the message. Next, the probability that none of the one-hop

receivers receive the broadcast message successfully is computed as the product of n single vehicle's message failure probabilities. Finally, by unconditioning with respect to the number of nodes $N(R)=n$, and subtracting from 1, we obtain the probability that at least one vehicle receives the broadcast message successfully, which is equivalent to the message-centric rebroadcast probability:

$$\begin{aligned} P_{rb} &= 1-\sum_{n=0}^{\infty}\left\{\prod_{i=1}^{n}\left[\int_{t_i=0}^{t_i=R}\left(1-P_s(t_i)\right)\cdot f_{T_i}\left[t_i \mid N(R)=n\right]dt_i\right]\right\}\cdot P\left(N(R)=n\right) \\ &= 1-\sum_{n=0}^{\infty}\left\{\prod_{i=1}^{n}\left[\int_{t_i=0}^{t_i=R}\left(1-P_s(t_i)\right)\cdot\frac{1}{R}dt_i\right]\right\}\frac{(\lambda R)^n e^{-\lambda R}}{n!} \\ &= 1-\sum_{n=0}^{\infty}\left[I(0)^n\cdot\frac{\lambda^n e^{-\lambda R}}{n!}\right] \\ &= 1-e^{-\lambda R}\cdot\sum_{n=1}^{\infty}\frac{\left(\lambda I(0)\right)^n}{n!} \\ &= 1-e^{-\lambda R+\lambda I(0)} \end{aligned} \tag{7.10}$$

where

$$\begin{aligned} I(x) &= \int_{t=x}^{t=R}\left(1-P_s(t)\right)dt = \int_{t=x}^{t=R}\left(\frac{m^m}{\Gamma(m)}\int_0^{(t/R)^\gamma} z^{m-1}e^{-mz}dz\right)dt \\ &= \int_{t=x}^{t=R}\frac{m^m}{\Gamma(m)}\cdot\left(\int_0^{(t/R)^\gamma} z^{m-1}e^{-mz}dz\right)dt = f(x,m) \end{aligned} \tag{7.11}$$

The $f(x,m)$ in Eq. (7.11) can be significantly simplified to reduce the computational complexity by changing the order of integration in the double integral. The detailed simplification is shown in Section 7.5.

7.3.2.2 Receiver-centric rebroadcast probability

Besides the message-centric rebroadcast probability, we are also interested in: given a receiver located at a distance x from the sender, what is the probability that this

receiver will rebroadcast the message? Based on the two conditions for selecting a relay node in Section 7.2, we know that a vehicle will rebroadcast a message if it successfully receives the broadcast message from the sender, and all one-hop nodes farther than this vehicle have not received this message.

Denote a random receiver in the rebroadcast direction to be *A*, located at a distance *x* from the sender *O* as shown in Fig. 7.1. In addition, assume that there are *n* nodes located farther than node *A* from the sender *O* but within *O*'s transmission range *R*. According to Theorem 6.2 in [9], the conditional *pdf* of the *n* nodes' un-ordered locations T_1, T_2, …, T_n respectively is given by:

$$f_{T_i}\left[t_i \mid N(R-x)=n\right]=\frac{1}{R-x},\ \ x \le t_i \le R,\ i=1,2,...,n \tag{7.12}$$

Therefore, the rebroadcast probability of node *A*, conditioned on there being *n* one-hop nodes farther than *A*, can be computed as follows:

- If n=0

$$P_{rb1}\left(x \mid N(R-x)=0\right)=P_s\left(x\right) \tag{7.13}$$

- If n>0

$$
\begin{aligned}
P_{rb2}\left(x \mid N(R-x)=n\right) &= P_s\left(x\right)\cdot\left\{\prod_{i=1}^{n}\left[\int_{t_i=x}^{t_i=R}\left(1-P_s(t_i)\right)\cdot f_{T_i}\left[t_i \mid N(R-x)=n\right]dt_i\right]\right\} \\
&= P_s\left(x\right)\cdot\left\{\prod_{i=1}^{n}\left[\int_{t_i=x}^{t_i=R}\left(1-P_s(t_i)\right)\cdot\frac{1}{R-x}dt_i\right]\right\} \\
&= P_s\left(x\right)\cdot\left[\int_{t=x}^{t=R}\left(1-P_s(t)\right)dt\right]^n\cdot\left(\frac{1}{R-x}\right)^n \\
&= P_s\left(x\right)\cdot I\left(x\right)^n\cdot\left(\frac{1}{R-x}\right)^n
\end{aligned}
\tag{7.14}
$$

Therefore, the un-conditioned rebroadcast probability for A (*i.e.*, the rebroadcast probability for a receiver located at a distance x from the sender) is given by:

$$
\begin{aligned}
P_{rbA}\left(x\right) &= P_{rb1}\left(x\right)\cdot e^{-\alpha(R-x)}+\sum_{n=1}^{\infty}\left[P_{rb2}\left(x\right)\cdot\frac{\left(\alpha\left(R-x\right)\right)^n e^{-\alpha(R-x)}}{n!}\right] \\
&= P_s\left(x\right)\cdot e^{-\alpha(R-x)+\alpha I(x)}
\end{aligned}
\tag{7.15}
$$

7.3.3 Average Rebroadcast Distance

For multi-hop message dissemination, the number of hops to reach a specific distance is one of the most important metrics to evaluate how fast a message can be transmitted. Hence, one-hop rebroadcast distance needs to be analyzed first, based on which the number of hops to reach a distance can be easily computed.

In Section 7.3.2, the un-ordered statistics for vehicles are considered for both message-centric and receiver-centric rebroadcast probability calculation, since the output measures do not depend on the order of vehicles within an area. However, to assess the rebroadcast distance for a message, we need to pay attention to the ordered statistics of the receivers because their locations impact the rebroadcast distance.

Suppose there are n vehicles located in the rebroadcast direction of the sender O within its transmission range R. According to the Theorem 6.1 in [9], the conditional joint *pdf* of the n vehicles' ordered locations Y_1, Y_2, …, Y_n is given by:

$$f\left[y_1, y_2, \cdots, y_n \mid N(R)=n\right]=\frac{n!}{R^n}, \qquad 0 \le y_1 \le y_2 \le \cdots \le y_n \le R \tag{7.16}$$

Any vehicle among these n vehicles has the potential to rebroadcast the message originally broadcast from the sender. Suppose the ith vehicle with distance y_i rebroadcasts the message, the average rebroadcast distance is:

$$\begin{aligned} J_1(n,i) &= \int_{y_n=0}^{y_n=R} \cdots \int_{y_2=0}^{y_2=y_3} \int_{y_1=0}^{y_1=y_2} \left[P_s(y_i) \prod_{j=i+1}^{n} \left(1-P_s(y_j)\right) \right] \cdot y_i \cdot \frac{n!}{R^n} \cdot dy_1 dy_2 \cdots dy_n \\ &= \int_{y_n=0}^{y_n=R} \cdots \int_{y_i=0}^{y_i=y_{i+1}} \left[P_s(y_i) \prod_{j=i+1}^{n} \left(1-P_s(y_j)\right) \right] \frac{y_i^{i-1}}{(i-1)!} \cdot y_i \cdot \frac{n!}{R^n} \cdot dy_i \cdots dy_n \\ &= \frac{n!}{(i-1)!R^n} \int_{y_n=0}^{y_n=R} \cdots \int_{y_i=0}^{y_i=y_{i+1}} \left[P_s(y_i) \prod_{j=i+1}^{n} \left(1-P_s(y_j)\right) \right] \cdot y_i^{\,i} dy_i \cdots dy_n \\ &= \frac{n!}{R^n} K_1(n,i) \end{aligned} \tag{7.17}$$

where

$$K_1(n,i)=\frac{1}{(i-1)!} \int_{y_n=0}^{y_n=R} \cdots \int_{y_i=0}^{y_i=y_{i+1}} \left[P_s(y_i) \prod_{j=i+1}^{n} \left(1-P_s(y_j)\right) \right] \cdot y_i^{\,i} dy_i \cdots dy_n \tag{7.18}$$

Due to the computational complexity of Eq. (7.18), we use polynomial to approximate the integrand for $P_s(y_i)$, and then do the multiple integrals symbolically to obtain $K_1(n,i)$. Next, taking into account of all receivers rebroadcast behavior and un-conditioning on the number of receivers, the average rebroadcast distance is:

$$
\begin{aligned}
D_{rb} &= \sum_{n=0}^{\infty}\left[\sum_{i=1}^{n} J_1(n,i)\right]\cdot P\left(N(R)=n\right) \\
&= \sum_{n=0}^{\infty}\left[\sum_{i=1}^{n} J_1(n,i)\right]\cdot \frac{(\alpha R)^n}{n!}e^{-\alpha R} \\
&= \sum_{n=0}^{\infty}\left[\sum_{i=1}^{n} K_1(n,i)\right]\cdot \alpha^n e^{-\alpha R}
\end{aligned}
\tag{7.19}
$$

7.3.4 Average Number of Hops to Reach a Distance

Based on the average rebroadcast distance for a message derived in the previous section, we can compute the average number of hops to reach a specific distance l for a broadcast safety message:

$$
E_h(l) = \left\lceil \frac{l}{D_{rb}} \right\rceil \tag{7.20}
$$

7.3.5 Average Rebroadcast Delay

As mentioned in Section 7.1, one-hop receivers that successfully receive the broadcast message from the sender will trigger their respective distance-based AD timers before the winner whose timer expires first rebroadcasts the message. Such AD timer leads to delay in the message rebroadcast process. Hence, in this section, we evaluate the rebroadcast delay induced by the AD timer. Following an approach similar to the one in Section 7.3.3 for rebroadcast distance computation, we utilize the ordered statistics for receivers and obtain the average delay if the ith vehicle with distance y_i rebroadcasts the message given that there are n one-hop receivers:

$$J_2(n,i) = \int_{y_n=0}^{y_n=R} \cdots \int_{y_2=0}^{y_2=y_3} \int_{y_1=0}^{y_1=y_2} \left[P_s(y_i) \prod_{j=i+1}^{n} \left(1 - P_s(y_j)\right) \right] \cdot t_{AD}(y_i) \cdot \frac{n!}{R^n} dy_1 dy_2 \cdots dy_n$$
$$= \frac{n!}{R^n} K_2(n,i) \tag{7.21}$$

where

$$K_2(n,i) = \frac{1}{(i-1)!} \int_{y_n=0}^{y_n=R} \cdots \int_{y_i=0}^{y_i=y_{i+1}} \left[P_s(y_i) \prod_{j=i+1}^{n} \left(1 - P_s(y_j)\right) \right] \cdot y_i^{i-1} \cdot T_{\max} \left(1 - \frac{y_i}{R}\right) \cdot dy_i \cdots dy_n \tag{7.22}$$

Considering all receivers rebroadcast behavior and un-conditioning on the number of receivers, the average rebroadcast delay induced by AD timer for a message is:

$$E_{AD} = \sum_{n=0}^{\infty} \left[\sum_{i=1}^{n} J_2(n,i) \right] \cdot P\left(N(R) = n\right) = \sum_{n=0}^{\infty} \left[\sum_{i=1}^{n} K_2(n,i) \right] \cdot \alpha^n e^{-\alpha R} \tag{7.23}$$

7.3.6 Average Delay to Reach a Distance

The transmission delay for a safety message to reach a specific distance includes two parts: the time spent to actually transmit the message through the wireless channel, and the delay induced by the AD timer.

Let T denote the real transmission time for a safety message through a wireless channel, which is given by:

$$T = \frac{PL}{R_d} + T_H \tag{7.24}$$

In the Eq. (7.24), PL represents the packet length, R_d represents the transmission data rate, and T_H represents the time to transmit the header. For the first hop of message transmission, the sender needs to sense the channel for *DIFS* time before it can broadcast the message to avoid channel collisions. Since we reasonably assume that the safety

message occurs occasionally (*i.e.*, when an emergency event presents on the road), the channel contentions between different safety messages are not considered. Therefore, the average delay for a safety message to reach distance l is:

$$E_d(l) = DIFS + T + \left[E_h(l) - 1\right] \cdot (E_{AD} + T) \tag{7.25}$$

7.3.7 Metrics Related to Message Vanishing

Having been broadcast by a sender for the first time, a safety message may be rebroadcast several times before it cannot be rebroadcast any further in the rebroadcast direction (*i.e.*, it vanishes). Several previous papers [96] show interest in evaluating metrics until a message vanishes from the network:

- What is the total distance travelled by the safety message before it vanishes?
- What is the total number of hops of the message before it vanishes?
- What is the total transmission delay for a message before it vanishes?

Based on the metrics derived earlier in Section 7.3, these metrics can be easily computed.

The average total distance travelled by a message is:

$$\begin{aligned} D_{total} &= \sum_{i=1}^{\infty}\left[i \cdot D_{rb} \cdot {P_{rb}}^{i}\left(1 - P_{rb}\right)\right] \\ &= D_{rb} \cdot \left(1 - P_{rb}\right)\sum_{i=1}^{\infty}\left[i \cdot {P_{rb}}^{i}\right] \\ &= \frac{D_{rb} \cdot P_{rb}}{1 - P_{rb}} \end{aligned} \tag{7.26}$$

The average total number of hops travelled by a message is:

$$H_{total} = \frac{D_{total}}{D_{rb}} = \sum_{i=1}^{\infty} \left[i \cdot P_{rb}{}^{i} \left(1 - P_{rb}\right) \right] = \frac{P_{rb}}{1 - P_{rb}} \tag{7.27}$$

The average total transmission delay for a message is:

$$E_{total} = DIFS + T + H_{total} \cdot \left(E_{AD} + T\right) \tag{7.28}$$

7.4 Numerical Results

To evaluate the accuracy and efficiency of our proposed analytic model, we compare the analytic-numeric results with the discrete event simulation results conducted in Matlab. The network parameters are chosen reasonably and most of them are from real testbeds [96][97], which are listed in Table 7.1. The assumptions made for the analytic model in Section 7.2 are all made in the simulative solution as well. We conducted 300 simulation runs. The mean for an output measure is computed for every 10 runs and hence the number of means obtained for each output measure is 30. Due to the Central Limit Theorem, normal distribution is assumed for these 30 sample means to compute 99% confidence intervals for the population mean.

Table 7.1: Network parameter

Parameters	Values	Parameters	Values
Transmission range R	300 m	Packet length PL	300 *bytes*
$DIFS$	64 us	T_{max}	1 *second*
PHY preamble T_{H1}	40 μs	path loss exponent γ	2
MAC header T_{H2}	272 bits	Fading Parameter m	3 for d<50m 1.5 for 50m≤d<150 m 1 for d≥150m
PLCP header T_{H3}	4 μs		
Data rate R_d	6 *Mbps*		

Fig. 7.2 shows the point-to-point node reception probability (NRP) incorporating channel fading impact and receiver-centric rebroadcast probability (P_{rbA}) with respect to

distance from the sender. The lines represent the analytic-numeric results, whereas the symbols represent the simulation results for 99% confidence interval. In Fig. 7.2, NRP decreases as distance increases due to channel fading's effect. In addition, the receiver-centric rebroadcast probability for a receiver $P_{rbA}(x)$ is nearly zero when the distance is less than $150m$, and it generally increases when the distance approaches the transmission range R=$300m$. This is because the rebroadcast vehicle is most likely to be the farthest one from the sender, which is close to the transmission range. In addition, at the transmission range point R=$300m$, we notice that NRP almost equals P_{rbA}. This observation results from the fact that P_{rbA} is the probability that the vehicle located at R receives the message (given by NRP) and no farther receivers receive the message. Since there is no receiver farther than the one located with distance R, the P_{rbA} is equivalent to NRP for such a vehicle. The good match between the simulation and analytic results validates the accuracy of our model.

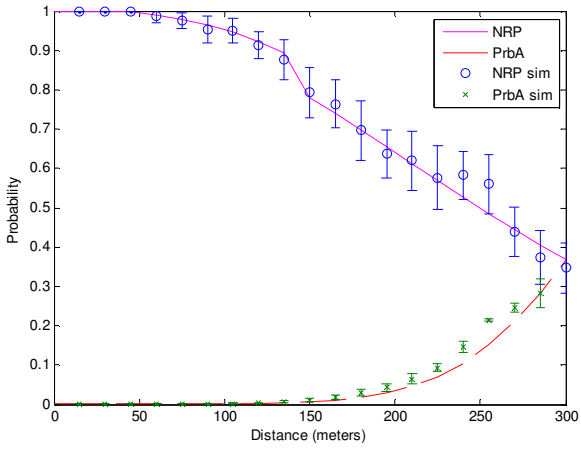

Figure 7.2: NRP and receiver-centric rebroadcast probability

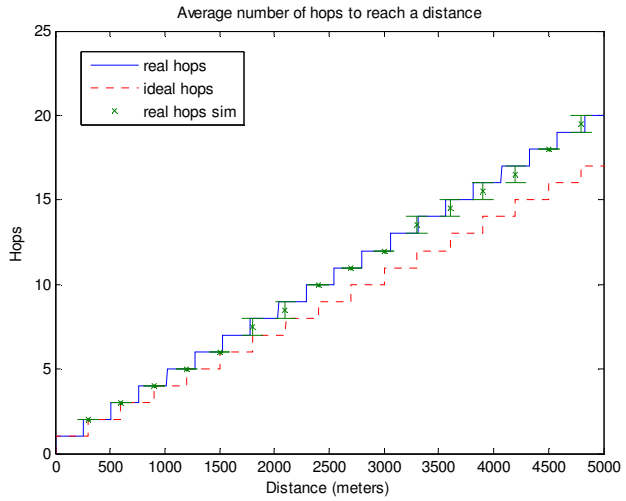

Figure 7.3: Number of hops to reach a distance

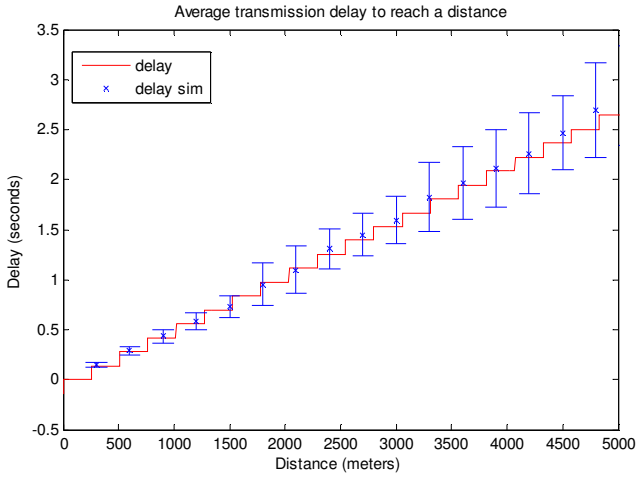

Figure 7.4: Average transmission delay

Fig. 7.3 shows that as the distance becomes larger, the average number of hops generally increases. For better comparison, the ideal hop to reach a distance l is also plotted, which is defined as:

$$E_{h\_ideal} = \left\lceil \frac{l}{R} \right\rceil \tag{7.29}$$

The figure shows that the real number of hops for a message to reach a specific distance is larger than the ideal hop number. Such difference is more obvious when the distance is larger. This phenomenon results from the fact that the rebroadcast vehicle is at a distance less than the transmission range. The simulation results match very well with our analytic results, which again verifies the correctness of our approach.

Fig. 7.4 shows that when the distance becomes larger, the transmission delay for a message increases. This increase follows similar pattern as the average number of hops because the average transmission delay is a linear function of the average number of hops to reach a specific distance as shown in Eq. (7.25).

The other output measures, which are not distance-based metrics, are listed in Table 7.2. The average rebroadcast distance is around 254m, which is less than the transmission range 300m. The average rebroadcast delay is about 0.139s, and this time accounts for the AD timer delay in the rebroadcast process. Compared to the simulation results, the analytic results fall within 99% confidence interval of the simulation results. Hence, this verifies the accuracy of our proposed analytic models. In addition, the analytic model takes about 1 minute to obtain the numerical results, whereas the simulation takes 28 minutes. The simulation time will be longer if we need to obtain tighter confidence intervals. Therefore, our analytic model is much more efficient than simulations.

The message-centric rebroadcast probability for a message is very large because in the general case, at least one of the receivers can successfully receive the message in order to rebroadcast it. Since the un-rebroadcast message is an extremely rare event, which is very difficult to be captured, we have not conducted simulation for such an output measure. In addition, the average total distance traveled before the message vanishes is extremely long. As a result, the average total number of hops and the average total transmission delay are also very high before the message vanishes. In practice, there could be a lifetime setting for multi-hop broadcast message so that the rebroadcasting will be terminated if either a destination is reached or the life time expires.

Table 7.2: Non distance-based metrics

Definitions	Symbols	Analytic Results	Simulation Results 99% CI	
			Low bound	High bound
Average rebroadcast distance (m)	D_{rb}	2.54419e+02	2.501e+02	2.631e+02
Average rebroadcast delay (s)	E_{tAD}	0.13857762	0.122911	0.166271
Message-centric rebroadcast probability	P_{rb}	0.99999393	-	
Average total distance (m)	D_{total}	4.196314e+07	-	
Average total number of hops	H_{total}	1.649371e+05	-	
Average total transmission delay (s)	E_{total}	2.293730e+04	-	

7.5 Simplification of f(x,m)

This section shows the detailed method to simplify the expression of $f(x,m)$ in Eq. (7.11) in order to reduce the computation complexity.

Denote:

$$h(d,m)=\int_{t=0}^{t=d}\frac{m^m}{\Gamma(m)}\left[\int_0^{(t/R)^\gamma} z^{m-1}e^{-mz}dz\right]dt \tag{7.30}$$

Therefore,

$$\begin{aligned} f(x,m) &= \int_{t=x}^{t=R}\frac{m^m}{\Gamma(m)}\left[\int_0^{(t/R)^\gamma} z^{m-1}e^{-mz}dz\right]dt \\ &= \int_{t=0}^{t=R}\frac{m^m}{\Gamma(m)}\left[\int_0^{(t/R)^\gamma} z^{m-1}e^{-mz}dz\right]dt \\ &\quad -\int_{t=0}^{t=x}\frac{m^m}{\Gamma(m)}\left[\int_0^{(t/R)^\gamma} z^{m-1}e^{-mz}dz\right]dt \\ &= h(R,m)-h(x,m) \end{aligned} \tag{7.31}$$

Next, we simplify $h(d,m)$, based on which $f(x,m)$ can be easily simplified. The fading parameter m in practice can be either modeled as a constant or, more frequently, as a piecewise function to more precisely capture the real traffic scenarios.

7.5.1 *m* is a constant over [0, *d*]

By changing the order of integration in double integral in Eq. (7.30) as shown in Fig. 7.5, we obtain:

$$\begin{aligned} h(d,m) &= \int_{t=0}^{t=d}\frac{m^m}{\Gamma(m)}\cdot\left[\int_0^{(t/R)^\gamma} z^{m-1}e^{-mz}dz\right]dt \\ &= \frac{m^m}{\Gamma(m)}\cdot\int_{z=0}^{z=(d/R)^\gamma}\left(\int_{R\cdot z^{1/\gamma}}^{d}dt\right)z^{m-1}e^{-mz}dz \\ &= \frac{d}{\Gamma(m)}Y\left[m,m\left(\frac{d}{R}\right)^\gamma\right]-\frac{R}{\Gamma(m)m^{1/\gamma}}\cdot Y\left[\frac{1}{\gamma}+m,m\left(\frac{d}{R}\right)^\gamma\right] \end{aligned} \tag{7.32}$$

where

$$Y(a,b)=\int_{u=0}^{u=b}u^{a-1}e^{-u}du \tag{7.33}$$

represents the lower incomplete *Gamma* function, which can be easily computed through built-in functions in software such as Matlab. Let's denote:

$$g(d,m)=\frac{d}{\Gamma(m)}Y\left[m,m\left(\frac{d}{R}\right)^{\gamma}\right]-\frac{R}{\Gamma(m)m^{1/\gamma}}\cdot Y\left[\frac{1}{\gamma}+m,m\left(\frac{d}{R}\right)^{\gamma}\right] \tag{7.34}$$

Hence,

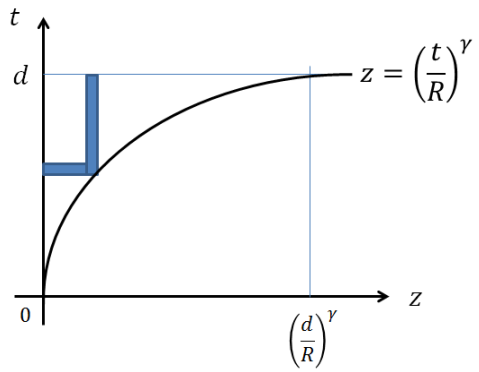

Figure 7.5: Change order of double integral

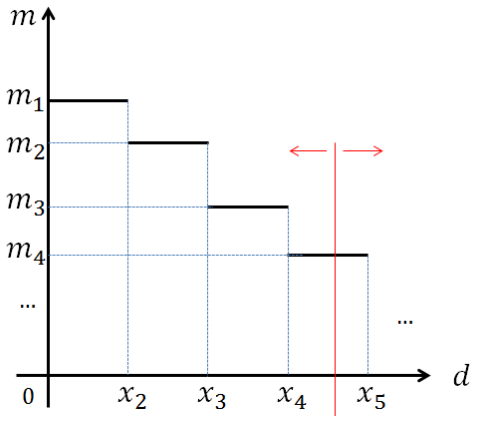

Figure 7.6: Fading parameter as a piecewise function

$$
\begin{aligned}
f(x,m) &= h(R,m) - h(x,m) \\
&= g(R,m) - g(x,m) \\
&= \frac{R}{\Gamma(m)} Y[m,m] - \frac{R}{\Gamma(m) m^{1/\gamma}} \cdot Y\left[\frac{1}{\gamma} + m, m\right] \\
&\quad - \frac{x}{\Gamma(m)} Y\left[m, m\left(\frac{x}{R}\right)^{\gamma}\right] + \frac{R}{\Gamma(m) m^{1/\gamma}} \cdot Y\left[\frac{1}{\gamma} + m, m\left(\frac{x}{R}\right)^{\gamma}\right]
\end{aligned}
\tag{7.35}
$$

7.5.2 *m* is a piecewise function over [0, *d*]

Normally, the fading parameter m is a piecewise constant function of communication distance in most MANET channels, that is:

$$
\begin{aligned}
&m = m_i \quad \text{for } x_i \le d < x_{i+1}, i = 1, 2, \ldots \\
&x_1 = 0
\end{aligned}
\tag{7.36}
$$

where x_i are jump points and m_i are constant fading parameter values. Through some mathematic manipulations for $h(d,m)$ in Eq. (7.30), we obtain:

$$
\begin{aligned}
&h(d,m) = \left\{ \sum_{i=2}^{N} \left[g\left(x_i, m_{i-1}\right) - g\left(x_i, m_i\right) \right] \right\} + g\left(d, m_N\right) \\
&N = \max\left\{ i : x_i \le d \right\}
\end{aligned}
\tag{7.37}
$$

where $g(d,m)$ is given by Eq. (7.34) and can be easily computed in Matlab. Therefore,

$$
\begin{aligned}
f(x,m) &= h(R,m) - h(x,m) \\
&= \left\{ \sum_{i=N_2+1}^{N_1} \left[g\left(x_i, m_{i-1}\right) - g\left(x_i, m_i\right) \right] \right\} \\
&\quad + g\left(R, m_{N_1}\right) - g\left(x, m_{N_2}\right) \\
&N_1 = \max\left\{ i : x_i \le R \right\} \\
&N_2 = \max\left\{ i : x_i \le x \right\}
\end{aligned}
\tag{7.38}
$$

7.6 Conclusions

This chapter presents an accurate and efficient analytic model to evaluate the impact of channel fading on multi-hop safety message disseminations in VANET. We utilize a distance-based timer to ensure the farthest node from the sender has highest priority to be chosen to relay the safety message. Various important performance and reliability metrics are derived and analyzed for thorough understanding of the safety message transmission behavior. Simulations conducted in Matlab cross validate the accuracy of our proposed model. In addition, our model is much more efficient in terms of evaluation time than simulations. The analytic model can also be used to analyze essential metrics that are difficult to capture in simulations as shown in Table 7.2.

8. Two-Dimensional Network Evaluation

8.1 Motivation

Broadcast services are provided widely in various ad hoc network applications such as safety-related message channels in vehicle-to-vehicle communication, and military battle field communication [104]. These applications require highly reliable and real-time communications between mobile nodes under adverse environments. Broadcast in IEEE 802.11 does not use the virtual carrier sensing and thus only relies on physical carrier sensing to reduce collisions. Thus, hidden terminal problem in broadcast VANETs is quite different from that in unicast systems [105]. Normally, the performance of broadcast VANETs is evaluated by simulations [3] although many analytical models have been constructed for the performance of IEEE 802.11 based VANETs [106][107]. In [39][105][41][36], analytical models are proposed to obtain *PRR* expressions in one-dimensional (1-D) IEEE 802.11 based broadcast VANETs with hidden terminals. However, the impact analysis of fading channel model, if any, is approximated by a constant bit error rate (BER). Assuming spatial Poisson distributed nodes and saturated packet generation condition, *PRR* of beacon message broadcast in DSRC VANETs is investigated in [24] taking into account the impact of *Rayleigh* fading on IEEE 802.11 based 1-D broadcast VANET. Unfortunately, very few network scenarios in real applications can be abstracted as 1-D models. However, extension of 1-D VANET reliability analysis to general 2-D VANET reliability analysis is not trivial because the

potential hidden terminal area computation given distribution of nodes in 2-D area is still claimed to be an open problem [108][109]. For 1-D network, the hidden terminals for a tagged vehicle are shown in Fig. 8.1. Comparatively, the hidden terminal problem has more impact on 2-D network since more hidden nodes will exist as shown in Fig. 8.2 for open field (the area inside the red circle and outside the blue circle will be the hidden terminal area of the tagged vehicle). Recently, we have conducted *PRR* analysis in a special 2-D VANET (two parallel lines approximate two opposite roads on highway) [105][110]. As of now, there is no work on *PRR* evaluation in general 2-D IEEE 802.11 broadcast VANETs.

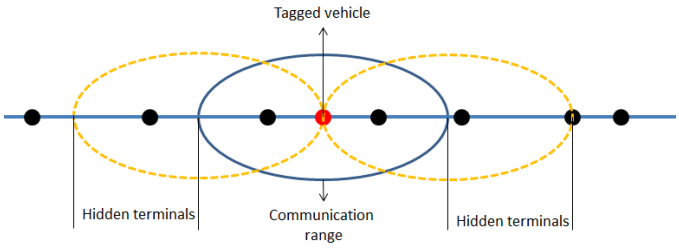

Figure 8.1: Hidden terminals problem for 1-D network

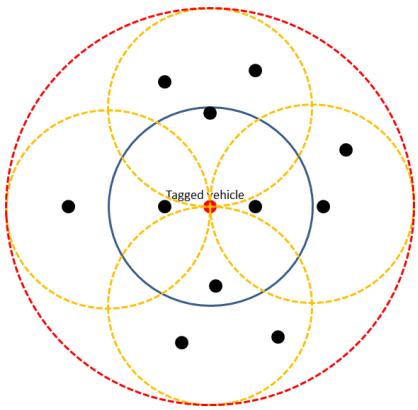

Figure 8.2: Hidden terminals problem for 2-D network

Compared with the existing models for performance analysis of broadcast in VANETs, the main contributions of the proposed analytic model in this chapter are: 1) general 2-D *PRR* is analytically derived accounting for IEEE 802.11 MAC, non-saturated packet generation, hidden terminal problem, and fading channel with path loss; 2) Deriving *PRR* using point-to-point integration of packet delivery probability makes the impact analysis of distance related *Nakagami* fading on the performance possible; 3) Introduction of SMP model [12] facilitates the accurate evaluation of IEEE 802.11 broadcast and hidden terminal impact that is one of the major factors on the degradation of the reliability; 4) *PRR* in 2-D VANETs is derived as a function of the receivers' distances to the broadcast sender, which provides a deeper insight into the performance as the distances change.

This chapter is organized as follows. Section 8.2 presents a brief description of system assumptions made in this chapter. Section 8.3 presents SMP analytic models and the fixed-point iteration algorithm. In Section 8.4, performance metrics such as mean transmission delay, packet delivery probability, and packet reception ratio are derived in the two-dimensional IEEE 802.11 broadcast VANETs. Section 8.5 demonstrates and discusses the numerical results from the analytic model and the simulation. The chapter is concluded in Section 8.6.

8.2 System Assumptions

In the proposed model, we assume that IEEE 802.11 broadcast DCF works under the following scenarios:

a. We consider a VANET with nodes distributed randomly according to the two-dimensional Poisson distribution. Let the average number of nodes per square unit (density) in the network be β. The probability $P(i, s)$ of finding i nodes in an area of s units is given by

$$P(i,s) = \frac{(\beta s)^i e^{-\beta s}}{i!} \tag{8.1}$$

For networks where transmitters and/or receivers are located or move around randomly over a large area, the Poisson point process is a good approximation [111].

b. All nodes have the same deterministic transmission range R, same carrier sensing range L_{cs}, $R \leq L_{cs} \leq 2R$, and same interference range L_{int}, $R \leq L_{int} \leq L_{cs}$.

c. At each mobile node, packet arrivals follow a Poisson process with rate λ (in packets per second). In addition to its tractability, the Poisson arrival process is a good approximation of message arrivals in packet-data networks [9].

d. Each vehicle has an infinite queue to store the packets at the MAC layer. Hence, each vehicle can be modeled as an M/G/1 type queue.

e. Impact of node mobility on the performance is not considered in this chapter. It was proven in [41] that high node mobility has a minor impact on the

performance of the one-hop direct message broadcast network with high data transmission rates.

f. *Nakagami* fading channel with path loss is assumed for studying the impact of channel fading on the performance.

Based on these assumptions, we can incorporate the analytic model presented in Chapter 3, in which the overall model can be seen as a set of interacting M/G/1 queues. The differences between the models in Chapter 3 are a few simplifications on the SMP model (this has minor influences on the results yet produces a more simplified model) and the derivation of performance metrics, which differ in the hidden terminal problem computation and include the channel fading's impact.

8.3 Analytic Models

8.3.1 SMP Model

The behavior of a tagged node for packet transmission is approximated by the SMP model shown in Fig. 8.3 [12]. The tagged node is in *idle* state if there is no packet in its queue. After a packet is generated, the node senses channel activity for DIFS time period. Next, the node will randomly choose a backoff counter in the range [0, W_0-1]. The backoff counter will be decreased by one if the channel is detected to be idle for a time slot σ (with probability 1-p_b), which is captured by the transition from W_0-i to W_0-i-1 state. If the channel is busy during a backoff time slot σ, the backoff counter of the tagged node will be suspended and deferred for the duration T of a packet transmission

time plus an idle DIFS, which presents the transition from state W_0-i to state $D_{W0\text{-}i\text{-}1}$ with probability p_b. When the backoff counter reaches zero, the packet will directly be transmitted (an SMP transition occurs from 0 state to state *XMT* with probability one). In *XMT* state, a packet is transmitting. After the packet transmission, if there is no packet left in the queue of the tagged node (with probability 1-ρ), the node will go from *XMT* to *idle* state and wait for a new incoming packet. If there are packets left in the queue after a packet transmission (with probability ρ), the node will sense the channel again for DIFS time and then randomly choose a backoff counter before transmitting the next packet. The fact that we simply use server utilization as a surrogate for the queue of waiting messages is a key approximation.

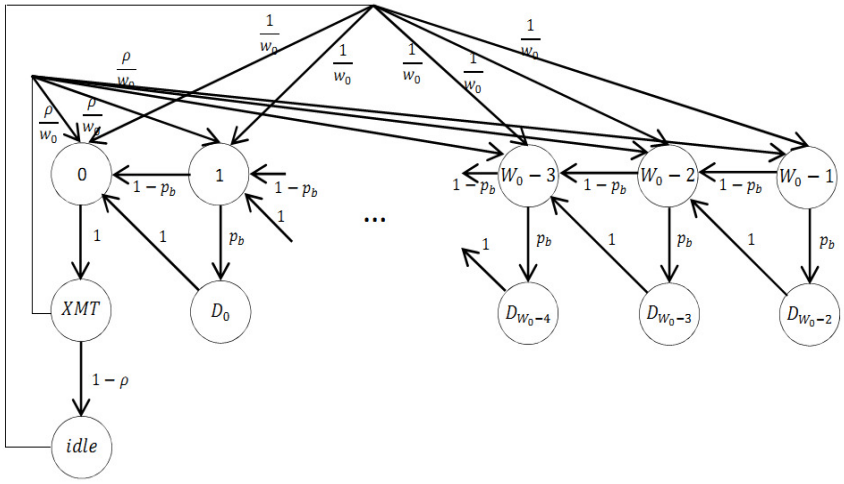

Figure 8.3: SMP model for IEEE 802.11 broadcast

Define the sojourn time in state j as T_j. The mean and variance of T_j in the SMP model are:

$$E[T_j]=\tau_j=\begin{cases}\sigma, & j=0,1,2,...,W_0-1\\ T & j=D_0,D_1,...,D_{W_0-2}\\ T & j=XMT\\ \dfrac{1}{\lambda}+DIFS & j=idle\end{cases} \tag{8.2}$$

$$Var[T_j]=\theta_j^2=\begin{cases}0, & j=0,1,2,...,W_0-1\\ Var[PA]\cdot\left(\dfrac{1}{R_d\cdot 10^6}\right)^2 & j=D_0,D_1,...,D_{W_0-2}\\ Var[PA]\cdot\left(\dfrac{1}{R_d\cdot 10^6}\right)^2 & j=XMT\\ 1/\lambda^2 & j=idle\end{cases} \tag{8.3}$$

where $T=E[PA]/(R_d\cdot 10^6)+T_H+DIFS+\delta$. The mean and variance of the packet transmission time are $E[PA]/(R_d\cdot 10^6)$ and $Var[PA]/(R_d\cdot 10^6)^2$ respectively. R_d (*Mbps*) presents the data rate. Hence, $E[PA]/(R_d\cdot 10^6)$ is the time to transmit the packet. T_H presents the packet header transmission time including physical layer header time and MAC layer header time. δ is the propagation delay.

For the SMP model in Fig. 8.3, the embedded DTMC is first solved for its steady-state probabilities:

$$v_i=\begin{cases}(W_0-j)v_{W_0-1}, & j=0,1,2,...,W_0-1\\ (W_0-j-1)p_b v_{W_0-1} & j=D_0,D_1,...,D_{W_0-2}\\ W_0 v_{W_0-1} & j=XMT\\ W_0(1-\rho)v_{W_0-1} & j=idle\end{cases} \tag{8.4}$$

In the above equations,

$$v_{W_0-1}=\frac{2}{(1+p_b)W_0^{\,2}+(5-p_b-2\rho)W_0}$$

Taking into account the mean sojourn time in each state, the steady-state probabilities of the semi-Markov process are given by:

$$\pi_i = \frac{v_i \tau_i}{\sum_j v_j \tau_j} \tag{8.5}$$

Therefore, the steady-state probability that a node is in the *XMT* state is given

$$\pi_{XMT} = \frac{2T}{(\sigma + p_b T)W_0 + \sigma - p_b T + 2T + 2(1-\rho)(1/\lambda + DIFS)} \tag{8.6}$$

Although the sojourn time in *XMT* state is *T*, the real packet transmission only occupies a portion of this sojourn time, which is $E[PA]/(R_d \cdot 10^6)+T_H+\delta=T-DIFS$. Hence, the probability that a node is transmitting in steady state is $\pi_{XMT}(T-DIFS)/T$.

In Eq. (8.6), two unknown parameters are: ρ (the probability that there are packets in the queue of the tagged vehicle) and p_b (the probability that the channel is detected busy in one time slot by the tagged vehicle). It is easy to see that p_b of the tagged vehicle depends on the transmitting state of other vehicles within the tagged vehicle's receiving range, and the transmitting probability of a vehicle can be described by Eq. (8.6) (as a function of p_b and ρ). Hence, p_b of the tagged vehicle can be expressed as a function of p_b and ρ of other vehicles. Clealry, we have made the homogenity assumption for all the vehicles. In addition, we know that ρ depends on the mean service time to transmit a packet. Therefore, the service time is derived first in the next subsection.

8.3.2 Service Time Computation

As mentioned above, each vehicle in the network is modeled as an M/G/1 queue. The MAC layer service time is defined as the time interval from the time instant when a packet becomes the head of the queue and starts to contend for transmission, to the time instant when the packet is received.

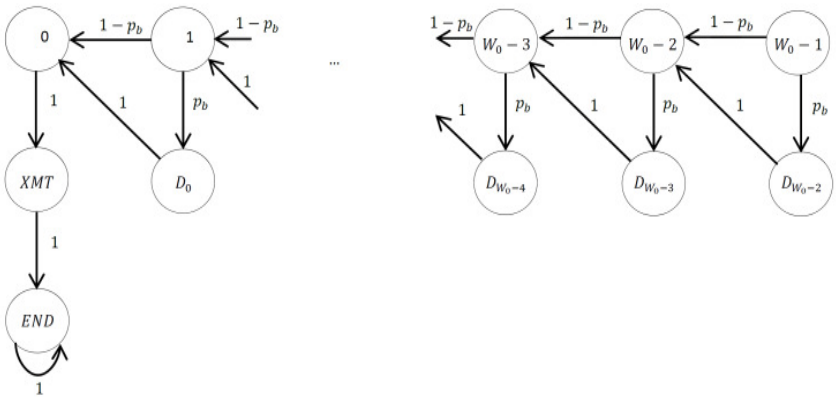

Figure 8.4: Embedded DTMC of the SMP model for the service time

The SMP model in Section 8.3.1 describes the behavior of a tagged vehicle transmitting packets in its queue. This SMP model takes the state of its own queue into account by means of a surrogale ρ. Hence, at the end of one packet transmission, it checks whether there are packets left in its queue or not to transmit the next packet. In this section, the service time for any one packet in the queue is derived. Therefore, the SMP model in Section 8.3.1 is modified to contain an absorbing state *END* as shown in Fig. 8.4. Thus, at the end of one packet transmission, the SMP model reaches an absorbing state instead of checking the status of the queue to transmit the next packet.

By proper choice of the initial probability vector, the time to reach the absorbing state will be the service time for a packet transmission.

For a newly generated packet in the tagged vehicle, the vehicle will randomly choose a backoff counter before the packet transmission. Therefore, the initial probability that a packet starts its service from state i (i=0,1,…,W_0-1) is $1/W_0$. Hence, the initial probability vector is:

$$q_i = \begin{cases} \dfrac{1}{W_0} & i = 0,1,2,...,W_0 - 1 \\ 0, & i = D_0, D_1, D_2, ..., D_{W_0-2}, XMT \end{cases} \tag{8.7}$$

Since the embedded DTMC contains an absorbing state (state *END* in Fig. 8.4), taking advantage of the acyclic nature of the DTMC model in Fig. 8.4, the mean service time for a packet transmission conditioned on starting from state i is derived from [12]:

$$E[S_i] = i\sigma + i \cdot p_b \cdot T + T \qquad for \quad i = 0,1,...,W_0 - 1 \tag{8.8}$$

Therefore, the mean of the service time is given by

$$E[S] = \sum_i E[S_i] q_i = \frac{(\sigma + p_b T)(W_0 - 1)}{2} + T \tag{8.9}$$

8.3.3 Fixed-Point Iteration

In the previous section, the mean service time $E[S]$ is shown to depend on two unknown parameters ρ and p_b. But ρ in turn depends on the mean service time as per the M/G/1 queue equation $\rho=\lambda E[S]$. As shown below, p_b also depends on ρ. Because of this cyclic dependence among the parameters, fixed-point iteration algorithm is utilized to obtain the final converged solutions.

From the tagged vehicle's point of view, p_b is the probability that it senses channel busy during one time slot in the backoff process. Since channel is detected busy if there is at least one neighbor (*i.e.*, a vehicle in the transmission range of the tagged vehicle) transmitting in a backoff time slot of the tagged vehicle, we have

$$p_b = 1 - \sum_{i=0}^{\infty} (1 - P_{XMT})^i \frac{(\beta \pi L_{cs}{}^2)^i}{i!} e^{-\beta \pi L_{cs}{}^2} = 1 - e^{-\beta \pi L_{cs}{}^2 P_{XMT}} \tag{8.10}$$

where P_{XMT} is the probability that a neighbor is transmitting in a backoff time slot of the tagged vehicle, to be derived later in this chapter.

For the first backoff time slot of the tagged vehicle, the time duration that can capture the transmission of the neighbor is $T\text{-}DIFS+2\sigma$. One extra time slot σ is the one just before transmission and another is the one just after transmission, which can capture the starting time instant and ending time instant of the packet transmission. Therefore, the probability that a neighbor's transmission is detected in the first backoff time slot of the tagged vehicle is $\pi_{XMT}(T\text{-}DIFS+2\sigma)/T$.

For a backoff time slot that is not the first backoff time slot of the tagged vehicle, the time duration that captures the transmission of the neighbor is 2σ [12]. Therefore, the probability that a neighbor's transmission is detected in non-first backoff time slot of the tagged vehicle is $\pi_{XMT} \times 2\sigma/T$.

Since the probability that a backoff time slot is the first backoff time slot is $1/W_0$ and non-first backoff time slot is $(1\text{-}1/W_0)$, the probability that a neighbor's transmission is detected by a backoff time slot of the tagged vehicle is given by

$$P_{XMT} = \frac{1}{W_0}\frac{T - DIFS + 2\sigma}{T}\pi_{XMT} + \left(1 - \frac{1}{W_0}\right)\frac{2\sigma}{T}\pi_{XMT} \tag{8.11}$$

From the above analysis of the relationship between two parameters ρ and p_b, we notice that p_b depends on ρ and p_b itself. Hence, we denote $p_b=g(\rho,p_b)$ and the reciprocal of mean service time for M/G/1 queue to be $\mu=h(\rho,p_b)$. The fixed-point iteration algorithm is outlined below.

Step 1: Initialize ρ=1, which is the saturation condition;

Step 2: With ρ, solve p_b using Eqs. (8.6)(8.10)(8.11);

Step 3: With ρ and p_b, calculate service rate $\mu=1/E[S]$ using Eq. (8.9);

Step 4: If $\lambda<\mu$, $\rho=\lambda/\mu$; otherwise, ρ=1;

Step 5: If ρ converges, then stop the iteration. Otherwise, go to step 2 with the updated ρ.

By utilizing the fixed-point iteration, the parameters ρ, p_b, π_{XMT} as well as the mean and the variance of the service time are determined, which are subsequently used for the performance indices computation in the next section.

8.4 Performance Metrics

8.4.1 Mean Transmission Delay

The packet transmission delay is defined as the average delay a packet experiences from the time at which the packet is generated until the time at which the packet is successfully received by all neighbors of the node that generates the packet. The transmission delay $E[D]$ includes the queuing delay and medium service time (due to backoff, packet transmission, and propagation delay, *etc.*).

The expected queuing delay is obtained from the *Pollaczek-Khinchin* mean value formula of M/G/1 queue:

$$E[D_q] = \frac{\lambda Var[S] + (E[S])^2}{2(1 - \lambda E[S])} \tag{8.12}$$

The average packet transmission delay is then calculated as

$$E[D] = E[D_q] + E[S] \tag{8.13}$$

8.4.2 Packet Delivery Probability

Packet Delivery Probability (*PDP*) (also is referred as Node Reception Probability in Chapter 6-7) is defined as the probability that a node within the transmission range of the sender successfully receives a packet from the tagged node (*i.e.*, sender). There are three factors affecting the performance of a packet reception: hidden terminal problems, collisions due to concurrent packet transmissions, and interference as a result of the fading channel.

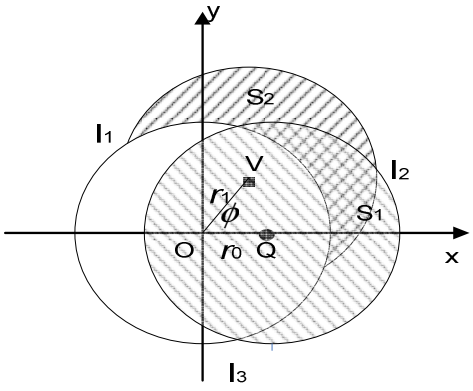

Figure 8.5: 2-D MANET model for performance analysis

The transmission scenario is shown pictorially in Fig. 8.5. Given a transmitting node O placed at the origin, Q is one of the receivers within the transmission range (*i.e.*, a circular coverage area having radius R) of node O. Q is placed on the x axis at a distance r_0 from O.

Let V: ($r_1 cos\Phi$, $r_1 sin\Phi$) be another node in the transmission range of O and Q. In order to evaluate the impact of hidden terminals and concurrent transmissions on *PDP*, two areas need to be considered. $S_1(r_0)=D(Q, L_{int})-D(O, L_{cs})$ denotes the hidden terminal area of node O, where $D(s,l)$ represents the disk of radius l centered at s. Denote $S_2(\Phi, r_1, r_0)= D(V, L_{cs})-D(O, L_{cs}) \cup D(Q, L_{int})$ as the area within the carrier sensing range of V that is not in the carrier sensing range of O or interference range of Q.

a. Impact of Hidden Terminals

We observe that since the transmission time for a packet is $T\text{-}DIFS=E[PA]/(R_d \cdot 10^6)+T_H+\delta$, the transmissions from hidden terminals collide with the tagged node's transmission only happens when hidden terminals start to transmit during the vulnerability period $2(T\text{-}DIFS)=2(E[PA]/(R_d \cdot 10^6)+T_H+\delta)$. Given the probability that a node starts to transmit during the vulnerable period is $\pi_{XMT} \cdot 2(T\text{-}DIFS)/T$ [12], we have

$$\begin{aligned} P_H(r_0) &= \sum_{i=0}^{\infty}\left(1-\pi_{XMT}\frac{2(T-DIFS)}{T}\right)^i \frac{|\beta S_1(r_0)|^i}{i!} e^{-|\beta S_1(r_0)|} \\ &= \exp\left(-\frac{2(T-DIFS)|\beta S_1(r_0)|\pi_{XMT}}{T}\right) \end{aligned} \tag{8.14}$$

where $|S_1(r_0)|$ is the area of $S_1(r_0)$. Derivation of $|S_1(r_0)|$ is described next.

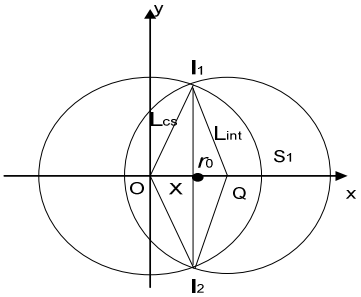

Figure 8.6: Illustration of S_1 area calculation

As shown in Fig. 8.6, given distance r_0 (r_0<L_{cs}) between center O for circle $D(O, L_{cs})$ and center Q for circle $D(Q, L_{int})$, intersection points of two circles denoted as I_1 and I_2, and X the range on x axis projected by line I_1O, we have equation:

$$\sqrt{L_{cs}{}^2 - X^2} = \sqrt{L_{\text{int}}{}^2 - (r_0 - X)^2} \tag{8.15}$$

Solve above equation, we obtain

$$X = \frac{L_{cs}{}^2 + r_0{}^2 - L_{\text{int}}{}^2}{2r_0} \tag{8.16}$$

Let ψ_1, ψ_2 be radian of I_1O and I_1Q, respectively. Then

$$\begin{aligned} \psi_1 &= \arccos\left(\frac{X}{L_{cs}}\right) = \arccos\left(\frac{L_{cs}{}^2 + r_0{}^2 - L_{\text{int}}{}^2}{2L_{cs}r_0}\right) \\ \psi_2 &= \arccos\left(\frac{r_0 - X}{L_{\text{int}}}\right) = \arccos\left(\frac{L_{\text{int}}{}^2 + r_0{}^2 - L_{cs}{}^2}{2L_{\text{int}}r_0}\right) \end{aligned} \tag{8.17}$$

Denote $S_1'(r_0)$ as the overlapping area of $D(O, L_{cs})$ and $D(Q, L_{int})$, we have

$$S_1'(r_0) = L_{cs}{}^2\psi_1 + L_{\text{int}}{}^2\psi_2 - r_0\sqrt{L_{cs}{}^2 - X^2} \tag{8.18}$$

Therefore,

$$| S_1(r_0) | = \pi L_{\text{int}}^2 - | S_1'(r_0) | \tag{8.19}$$

b. Impact of Concurrent Transmissions

In addition to collisions caused by the hidden terminals, transmissions from nodes within the interference range of the tagged node in the meantime at which the tagged node transmits may also cause collisions. When the tagged node transmits in a slot time, concurrent collisions will take place if any node in the interference range of the tagged node transmits in the slot.

Given that both *O* and *Q* sense the channel idle, *V* will transmit within the duration of a slot with probability $\tau=\pi_0$. It should be noted that the slots of *O* and *V* are not necessarily synchronized. Now, given that all nodes inside the union of two circles center *O*, *Q*, radius *R* and L_{int}, respectively, are idle at the beginning of the slot, the probability that a node *V* starts transmitting during the slot is the probability that node *V* intends to transmit and all nodes in S_2 are not in the transmitting state, which is expressed as

$$\begin{aligned} P_2'(\varphi, r_1, r_0) &= \pi_0 \sum_{i=1}^{\infty} (1 - P_{XMT})^i \frac{(\beta | S_2(\varphi, r_1, r_0) |)^i}{i!} e^{-\beta | S_2(\varphi, r_1, r_0) |} \\ &= \pi_0 \exp(-\beta P_{XMT} | S_2(\varphi, r_1, r_0) |) \end{aligned} \tag{8.20}$$

where $| S_2(\Phi, r_1, r_0) |$ is the area of $S_2(\Phi, r_1, r_0)$. Derivation of $| S_2(\Phi, r_1, r_0) |$ is shown next.

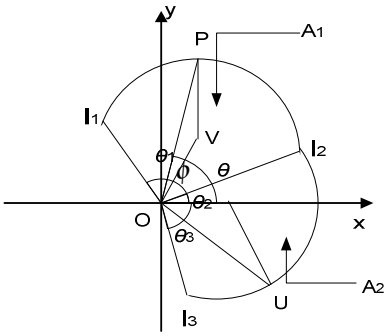

Figure 8.7: Illustration of S_2 area calculation

Given coordinates of nodes P: (0,0), Q: (r_0,0), and V: ($r_1 cos\Phi$, $r_1 sin\Phi$), the contour functions of the transmission (or receiving) area of the nodes are: $D(O, L_{cs})$: $x^2+y^2=L_{cs}^2$, $D(Q, L_{int})$: $(x-r_0)^2+y^2=L_{int}^2$, $D(V, L_{cs})$: $(x-r_1 cos\ \Phi)^2+(y-r_1 sin\ \Phi)^2=L_{cs}^2$.

Solve the above contour equations, we find the coordinates of all the intersection points I_{PQ}^1, I_{PQ}^2, I_{PV}^1, I_{PV}^2, I_{QV}^1, and I_{QV}^2. Only three out of six intersection points determine the shape of outmost contour. These intersection points can be selected through the following criterion: if the given intersection point (x', y') is one of the outmost intersection points, the following inequities must hold

$$\begin{aligned} & x'^2 + y'^2 \geq L_{cs}^{\ 2} \\ & (x' - r_0)^2 + y'^2 \geq L_{\text{int}}^{\ 2} \\ & (x' - r_1 \cos\varphi)^2 + (y' - r_1 \sin\varphi)^2 \geq L_{cs}^{\ 2} \end{aligned} \tag{8.21}$$

It is easy to prove that the criterion is both sufficient and necessary.

By knowing the outmost intersection points and corresponding outmost curves, we are able to calculate the area surrounded by the outmost contour. Two neighboring outmost intersection points determine one outmost curve. Outmost curves all together

form the outmost contour. In Fig. 8.7, the outmost contour consists of the following curves:

Given the three outmost intersection points I_1 with coordinate (x_1, y_1), I_2 with coordinate (x_2, y_2), and I_3 with coordinate (x_3, y_3), whose radian coordinates are (r_{i1}, θ_1), (r_{i2}, θ_2), and (r_{i3}, θ_3), respectively, where $r_{i1}= r_{i3}=L_{cs}$; $r_{i2}= (x_{i2}^2+y_{i2}^2)^{1/2}$; θ_1=arctg(y_{i1}/x_{i1}), θ_2=arctg(y_{i2}/x_{i2}), θ_3=arctg(y_{i3}/x_{i3}).

Outmost curves connected by I_1, I_2, and I_3 divide the total area into two sections: section 1 (I_1I_2) center V and section 2 (I_2I_3) center Q, as shown in Fig. 8.7. Areas of the two sections are denoted as A_1 and A_2, respectively. Given O at the origin, radian of section 1 ranges from θ_2 to θ_1; radian of section 2 ranges from θ_3 to θ_2; and radian of VO is Φ.

Given that P is a point on the outmost curve of section 1 and the radian of PO is θ, the area of section 1 is:

$$\begin{aligned} A_1 &= \frac{1}{2}\int_{\theta_2}^{\theta_1} |PO|^2 \, d\theta \\ &= \frac{1}{2}\int_{\theta_2}^{\theta_1} (r_1\cos(\theta-\varphi) + \sqrt{L_{cs}^{\ 2} - r_1^{\ 2}\sin^2(\theta-\varphi)})^2 \, d\theta \\ &= \frac{(L_{cs}^{\ 2} - r_1^{\ 2})(\theta_1-\theta_2)}{2} + r_1^{\ 2}[\frac{\theta-\varphi}{2} + \frac{\sin 2(\theta-\varphi)}{4}] - r_1^{\ 2}\frac{\sin(\theta-\varphi)\sqrt{(\frac{L_{cs}}{r_1})^2 - \sin^2(\theta-\varphi)}}{2} \\ &\quad - \frac{L_{cs}^{\ 2}\arcsin(\frac{r_1\sin(\theta-\varphi)}{L_{cs}})}{2}\Bigg|_{\theta_2}^{\theta_1} \end{aligned} \tag{8.22}$$

Given that U is a point on the outmost curve of section 2 and the radian of UO is θ, the area of section 2 is:

$$
\begin{aligned}
A_2 &= \frac{1}{2}\int_{\theta_3}^{\theta_2} |UO|^2 \, d\theta \\
&= \frac{1}{2}\int_{\theta_3}^{\theta_2} (r_0\cos\theta + \sqrt{{L_{\text{int}}}^2 - {r_0}^2\sin^2\theta})^2 d\theta \\
&= \frac{({L_{\text{int}}}^2 - {r_0}^2)(\theta_2-\theta_3)}{2} + {r_0}^2[\frac{\theta}{2} + \frac{\sin(2\theta)}{4}] - {r_0}^2 \frac{\sin\theta\sqrt{(\frac{L_{\text{int}}}{r_0})^2 - \sin^2\theta}}{2} - \frac{{L_{\text{int}}}^2 \arcsin(\frac{r_0\sin\theta}{L_{\text{int}}})}{2}\Bigg|_{\theta_3}^{\theta_2}
\end{aligned}
\tag{8.23}
$$

Then, the extended coverage area $S_2(\Phi, r_1, r_0)$, as shown in Fig. 8.7, can be calculated as the sum of A_1 and A_2 excluding the area of $D(O, R)$ and node O's hidden terminal area in A_1 and A_2, which is expressed as:

$$
S_2(\varphi, r_1, r_0) = A_1 + A_2 - \frac{1}{2}(\theta_1 - \theta_3){L_{cs}}^2 - |S_1(r_0)| \tag{8.24}
$$

Therefore, the average number of nodes that start transmission during the slot that collides with the transmission from O within the circle with center Q radius L_{int} is

$$
\bar{n}_T = \beta\int_0^{2\pi}\int_0^{L_{\text{int}}} rP_2'(\varphi, r, r_0)\,dr\,d\varphi \tag{8.25}
$$

Therefore, given Poisson node distribution, the probability that no node within the circle center Q radius L_{int} start transmission during the slot that collides with the transmission from O is:

$$
P_{con}(r_0) = \frac{(\bar{n}_T)^0}{0!}\exp(-\bar{n}_T) = \exp(-\bar{n}_T) \tag{8.26}
$$

c. Impact of Channel Fading and Path Loss

VANETs present scenarios with unfavorable characteristics to develop wireless communications, *i.e.*, multiple reflecting objects able to degrade the strength and quality of the received signal. Additionally, fading effects resulting from the mobility of the

surrounding objects and/or the sender and receivers themselves have to be taken into account. Therefore, similar to Section 7.3.1 in Chapter 7, we incorporate the channel fading's effect and the probability of successfully receiving a message at a distance r_0 considering channel fading with path loss effects is given by:

$$P_F(r_0) = 1 - \frac{m^m}{\Gamma(m)} \int_0^{(r_0/R)^\gamma} z^{m-1} e^{-mz} \, dz \tag{8.27}$$

Taking hidden terminals, possible packet collisions, and channel fading with path loss into account, and assuming these three events are independent, the probability that the node Q receives the broadcast message from the tagged node O is:

$$P_s(r_0) = P_H(r_0) P_F(r_0) P_{con}(r_0) \tag{8.28}$$

8.4.3 Packet Reception Ratio

Packet Reception Ratio (*PRR*) is defined as the percentage of nodes that successfully receive a packet from the tagged node given that all receivers are within the transmission range of the sender at the moment that the packet is sent out [3]. From the above definition, *PRR* can be interpreted as the percentage of the mobile nodes in the tagged node's transmission range that receive the broadcast message successfully.

We approach *PRR* evaluation in two steps. First, compute the probability that the individual node Q successfully receives the broadcast packet from the sender O. Then, *PRR* is derived through integration of the probabilities over the transmission range of O. Assuming the distribution of nodes along a 2-D area follows Poisson process, the average number of nodes within an incremental area dA should be βdA [110]. Given the

reception probability of each node in Eq. (8.28), the average number of nodes within dA that successfully receive the broadcast message from the tagged node is $P_s(r)\beta dA$. For a circular coverage area having radius R from node O, PRR over a coverage area with radius d ($d \le R$) found by integrating the probabilities that nodes with distance r to the source node O within an incremental area dA successfully receive the broadcast message from O. Hence,

$$PRR(d) = \frac{1}{\pi d^2}\int_0^{2\pi}\int_0^d P_s(r) r dr d\varphi = \frac{2}{d^2}\int_0^d P_s(r) r dr \tag{8.29}$$

8.5 Numerical Results

Table 8.1: DSRC communication parameter

Parameters	Values	Parameters	Values
Modulation	BPSK, QPSK, 16-QAM, 64-QAM	Slot time, σ	16 μs
Coding Rates	1/2, 2/3, 3/4	SIFS	32 μs
OFDM Symbol Duration	8 μs	Propagation delay, δ	1 μs
Signal Bandwidth	10 *MHz*	Preamble Length	40 μs
Channel Data rate	6, 9, 12, 36, 54 *Mbps*	PLCP Header Length	8 μs
DIFS	64 μs	CWMin	15~1024

In this section, we apply the proposed model to a typical VANET environment: vehicular ad hoc communication system in battlefield. Each node is equipped with IEEE 802.11 based wireless ad hoc network capability with communication parameters as listed in Table 8.1. Communication range (transmission/carrier sensing) is R=500 m. Each node generates broadcast messages with rate λ and the average message length $E[PA]$=200~400 bytes. Two dimensional numerical integrations in MATLAB (double integral over rectangle) are used to compute overlapping areas and the impact of

Nakagami fading needed for derivation of *PRR*s. In order to cross-validate the proposed analytic model, we extend 1-D event-driven simulation program developed for research in [36] to 2-D simulation with *Nakagami* fading and path loss using both NS2 and MATLAB. The communication nodes are Poisson distributed with density β (nodes/m^2) on a 2-D area with radius of 3000 m. The free space propagation model is adopted (γ=2). Most of assumptions made in the analytic solution are relaxed in the simulation. In the NS2 program, the communication nodes are connected through setting up transmission powers and receiving thresholds so that the communication ranges are random variables. With distributed asynchronous time scale and limited communication ranges, asynchronous time channel access and the hidden terminal problem are naturally reflected in the simulation process. In addition, different from the decomposition method used in the analytic model, the simulation process simulates the overall system behavior.

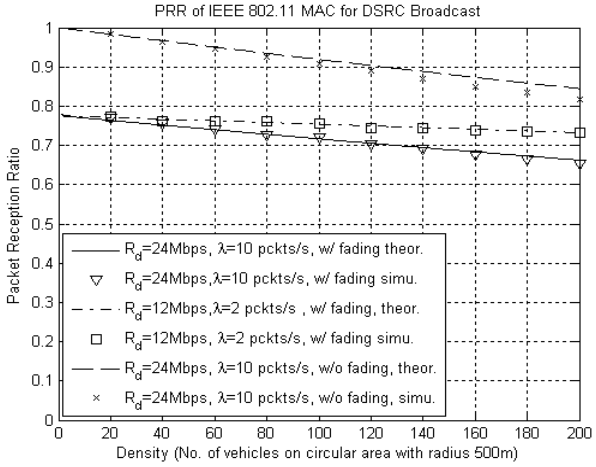

Figure 8.8: PRR with W_0=15

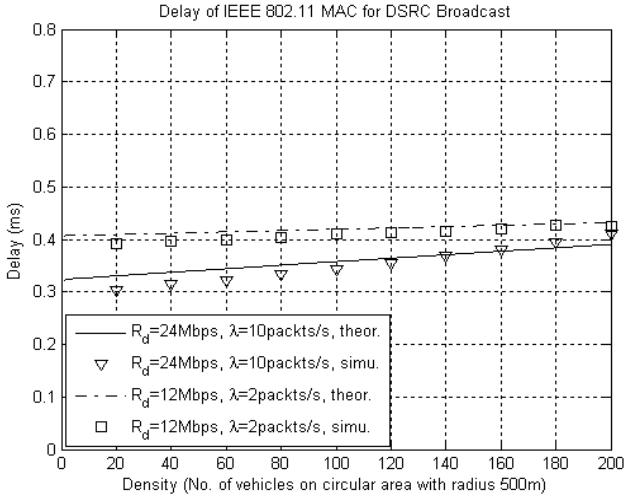

Figure 8.9: Mean transmission delay with W_0=15

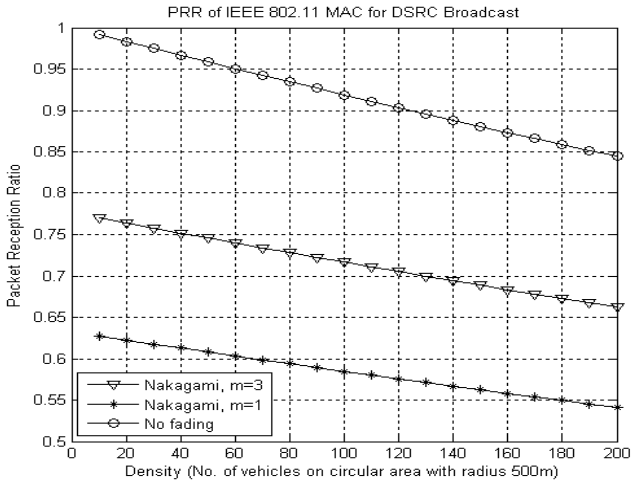

Figure 8.10: Impact of Nakagami fading on PRR of DSRC broadcast with network parameters W_0=15, λ=10 packets/s, R_d=24Mbps

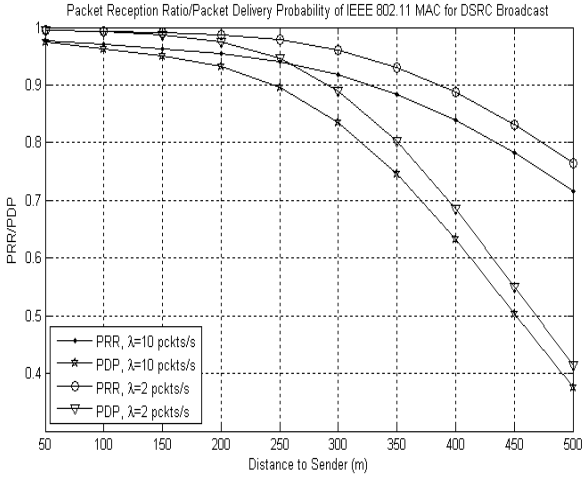

Figure 8.11: PRR and PDP of DSRC broadcast with network parameters W_0=15, R_d=24Mbps, β=100/(πR^2)

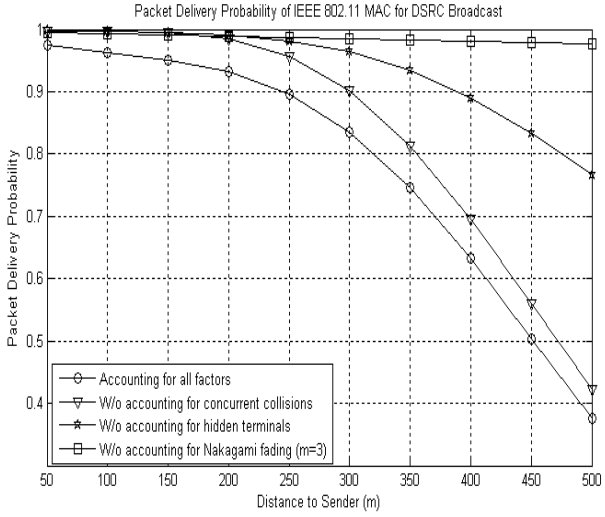

Figure 8.12: PDP with network parameters λ=10 packets/s, W_0=15, R_d=24Mbps, β=100/(πR^2)

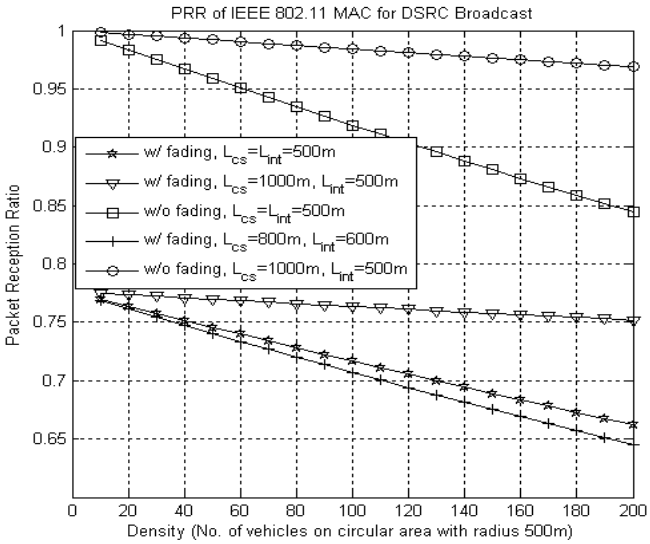

Figure 8.13: Impact of Communication range on PRR of DSRC broadcast with network parameters W_0=15, λ=10 packets/s, R_d=24Mbps

Fig. 8.8 and Fig. 8.9 depict the packet reception ratios (*PRR*s) and packet transmission delay, respectively, over the average number of nodes in the transmission range of a transmitting (or tagged) node. As shown in Fig. 8.8 and Fig. 8.9, analytical results (lines) practically coincide with the simulation results (symbols). The relative errors between analytical results and simulation results are 0.84% for *PRRs*, and 3.45% for packet transmission delays. We also observe that *PRR*s get lower with the density of nodes in the network because more nodes introduce more data traffic on the ad hoc broadcast network. Fig. 8.8 also shows that increasing packet generation rate λ (from 2 packets/second to 10 packets/second) degrades *PRRs* since more collisions and transmissions of hidden terminals are introduced as the packet generation rate λ goes up. This degradation cannot be compensated by lifting transmission data rate (from 12

Mbps to 24 *Mbps*). From Fig. 8.8, we can see a significant difference between *PRR*s with *Nakagami* fading (*m*=3) and *PRR*s without any fading, which indicates that, in addition to hidden terminal problem, channel fading is another major factor for the degradation of reliability. From Fig. 8.9, we observe that channel fading does not affect the packet transmission delay.

Fig. 8.10 shows how *Nakagami* fading with different *m* values affect *PRR*s of the MANET broadcast communication. As stated earlier, fading degrades *PRR*s significantly. *PRR*s with *m*=3 are bigger than *PRR*s with *m*=1 (*Rayleigh* distribution), which means bigger fading parameters bring smaller fading to the communications.

Fig. 8.11 demonstrates how packet reception ratios (*PRR*s) and packet delivery probability (*PDP*s) of a node change with the receivers' distances to the sender. Both *PRR*s and *PDP*s are reduced with the receiver's distance to the sender, and are degraded with much higher rate as the receiver's distance to the sender is longer than 300 *m*. The observation is due to the fact that the longer the receiver's distance to the sender, the more likely the receiver is affected by hidden terminals problem and channel fading. This observation alleviates the difficulty of selecting network parameters to meet the strict reliability requirements in some applications such as VANET safety message broadcast where high *PRR* is required for the receiving nodes that are closer to the transmitting node.

Fig. 8.12 shows how *PDP*s are affected by respective factors listed as hidden terminal problem, concurrent collisions, and channel fading. Given the same network parameters, separate *PDP* curves ignoring individual factors are compared with *PDP*s taking all factors into account. It is observed that the curve without accounting for *Nakagami* fading has the biggest difference from the curve taking all factors into account among the other two curves, and the curve without accounting for concurrent collisions has the smallest difference from the curve taking all factors into account among the other two curves. This observation reveals that fading channel and hidden terminals problem are major factors to degrade the broadcast reliability, while concurrent collisions affect the reliability slightly.

Fig. 8.13 depicts the impact of communication ranges on the reliability with certain network setting. When carrier sensing range increases from 500 *m* to 1000 *m* (means w/o hidden terminals), *PRRs* increase accordingly because the bigger the carrier sensing range, the less the number of hidden terminals. It is interesting to see that the impact of fading is more significant than the impact of hidden terminals. If the interference range increases (from 500 *m* to 600 *m*), *PRR*s are getting worse even though carrier sensing range is extended (from 500 *m* to 800 *m*).

8.6 Conclusions

In this chapter, we propose an analytical model to evaluate the performance of IEEE 802.11 based broadcast two-dimensional VANETs. A semi-Markov process model

interacts with M/G/1 queuing model to characterize the behavior of communicating nodes under IEEE 802.11 broadcast. The derived *PRR* expressions take into account the impact of *Nakagami* fading channel with path loss, hidden terminals problem, concurrent transmissions, unsaturated message arrivals and varied communication ranges of IEEE 802.11 MAC, and DCF backoff process. As an example, the analytical model is applied to a vehicular ad hoc system for the broadcast of safety messages. *PRR* derivation using point-to-point integration facilitates the accurate impact analysis of fading channel. Numerical results prove the effectiveness and correctness of the proposed model, and reveal the characteristics of 2-D broadcast VANETs, which can be beneficial to the design of such systems. From the numerical results and discussions, some very important observations of such networks are described. Our future research will focus on building more specific models to fit various road conditions such as intersections, streets of cities, *etc.*, and extend the proposed 2-D model to the models with more general node distributions and more general packet arrivals.

9. Summary

In this chapter, we summarize the work in this dissertation. The main theme of this dissertation is to develop comprehensive and high fidelity analytic models for the effective performance and reliability analysis of various V2V DSRC safety communication scenarios. A major hurdle in the development of VANET for safety-critical services in the DSRC system is the lack of established models and metrics which can be utilized to determine the effectiveness of VANET design mechanisms for predictable QoS and allows one to evaluate the tradeoff between network parameters. Simulation methods usually consume long time to collect sufficient data for accurate system performance analysis. Real world testbeds can capture more practical network dynamics but are limited by extremely high equipment cost. In this dissertation, we have proposed accurate and efficient analytic models to assess the effectiveness of message dissemination schemes for safety applications. Important MAC and application level performance and reliability metrics are derived and evaluated. The major point is that analytic models that reflect important details of the protocol and user behavior can be developed and solved efficiently thus avoiding costly simulations. Based on the numerical results, we also analyze the tradeoff of network parameters and provide insights to tune the network parameters to meet the application requirements.

In Chapter 3, we presented a general analytic model to evaluate the performance of safety message broadcasting, which is suitable for event-driven safety messages

(ESMs) assuming Poisson arrivals and infinite MAC-layer queue. To produce a tractable analytic model, we utilize model decomposition and fixed-point iteration to obtain converged solutions. Important MAC-level performance and reliability metrics are subsequently derived. Chapter 4 describes a more accurate analytic model compared to Chapter 3 to capture the basic safety messages (BSMs) broadcasting, where associated features such as periodic message generation, out-dated message replacement and no queuing in MAC-layer are incorporated. Such a model for BSMs is compared with the model presented in Chapter 3 for ESMs. The results prove that the simplified analytic model for ESMs can be used to approximately evaluate the BSMs transmission. Besides MAC-level metrics, application-level metrics are also derived in Chapter 4. Simulations in Matlab are conducted for the comparison purpose in both Chapter 3 and 4.

Since different types of messages (including BSMs and ESMs with different priorities) maybe transmitted in a single channel, in Chapter 5, multiple types of services transmission over a single channel (*e.g.*, control channel) is evaluated based on the extension of the analytic model developed in Chapter 3. The EDCA mechanism specified in the IEEE 802.11p protocol is shown to be ineffective to guarantee priorities for different services. Important conclusions are also drawn to tune network parameters in order to improve the performance and reliability for high priority services.

At the early stage of DSRC technology deployment, a radio device can switch between channels to support concurrent applications on different channels. Therefore, in

Chapter 6, we consider IEEE 1609.4 multi-channel operation's impact to evaluate the performance and reliability of the BSMs transmission on the control channel (CCH). The impact of various factors such as concurrent transmission, hidden terminals problem, channel fading with path loss and channel switching mechanism are evaluated. Simulations are developed in NS2 to validate the accuracy and efficiency of the proposed analytic model.

Channel 172 may be reserved for highly critical safety applications with no time division, and hence ESMs are most likely to be transmitted in Channel 172. Since some event-driven safety applications (*e.g.*, post-crash notification, road hazard warning) may require longer transmission distance than the one-hop communication range, multi-hop dissemination of ESMs is necessary. Therefore, Chapter 7 introduces an accurate analytic model to evaluate multi-hop propagation of ESMs. Extensive Matlab simulations are performed to cross-validate the analytic model. Important conclusions are drawn to provide deeper understandings of the performance and reliability of the ESMs transmission behavior.

Besides 1-D traffic scenario presented in Chapter 3-7, we first introduce an analytic model for the performance and reliability evaluation of 2-D traffic at open field to capture more realistic message transmission behaviors. Simulations in NS2 are carried out and the numerical results are compared with the analytic-numerical results under a large range of network parameter settings.

In future, vehicle mobility may be taken into account to characterize the dynamic behavior in vehicular safety communications. Even though vehicle mobility has been proven that high mobility of vehicles has very minor impact on the performance of the direct message broadcasting with high data rate, it may have great impact on application level performance metrics. In addition, more realistic two-dimensional traffic scenarios such as intersections, parallel lanes and square grid for downtown area will be considered.

For event-driven safety messages that are highly critical to safety on the road, it is essential to ensure their successfully transmission. Therefore, the safety message can be broadcasted multiple times over the communication range to increase the receptions probability, which is referred as one-hop multi-cycle broadcast. However, due to the increase number of packets transmitted resulting from rebroadcast of the same message, the packets will suffer from more collisions. Therefore, the evaluation of multi-cycle broadcast of safety messages is necessary to ensure the effective of multi-cycle schemes.

The analytic model will also be extended to incorporate different packet arrival processes such as Markov modulated Poisson process (MMPP), Markovian arrival process (MAP) etc. to capture more general safety message generations. For event-driven safety messages that generated occasionally for a vehicle, it is possible that the over different time periods, safety messages are generated with different arrival rates. For example, the emergency events may occur quite less frequently over an area in

which vehicle density is low or road condition is very good, while occur more frequently over another area in which vehicle density is high or road condition is bad. For such scenario, MMPP can be used to capture the packets arrivals instead of assuming Poisson arrival for event-driven safety messages.

Bibliography

[1] ASTM E2213-03, "Standard Specification for Telecommunications and Information Exchange Between Roadside and Vehicle Systems 5GHz Band Dedicated Short Range Communications (DSRC) Medium Access Control (MAC) and Physical Layer (PHY) Specifications", *ASTM Intl.* Jul, 2003.

[2] J. Yin, T. Elbatt, et al., "Performance evaluation of safety applications over DSRC vehicular ad hoc networks", *ACM VANET*, pp. 1-9, 2004.

[3] M. T. Moreno, D. Jiang, and H. Hartenstein, "Broadcast reception rates and effects of priority access in 802.11-based vehicular ad-hoc networks", *ACM VANET*, pp. 10-18, 2004.

[4] Q. Xu, T. Mak, J. Ko, and R. Sengupta, "Vehicle-to-vehicle safety messaging in DSRC", *ACM VANET*, pp. 19-28, 2004.

[5] F. Bai and H. Krishnan, "Reliability analysis of DSRC wireless communication for vehicle safety applications", *IEEE Intelligent Transportation Systems Conference*, ITSC'06., pp. 355–362, Sept. 2006.

[6] X. Ma, X. Chen, and H. H. Refai, "Unsaturated performance of IEEE 802.11 broadcast service in vehicle-to-vehicle networks", *IEEE VTC*, pp. 1957-1961, 2007.

[7] X. Chen, H. H. Refai, and X. Ma, "A Quantitative Approach to evaluation DSRC Highway Inter-vehicle Safety Communication", *IEEE GLOBECOM*, pp. 151-155, 2007.

[8] X. Ma, X. Chen, and H. H. Refai, "Performance and reliability of DSRC vehicular safety communication: a formal analysis", *EURASIP J. on Wireless Comm. and Networking*, pp. 1-13, 2009.

[9] K. S. Trivedi, *Probability and Statistics with Reliability, Queuing and Computer Science Applications,* Second Edition, John Wiley, 2002.

[10] L. Tomek and K.S. Trivedi, "Fixed-Point Iteration in Availability Modeling", *Informatik-Fachberichte*, Vol. 283, M. DalCin (ed.), pp. 229-240, Springer-Verlag, Berlin, 1991.

[11] IEEE 802.11 Working group, "Part 11: wireless LAN medium access control (MAC) and physical layer (PHY) specifications", *ANSI/IEEE Std. 802.11*, Sep. 1999.

[12] X. Yin, X. Ma and K. S. Trivedi, "Performance Evaluation for DSRC Vehicular Safety Communication: A Semi-Markov Process Approach", *International Conference on Communication Theory, Reliability, and Quality of Service*, 2011.

[13] P. D. Welch, "On a Generalized M/G/l Queueing Process in which the First Customer of Each Busy Period Receives Exceptional Service", *Operations Research*, Vol, 12, No, 5, pp. 736-752, 1964.

[14] V. Mainkar and K. S. Trivedi, "Sufficient conditions for existence of a fixed point in stochastic reward net-based iterative models", *IEEE Transactions. on Software Engineering*, 1996.

[15] G. Haring, R. Marie, R. Puigjaner, K.S. Trivedi, "Loss formulae and their optimization for cellular networks", *IEEE Transactions on Vehicular Technology*, 50 (3) pp. 664-673, 2001.

[16] G. Ciardo and K. S. Trivedi, "A Decomposition Approach for Stochastic Reward Net Models", *Performance Evaluation*, 18(1), pp. 37-59, 1993.

[17] J. Medhi, *Stochastic Processes*, Wiley Eastern, New Delhi, 1994.

[18] J. M. Ortega and W. C. Rheinboldt, *Iterative Solution of Nonlinear Equations in Several Variables*, Academic Press, 1970.

[19] P. M. Fitzpatrick, *Advanced Calculus*, 2nd edition, Thomson, Brooks/Cole, 2006.

[20] R. L. Burden, J. D. Faires, *Numerical Analysis*, 7th edition, Brooks/Cole, 2000.

[21] S. C. Malik, S. Arora, *Mathematical Analysis*, 3rd edition, New Age Science, 2009.

[22] E. Cinlar, *Introduction to Stochastic Processes*, Prentice-Hall, Englewood Cliffs, New Jersey, 1975.

[23] X. Ma and X. Chen, "Performance analysis of IEEE 802.11 broadcast scheme in ad hoc wireless LANs", *IEEE Transactions on Vehicular Technology*, 57(6): 3757-3768, Nov. 2008.

[24] F. Ye, R. Yim, S. Roy, and J. Zhang, "Efficiency and reliability of one-hop broadcasting in vehicular ad hoc networks", *IEEE Journal of Selected Areas in Communications*, 29(1): 151-160, Jan. 2011.

[25] Md. I. Hassan, H. L. Vu, T. Sakurai, "Performance analysis of the IEEE 802.11 MAC protocol for DSRC with and without retransmissions", *IEEE Int. Symposium on a World of Wireless Mobile and Multimedia Networks*, 2010.

[26] C. Campolo, A. Vinel, A. Molinaro, Y. Koucheryavy, "Modeling Broadcasting in IEEE 802.11p/WAVE Vehicular Networks", *IEEE Communications Letters*, vol.15, no.2, pp.199-201, February 2011.

[27] G. Bianchi, "Performance analysis of the IEEE 802.11 distributed coordination function", *IEEE Journal on Selected Areas in Communications*, vol.18, no.3, pp.535-547, Mar 2000.

[28] J. W. Robinson and T. S. Randhawa, "Saturation throughput analysis of IEEE 802.11e enhanced distributed coordination function", *IEEE Journal on Selected Areas in Communications*, vol. 22, no. 5, pp. 917–928, Jun. 2004.

[29] R. Battiti and B. Li, "Supporting service differentiation with enhancements of the IEEE 802.11 MAC protocol: models and analysis", University of Trento, Italy, Tech. Rep. DIT-03-024, May 2003.

[30] D. Malone, K. Duffy, D. Leith, "Modeling the 802.11 Distributed Coordination Function in Nonsaturated Heterogeneous Conditions", *IEEE/ACM Transactions on Networking*, vol.15, no.1, pp.159-172, Feb. 2007.

[31] J.R. Gallardo, D. Makrakis, and H.T. Mouftah, "Mathematical Analysis of EDCA's Performance on the Control Channel of an IEEE 802.11 WAVE Vehicular Network", *EURASIP Journal on Wireless Communications and Networking*, 2010.

[32] G. Badawy, J. Misic, T. Todd, and D. Zhao, "Performance Modeling of Safety Message Delivery in Vehicular Ad Hoc Networks", *IEEE WiMob*, 2010.

[33] J. R. Gallardo, D. Makrakis, and H. T. Mouftah, "Performance analysis of the EDCA medium access mechanism over the control channel of an IEEE 802.11p WAVE vehicular network", *IEEE International Conference on Communications (ICC)*, pp. 1-6, 2009.

[34] N. Wisitpongphan, B. Fan, P. Mudalige, V. Sadekar, O. Tonguz, "Routing in sparse vehicular ad hoc wireless networks", *IEEE Journal on Selected Areas in Communications*, 25(8): 1538-1556, 2007.

[35] H. Zhu, L. Fu, G. Xue, Y. Zhu, M. Li, L. Ni, "Impact on traffic influxes: understanding exponential inter-contact time in VANETs", *IEEE INFOCOM'10*, 2010.

[36] X. Ma, J. Zhang, T. Wu, "Reconsider Broadcast Packet Reception Rates in One-Dimensional MANETs". *IEEE GLOBECOM*, 2010: 1-6.

[37] I. Tinnirello, G. Bianchi, "Rethinking the IEEE 802.11e EDCA performance modeling methodology". *IEEE/ACM Transactions on Networking* (*TON*), 18(2):540-553, 2010.

[38] J. Y. Lee, H. S. Lee, "A performance analysis model for IEEE 802.11e EDCA under saturation condition". *IEEE Transactions on Communications (TCOM)* 57(1):56-63, 2009.

[39] F. Bai and B. Krishnamachari, "Spatio-temporal Variations of Vehicle Traffic in VANETs: Facts and Implications". *In ACM VANET*, 2009.

[40] M. T. Moreno, S. Corroy, H. Hartenstein, "IEEE 802.11-based one-hop broadcast communications: understanding transmission success and failure under different radio propagation environments" *ACM International Workshop on Modeling Analysis and Simulation of Wireless and Mobile Systems* (*MSWiM'06*), pp. 68-77, Spain, 2004.

[41] X. Ma and X. Chen, "Delay and Broadcast Reception Rates of Highway Safety Applications in Vehicular Ad Hoc Networks", *IEEE INFOCOM2007 Workshop on Mobile Networks for Vehicular Environments*, pp. 85-90, 2007.

[42] M. V. Eenennaam, W. K. Wolterink, G. Karagiannis, and G. Heijenk, "Exploring the Solution Space of Beaconing in VANETs", *In: First IEEE Vehicular Networking Conference*, VNC2009, 28-30 Oct 2009, Tokyo, Japan.

[43] X. Chen, H. H. Refai, X. Ma, "Saturation Performance of IEEE 802.11 Broadcast Scheme in Ad Hoc Wireless LANs", *IEEE VTC Fall 2007*: 1897-1901.

[44] IEEE Standard for Information Technology-Telecommunications and Information Exchange between Systems-Local and Metropolitan Area Networks-Specific Requirements; Part 11: Wireless LAN Medium Access Control (MAC) and Physical Layer (PHY) Specifications; Amendment 6: Wireless Access in Vehicular Environments, IEEE Std. 802.11p, Jul. 2010.

[45] J. B. Kenney, "Dedicated short range communications (DSRC) standards in the United States", *Proceedings of the IEEE*, vol. 99, no. 7, pp. 1162-1182, 2011.

[46] "Dedicated Short Range Communications (DSRC) Message Set Dictionary", *SAE Std. J2735, SAE Int.*, DSRC Committee, Nov. 2009.

[47] T. A. ElBatt, S. K. Goel, G. Holland, H. Krishnan, J. S. Parikh, "Cooperative collision warning using dedicated short range wireless communications," *Proceeding of ACM VANET workshop*, 2006.

[48] S. Yousefi, M. Fathy and A. Benslimane, "Performance of beacon safety message dissemination in Vehicular Ad hoc NETworks (VANETs)," *Journal of Zhejiang University SCIENCE A*, 2007.

[49] M. Torrent-Moreno "Inter-Vehicle Communications: Achieving Safety in a Distributed Wireless Environment: Challenges, Systems and Protocols", PhD-dissertation, Karlsruhe, 2007.

[50] A. Vinel, V. Vishnevsky, Y. Koucheryavy, "A simple analytical model for the periodic broadcasting in vehicular ad-hoc networks", *Proc. 4th BWA Workshop, co-located with IEEE GLOBECOM*, 2008.

[51] S. Bastani, B. Landfeldt and L. Libman, "On the Reliability of Safety Message Broadcast in Urban Vehicular Ad hoc Networks", *Proc. ACM int. conf. on Modeling, Analysis and Simulation of Wireless and Mobile Systems*, 2011.

[52] X. Yin, X. Ma, and K. S. Trivedi, "An Interacting Stochastic Models Approach for the Performance Evaluation of DSRC Vehicular Safety Communication", *IEEE Transactions on Computers*, vol. 62, no. 7, 2013.

[53] F. Bai, H. Krishnan, V. Sadekar, G. Holland, T. ElBatt, "Towards characterizing and classifying communication-based automotive applications from a wireless networking perspective", *IEEE Workshop on Autonet*, 2006.

[54] N. An, T. Gaugel, and H. Hartenstein, "VANET: is 95% probability of packet reception safe?" *IEEE 11th International Conference on ITS Telecommunications*, 2011.

[55] H. Lu, and C. Poellabauer, "Analysis of application-specific broadcast reliability for vehicle safety communications", *ACM VANET'11*.

[56] K. Matthes, Zur Theorie der Bedienungsprozesse, in: Trans. of the 3rd Prague Conf. on Information Theory, Stat. Dec. Fns. and Random Processes, 1962, pp. 513–528.

[57] P. Glynn, "A GSMP formalism for discrete event systems", *Proc. of the IEEE*, 77, (1989).

[58] ETSI TC ITS, "ITS; Vehicular Communications; Basic Set of Applications; Definitions", Tech. Rep. TR 102 638, 2009.

[59] A. Buchenscheit, F. Schaub, F. Kargl, M. Weber, "A VANET-based emergency vehicle warning system", *IEEE Vehicular Networking Conference* (*VNC*), pp.1-8, 28-30 Oct. 2009.

[60] R. Chen, D. Ma, and A. Regan, "TARI: Meeting Delay Requirements in VANETs with Efficient Authentication and Revocation", *IEEE International Conference on Wireless Access in Vehicular Environment*, 2009.

[61] Q. Chen, D. Jiang, L. Delgrossi, "IEEE 1609.4 DSRC Multi-Channel Operations and Its Implications on Vehicle Safety Communications" *VNC* 2009.

[62] A. Lyakhov, V. Vishnevsky, and P. Poupyrev, "Analytical Study of Broadcasting in 802.11 Ad Hoc Networks", *Proc. 2nd International Conference on e-Business and Telecommunication Networks (ICETE 2005)*, October 3-7, 2005, Reading, U.K. Vol. II, pp.86-91

[63] "IEEE Trial-Use Standard for Wireless Access in Vehicular Environments (WAVE) – Multi-Channel Operation," IEEE 1609.4-2006.

[64] K. Hong, J. B. Kennedy, V. Rai and K. P. Laberteaux, "Evaluation of Multi-Channel Schemes for Vehicular Safety Communications", *in Proc. of IEEE VTC-Spring*, Taipei, pp. 1-5, 2010.

[65] J. Misic, G. Badawy and V. Misic, "Performance Characterization for IEEE 802.11p Network with Single Channel Devices", *IEEE Transactions on Vehicular Technology*, 68(4), pp. 1775-1789, 2011.

[66] A. J. Ghandour, M. D. Felice, L. Bononi, H. Artail, "Modeling and simulation of WAVE 1609.4-based multi-channel vehicular ad hoc networks", *Proceedings of the 5th International ICST Conference on Simulation Tools and Techniques*, pp. 148-156, 2012

[67] Y. Du, L. Zhang, Y. Feng, Z. Ren and Z. Wang, "Performance Analysis and Enhancement of IEEE 802.11p/1609 Protocol Family in Dense Vehicular Environments", *In Proc. of 13th International IEEE Conference on Intelligent Transportation Systems*, ITSC 2010, 19-22 Sep 2010.

[68] X. Yin, X. Ma and K. S. Trivedi, "MAC and Application Level Performance Evaluation of Beacon Message Dissemination in DSRC Safety Communication", submitted to Performance Evaluation, 2012.

[69] IEEE Trial-Use Standard for Wireless Access in Vehicular Environments (WAVE)—Multi-Channel Operation, IEEE Std. 1609.4-2007, 2007.

[70] IEEE Trial-Use Standard for Wireless Access in Vehicular Environments (WAVE)—Networking Services, IEEE Std. 1609.3-2007, 2007.

[71] IEEE Trial-Use Standard for Wireless Access in Vehicular Environments (WAVE)—Security Services for Applications and Management Messages, IEEE Std. 1609.2-2007, 2007.

[72] X. Ma, X. Yin and K. S. Trivedi, "Performance Evaluation of Two-Dimensional Broadcast Ad Hoc Network", submitted to *IEEE Transaction on Computers*, 2012.

[73] X. Ma, J. Zhang, X. Yin, and K. S. Trivedi, "Design and analysis of a robust broadcast scheme for vanet safety-related services," *IEEE Transactions on Vehicular Technology*, vol. 61, no. 1, pp. 46–61, Jan 2012.

[74] A. Vinel, "3GPP LTE Versus IEEE 802.11p/WAVE: Which Technology is Able to Support Cooperative Vehicular Safety Applications?", *IEEE Wireless Communication Letters*, Vol. 1, No. 2, April 2012.

[75] S. Bastani, B. Landfeldt, and L. Libman, "A traffic density model for radio overlapping in urban vehicular ad hoc networks", *IEEE Conference on Local Computer Networks* (*LCN*), Bonn, Germany, Oct. 2011.

[76] S. Bastani, B. Landfeldt, and L. Libman, "On the reliability of safety message broadcast in urban vehicular ad hoc networks", *ACM MSWiM'11*, Miami Beach, 2011.

[77] A. Zanella, G. Pierobon, and S. Merlin, "On the limiting performance of broadcast algorithms over unidimensional ad hoc radio networks", *WPMC*' 04, Italy, Sep. 2004.

[78] S. Ni, Y. Seng, Y. Chen and J. Sheu, "The broadcast storm problem in a mobile ad hoc networking and computing", *ACM MOBIHOC*, Lausanne, Switzerland, 2002.

[79] E. Fasolo, R. Furiato, and A. Zanella, "Smart broadcast algorithms for Inter-vehicular communications", *IWS 2005/WPMC'05*, Aaborg, Denmark, 2005.

[80] B. William and T. Camp, "Comparison of broadcasting techniques for mobile ad hoc networks", *Proc. ACM Symp. Mobile Ad Hoc Networking* (*MOBIHOC*), pp. 194-205, 2002.

[81] J. H. Zhu and I. Chlamtac, "Performance analysis for IEEE 802.11e EDCF service differentiation", *IEEE Transactions on Wireless Communication*, vol. 4, no. 4, pp. 1779–1788, July 2005.

[82] K. Z. Tao and S. Panwar, "Throughput and delay analysis for the IEEE 802.11e enhanced distributed channel access", *IEEE Transactions on Communication*, pp. 596–602, Apr. 2006.

[83] I. Inan, F. Keceli, and E. Ayanoglu, "Saturation throughput analysis of the 802.11e enhanced distributed channel access function", *in Proc. IEEE ICC '07*, June 2007.

[84] C. Huang, and W. Liao, "Throughput and delay performance of IEEE 802.11e enhanced distributed channel access (EDCA) under saturation condition", *IEEE Transactions on Wireless Communications* (*TWC*) 6(1):136-145 (2007).

[85] P. E. Engelstad, and O.N. Østerbø, "Non-saturation and saturation analysis of IEEE 802.11e EDCA with starvation prediction", *in Proceedings of the eighth ACM International Symposium on Modeling, Analysis and Simulation of Wireless and Mobile Systems*. October 2005.

[86] J. Hu, G. Min, M.E. Woodward, and W. Jia, "A comprehensive analytical model for IEEE 802.11e QoS differentiation schemes under unsaturated traffic loads", *in Proceedings of the ICC'08*, May 2008.

[87] J.-H. Lim, J.-H. Yun, and S.-W. Seo, "Throughput model of IEEE 802.11e EDCF with consideration of delay bound constraint", *IEEE ICC'08*, May 2008.

[88] I. Inan, F. Keceli, E. Ayanoglu, "Analysis of the 802.11e enhanced distributed channel access function", *IEEE Transactions on Communications*, vol.57, no.6, pp.1753-1764, June 2009.

[89] K. Kosek-Szott, M. Natkaniec, and A.R. Pach, "A simple but accurate throughput model for IEEE 802.11 EDCA in saturation and non-saturation conditions", *Computer Networks* (*CN*) 55(3):622-635 (2011).

[90] K. A. Hafeez, L. Zhao, Z. Liao, and B. N. Ma, "Performance Analysis of Broadcast Messages in VANETs Safety Applications", *IEEE Global Telecommunications Conference*, pp.1-5, 6-10 Dec. 2010.

[91] M. Khabazian, S. Aïssa, and M. Mehmet-Ali, "Performance Modeling of Message Dissemination In Vehicular Ad Hoc Networks with Priority", *IEEE Journal on Selected Areas in Communications*, vol.29, no.1, pp.61-71, January 2011.

[92] M. Barradi, A. S. Hafid, and J. R. Gallardo, "Establishing Strict Priorities in IEEE 802.11p WAVE Vehicular Networks", *IEEE Global Telecommunications Conference*, pp.1-6, 6-10 Dec. 2010.

[93] IEEE 802.11 Working group, "IEEE Standard for Information technology--Telecommunications and information exchange between systems--Local and metropolitan area networks--Specific requirements Part 11: Wireless LAN Medium Access Control (MAC) and Physical Layer (PHY) Specifications Amendment 6: Wireless Access in Vehicular Environments," *IEEE Std 802.11p-2010,* pp.1-51, July 15 2010.

[94] C. Campolo, A. Molinaro, and A. Vinel, "Understanding the Performance of Short-lived Control Broadcast Packets in 802.11p/WAVE Vehicular Networks", *Proc. of the 3rd IEEE Vehicular Networking Conference* – IEEE VNC-2011, Amsterdam, Netherlands, 2011.

[95] C. Patel, G. Stuber and T. Pratt. "Simulation of Rayleigh-Faded Mobile-to-Mobile Communication Channels", *IEEE Transactions on Vehicular Technology*. Nov 2005.

[96] G. Marfia, M. Roccetti, A. Amoroso, and G. Pau, "Safe Driving in LA: Report from the Greatest Intervehicular Accident Detection Test Ever", *IEEE Transactions on Vehicular Technology*, Vol. 62, n. 2, February 2013.

[97] F. Bai, D. D. Stancil, and H. Krishnan, "Toward understanding characteristics of Dedicated Short Range Communications (DSRC) from a perspective of vehicular network engineers", *in Proc. 16th Annu. Int. Con. MobiCom*, 2010, pp. 329–340.

[98] G. Resta, P. Santi, and J. Simon, "Analysis of multi-hop emergency message propagation in vehicular ad hoc networks", *Proc. of the 8th ACM International Symposium on Mobile Ad Hoc Networking and Computing*, 2007.

[99] T. Osafune, L. Lin, and M. Lenardi, "Multi-hop vehicular broadcast (MHVB)", *6th International Conference on ITS Telecommunications*, 2006.

[100] R. Chen, W. Jin, and A. Regan, "Multi-hop broadcasting in vehicular ad hoc networks with shockwave traffic", *7th IEEE Consumer Communications and Networking Conf.*, 2010.

[101] Q. Yang, and L. Shen, "A multi-hop broadcast scheme for propagation of emergency messages in vanet", *12th IEEE Int. Conf. on Communication Technology* (*ICCT*), 2010.

[102] M. Jerbi, and S. M. Senouci, "Characterizing multi-hop communication in vehicular networks", *IEEE Wireless Communications and Networking Conference*, 2008.

[103] J. Santa, et al., "Experimental analysis of multi-hop routing in vehicular ad-hoc networks", *IEEE 5th Int. Conf. on Testbeds and Research Infrastructures for the Development of Networks & Communities and Workshops*, 2009.

[104] C. Rajabhushanam and A. Kathirvel, "Survey of wireless MANET application in battlefield operations", *International Journal of Advanced Computer Science and Applications*, 2(1), Jan. 2011.

[105] X. Ma, Xianbo Chen, and Hazem Refai, "On the broadcast packet reception rates in one-dimensional MANETs", *IEEE GLOBECOM*, Nov. 30-Dec. 4, New Orleans, 2008.

[106] D. Huang, "Unlinkability measure for IEEE 802.11 based MANETs", *IEEE Trans. on Wireless Communications*, 7(3): 1025-1034, March, 2008.

[107] C. H. Foh, M. Zukerman, and J. W. Tantra, "A Markovian framework for performance evaluation of IEEE 802.11", *IEEE Trans. on Wireless Communications*, 6(4): 1276-1285, April, 2007.

[108] X. Li, Thu D. Nguyen, and R. P. Martin, "An analytic model predicting the optimal range for maximizing 1-hop broadcast coverage in dense wireless networks", *Proceedings of the 3rd International Conferences on Ad-Hoc Networks & Wireless*, pp. 172-182, Vancouver, Canada, July 2004.

[109] J. Choi, J. So, and Y. Ko, "Numerical analysis of IEEE 802.11 broadcast scheme in multihop wireless ad hoc networks", *19th International Conference on Information Networking*, pp. 1-10, 2005.

[110] X. Ma, "On the Reliability and Performance of Real-Time One-Hop Broadcast MANETs", *ACM/Springer Wireless Networks*, 17(5): 1323-1337, May 2011.

[111] J. G. Andrews, R. K. Ganti, M. Haenggi, N. Jindal, and S. Weber, "A Primer on Spatial Modeling and Analysis in Wireless Networks", *IEEE Communications Magazine*, Nov. 2010. 48(11): 156-163, Nov. 2010.

[112] "Federal Communications Commission. FCC 03-324. FCC Report and Order," February 2004.

[113] O. Andrisano, R. Verdone, and M. Nakagama, "Intelligent Transportation Systems: The role of Third-Generation Mobile Radio Networks", *IEEE Communications Magazine*, 38(9), pp.144-151, 2000.

[114] P. Roberto, S. Russo, and K. S. Trivedi, "Software reliability and testing time allocation: an architecture-based approach", *IEEE Transactions on Software Engineering*, 36.3 (2010): 323-337.

[115] G. Katerina, and K. S. Trivedi, "Failure correlation in software reliability models", *IEEE 10th International Symposium on Software Reliability Engineering*, 1999.

[116] D. Salvatore, and K. S. Trivedi, "Non-Markovian State-Space Models in Dependability Evaluation", *Quality and Reliability Engineering International* (2012).

[117] A. I. Lyakhov, and P. Poupyrev, "Evaluation of Broadcasting Technologies Performance in IEEE 802.11 Networks", *Proc. International Workshop on Distributed Computer and Communication Networks (DCCN-2005)*. Sofia, Bulgaria, April 23-29, pp. 84-94, 2005.

Biography

Xiaoyan Yin was born in Anhui, China, on October 6th, 1983. She received her B.S. degree in Electrical Engineering and Computer Science from Peking University, China, in 2006, and her M.S. degree in Electrical and Computer Engineering from Duke University, USA, in 2010. She received the teaching assistantship in Electrical and Computer Engineering department of Duke University in academic year of 2009-10, Fellowship from the academic year of 2010-11, and then research assistantship for the academic years from 2011-12 to 2012-13. She worked as a research intern at General Motors (Palo Alto office) in 2011. Her research interests include performance and dependability analysis of vehicular ad hoc networks (VANETs), data backup and restore operations in storage systems, and IMS-based telecommunication networks. Her scientific publications are listed below.

Publications

1. Xiaoyan Yin, Xiaomin Ma, and Kishor Trivedi, "Performance Evaluation for DSRC Vehicular Safety Communication: A Semi-Markov Process Approach", *The Fourth International Conference on Communication Theory, Reliability, and Quality of Service*, April 16-17, 2011.
2. Xiaoyan Yin, Xiaomin Ma, and Kishor Trivedi, "An Interacting Stochastic Models Approach for the Performance Evaluation of DSRC Vehicular Safety Communication," *IEEE Transaction on Computers*, vol. 62, no. 5, pp. 873-885, 2013.

3. Xiaomin Ma, Xiaoyan Yin, and Kishor Trivedi, "A Robust Broadcast Scheme for VANET One-Hop Emergency Services," *IEEE Vehicular Technology Conference*, pp.1-5, 5-8 Sept. 2011.
4. Xiaomin Ma, Jingsong Zhang, Xiaoyan Yin, and Kishor Trivedi, "Design and Analysis of a Robust Broadcast Scheme for VANET Safety-Related Services," *IEEE Trans. on Vehicular Technology*, vol.61, no.1, pp.46-61, Jan. 2012.
5. Xiaomin Ma, Xiaoyan Yin, and Kishor Trivedi, "On the Reliability of Safety Applications in VANETs", *International Journal of Performability Engineering Special Issue on Dependability of Wireless Systems and Networks,* 2012.
6. Yang Zhao, Xiaoyan Yin, Rui Kang, and Kishor S. Trivedi, "A review of the research on quantitative reliability Prediction and Assessment for electronic components," *IEEE Prognostics and System Health Management Conference*, pp.1-7, 24-25, May 2011.
7. Maurizio Guida, Maurizio Longo, Fabio Postiglione, Kishor S. Trivedi and Xiaoyan Yin, "Semi-Markov Models for Performance Evaluation of Telecommunication Networks in the Presence of Failures", *PSAM11 & ESREL*, 2012.
8. Kishor S. Trivedi, Dong Seong Kim, Xiaoyan Yin, "Multi-State Availability Modeling in Practice", book chapter in *Recent Advances in System Reliability: Signature, Multi-state Systems and Statistical Inference*, Eds. Anatoly Lisnianski, Ilia Frenkel, Springer, 2011.

9. Xiaoyan Yin, Javier Alonso, Fumio Machida, Ermeson Andrade and Kishor Trivedi, "Availability Modeling and Analysis for Data Backup and Restore operations", in *Proc. of the 31st IEEE International Symposium on Reliability Distributed Systems (IEEE SRDS 2012)*, 2012.
10. Xiaoyan Yin, Xiaomin Ma, Kishor S. Trivedi, "Performance of BSM Dissemination in Multi-channel DSRC", *IEEE 77th Vehicular Technology Conference (IEEE VTC 2013)*, June, 2013.
11. Xiaomin Ma, Xiaoyan Yin, Matthew Wilson, Kishor S. Trivedi, "Performance of VANET Safety Message Broadcast at Rural Intersections", *IEEE IWCMC* 2013.
12. Maurizio Guida, Maurizio Longo, Fabio Postiglione, Kishor S. Trivedi, Xiaoyan Yin, "Semi-Markov models for performance evaluation of failure-prone IMS core networks", *Proceedings of the Institution of Mechanical Engineers, Part O: Journal of Risk and Reliability*, Volume 227 Issue 3, June 2013, pp. 290-301.
13. Kishor S. Trivedi, Fabio Postiglione and Xiaoyan Yin, "Performance and Availability Evaluation of IMS-based Core Networks", book chapter in *Applied Reliability Engineering and Risk Analysis: Probabilistic Models and Statistical Inference*, John Wiley & Sons, 2013.
14. Xiaoyan Yin, Xiaomin Ma, Kishor S. Trivedi and Alexey Vinel, "Performance and Reliability Evaluation of BSM Broadcasting in DSRC with Multi-channel Schemes", *IEEE Trans. on Computers*, 2013, accepted.

15. Xiaoyan Yin, Xiaomin Ma and Kishor S. Trivedi, "Channel Fading Impact on Multi-hop DSRC Safety Communication", *16th ACM International Conference on Modeling, Analysis and Simulation of Wireless and Mobile Systems* (MSWIM), Spain, 2013.
16. Xiaoyan Yin, Xiaomin Ma and Kishor S. Trivedi, "MAC and Application Level Performance Evaluation of Beacon Message Dissemination in DSRC Safety Communication", *Performance Evaluation*, 2014, to appear.